# Structural-geological setting of Ivanščica Mountain and its tectonic position at the junction of the Alps, Dinarides and Pannonian basin

**Vukovski, Matija**

University of Zagreb

Faculty of Mining, Geology and Petroleum Engineering

Matija Vukovski

# STRUCTURAL-GEOLOGICAL SETTING OF IVANŠČICA MOUNTAIN AND ITS TECTONIC POSITION AT THE JUNCTION OF THE ALPS, DINARIDES AND PANNONIAN BASIN

DOCTORAL THESIS

Zagreb, 2024

University of Zagreb

Faculty of Mining, Geology and Petroleum Engineering

Matija Vukovski

# STRUCTURAL-GEOLOGICAL SETTING OF IVANŠČICA MOUNTAIN AND ITS TECTONIC POSITION AT THE JUNCTION OF THE ALPS, DINARIDES AND PANNONIAN BASIN

DOCTORAL THESIS

Supervisors:
Prof. Bruno Tomljenović, PhD
Damir Slovenec, PhD

Zagreb, 2024

Sveučilište u Zagrebu

Rudarsko-geološko-naftni fakultet

Matija Vukovski

# STRUKTURNO-GEOLOŠKA GRAĐA IVANŠČICE I NJEZIN TEKTONSKI POLOŽAJ U DODIRNOM PODRUČJU ALPA, DINARIDA I PANONSKOG BAZENA

DOKTORSKI RAD

Mentori:
Dr. sc. Bruno Tomljenović, redoviti profesor u trajnom izboru
Dr. sc. Damir Slovenec, znanstveni savjetnik u trajnom izboru

Zagreb, 2024

**Supervisors:**

Prof. Bruno Tomljenović, PhD
University of Zagreb
Faculty of Mining, Geology and Petroleum Engineering
Department of Geology and Geological Engineering

Damir Slovenec, PhD
Croatian Geological Survey
Department of Geology

*Mojoj obitelji*

***ZAHVALE***

*Doktorsko istraživanje putovanje je obilježeno brojnim izazovima, osobnim rastom i radosnim trenucima otkrića. Međutim, ovo putovanje također je bilo obilježeno trenucima frustracija, sumnji i borbe. Ti trenuci, iako teški, bili su jednako važni za moj razvoj, poučivši me vrijednosti ustrajnosti i važnosti podrške onih oko mene. Iako sama disertacija nosi moje ime, ona je rezultat zajedničkih napora, ohrabrenja i nepokolebljive podrške mnogih koji su hodali ovim putem sa mnom. Ovo poglavlje posvećeno je priznavanju dubokog utjecaja koji su moji kolege, prijatelji i obitelj imali na moje akademsko i osobno putovanje.*

*Veliko hvala prvom mentoru dr. sc. Bruni Tomljenoviću na ukazanom povjerenju, potpori i podršci, kako za vrijeme doktorata tako i unazad već 8 godina, na nesebičnom prijenosu znanja i iskustava te slobodnom vremenu uloženom za rad na mom znanstvenom radu i disertaciji. Hvala na brojnim konstruktivnim, ponekad žustrim, ali uvijek vrlo korisnim raspravama, vođenim što u kabinetu što na terenu uz izdanke. Hvala na omogućenoj znanstvenoj slobodi i što ste me naučili ispravnom znanstvenom pristupu.*

*Drugom mentoru dr. sc. Damiru Slovenecu također veliko hvala na ukazanom povjerenju te kao voditelju projekta GOST, hvala na pokretanju samog projekta i ove doktorske disertacije. Trebam naglasiti da bez planirane ovoliko velike količine terenskih dana ne bi bilo moguće realizirati ovu disertaciju.  Hvala na stalnoj brizi i podsjećanju oko ispunjenja brojnih obaveza. Hvala na otvorenosti i spremnosti za odgovaranje na sva moja pitanja te na brojnim često dugotrajnim razgovorima od kojih me svaki doveo barem jedan korak bliže da postanem bolji znanstvenik.*

*Doc. dr. sc. Duji Smirčiću predsjedniku Povjerenstva za ocjenu i obranu doktorskog rada, veliko hvala na pažljivom i vrlo pedantnom čitanju disertacije, te komentarima koji su značajno poboljšali njenu kvalitetu. Hvala na zajedničkim diskusijama što geološkim što životnim te jakoj podršci i motivaciji u onim teškim trenucima.*

*Najiskrenije zahvaljujem dr. sc. Špeli Goričan, članici Povjerenstva za obranu i ocjenu doktorskog rada, na vrlo pažljivom čitanju doktorskog rada, na korisnim komentarima ali ponajviše na pitanjima koja su me uvijek natjerala da još jednom ili više puta promislim. Zelo hvala za izjemno kakovostne razprave in za veliko prenesenega znanja v zelo kratkem času, kolikor se poznava.*

*Hvala prof. dr. sc. Marku Vrabecu članu povjerenstva za obranu i ocjenu doktorskog rada na strpljivom čitanju disertacije i korisnim sugestijama. Hvala za preneseno znanje in odpiranje vrat v geologijo Alp ter za koristne nasvete in konstruktivne razprave.*

*Najiskrenije zahvaljujem svojim dragim kolegama, članovima projektnog tima projekta GOST, koji su me od prvog dana prihvatili i tretirali kao ravnopravnog člana ekipe. Uz rad s vama ja sam rastao, a vi ste svojim iskustvom, znanjem i savjetima bitno doprinijeli mom profesionalnom razvoju pa tako i ovoj disertaciji. Hvala dr. sc. Tonćiju Grgasoviću i dr. sc. Duji Kukoču s kojima sam proveo najviše dana na terenu i naučio mnogo o sedimentologiji i paleontologiji. Tonćiju veliko hvala na nesebičnom dijeljenju neprocjenjivog znanja i iskustva stečenog tijekom dugogodišnjih terenskih istraživanja te na konstruktivnim diskusijama. Duji hvala na brojnim* konstruktivnim diskusijama i spremnosti da uvijek odgovori na svako moje pitanje. Kad bih imao trećeg mentora to bi bio Duje. Veliko hvala već spomenutom doc. dr. sc. Duji Smirčiću na prenesenom terenskom znanju i diskusijama. Veliko hvala sada već umirovljenom dr. sc. Mirku Belaku, prije svega na ukazanom povjerenju tijekom terenskih istraživanja, ali i na ogromnoj količini nesebično prenesenog znanja i terenskog iskustva te zajedničkim diskusijama. Dr. sc. Mariji Horvat, mojoj prvoj cimerici, hvala na stalnoj spremnosti za pomoć, posebice u prvim danima tjednima i mjesecima po zaposlenju. Na kraju još jednom hvala već spomenutom dr. sc. Damiru Slovenecu voditelju projekta na osmišljanju i vođenju projekta GOST bez kojeg ne bi bilo niti ove doktorske disertacije. Hvala i ostalim članovima projekta, koji su doprinijeli njegovu planiranju i realizaciji.

Moram zahvaliti i Hrvatskoj zakladi za znanost koja je financirala projekt GOST i ovo doktorsko istraživanje.

Zahvaljujem se i svim drugim kolegama u svojoj matičnoj kući, Hrvatskom geološkom institutu, u kojem je izrađena ova doktorska disertacija. Osobito hvala kolegama Zavoda za geologiju na čelu s bivšom predstojnicom dr. sc. Koraljkom Bakrač i sadašnjom predstojnicom dr. sc. Anitom Grizelj, koji su me također od prvog dana srdačno primili i prihvatili i s kojima mi je vrlo ugodno raditi.

Mojoj drugoj cimerici i kumi Ani Kamenski mag. geol., hvala na velikoj pomoći po mom zaposlenju, i važnije, na stalnoj čvrstoj podršci i korisnim savjetima.

Veliko hvala mojim svim mojim koautorima, prvenstveno članovima projektnog tima projekta GOST. Od preostalih tu je kolega i susjed Ladislav Fuček dipl. ing. geol., kojem hvala na određivanju mikrofosila, ali još više na prenesenom neprocjenjivom znanju i iskustvu u geološkom kartiranju. Dragoj dr. sc. Tamari Troskot-Čorbič na spremnosti za pomoć te na urađenim analizama. Kolegi dr. sc. Marku Špeliću na interpretaciji refleksijskih seizmičkih profila i kvalitetnim zajedničkim diskusijama.

Zahvaljujem svim djelatnicima laboratorija Zavoda za geologiju, koji su sudjelovali u pripremi uzoraka korištenih u ovom doktorskom radu.

Najiskrenije zahvaljujem gospođama Željki Kurelec i Andrei Gmajnički Drvar na velikoj srdačnosti, ljubaznosti i svestranoj administrativnoj i drugoj pomoći tijekom doktorskog studija.

Želim zahvaliti i onim ljudima koji su u meni prepoznali te kasnije pomogli pri odabiru moga prirodoslovnog puta i dali mi čvrste temelje na kojima je kasnije bilo lako graditi. To su moji bivši susjedi Branko Jalžić, njegova žena Đurđa i sin Vedran, koji su od najranijeg djetinjstva svojim pričama i dogodovštinama, darovanim knjigama i izletima na koje su me vodili, u meni još više rasplamsali ljubav prema prirodi i prirodoslovlju. Veliko hvala mojim učiteljima iz Prirodoslovne srednje škole Vladimira Preloga. Tatjani Horvat, Danku Antunoviću, svojem prvom mentoru Mirku Hećimoviću i Josipu Završkom kojem posebno zahvaljujem na savjetima u dvojbi prilikom odabira fakulteta.

Hvala mojim trenerima veslanja, Aleksandru Vukojičiću i Krešimiru Petroviću s kojima sam proveo gotovo pola svojeg dosadašnjeg života, i koji su me naučili radu, strpljenju, trpljenju, disciplini i odgovornosti.

Veliko hvala svim članovima obitelji Jurič na velikoj pomoći i toplom domu čime ste mi omogućili da napravim za mene toliko veliku stepenicu u profesionalnom životu.

Hvala mojim dragim prijateljima i kumovima kojih je previše da ih sve nabrojim, a uvijek ste bili velika podrška i oslonac na koji sam uvijek mogao računati.

Od srca veliko hvala Graciji, Antoniu, Mariji, Ruži, Branku, Katarini, braći Lovru i Petru te roditeljima na ogromnoj pomoći pri čuvanju djece, pogotovo u najtežim trenucima. Puno puta ste baš vi bili jedini razlog koji mi je omogućio da tih dana radim na disertaciji.

Veliko hvala mojim roditeljima, što su me odgojili kakav jesam i usadili u mene ispravne vrijednosti. Što su me uvijek podržavali u životnim odlukama i konstantno podupirali na mome putu.

Na kraju posebno zahvaljujem svojoj ženi Mihaeli, na snazi koju ima, na razumijevanju, podršci i motivaciji, na trpljenju i žrtvi, jednom riječju ljubavi. Hvala ti što si uvijek vjerovala u mene i bodrila me. Tvoja prisutnost pogotovo u najtežim trenucima bila mi je neprocjenjiva, i mnogo puta jedini razlog zbog kojeg sam se nastavljao truditi. Hvala ti što me činiš boljim! Hvala našoj djeci Rafaeli i Tereziji koje su mi najveće učiteljice u jednostavnosti, ljubavi i poniznosti, te našoj prerano preminuloj kćerki Mariji koja me u najtežim trenucima, za tako malo vremena, naučila istinskim pravim vrijednostima. Ponosan sam što sam vaš tata!

Hvala dragom Bogu!

*"I will see you again.*

*But not yet…*

*Not yet…"*

- David Franzoni, Gladiator

## ABSTRACT

Over the last decades, geologic and geophysical research has revealed the complexity of the Alpine-Carpathian-Dinaridic orogenic system. In large orogenic systems crustal and upper mantle structures can be traced for hundreds or thousands of kilometers. Contrary, Alpine-Carpathian-Dinaridic orogenic system is characterized by the spatially limited subduction zones, detached and torn slabs, slabs that reverse subduction polarity along strike, subduction of heterogeneous lithosphere with oceanic or continental crust, and collision between continental lithosphere. Such complexity raises many controversies and multiple hypotheses which can be resolved only by obtaining high quality images of the deep subsurface and their integration with quality surface studies.

One such controversial area is the study area comprising the Ivanščica Mt. with its close surroundings. This area represents the zone of subduction polarity reversal between the Dinarides, where the Adriatic plate represents the lower plate, and the Alps, where Adriatic plate represents the upper plate. This makes Ivanščica Mt. a significant site for the implementation of structural research aimed at understanding the crustal structures, deformation patterns and tectonic history of the region. Therefore, the main objective of this doctoral research was to investigate the Mesozoic and Cenozoic tectono-stratigraphic evolution of this transitional zone between the Alps and the Dinarides, in the SW part of the Pannonian Basin.

The conducted interdisciplinary research combined implementation of sedimentological, biostratigraphic, petrological, geochemical, structural and thermochronological methods which resulted in novel findings regarding the Mesozoic lithostratigraphic evolution and tectonic history of the transitional area of the Alps and the Dinarides in the SW Pannonian Basin.

In the Mesozoic Adriatic passive margin successions preserved on Ivanščica Mt., two extensional events were recognized by their syn-rift deposits. First extensional event (D1) is marked by the upper Anisian to Upper Ladinian deep-marine volcano-sedimentary deposits and is related to the opening of the Neotethys Ocean. Second extensional event (D2) is induced by the opening of the Alpine Tethys Ocean and characterized by the deposition of the Lower Jurassic deep-marine sedimentary succession. The oldest contractional event (D3) is related to the Berriasian - Valanginian (~ 140 Ma) obduction of the Neotethyan ophiolitic mélange above the sedimentary successions of the eastern Adriatic passive margin. This event was soon followed by the second contractional event (D4), which occurred in Hauterivian to Albian (~ 133–100 Ma) and was characterized by thrusting and imbrication of the Adriatic passive margin successions together with previously emplaced ophiolitic mélange. The Mesozoic structures were dextrally rotated in post-Oligocene times and brought from the initially Dinaridic SE striking and SW verging structures to the recent SW striking and NW verging structures. The following Ottnangian to middle Badenian (~ 18–14 Ma) extensional event (D5) is associated with the formation of SE striking and mostly NE dipping normal listric faults, and ENE striking dextral transfer faults accommodating top-NE extension in the Pannonian Basin. A short-lasting contraction (D6) was registered in the late Sarmatian (~ 12 Ma). The late Pannonian (~ 6 Ma) to present contractional event (D7) resulted in reactivation of ENE striking dextral faults, formation of SE striking dextral faults as well as the formation of E to ENE trending folds and reverse faults.

Documented stratigraphic evolution of the Ivanščica Mt. is in good accordance with the passive margin successions originating from the Adria plate, preserved today in the Alps, and the Pre-Karst unit of the Dinarides. Recognized deformational events and their timings indicate that Ivanščica Mt. was mainly affected by deformational phases related to the Mesozoic evolution of the Neotethys Ocean, as well as the Miocene opening and inversion of the Pannonian Basin. Therefore, the Mesozoic tectono-stratigraphic evolution of Ivanščica Mt. proves the paleogeographic affiliation of its non-ophiolitic Mesozoic structural-stratigraphic entities to the Pre-Karst unit of the Dinarides.

# PROŠIRENI SAŽETAK

Tijekom posljednjih desetljeća, geološka i geofizička istraživanja otkrila su složenost Alpsko-Karpatsko-Dinaridskog orogenog sustava. U velikim orogenim sustavima, strukture Zemljine kore i gornjeg plašta mogu se pratiti stotinama ili tisućama kilometara. Suprotno tomu, Alpsko-Karpatsko-Dinaridski orogeni sustav karakteriziraju prostorno ograničene zone subdukcije, odvojene i pocijepane ploče, ploče koje po pružanju mijenjaju polaritet subdukcije, subdukcija heterogene litosfere s oceanskom ili kontinentalnom korom te kolizija između kontinentalnih litosfera. Takva složenost rađa brojne kontroverze i mnogo hipoteza koje se mogu razriješiti samo prikupljanjem visokokvalitetnih geofizičkih slika dubokog podzemlja i integracijom s rezultatima kvalitetnih površinskih geoloških istraživanja.

## Ciljevi i hipoteze

Jednom takvom kontroverznom području pripada i istraživano područje koje uključuje planinu Ivanščicu sa svojoj širom okolicom. Ono predstavlja zonu promjene polariteta subdukcije između Dinarida, gdje Adrija predstavlja donju ploču, i Alpa, gdje Adrija predstavlja gornju ploču. To čini planinu Ivanščicu značajnim mjestom za provođenje strukturnih istraživanja s ciljem razumijevanja struktura Zemljine kore, deformacijskih obrazaca i tektonske povijesti regije. Stoga su glavni ciljevi ovog doktorskog istraživanja bili: (1) nadopuniti postojeća saznanja o starosti, litostratigrafskim značajkama i paleogeografskom porijeklu mezozojskih naslaga na području Ivanščice; (2) odrediti današnji prostorni raspored i geodinamske značajke glavnih tektonsko-stratigrafskih jedinica te kinematsku karakterizaciju njihovih graničnih rasjeda; (3) rekonstruirati tektonsko-termalnu evoluciju, kinematske pokrete i režime paleonaprezanja tijekom glavnih mezozojskih i kenozojskih deformacijskih događaja u geodinamskom razvoju istraživanog područja te (4) predložiti regionalnu korelaciju tektonsko-stratigrafskih jedinica i deformacijskih događaja s odgovarajućim jedinicama i događajima u okolnim područjima Alpa, Dinarida i Panonskog bazena. Kako bi se ostvarili postavljeni ciljevi, zadane su sljedeće hipoteze: (i) sedimentološke i biostratigrafske analize srednje trijaskih i jurskih sedimentnih sukcesija mogu pružiti informacije o njihovoj preciznoj starosti i paleogeografskom porijeklu, kao i o starosti sin-sedimentnih tektonskih događaja; (ii) jedinica vulkanogeno-sedimentnog kompleksa može se podijeliti u dvije formacije, turbidite formacije Oštrc i ofiolitni melanž kompleksa Repno, s određivanjem njihove prostorne distribucije i karaktera njihove geološke granice; (iii) izolirana tijela gornjotrijaskih karbonata predstavljaju navlačke, olistolite unutar ofiolitnog melanža ili erozijske ostatke podloge ofiolitnog melanža sačuvane u jezgrama antiklinala; (iv) osim rasjeda koji su prema OGK 1:100.000 listu Varaždin na planini Ivanščici isključivo kenozojske starosti, moguće je kartografski odvojiti rasjede čija je starost predkenozojska; (v) neki od rasjeda koji su nastali u prethodnom aktivnom režimu tektonskog naprezanja, naknadno su reaktivirani ili invertirani pod utjecajem mlađih tektonskih naprezanja; (vi) tijekom mezozoika i kenozoika, istraživano područje bilo je pod utjecajem tektonskih deformacijskih događaja vezanih uz Dinaride, Alpe i Panonski bazen čije je učinke i deformacijske strukture moguće odrediti na terenu; (vii) moguće je odrediti kinematske karakteristike navlake prvog reda između tektonske jedinice Južnih Alpa i Dinarida te je isti navlačni kontakt moguće kartirati i pratiti na terenu.

Potvrđivanjem ili opovrgavanjem iznesenih hipoteza dobiveni su i odgovori na zadane ciljeve doktorskog istraživanja koji su prezentirani u objavljenim znanstvenim radovima i sažeti u okviru diskusije ove disertacije.

**Metodološki pristup**

Provedena interdisciplinarna istraživanja uključivala su primjenu različitih metoda geološkog kartiranja te sedimentoloških, biostratigrafskih, petroloških, geokemijskih, strukturnih i termokronoloških metoda što je rezultiralo novim spoznajama vezanim uz mezozojsku litostratigrafsku evoluciju i tektonsku povijest istraživanog područja. Uvjeti na terenu zahtijevali su korištenje metoda geološkog kartiranja u svrhu prikupljanja maksimalne količine podataka tijekom samih terenskih istraživanja. Sedimentološke i biostratigrafske analize korištene su za određivanje taložnih okoliša i starosti mezozojskih sedimentnih i vulkanoklastičnih stijena. Petrološke i geokemijske metode korištene su pri analizi mezozojskih vulkanskih i vulkanoklastičnih stijena. Metodom određivanja vitrinitne refleksije analizirane su sedimentne stijene mezozojske starosti u svrhu određivanja maksimalnih temperatura pri kojima su iste bile izložene. *Fission track* analiza korištena je u svrhu otkrivanja povijesti hlađenja istraživanih stijena tijekom geološke prošlosti. Deskriptivna, kinematička i dinamička strukturna analiza sustavno je provedena na stijenama mezozojske i kenozojske starosti te u kombinaciji s rezultatima preostalih korištenih metoda, bila je osnova za razumijevanje mezozojske i kenozojske tektonsko-stratigrafske evolucije ove prijelazne zone između Alpa i Dinarida, u jugozapadnom dijelu Panonskog bazena.

**Rezultati**

U mezozojskoj sukcesiji pasivnog kontinentalnog ruba Adrije očuvanoj na Ivanšćici, prepoznate su te sedimentološki i biostratigrafski dokumentirane sin-riftne naslage dvaju ekstenzijskih događaja. Prvi ekstenzijski događaj (D1) karakteriziraju gornjo anizičke do gornjo ladiničke dubokomorske vulkano-sedimentne naslage, a povezan je s otvaranjem oceana Neotetis. Drugi ekstenzijski događaj (D2) uvjetovan je otvaranjem Alpskog Tetiskog oceana i karakteriziran je taloženjem donjo jurske dubokomorske sedimentne sukcesije. Najstariji kontrakcijski događaj (D3) vezan je uz berijas-valendijsku (~140 Ma) obdukciju neotetiskog ofiolitnog melanža preko sedimentnih sukcesija istočnog pasivnog ruba Adrije. Ovaj događaj je ubrzo praćen drugim kontrakcijskim događajem (D4) koji je rezultirao otrivsko-albskim (~133–100 Ma) navlačenjem i ljuskanjem sukcesija pasivnog ruba Adrije zajedno s ranije obduciranim ofiolitnim melanžem. Mezozojske deformacijske strukture su potom rotirane u post-oligocenskom vremenu iz prvotno tipično dinaridskih struktura s JI pružanjem i JZ vergencijom u recentne strukture s JZ pružanjem i SZ vergencijom. Sljedeći ekstenzijski događaj (D5) koji je trajao od otnanga do kraja srednjeg badena (~18–14 Ma) povezan je s formiranjem normalnih lističkih rasjeda s JI pružanjem i smjerom nagiba uglavnom prema SI te desnih rasjeda s pružanjem prema I-SI koji akomodiraju novonastalu ekstenziju u Panonskom bazenu sa smjerom prema SI. Kratkotrajna kontrakcija (D6) zabilježena je u kasnom sarmatu (~12 Ma) i rezultirao je reversnim rasjedanjem i inverzijom djela starije miocenskih lističkih rasjeda. Sadašnji kontrakcijski događaj (D7) koji započeo je u kasnom panonu (~6 Ma), a rezultirao je reaktivacijom desnih rasjeda s pružanjem prema I-SI, formiranjem novih desnih rasjeda s pružanjem prema JI te formiranjem bora i reversnih rasjeda s pružanjem prema I odnosno I-SI.

Mezozojska i kenozojska tektonsko-stratigrafska evolucija Ivanšćice ukazuje na tektonsku i paleogeografsku pripadnost njezinih ne ofiolitnih mezozojskih strukturno-stratigrafskih jedinica Predkrškoj jedinici Unutarnjih Dinarida. Repno kompleks predstavlja najsjeverozapadniju pojavu Zapadnovardarske ofiolitne jedinice. Do sada, ovo je jedino poznato mjesto gdje se ofiolitni melanž Zapadnovardarske ofiolitne jedinice nalazi u primarnom obdukcijskom navlačnom kontaktu sa sukcesijama Predkrške jedinice koje čine njegovu podinu. Ova spoznaja predstavlja značajan doprinos poznavanju strukturno-tektonske građe i dinamike Dinaridskog orogena.

**Zaključci**

Dokumentirana mezozojska litostratigrafska sukcesija Ivanščice korelativna je sa sukcesijama pasivnog kontinentalnog ruba Adrije, koje su danas očuvane u Alpama i Predkrškoj tektonsko-stratigrafskoj jedinici Dinarida. Prepoznati deformacijski događaji i njihovo vrijeme ukazuju na to da je Ivanščica uglavnom bila pod utjecajem deformacijskih događaja vezanih uz mezozojsku evoluciju Neotetiskog oceana kao i miocensko otvaranje i inverziju Panonskog bazena. Stoga, mezozojska tektonsko-stratigrafska evolucija Ivanščice dokazuje paleogeografsku pripadnost njezinog ne-ofiolitnog mezozojskog strukturno-stratigrafskog entiteta Predkrškoj jedinici Unutrašnjih Dinarida.

**KEYWORDS**

Adriatic passive continental margin
Northern Neotethys Ocean
Mesozoic
Cenozoic
Rifting
Ophiolite obduction
Continental collision
Geological mapping
Structural analysis
Biostratigraphy
Thermochronology
Mountain building
Structural inheritance
Tectonic inversion

**KLJUČNE RIJEČI**

Pasivni kontinentalni rub Adrije
Sjeverni Neotetis
Mezozoik
Kenozoik
Riftanje
Obdukcija ofiolita
Kontinentalna kolizija
Geološko kartiranje
Strukturna analiza
Biostratigrfija
Termokronologija
Orogeneza
Naslijeđene strukture
Tektonska inverzija

# TABLE OF CONTENTS

## LIST OF FIGURES

# 1. INTRODUCTION

## 1.1. Thesis motivation

This PhD thesis is a part of the Croatian Science Foundation Research project entitled "Revealing Middle Triassic Paleotethyan Geodynamics Recorded in the Volcano-Sedimentary Successions of NW Croatia" (Project no. IP-2019-04-3824). The Project was aimed to unveil the geodynamic, tectonic and paleogeographic evolution of the eastern Adriatic passive continental margin in the context of Middle Triassic opening of the Neotethys Ocean and closure of the Paleotethys Ocean. These objectives were intended to be achieved by detail study of Middle Triassic syn-tectonic volcano-sedimentary successions exposed on inselbergs of N Croatia including Desinić gora Mt., Kuna gora Mt., Strahinjčica Mt., Ravna gora Mt. and Ivanščica Mt. The Project was designed to perform an interdisciplinary study by integration of mineralogical, petrological, geochemical, paleontological, sedimentological, isotopic and structural investigations. As a part of the Project, this PhD study is focused on Ivanščica Mt., the largest inselberg in N Croatia located in the SW Pannonian Basin, in a transition area between the Alps and the Dinarides (**Fig. 1**). This transition area is characterized by rather complex overprinting structural relationships related to different deformation events recorded so far in neighbouring inselbergs (**e.g., Fodor et al., 1998, 2021; Tomljenović et al., 2008; van Gelder et al., 2015**), however, not yet studied in detail on Ivanščica Mt. Besides, as this inselberg exposes Permo-Mesozoic and Cenozoic lithostratigraphic units, some of which are recognized as syn-tectonic with respect to different deformation events in the tectonic evolution of the Dinarides, Alps and Pannonian Basin (**e.g., Babić et al., 2002; Goričan et al., 2005; Lužar-Oberiter et al., 2012; Brlek et al., 2023 with references therein**), it is considered as a "type area" for reconstruction of Mesozoic to Cenozoic tectono-stratigraphic evolution of this transition area. Such a place with polyphase deformation history represents a natural laboratory for studying the processes of reactivation and/or inversion of older structures and their role in strain localization during newly established tectonic stress field. This allowed the definition of the Ivanščica Mt. as a target area for the investigation of Mesozoic to Cenozoic stratigraphic and tectonic evolution of the Alps-Dinarides-Pannonian Basin transition zone and potential influence of two orogens in the architecture of N Croatia.

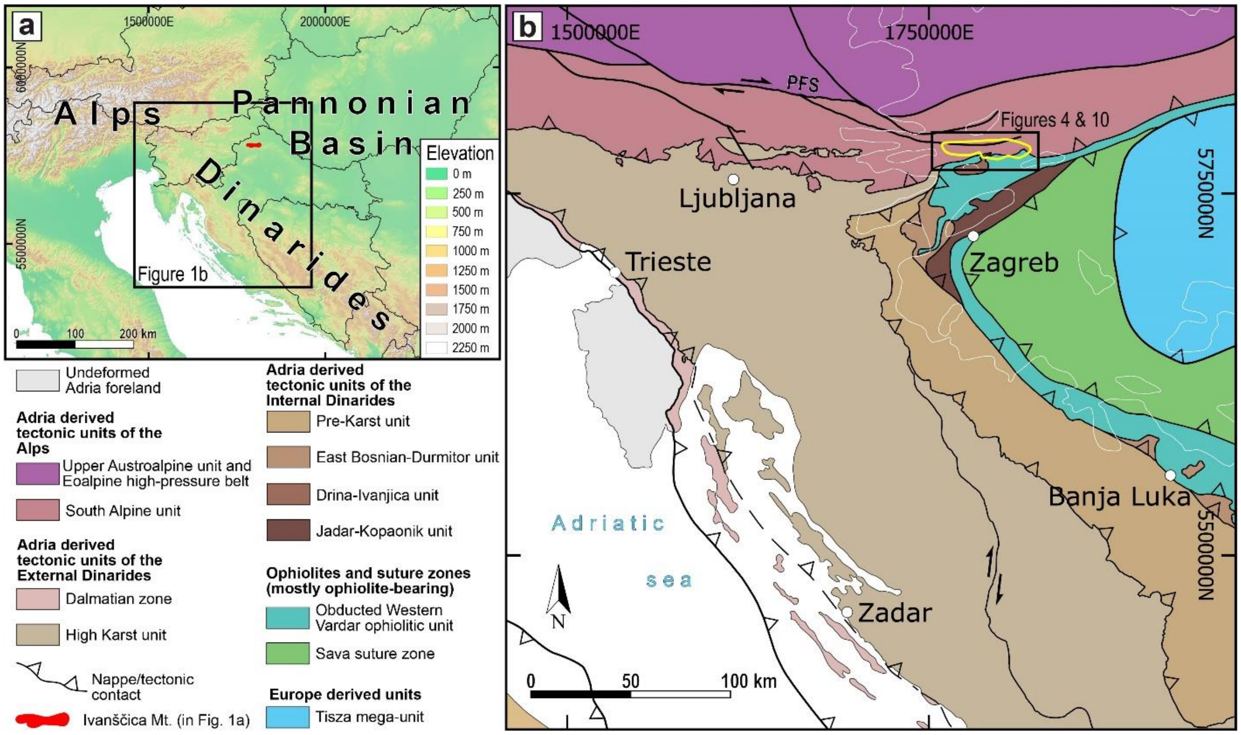


***Figure 1. a** Topographic map showing geographic location of Ivanščica Mt. (red polygon) positioned in the transition zone of the Alps and the Dinarides in the SW part of the Pannonian Basin. **b** Tectonic map after **Schmid et al. (2020)** showing constituent tectonic units of the Dinarides and the Alps. Ivanščica Mt. (marked with yellow line) occupies the position at the junction of the Western Vardar ophiolitic unit of the Dinarides and the South Alpine unit of the Alps in the SW part of the Pannonian Basin (white outlines). PFS – Periadriatic Fault System. Location of figure is shown in Fig. 1a*

## 1.2. An overview of lithostratigraphic characteristics of Ivanščica Mountain based on hitherto published data

### 1.2.1. Permo-Mesozoic sedimentary succession

The oldest deposits on Ivanščica Mt. consists of Permian brown-red conglomerates, sandstones and black shales, which are continuously overlain by Lower Triassic sediments (**Fig. 2; Šimunić et al., 1981; Šimunić & Šimunić, 1997**). These Permian to Lower Triassic deposits are exclusively documented on the northern slopes of Ivanščica Mt. (**Šimunić et al., 1982**). Lower Triassic deposits are represented by micaceous sandstones, siltstones, shale and marls, which occasionally alternate with ooid grainstones (**Šimunić et al., 1981; Šimunić & Šimunić, 1997**). These dominantly siliciclastic deposits grade into predominantly carbonate deposits represented by dark-grey, tabular, thin-bedded limestones (**Fig. 2**). Lower Triassic carbonate deposits gradually pass into indistinctively bedded Middle Triassic dark-grey dolostones and into continuously overlaying grey to light-grey massive dolostones (**Šimunić et al., 1981; Šimunić & Šimunić, 1997**).

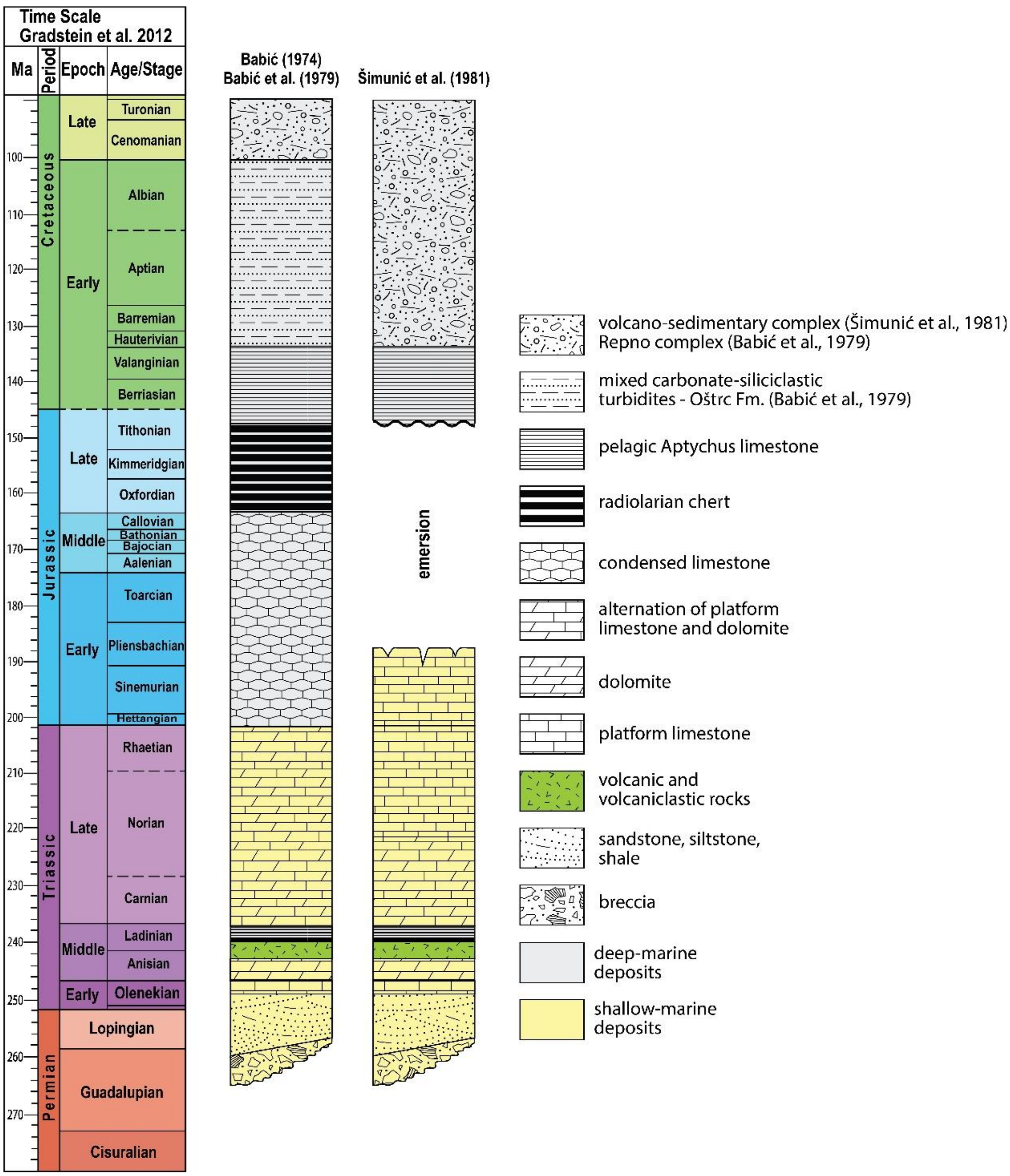


***Figure 2.*** *Stratigraphic columns showing detail lithostratigraphy of Permo-Mesozoic successions of the Ivanščica Mt. Two sections illustrate two different interpretations of the depositional environments during the Jurassic times*

Permian to lower Middle Triassic clastic to carbonate shallow-marine deposits are conformably overlain by an alternation of late Anisian to Late Ladinian hemipelagic and pelagic limestones, radiolarian cherts and acidic to intermediate volcanic and volcaniclastic rocks (**Fig. 2; Goričan et al., 2005**). That rapid change in the depositional environment indicate diversification of previously uniform depositional environments as a result of the Middle Triassic continental rifting and related extensional tectonics that finally resulted in break-up of Gondwana, separation of Adria and formation of its passive margins, and the opening of the Neotethys Ocean to the east (**Goričan et al., 2005; Slovenec et al., 2020).** Middle Triassic rift basins were filled by progradation of surrounding carbonate platforms already in the Late Ladinian when shallow-marine environments were re-established (**Fig. 2; Goričan et al., 2005**). Late Triassic was characterized by continuous deposition of shallow-marine dolostones and limestones (**Fig. 2; Šimunić et al. 1979; Šimunić et al. 1982; Šimunić and Šimunić 1997).** Due to a poor availability of outcrops on Ivanščica Mt., two different interpretations regarding the Jurassic depositional history arose (**Fig. 2**). One group of authors proposed the persistence of the continuous shallow-marine carbonate sedimentation until the middle Early Jurassic, followed by an emersion phase, which lasted until the late Tithonian and the deposition of pelagic Aptychus limestone (**Fig. 2**; **Šimunić et al., 1981; Šimunić, 1992**). Second group of authors proposed the continuous Jurassic pelagic sedimentation lasting since the Triassic/Jurassic transition. This pelagic succession starts with up to 1 m thick predominantly red Lower Jurassic condensed limestones, conformably overlaying Upper Triassic shallow-marine carbonates (**Fig. 2; Babić, 1974; 1976**). These are followed by up to few meters thick Middle Jurassic pink to grey condensed limestone with 'protoglobigerinas', Upper Jurassic radiolarian chert and late Tithonian to Valanginian pelagic Aptychus limestone (**Fig. 2; Babić and Zupanič, 1973; Babić, 1974**). Therefore, regarding two contrasting interpretations, the question of probably continuous or discontinuous sedimentation during the Jurassic times in preserved sedimentary succession on Ivanščica Mt. so far remained unsolved. Pelagic carbonate sedimentation of Aptychus limestone was interrupted in Hauterivian by terrigenous input and deposition of thin-bedded mixed carbonate–siliciclastic turbidites known as the Oštrc Formation (**Fig. 2; Zupanič et al., 1981; Lužar-Oberiter et al., 2012**). The youngest strata in the turbidites of the Oštrc Fm. are of Albian age (**Babić and Zupanič, 1978**).

### 1.2.2. Neogene to Quaternary sedimentary succession

The oldest Cenozoic transgressive deposits on Ivanščica Mt. are late Egerian brackish to marine siliciclastic deposits with coal seams (**Fig. 3; Šimunić et al., 1982; Avanić et al., 2021**). These sediments were deposited in the southernmost marginal segment of the Hrvatsko Zagorje Basin which occupied position on the SW margin of the Central Paratethys (**Avanić et al., 2021**). After the Early Miocene emersion, the deposition on Ivanščica Mt. started with the regional late Badenian transgression of coarse- to fine-grained clastic deposits, limestones and marls (**Fig. 3; Šimunić et al., 1981**). These are continuously overlain by Sarmatian laminated marls and only locally sandstones and conglomerates (**Fig. 3; Šimunić et al., 1981**).

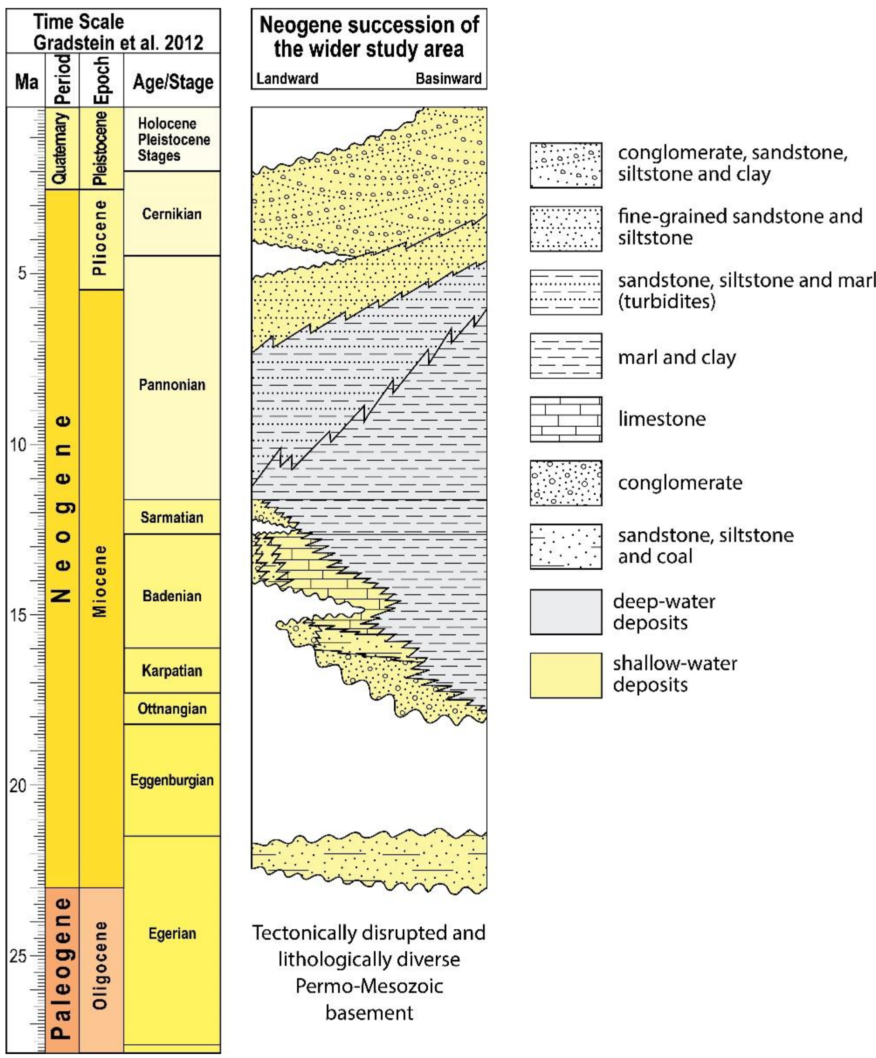


***Figure 3.*** *Stratigraphic column showing detail lithostratigraphy of the Neogene to Quaternary succession of the Ivanščica Mt. Compiled after* ***Avanić (2012)*** *and* ***Pavelić & Kovačić (2018)***

Lower Pannonian deposits are characterized by sedimentation of brackish marl and limestone which are overlain by Pannonian to Pliocene time-transgressive regressive sequence consisting of turbiditic, shelf-margin slope, deltaic and alluvial sediments (**Fig. 3; Šimunić et al., 1981, 1982; Pavelić and Kovačić, 2018**). Pliocene deposits are overlain by fine- to coarse-grained clastic Quaternary deposits of continental origin (**Fig. 3; Šimunić et al., 1981, 1982**). However, in the neighbouring areas located slightly N and S of Ivanščica Mt. different depositional histories were recorded during the Oligocene and Early Miocene times. Although the Cenozoic deposition on Ivanščica Mt. started in the late Egerian (**Fig. 3**), only few kilometres to the N of the mountain continuous Kiscellian to lowermost Badenian clastic shallow-marine succession was recorded (**Avanić et al., 2021**). Additionally, rare outcrops of upper Eocene Foraminiferal limestone that unconformably overlay Triassic carbonates were found on the Ravna gora and Boč mountains (**Šimunić et al., 1982; Ćovocić and Drobne, 2000**). Contrastingly, in the area S of Ivanščica Mt. the oldest Cenozoic deposits represent Ottnangian to Karpatian continental predominantly coarse clastic alluvial deposits which mark the onset of extensional subsidence and sedimentation of syn-rift deposits within North Croatian Basin (**Pavelić et al., 2001; Pavelić & Kovačić, 2018**). Ottnangian to Karpatian deposits are continuously overlain by lower to middle Badenian lacustrine to marine marls, limestones and fine clastic deposits with occasional occurrences of acidic to basic volcanic and volcaniclastic lithologies (**Šimunić et al., 1981; Pavelić & Kovačić, 2018**).

### 1.3. Structural characteristics of Ivanščica Mt.

Ivanščica Mt. is located within the Alps-Dinarides transition zone, which extends in W-E direction from the Dolomites in the NE Italy, across N Slovenia and N Croatia and continues further eastward into the Mid-Hungarian shear zone in Hungary (**e.g., Schmid et al., 2020**).

The first geological research on the Ivanščica Mt. has been done in the middle of the 19th century when the first geological map of this part of the Austro-Hungarian Monarchy has been published (**Hauer, 1868**). At the beginning of the 20th century, **Gorjanović-Kramberger** (**1904, 1907**) released a set of geological maps covering this and surrounding area, supplemented by a geotectonic study where the author proposed that Ivanščica Mt. makes a part of the eastern Alpine branches. **Winkler-Hermaden** (**1957**) proposed that the area of north-western Croatia is built up by a series of anticlines and synclines formed in the late Pliocene (known as the Sava folds ***sensu***

**Winkler, 1923**). **Petković** (**1961**) was the first to state that the border between the Alps, Dinarides and the Pannonian Basin is located in the area of northwestern Croatia. The structural-geological setting of the Ivanščica Mt. was described by **Šimunić et al.** (**1976, 1979, 1981**), **Šimunić & Hećimović** (**1979**) and **Šimunić & Šimunić** (**1987**). Mentioned authors consider the mountains of Hrvatsko zagorje to represent the eastern extension of the Sava folds (***sensu*** **Placer, 1999a**). They also highlighted the allochthonous nature of many parts of the Ivanščica Mt. and interpreted the northern vergence of its reverse faults and thrusts. So far, the most detailed geological investigations on Ivanščica Mt. were carried out in 1970s during geological mapping campaign for releasing the Basic Geological Map of the Yugoslavia in 1:100.000 scale, sheets Varaždin (**Šimunić et al., 1981, 1982**) and Rogatec (**Aničić & Juriša, 1984, 1985**). These authors consider all faults presented on these map sheets (**Fig. 4**) as Cenozoic in age, proposing that presented sets of E-W striking folds and faults have been formed during the Miocene. Šimunić et al. (**1979, 1981**) interpreted Ivanščica Mt. as a N verging nappe, which brought Palaeozoic and Mesozoic formations over Oligocene and lowermost Miocene sediments during the Early Miocene (i.e., during the Eggenburgian; **Fig. 4**). Numerous occurrences of decametre to hectometre isolated rock bodies of Upper Triassic to Lower Jurassic carbonates located in the southern part of central Ivanščica (**Fig. 4**) were interpreted as erosional remains of a structurally higher nappe (**Šimunić et al., 1979, 1982**). Alternatively, **Babić & Zupanič** (**1978**) proposed that these carbonates represent olistoliths embedded in the ophiolitic mélange of the Repno complex.

More recent studies consider Ivanščica and other mountains of Hrvatsko zagorje as a part of the Southern Alps tectonic unit (**Placer, 1999b**). Based on regional scale correlation of Alpine and Dinaridic tectonic units, **van Gelder et al.** (**2015**) and **Schmid et al.** (**2020**) consider that Ivanščica Mt. partly comprises regional S verging nappe derived from Southern Alps and thrusted over tectonic units of the Internal Dinarides (**Fig. 1**). However, as modern and more detailed structural research on Mesozoic and Cenozoic units, outcropping on this mountain, have not been performed yet, their tectonic position and paleogeographic origin could be still considered as tentative and worth to study.

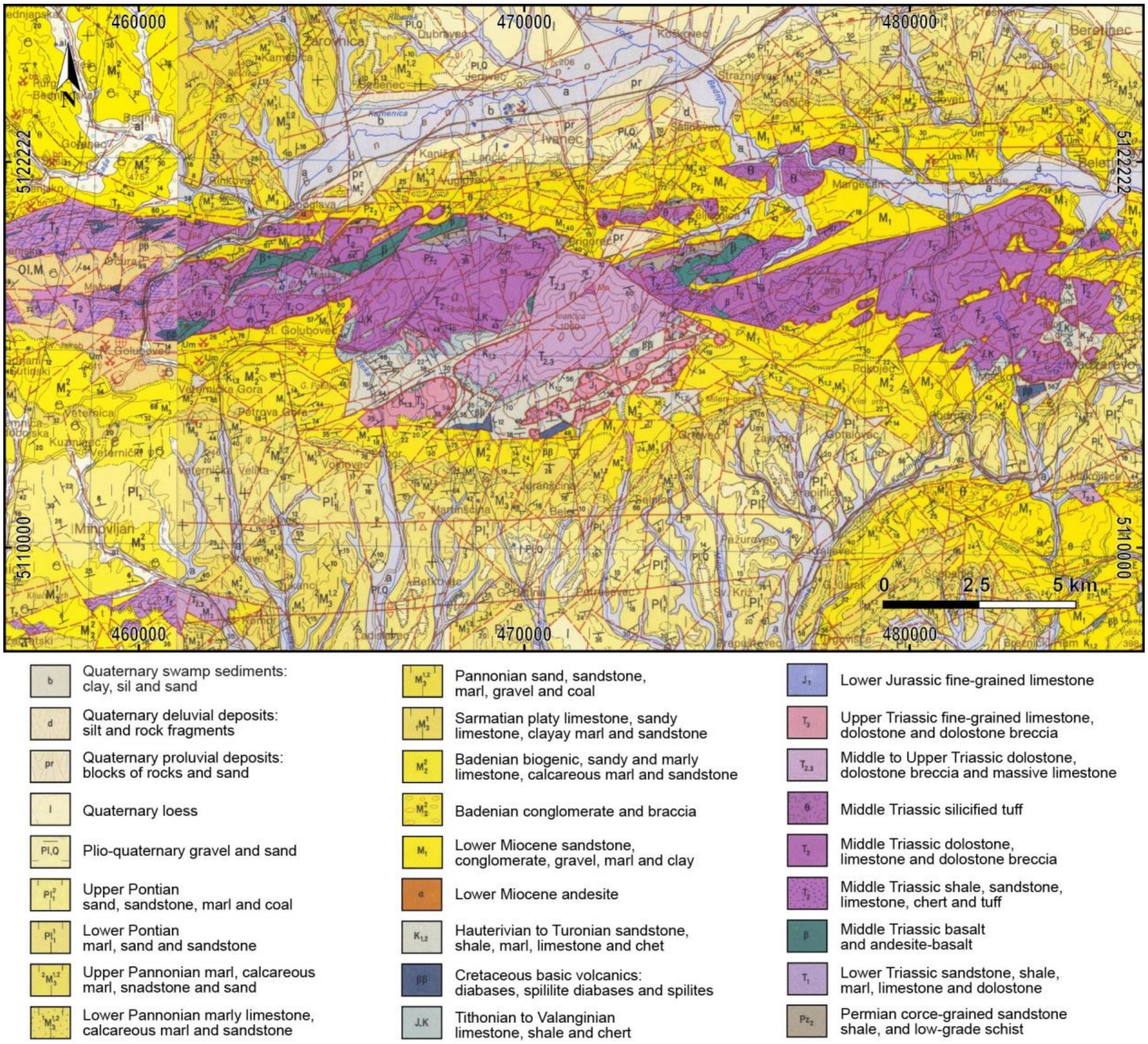


***Figure 4.*** *Fragment of the Basic Geological Map of Yugoslavia, in 1:100.000 scale, sheet Rogatec (**Aničić & Juriša, 1984**) and sheet Varaždin (**Šimunić et al., 1982**) showing the Ivanščica Mt. and the neighbouring area*

### 1.4. Objectives and hypotheses

The aim of this study can be summed up in terms of the following main objectives:

(1) to improve the existing knowledge on the age, lithostratigraphic features and paleogeographic provenance of the Mesozoic deposits of Ivanščica Mt.,

(2) to determine the present-day spatial arrangement and geodynamic features of the main tectonostratigraphic units and kinematic characterization of their bounding faults,

(3) to reconstruct tectono-thermal evolution, kinematics and paleostress regimes during the main Mesozoic and Cenozoic deformation events in the geodynamic development of the researched area,

(4) to propose regional correlation of tectonostratigraphic units and deformational events with the corresponding units and events in the surrounding area of the Alps, Dinarides and Pannonian Basin.

These objectives were based on the following hypotheses:

(i) sedimentological and biostratigraphic analyses of Middle Triassic and Jurassic sedimentary successions can provide information on their precise age and paleogeographic provenance as well as the age of syn-sedimentary tectonic events,

(ii) the unit of the volcanogenic-sedimentary complex can be separated into two formations, turbidites of the Oštrc Fm. and an ophiolitic mélange of the Repno complex, with the determination of their spatial distribution and the character of their geological boundary,

(iii) isolated bodies of Upper Triassic carbonates represent either tectonic klippes, olistoliths within ophiolitic mélange or erosional remnants of the ophiolitic mélange basement preserved in the cores of the anticlines,

(iv) apart from the faults which, according to the OGK 1:100,000 sheet Varaždin at the Ivanščica Mt. are exclusively of Cenozoic age, it is possible to cartographically separate faults whose age is pre-Cenozoic,

(v) some of the faults that were created in the former active regime of tectonic stress, were subsequently reactivated or inverted under the influence of younger tectonic stress,

(vi) during Mesozoic and Cenozoic, study area was affected by Dinarides, Alps and Pannonian Basin related tectonic deformational events whose effects and deformational structures is possible to determine in the field,

(vii) kinematic characteristics of the first order thrust between the nappe of the South Alpine unit and the Dinarides can be determined and the thrust contact can be mapped and traced on the field.

### 1.5. Methodological approach

The geological maps of the study area sheet Rogatec (**Aničić & Juriša, 1984**) and sheet Varaždin (**Šimunić et al., 1982**) provide valuable information about the geology but lack a modern tectonic and stratigraphic understanding. For that reason, interdisciplinary approach involving methods of various geological sub-disciplines were implemented to decipher the addressed questions.

Sedimentological and biostratigraphic methods were used in order to unveil the complete Mesozoic and Cenozoic sedimentary successions, crucial for distinguishing tectonic omissions from stratigraphic hiatuses, as well as for identification of tectonic deformational events whose effects are registered in the sedimentological record. Sedimentological and biostratigraphic methods were used in the context of the three presented scientific papers. A detailed description of used sedimentological and biostratigraphic methods, as well as the obtained results, are described in detail under the chapters 2, 3, and 4.

Petrological and geochemical analytical methods were used for petrological and geochemical characterisation of the Mesozoic volcanic and volcaniclastic rocks. A detailed description of used analytical methods and the obtained results can be found in the chapter 4.

Vitrinite reflection and fission track analyses were used for the reconstruction of the tectono-thermal evolution of the study area. Vitrinite reflection is used with intention to determine the maximum temperatures that individual rocks have reached. This was also essential in the selection of mineral suitable for fission track dating. Considering the results of the vitrinite reflection, only Lower Triassic clastic deposits would barely reach the temperature required for reset of the zircon grains. Therefore, apatite grains that require a much lower temperature for their reset were chosen for the fission track dating in order to reconstruct style and timing of cooling of the Mesozoic successions of Ivanščica Mt.

At the locations considered as essential for better understanding of deformational history of study area, detail geological mapping in scales 1:25 000 and locally 1:5 000 was conducted. Special attention was given to the collection of field structural and kinematic data, later used in descriptive, kinematic and dynamic structural analysis. Reflection seismic data and well data were used for investigations of deformational structures in the Neogene sedimentary cover. These results, as well as the results of vitrinite reflectance and fission track analysis, are described together with a detailed description of the methodology in chapter 5.

### 1.6. Organisation of the thesis

The thesis is organized in a cumulative manner and consists of seven chapters, four of which represent original scientific papers that were published in scientific journals. The scientific papers are arranged in chronological order in such a way that their results explain the tectono-stratigraphic development of the investigated area through geological history, starting from the Middle Triassic to the Present.

Chapter 1 (introduction) outlines the thesis motivation and gives a review on the research conducted hitherto regarding the lithostratigraphic and structural characteristics of Ivanščica Mt. and its close surroundings. In the same chapter, objectives and hypotheses of the thesis are specified as well as the methodological approach that was chosen for implementation of set objectives.

Chapter 2 represents the first published paper entitled "*Biostratigraphy and facies description of Middle Triassic rift-related volcano-sedimentary successions at the junction of the Southern Alps and the Dinarides (NW Croatia)*". This chapter addresses the lithological descriptions and interpretation of depositional mechanism for Middle Triassic rift-related volcano-sedimentary successions as well as their biostratigraphic constraints.

Chapter 3 represents the second published paper, under the title "*Evolution of eastern passive margin of Adria recorded in shallow- to deep-water successions of the transition zone between the Alps and the Dinarides (Ivanščica Mt., NW Croatia)*". This chapter describes facies description and biostratigraphic data of Upper Triassic to Lower Cretaceous succession of Ivanščica Mt. and thus presents, for the first time, the complete Jurassic pelagic succession preserved in the Croatian part of the eastern Adriatic passive margin. Described succession testify for the so far unrecognized Early Jurassic extensional event.

Chapter 4 represents the third paper, published under the title "*The early history of the Neotethys archived in the ophiolitic mélange of northwestern Croatia*". This chapter investigates various blocks in the Repno complex (ophiolitic mélange) exposed on the southern slopes of the Ivanščica Mt. Study presents new petrological and geochemical data for basalt blocks and biostratigraphic data for the associated radiolarian cherts, providing valuable information about the geological setting, petrogenesis and geodynamic evolution of the early Neotethyan history.

Chapter 5 represent the fourth published paper entitled "*Unravelling the Tectonic Evolution of the Dinarides – Alps – Pannonian Basin Transition Zone: Insights from Structural Analysis and Low-Temperature Thermochronology from Ivanščica Mt., NW Croatia*". This chapter present new structural, field kinematic and thermochronological data obtained from Ivanščica Mt., that enable reconstruction of seven Mesozoic to Cenozoic deformational events, their kinematics and age. Based on determined tectono-sedimentary evolution of Ivanščica Mt., new tectono-paleogeographic position is proposed.

Chapter 6 (discussion) discusses the results regarding the set hypothesis, provides a synthesis of published papers through the chronologically described tectono-stratigraphic evolution of the study area and gives a new interpretation of the tectonic position of Ivanščica Mt.

Chapter 7 (conclusion) summarizes the main results described in the previous chapters.

## 2. BIOSTRATIGRAPHY AND FACIES DESCRIPTION OF MIDDLE TRIASSIC RIFT-RELATED VOLCANO-SEDIMENTARY SUCCESSIONS AT THE JUNCTION OF THE SOUTHERN ALPS AND THE DINARIDES (NW CROATIA)

By

Duje Kukoč, Duje Smirčić, Tonći Grgasović, Marija Horvat, Mirko Belak, Dražen Japundžić, Tea Kolar-Jurkovšek, Branimir Šegvić, Luka Badurina, **Matija Vukovski** & Damir Slovenec

*Published in International Journal of Earth Sciences*

*DOI: https://doi.org/10.1007/s00531-023-02301-w*

International Journal of Earth Sciences
https://doi.org/10.1007/s00531-023-02301-w

ORIGINAL PAPER

# Biostratigraphy and facies description of Middle Triassic rift-related volcano-sedimentary successions at the junction of the Southern Alps and the Dinarides (NW Croatia)

Duje Kukoč[1] · Duje Smirčić[2] · Tonći Grgasović[1] · Marija Horvat[1] · Mirko Belak[1] · Dražen Japundžić[3] · Tea Kolar-Jurkovšek[4] · Branimir Šegvić[5] · Luka Badurina[5] · Matija Vukovski[1] · Damir Slovenec[1]

Received: 26 July 2022 / Accepted: 11 February 2023


## Abstract

The Middle Triassic volcano-sedimentary successions deposited on the passive continental margin during a period of intense extensional tectonics related to the opening of the Neotethys Ocean were investigated in NW Croatia. A new palaeogeographic term, the Northwestern Croatian Triassic Rift Basin (NCTRB), is introduced for these successions. Pelagic sediments were deposited on top of older shallow-marine carbonates from the early Illyrian to possibly late Ladinian. Pelagic limestones containing Illyrian ammonites and redeposited benthic foraminifers of the same age indicate the existence of a contemporaneous shallow-marine carbonate environment that supplied material to the deeper parts of the basin. Stratigraphically stacked volcanic and volcanogenic rocks are intercalated with pelagic sedimentary rocks. Submarine basaltic rocks, geochemically characterized as trachy-basalts, are related to deep-rooted faults. Trachy-basaltic hyaloclastites, found intercalated within pelagic limestones, were formed by the quenching of magma that came into contact with cold sea water and subsequent resedimentation of the newly formed basaltic fragments. The majority of volcanogenic deposits belong to the Pietra Verde deposits found higher in the sections. The material for these deposits was produced by explosive volcanic eruptions and deposited by gravitational mechanisms, including pyroclastic density currents. Radiolarians from intercalated radiolarian cherts indicate late Illyrian to early Fassanian age for volcanic activity, as well as episodic eruptions and deposition of pyroclastic material. The uppermost part of the NTCRB successions is characterized by secondary volcaniclastic deposits generated by the rapid reworking of unconsolidated pyroclastic detritus and is deposited as medium- to fine-grained turbidites, marking the gradual filling of the basin. Based on regional correlations, late Ladinian is the most likely age for these deposits, indicating a significant stratigraphic gap in the NTCRB successions.

**Keywords** Anisian · Ladinian · Volcanogenic deposits · Biostratigraphy · Northwestern Croatian Triassic Rift Basin

## Introduction

Middle Triassic volcano-sedimentary successions are common in the Southern Alps (e.g., Brack and Reiber 1986, 1993; Mundil et al. 1996; Gianolla et al. 1998; Brack et al. 2005; Stockar et al. 2012; Storck et al. 2018, 2020), Dinarides (e.g., Aubouin et al. 1970; Šćavinčar et al. 1984; Pamić 1984; Dimitrijavić 1997; Trubelja et al. 2004; Gawlick et al. 2012; Smirčić et al. 2016, 2018) and Transdanubian Range (e.g., Harangi et al. 1996; Pálfy et al. 2003; Budai and Vörös 2006; Karádi et al. 2022). These deposits mark the period of intense volcanic activity related to the opening of the Neotethys Ocean (sensu Schmid et al. 2008, 2020). While evidence of magmatic activity in this period has been extensively reported, the geodynamic framework remains a matter

✉ Damir Slovenec
damir.slovenec@hgi-cgs.hr

1 Department of Geology, Croatian Geological Survey, Sachsova 2, HR-10000 Zagreb, Croatia

2 Faculty of Mining, Geology and Petroleum Engineering, University of Zagreb, Pierottijeva 6, HR-10000 Zagreb, Croatia

3 Croatian Natural History Museum, Demetrova 1, HR-10000 Zagreb, Croatia

4 Geological Survey of Slovenia, Dimičeva Ulica 14, 1000 Ljubljana, Slovenia

5 Department of Geosciences, Texas Tech University, 1200 Memorial Circle, Lubbock, TX 79409, USA

Published online: 17 March 2023

of debate (for more detailed discussion, see Slovenec et al. 2020; Slovenec and Šegvić 2021 and references therein, and Slovenec et al. 2023). Extensional tectonics related to rifting disintegrated the previously stable shallow-marine depositional environment and created blocks of different subsidence, producing horst-and-graben topography along the continental margin. In large areas, hemipelagic and pelagic sediments were deposited on top of drowned carbonate platforms (e.g., Aubouin et al. 1970; Dimitrjević and Dimitrijević 1991; Brack and Reiber 1993; De Zanche et al. 1993; Haas and Budai 1995; Gianolla et al. 1998; Goričan et al. 2005; Budai and Vörös 2006; Brack et al. 2007; Gawlick et al. 2012; Celarc et al. 2013; Smirčić et al. 2018, 2020; Karádi et al. 2022). One of the prominent features of these pelagic successions is the occurrence of volcaniclastic deposits named Pietra Verde, which are often characteristically green in colour (e.g., Castellarin et al. 1988; Obenholzner 1991). Produced by explosive silicic eruptions, these deposits vary in grain size and thickness. Individual volcanic ash layers can be correlated over wide areas and are intercalated in both deep basinal successions and coeval shallow-marine carbonates (Brack and Reiber 1993; Mundil et al. 2003). This indicates that most volcanic products were primary airborne deposits (Mundil et al. 2003). The presence of thicker, often graded volcaniclastic beds in deep basin portions indicates that reworking of the material also occurred (Brack and Muttoni 2000; Smirčić et al. 2020). A large amount of data, including high-precision U–Pb zircon ages, obtained from these deposits show that volcaniclastic sediments were deposited over a span of approximately five million years across the Anisian-Ladinian boundary, with three major activity phases recognized (Mundil et al. 1996, 2010; Pálfy et al. 2003; Brack et al. 2005, 2007; Storck et al. 2018; Wotzlaw et al. 2018; Dunkl et al. 2019; Karádi et al. 2022).

In the mountains of northwestern Croatia, Middle Triassic volcano-sedimentary successions were deposited following carbonate platform break-up (Šimunić and Šimunić 1979; Goričan et al. 2005; Slovenec et al. 2020, 2023; Slovenec and Šegvić 2021). In this tectonically complex area, where Dinaridic and Alpine deformation structures overlap (Tomljenović et al. 2008; van Gelder et al. 2015), volcano-sedimentary successions of the rifted continental margin are tectonically juxtaposed with the ophiolitic mélange containing blocks of oceanic crust of the same age (Halamić et al. 1998; Goričan et al. 2005; Slovenec et al. 2011). These volcano-sedimentary successions were likely deposited on the portion of the margin proximal to the newly formed oceanic spreading centre of the Neotethys, located further to the east (Schmid et al. 2008, 2020). However, small amounts of data exist for the Middle Triassic rift-related successions of NW Croatia (Golub et al. 1969; Golub and Brajdić 1970; Šimunić and Šimunić 1979, 1997; Marci et al. 1984; Goričan et al. 2005), with only several recent studies offering more comprehensive analyses and interpretations of origin of volcanic and volcaniclastic rocks (Slovenec et al. 2020, 2023; Slovenec and Šegvić 2021). In this study, we present lithological descriptions and interpretations of depositional mechanisms for rift-related volcano-sedimentary successions in NW Croatia, as well as biostratigraphic constraints. New data enables a regional correlation of volcano-sedimentary deposits of NW Croatia, providing a better understanding of the early evolution of the western margin of the Neotethys.

## Geological setting

The studied sections are located on Mts. Ivanščica, Strahinjščica and Kuna gora in the Hrvatsko zagorje region of NW Croatia (Fig. 1). This is a tectonically complex area at the junction of the Dinarides, Southern Alps and Tisza Unit (e.g., Haas et al. 2000; Tomljenović et al. 2008; Schmid et al. 2008, 2020; Fig. 1a). The mountains of NW Croatia can be considered the southernmost part of the Southern Alps (Schmid et al. 2008, 2020) or the southwestern portion of the Zagorje Mid-Transdanubian Zone (Pamić and Tomljenović 1998). This tectonic block is bound to the south by the Zagreb-Zemplen Line and to the north by the Periadriatic-Balaton Line (Haas et al. 2000; Tomljenović et al. 2008). Because of the thick Neogene and Quaternary sedimentary deposits, pre-Tertiary formations are exposed only in uplifted basement units, often referred to as “inselbergs”. Units of oceanic and continental affinity are readily hosted in most of the inselbergs of NW Croatia, where they were brought into contact as a result of the long-lasting and complicated Mesozoic-Cenozoic tectonic evolution, which ultimately gave rise to a complex nappe stack (Haas et al. 2000; Tomljenović and Csontos 2001; Babić et al. 2002; Pamić et al. 2002; Csontos and Vörös 2004; Tomljenović et al. 2008). In this area, older Dinaridic structures are overprinted by younger retro-wedge Alpine thrusting (van Gelder et al. 2015). A characteristic deflection of structures that are almost perpendicular to NW–SE striking Dinaridic structures is a result of the clockwise rotation and eastwards escape of this tectonic block in the Late Paleogene and Neogene (Tomljenović et al. 2008).

Sedimentary successions of the continental margin preserved in the Southern Alps and the Dinarides were a part of the larger passive margin of Adria formed as a result of Middle Triassic rifting (e.g., Gawlick et al. 2008; Schmid et al. 2008, 2020; Ferriere et al. 2016; van Hinsbergen et al. 2020). During the Middle and Late Triassic, this part of the margin faced the inception of the Meliata-Maliac back-arc basin (Stampfli and Borel 2002; Csontos and Vörös 2004; Goričan et al. 2005). Today, most authors consider this

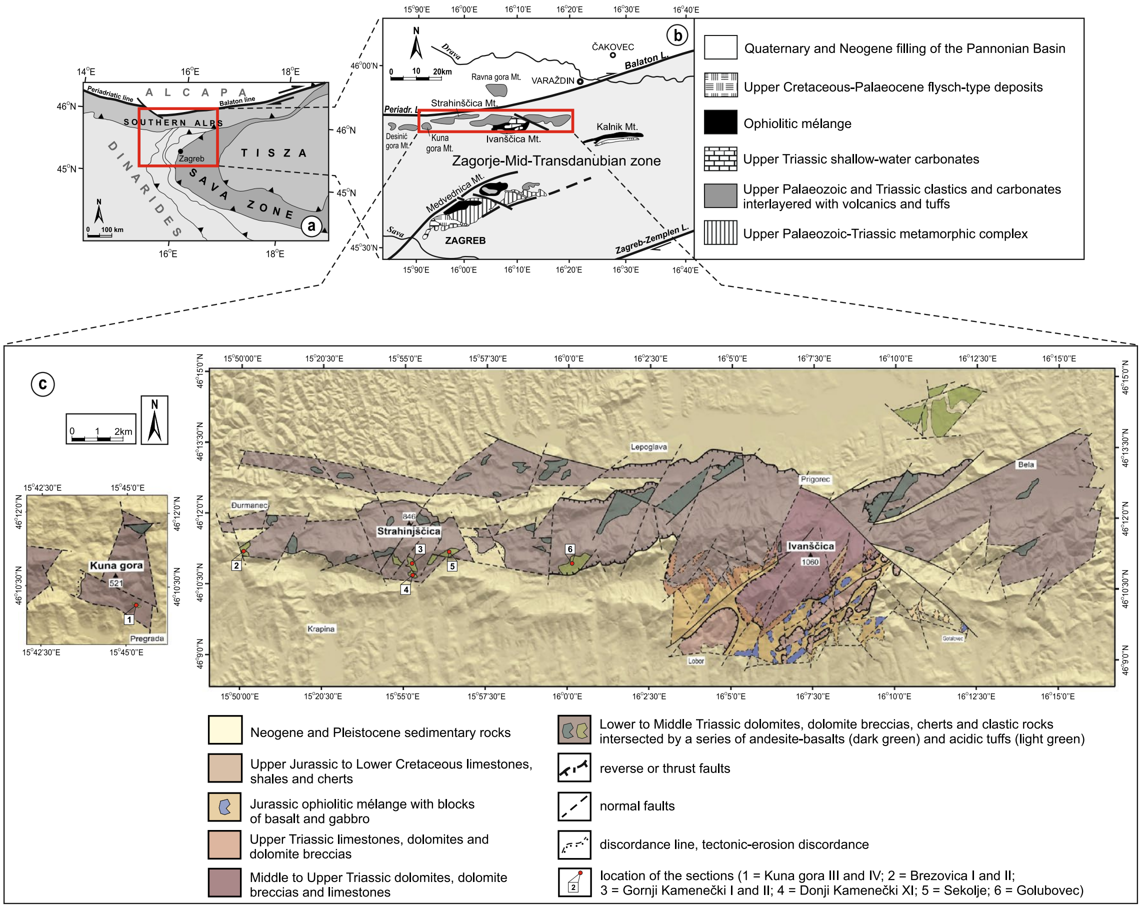


**Fig. 1** **a** Geotectonic sketch map of the major tectonic units (simplified from Schmid et al. 2008). **b** Geological sketch map of the Croatian part of the Zagorje-Mid-Trandanubian Zone (slightly modified from Pamić and Tomljenović 1998 and Haas et al. 2000). **c** Simplified geological sketch map of the Kuna gora, Strahinjščica and Ivanščica Mts. (modified from Aničić and Juriša 1984; Šimunić et al. 1983)

back-arc system to be a part of the Neotethys Ocean (sensu Schmid et al. 2008, 2020).

The oldest Mesozoic deposits in the area of NW Croatia are Lower Triassic sandstones, siltstones and shales, with oolitic limestones and marls also occurring (Šimunić and Šimunić 1979, 1997; Šimunić et al. 1981, 1983; Aničić and Juriša 1984, 1985). The Middle and Upper Triassic massive and bedded dolomites make up a large part of the NW Croatian mountains (Šimunić and Šimunić 1979, 1997; Šimunić et al. 1981, 1983; Aničić and Juriša 1985; Grgasović 1997). Limestones, limestone breccias and cherts occur only locally and are intercalated with volcanic and pyroclastic rocks (Golub et al. 1969; Šimunić et al. 1981, 1983; Šimunić and Šimunić 1979, 1997; Aničić and Juriša 1984, 1985; Goričan et al. 2005; Slovenec et al. 2020, 2023). Pyroclastic and effusive rocks range in composition from basaltic-andesitic to rhyolitic and are generally thoroughly altered (Golub et al. 1969; Golub and Brajdić 1970; Marci et al. 1984; Slovenec et al. 2020, 2023; Slovenec and Šegvić 2021). Younger Mesozoic deposits can be found only on Mt. Ivanščica, where Upper Triassic shallow-marine carbonates are overlayed by Jurassic to Cretaceous pelagic succession (Babić 1976; Šimunić et al. 1981; Lužar-Oberiter et al. 2009, 2012). Cretaceous pelagic sediments are found in tectonic contact with the ophiolitic mélange (Babić 1976; Babić and Zupanič 1978; Babić et al. 2002).

Sedimentary successions related to Middle Triassic rifting have been studied only on Mt. Ivanščica. The platform-to-basin succession consisting of carbonate breccia, siliceous limestones, cherts and pyroclastic deposits overlies dolomites and limestones (Goričan et al. 2005). Carbonate breccia and siliceous limestones were dated with calcareous algae and conodonts as Pelsonian to early Illyrian, while overlying cherts were dated as early Ladinian with radiolarians (Goričan et al. 2005). However, the described radiolarian assemblages are now considered late Anisian after the ratification of the GSSP for the base of the Ladinian stage by the IUGS (Brack et al. 2005). Upper Anisian radiolarian cherts and intercalated pyroclastics were also described by Slovenec et al. (2020). In another location on Mt. Ivanščica, carbonate breccias with rich reefal fossil assemblages of Illyrian age, limestones and tuffs overlie metabasalts (Goričan et al. 2005). These successions were likely deposited in a short-lived basin, formed on a continental margin in the vicinity of the active, ensialic and mature volcanic arc developed due to the subduction of an older oceanic lithosphere (Goričan et al. 2005; Slovenec et al. 2020; Slovenec and Šegvić 2021). This basin was quickly filled in the Ladinian by the prograding carbonate platform (Goričan et al. 2005).

## Description of lithologies

Eight sections containing volcanic and pyroclastic rocks in association with pelagic sediments were investigated in the mountains of NW Croatia (Figs. 1, 2). The exposures of the sections are limited due to dense forestation. The contacts with underlying and overlying lithologies are not accessible, except in the Brezovica I section, where clear contact with underlying dolomites is documented. In Golubovec on the western part of Mt. Ivanščica (Fig. 1), a 19 m-thick succession of red cherts and felsic pyroclastic deposits was also investigated but is not illustrated in this paper due to a lack of age data. All analysed radiolarian samples from this locality were barren. Representative rock samples were analysed using a polarization microscope at the Croatian Geological Survey and Faculty of Mining, Geology and Petroleum Engineering (Zagreb, Croatia). Bulk rock geochemistry data ($SiO_2$ and $K_2O$) for volcanic and pyroclastic rocks were obtained by XRF at Texas Tech University (Lubbock, TX, United States) and are illustrated in Fig. 4. XRF data were collected on fused glass discs using Thermo Scientific ARL Perform'X sequential and U.S. Geological Survey standards (for more details, see Slovenec et al. 2023).

### Carbonate deposits

Both dolostones and limestones were found in three of the studied sections (Fig. 2). The dolomite facies is represented

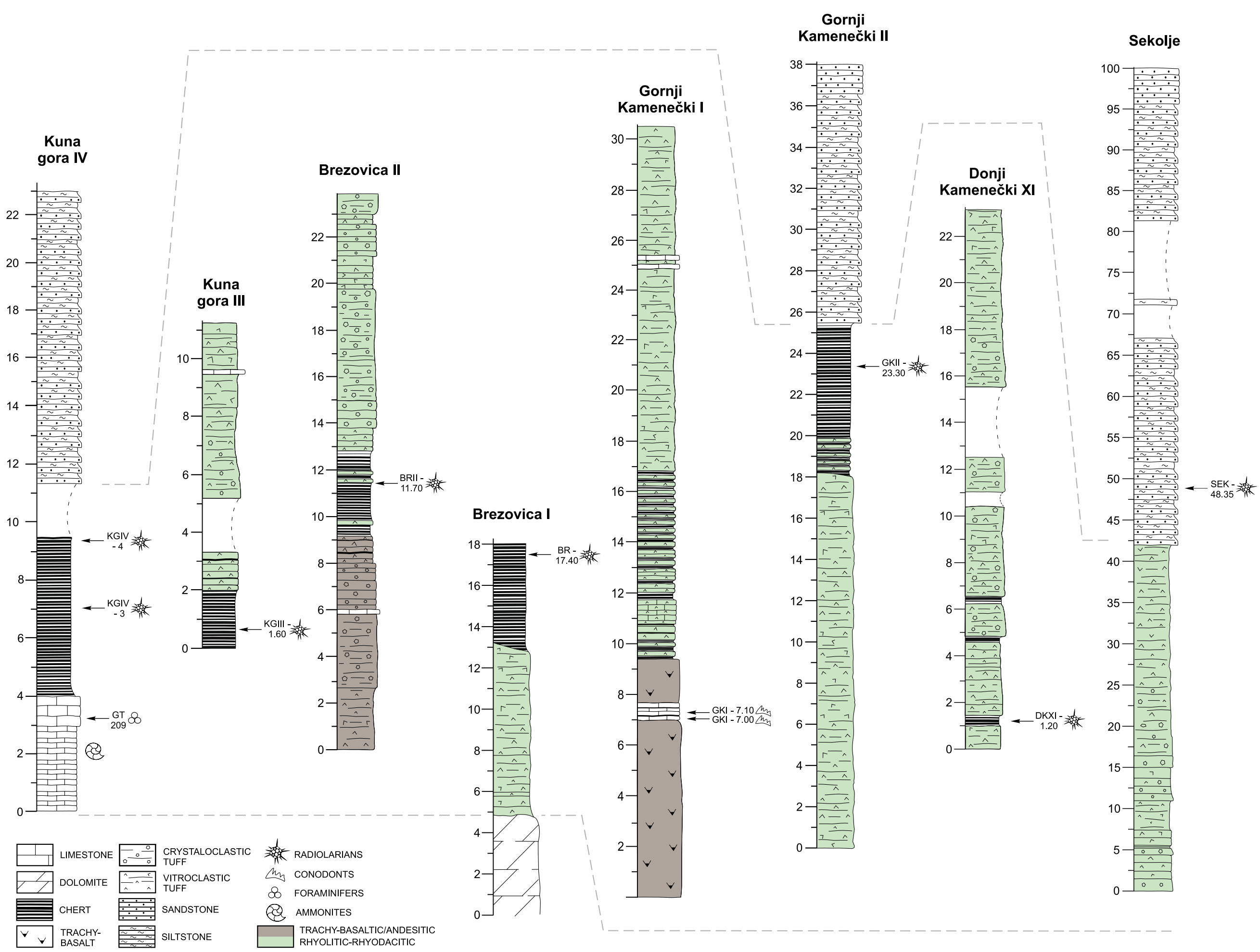


**Fig. 2** Lithological columns of investigated sections (for positions of the sections, see Fig. 1)

by xenotopic anhedral crystalline dolostones. The crystal size varies from micro- to macrocrystalline. Some faint lamination resembling stromatolite lamina can also be observed. The primary structure is mostly obliterated by late diagenetic processes (Fig. 3a). This lithofacies is found only at the base of section Brezovica I.

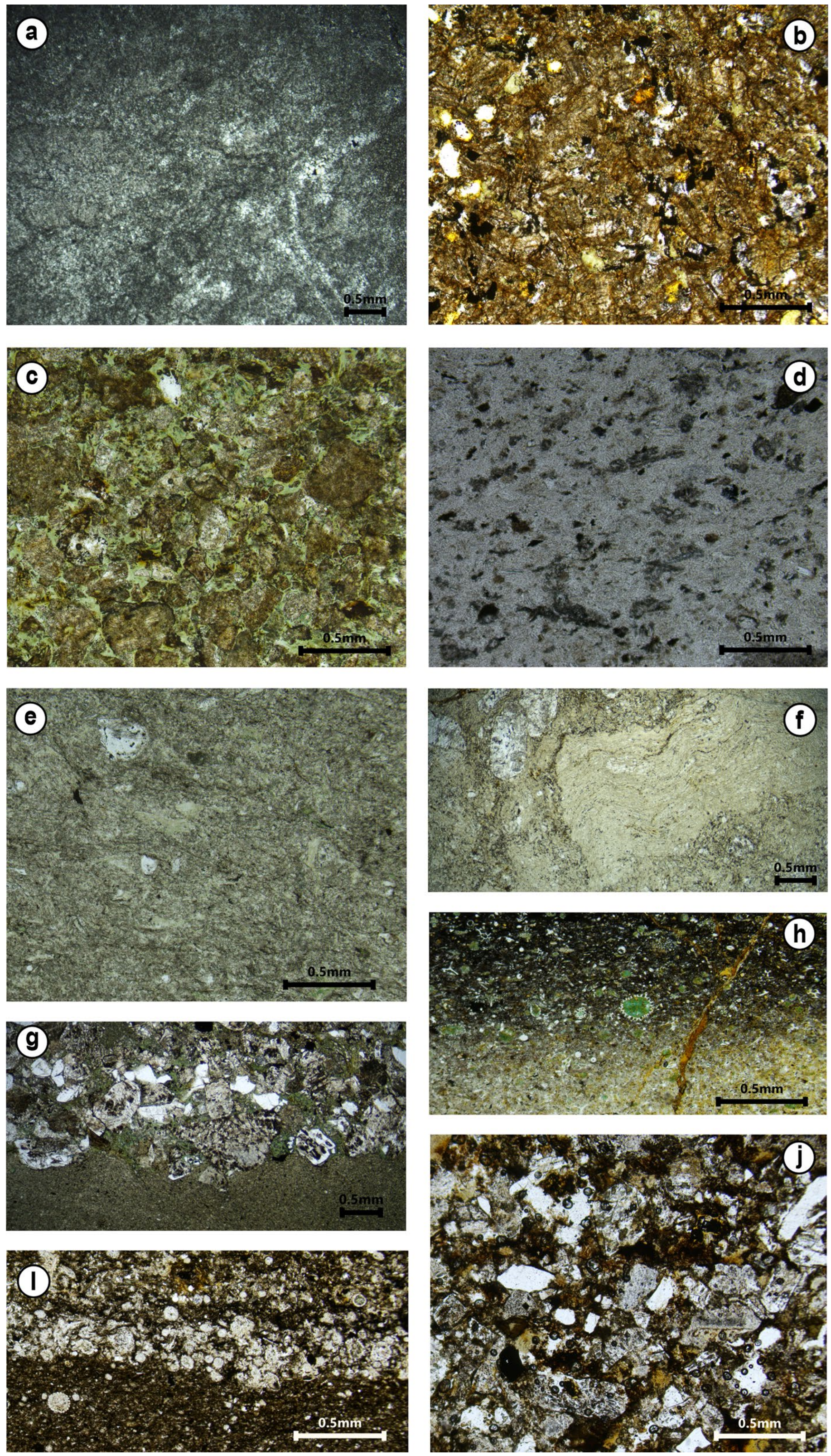


**Fig. 3** Microphotographs of the described lithotypes from the NW Croatian volcano-sedimentary successions. **a** Xenotopic anhedral dolomite crystals from the base of the BR section. Sample BR-2,20. **b** Heavily altered ophitic basalt with pyroxene crystals altered to chlorite. Sample GK-0,40. **c** Trachy-basaltic hyaloclastite composed of trachy-basalt fragments with a completely hyaline texture and scarce pyroxene crystaloclasts. Note the greenish glassy matrix between the clasts. Sample BR II-3,80. **d** Very fine ash vitroclastic tuff with barely visible platy and arcuate shards. Sample GK I-19,00. **e** Vitrocrystaloclastic tuffs with pumice fragments, glass shards and crystaloclasts of qtz, plag and K-feld; the most common lithotype of the Pietra Verde deposits; sample DK XI-5,10. **f** In some samples of the vitrocrystloclastic tuffs, pumice fragments can exceed the ash fraction and be lapilli sized. Also, note coarser K-feld crystaloclasts in the top left. Sample BR II-27,20. **g** Abrupt and irregular contact between the fine ash vitroclastic tuffs and coarse crystaloclastic tuffs, indicating fast sedimentation and likely erosion caused by gravitational currents. Sample SEK-15,55. **h** The transition from fine ash tuff to radiolarite is sometimes gradual and not clearly recognizable. Sample GK II—19,20. Note that sample GK II-19,00, which is mentioned before, is located just below GK II-19,20. **i** Secondary volcaniclastic deposits with radiolarian rich laminas or lenses. Sample SEK-48,35. **j** Coarse-grained sandstone found at the top of the Sekolje section. Sample SEK-98,35

Two microfacies of limestones were detected in the studied sections. Micritic, partially reddish limestones contain abundant thin-shelled bivalves, and in places, abundant calcified radiolarians and rare sponge spicules. This microfacies is found in the Gornji Kamenički I section directly overlaying basalts, at the base of the Kuna gora IV section, and sporadically as thin layers interbedded within the volcanogenic deposits. Ammonoid fauna is found in this microfacies on Kuna gora. The second microfacies is oncoid grainstone with benthic foraminifers. This microfacies is found only in the Kuna gora IV section above micritic reddish limestones and below radiolarian cherts. The oncoid grainstone is generally unsorted and contains oncoids, intraclasts, bioclasts, and carbonate lithoclasts. Oncoids are most abundant and range from 0.04 to 2 mm in size. They often have foraminifera or bivalve fragments in their cores. Intraclasts also vary in size up to 1 mm and are very well rounded. Benthic foraminifers and algal and bivalve fragments can be found as bioclasts. Carbonate lithoclasts account for 5–10% of the bulk carbonate grains. They are mostly biomicrite and biosparite limestones with foraminifera and intraclasts, and some grains are coated with an oncoidal coating. The cement is micro- to macrosparitic.

## Radiolarian chert deposits

Radiolarian chert deposits are present in all investigated sections, except for the Sekolje section (Fig. 2), as well-bedded red chert. The individual beds are up to 15 cm thick and often horizontally laminated. The amount of radiolarian skeletons is relatively low and accounts for up to 20% of the rock. Radiolarian skeletons, often deformed, are largely recrystallized and filled with microcrystalline quartz and calcite in lesser amounts. Sponge spicules are also present. Filaments, if present, are silicified and oriented parallel to lamination. Glass shards can also be distinguished. The transition between fine ash tuffs from the Pietra Verde deposits and the radiolarian cherts is sometimes not clear because it is gradual (Fig. 3h). In places, rocks have been tectonically crushed, thus making distinction between the two facies difficult.

## Volcanic and volcanogenic deposits

Volcanic rocks, geochemically determined as trachy-basalts recorded in the lower part of the Gornji Kamenečki I section are irregularly intercalated by pelagic limestones with filaments (Fig. 2). The trachy-basalts have an almost granular/ophitic texture and are composed of prismatic plagioclase, K-feldspar, and needle-like pyroxene (Fig. 3b). Feldspar is largely altered to various extents into prehnite aggregates. The pyroxene is chloritized, and its pristine nature cannot be unambiguously determined. Between the crystal phases, an amorphic volcanic groundmass can be seen. In places, rounded vesicles up to 2 mm in size can be found. The vesicles are filled with secondary calcite. The results gathered from bulk rock chemical analysis show that the investigated basalts crystallized from high-K shoshonitic magma ($K_2O$ up to 7.54 wt. %; Fig. 4).

Different volcanogenic deposits (sensu Di Capua et al. 2022) were recorded in the studied sections. Trachy-basaltic hyaloclasitic deposits were found only at the base of the Brezovica II section (Fig. 2). Here, these deposits are intercalated with biomicrite containing filaments and rare radiolarians. The individual layers are up to 20 cm thick and are horizontally laminated in places. Hyaloclastite is composed of hyaline trachy-basaltic lithoclasts with rare pyroxene and plagioclase phenocrysts (Fig. 3c). The amounts of lithoclasts and crystalloclasts vary among the samples. The lithoclasts range in size from 0.2 to 1.7 mm, varying from rounded to angular shapes. The crystalloclasts of feldspar and pyroxene are present in lesser amounts, as well as scoria fragments. The feldspar crystalloclasts are mostly euhedral to subhedral, and in places, exhibit in situ fragmentation and jigsaw-fit textures. They are altered into sericite, prehnite and clay mineral aggregates. The pyroxene crystalloclasts are less common and are altered to chlorite. Scoria fragments are the least common volcanic clasts in these deposits. The individual fragments can exceed 2 mm in size. They are irregularly elongated in shape and completely devitrified to chlorite. Rarely, the scoria fragments exhibit plastic deformation in contact with plagioclase crystalloclasts and/or incorporate them. The hyaloclastite is grain-supported and contains chlorite cement

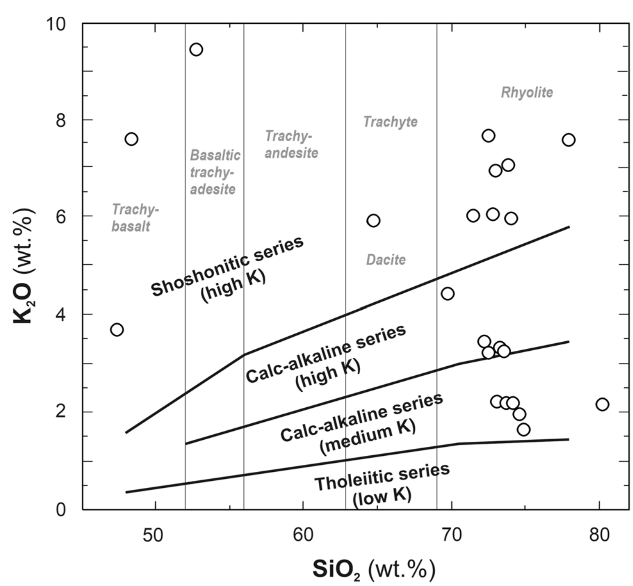


**Fig. 4** $K_2O$–$SiO_2$ discrimination diagram (modified from Peccerillo and Taylor 1976; Ewart 1982) for the volcanic and pyroclastic rocks from the Kuna Gora, Strahinjščica and Ivanščica Mts

between the volcanic clasts. Chemical analysis of hyaloclastite (sample BR II—3.80) shows high $K_2O$ concentrations (9.41 wt.%; Fig. 4), indicating that the magma belonged to the high-K shoshonitic series.

Pietra Verde deposits, the dominant volcanogenic deposits in the study area, were recorded in all sections, except the Kuna gora IV section (Fig. 2). These deposits are composed of different lithotypes, and a common feature is their greenish colour. Vitriclastic tuffs are composed of fine ash to medium ash glass shards. These tuffs are homogeneous to horizontally laminated (Fig. 3d). In most samples, the fine ash component is dominant, and the shard shapes are impossible to identify. The fine ash is devitrified to chlorite and celadonite. Radiolarians, sponge spicules and filaments occur in some samples. The medium-sized ash tuffs of this facies are composed of glass shards with visible forms, varying from arcuate, platy, X- to Y-shaped to rare bubble wall shards (Fig. 3e). In places, alteration processes have completely modified their primary mineralogy and structure. They are mostly devitrified to chlorite and to a lesser extent to albite, quartz, calcite, and clay minerals. The shards that are devitrified to calcite rarely exhibit opaque rims. Pumice fragments are also present in some samples, and their abundance varies from 5 to 40%. The size of the pumice fragments also varies from medium ash size to lapilli size (Fig. 3f). Alterations to chlorite and celadonite are practically omnipresent in all pumice fragments, with rare vesicles that are filled with microcrystalline quartz. Some pumice fragments exhibit imbrication patterns. The most common pyroclastic lithotype within the Pietra Verde deposits are vitricrystaloclastic tuffs, where the amounts of vitriclastic and crystaloclatic components are approximately equal. The size of the crystaloclasts varies from 0.05 to 1.50 mm. The dominant crystalloclasts are euhedral to subhedral plagioclase that is commonly lamellar and altered to sericite, prehnite and clay minerals. K-feldspars, quartz and biotite crystalloclasts are also present. Some quartz crystalloclasts are marked by oval cavities and are irregularly shaped. The plagioclase crystalloclasts are often fragmented, and in places, exhibit a jigsaw-fit texture. In places, pumice fragments are plastically deformed in contact with quartz and plagioclase crystalloclasts. Zircon, apatite, epidote, rutile, and opaque crystals are registered as accessory mineral phases. In rare samples, plagioclase and quartz crystaloclasts are the most abundant juvenile volcanic clast types (Fig. 3g). Bulk rock chemical analyses of this facies point to rhyolitic to rhyodacitic composition ($SiO_2$ = 64.47–80.18 wt. %; Fig. 4). The magma that generated the pyroclastic material found in the Pietra Verde deposits belonged to the medium-K to high-K calc-alkaline to shoshonitic series. Their $K_2O$ contents vary from 1.64 to 7.66 wt.% (Fig. 4).

Secondary volcaniclastic deposits (sensu Di Capua et al. 2022) are recorded in the upper parts of the Sekolje, Gornji Kamenečki II and Kuna gora IV sections (Fig. 2). These deposits are composed of three lithotypes: siltstones, fine- and coarse-grained sandstones. These deposits show a coarsening-upwards sequence. The siltstones are dark grey in colour and are generally horizontally laminated with light grey laminas (Fig. 5a, b). Lithoclasts of hyaline composition, as well as fragmented quartz and plagioclase mineral grains, are present. The plagioclase is almost completely altered to calcite. The accessory mineral phases present in the siltstones are muscovite, zircon, and opaque mineral grains. Radiolarians are sporadically dispersed in the siltstones or are organized in lenses or laminas (Fig. 3i). Lamination is also visible due to changes in cement/matrix ratios. Some of the laminas are cemented with calcite cement, while others are dominated by a dark matrix composed of very fine material containing volcanic particles, micrite and organic matter.

The fine sandstones are composed primarily of hyaline clasts and pumice fragments but crystalloclasts of quartz, plagioclase, and biotite are also present. The hyaline clasts are yellowish and irregular. The pumice fragments are devitrified to chlorite aggregates, while plagioclase is altered to calcite, prehnite, sericite and clay minerals. Accessory minerals include muscovite, zircon and opaque mineral phases

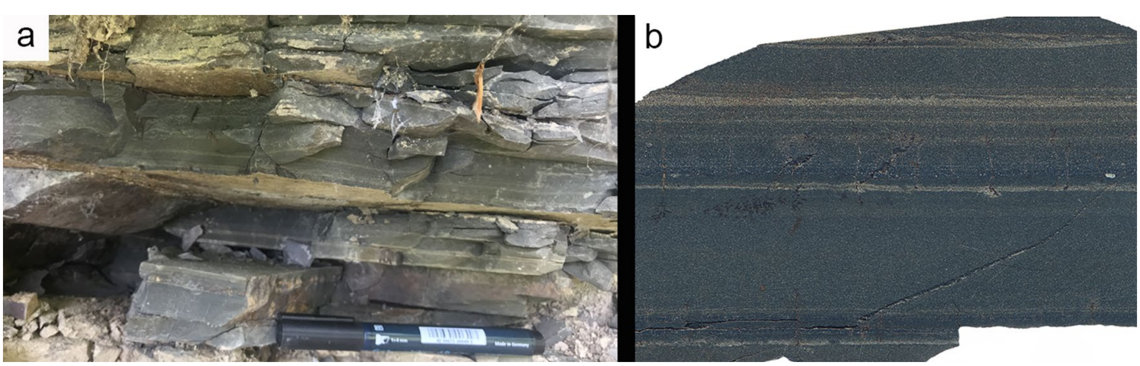


**Fig. 5** **a** Field photograph of the secondary volcaniclastic deposits. **b** Polished sample with horizontal laminations. Light grey laminas represent coarser turbiditic intervals with radiolarians

that are cubic in shape and can exceed 0.4 mm. They are either cemented with silicate cement or with a dark matrix made of very fine volcanic particles.

The coarse sandstones consist of grains up to 2.2 mm in size. They are chaotic, matrix supported and have a low degree of sorting (Fig. 3j). The individual layers are homogenous and up to 20 cm thick. The dominant clast types are lithic fragments of hyaline rocks, vitriclastic tuffs, pumice, and clasts of effusive rocks. The hyaline clasts are yellowish and completely altered to aggregates of chlorite. The vitriclastic tuff fragments are composed of fine ash particles, mainly fine glass shards. The clasts are yellowish to greenish, indicating devitrification of ash to chlorite. The pumice is devitrified to microcrystalline aggregates of quartz, albite and chlorite, while effusive rocks are recognized only by their porphyritic texture because their primary mineralogy has been completely obliterated by clay mineral-forming deuteric processes. Crystalloclasts are also present in this lithotype. The dominant crystalloclast type is quartz, followed by plagioclase. In some places, the quartz crystalloclasts exhibit oval cavities but also sharp and rough edges. In some places, in situ fragmentation can be seen, as indicated by the jigsaw-fit texture of the crystalloclasts. The plagioclase grains are usually anhedral in shape. Rare grains with subhedral habits are seen. The plagioclase crystalloclasts are altered to clay minerals and calcite. The matrix of this lithotype is dark brown and is composed of very fine fragments of volcanic material. In some places, remnants of glass shards can be recognized in the brown matrix.

## Biostratigraphy

### Radiolarians

Radiolarians were extracted using diluted (5%) HF acid from seven chert samples (at least one from each section) and from one sample of volcanogenic turbidites in the Sekolje section. Radiolarians are rare and are poorly to moderately well preserved in all samples. The inventory of radiolarian samples from chert samples is given in Table 1, and radiolarians are illustrated in Figs. 6 and 7. The radiolarians extracted from volcanogenic turbidites are illustrated in Fig. 8. Zonations by Kozur and Mostler (1994) and Kozur et al. (1996) were used for radiolarian dating (for a recent review, see Goričan et al. 2018). Compilations of stratigraphic ranges of Triassic radiolarian genera (O'Dogherty et al. 2009, 2010) were also used.

Stratigraphically, the most important occurrences are those of Oertlispongidae. The detached spines are present in all seven chert samples. The occurrence of *Oertlispongus inaequispinosus* Dumitrica, Kozur and Mostler in all samples means that the samples are not older than the *Spongosilicarmiger italicus* Zone (Kozur and Mostler 1994; Kozur et al. 1996). This zone has been subdivided into two subzones: the *Oertlispongus primitivus* Subzone and the *Oertlispongus inaequispinosus* Subzone (Kozur and Mostler 1994; Kozur et al. 1996). We do not assign samples to these subzones because we consider *Oertlispongus primitivus* Kozur and Mostler to be included in the variability of *Oertlispongus inaequispinosus* Dumitrica, Kozur and Mostler.

Based on the co-occurrence of *Baumgartneria bifurcata* Dumitrica and *Oertlispongus inaequispinosus* Dumitrica, Kozur and Mostler, the samples GKII-23,30, BR-17,40 and KGIV-4 have been assigned to the *Spongosilicarmiger italicus* Zone. This zone is correlated with the lower part of the Illyirian *Reitziites reitzi* Ammonoid Zone (Kozur 2003). Samples DKXI-1,20, BRII-11,70, KGIII-1,60 and KGIV-3 are assigned a broader range based on the occurrence of *Falcispongus falciformis* Dumitrica. This species last occurs in the *Ladinocampe vicentinensis* subzone of the *Ladinocampe multiperforata* Zone (Kozur and Mostler 1994; Stockar et al. 2012 and references therein). This subzone corresponds to the upper part of the Illyrian *Nevadites secedensis* Zone and the lower part of the Fassanian *Eoprotrachyceras curionii* Ammonoid Zone (Kozur 2003; Goričan et al. 2018). Because sample KGIV-3 is stratigraphically under sample KGIV-4, it is also assigned to the *Spongosilicarmiger italicus* Zone. The range of the genus *Celluronta* Sugiyama, as reported by O'Dogherty et al. (2009, 2010), was limited to the early and middle Anisian but has since been reported from the late Anisian and Ladinian (e.g., Gawlick et al. 2012; Dumitrica 2017). Similarly, *Monospongella rotunda* Kozur and Mostler, originally described from the Ladinian (Kozur and Mostler 1994), has been found in the Late Anisian assemblage (Gawlick et al. 2012).

Only rare and poorly preserved radiolarians were extracted from the secondary volcanicastic deposits in the Sekolje section (sample SEK-48,35, Fig. 8). Because of poor preservation, some specimens are assigned only generic designation. The age of this sample is based on compiled stratigraphic ranges of Triassic radiolarian genera (O'Dogherty et al. 2009, 2010) but should be considered tentative. Based on the last occurrence of *Tetrapaurinella* Kozur and Mostler and the first occurrence of *Poulpus* DeWever, the sample is assigned to the late Anisian.

### Ammonites

Approximately 30 specimens of ammonites were collected from the interval at the base of the Kuna gora IV section (Fig. 2). Ammonites were collected from the base of the section as primary samples and as secondary samples whose precise position in the section could not be determined. The ammonoid assemblage is illustrated in Figs. 9, 10 and 11. All specimens are deposited in the Stratigraphic collection

**Table 1** Occurrence of radiolarian species in samples from radiolarian cherts in investigated sections (see Fig. 2)

| Radiolarians | Samples | | | | | | |
|---|---|---|---|---|---|---|---|
| | DKXI-1,20 | GKII-23,30 | BR-17,40 | BRII-11,70 | KGIII-1,60 | KGIV-3 | KGIV-4 |
| Oertlispongidae | | | | | | | |
| *Baumgartneria bifurcata* Dumitrica | | • | • | | | | • |
| *Baumgartneria retrospina* Dumitrica | | | | • | • | | |
| *Falcispongus falciformis* Dumitrica | • | • | • | • | • | • | |
| *Oertlispongus inaequispinosus* Dumitrica, Kozur and Mostler | • | • | • | • | • | • | • |
| *Pararchaeospongoprunum* sp. | | | • | | | | |
| *Paroertlispongus multispinosus* Kozur and Mostler | | | | | | | • |
| *Paroertlispongus weddigei* (Lahm) | | • | | | • | | • |
| *Paroertlispongus* ? sp. 1 sensu Dumitrica 1999 | | | | • | • | • | |
| *Paroertlispongus* sp. | • | • | • | • | | • | |
| Other spumellaria | | | | | | | |
| *Archaeocenosphaera* sp. | • | | • | • | • | | • |
| *Astrocentrus pulcher* Kozur and Mostler | | | | | | • | |
| *Monospongella rotunda* Kozur and Mostler | | | • | • | | • | • |
| *Neopaurinella* sp. | | • | | | | | |
| *Paurinella latispinosa* Kozur and Mostler | | | | • | | | |
| *Spongopallium* sp. | | • | | | | | |
| *Tetrapaurinella discoidalis* Kozur and Mostler | | | cf | | | | |
| *Tripocyclia* sp. A sensu Nakaseko and Nishimura 1979 | | | | | | | • |
| Entactinaria | | | | | | | |
| *Cryptostephanidium cornigerum* Dumitrica | | | | | | • | |
| *Cryptostephanidium* sp. | | | | | | • | |
| *Eptingium manfredi* Dumitrica | | • | | | • | | |
| *Pentactinocapsa quadripes* Dumitrica | | | | | | | • |
| *Pseudostylosphaera acrior* (Bragin) | | | • | | | • | |
| *Pseudostylosphaera coccostyla* (Rüst) | | | | | | | • |
| *Pseudostylosphaera* aff. *japonica* (Nakaseko and Nishimura) | | | • | | • | | |
| *Pseudostylosphaera longispinosa* Kozur and Mostler | • | | | | • | | |
| *Pseudostylosphaera postjaponica* Kozur and Mostler | | • | | | | | |
| *Spongostephanidium spongiosum* Dumitrica | cf | | | | | • | • |
| *Tiborella anisica* Kozur and Mostler | | | | | | cf | |
| *Triassistephanidium laticornis* Dumitrica | | | • | | | | |
| Nassellaria | | | | | | | |
| *Celluronta conica* Sugiyama | | • | • | | | | |
| *Conospongocyrtis* sp. | | • | | | | | |
| *Hinedorcus* sp. | | • | | | | | |
| *Hozmadia* sp. | | • | | | | | |
| *Striatotriassocampe nodosoannulata* Kozur and Mostler | | • | | | | | |
| *Triassocampe coronata* Bragin | | | cf | | | | |
| *Triassocampe cylindrica* Kozur and Mostler | | | • | | | | |
| *Triassocampe deweveri* (Nakaseko and Nishimura) | | | • | • | • | • | • |
| *Triassocampe scalaris* Dumitrica | • | | • | | • | • | • |

of the Department of Geology and Palaeontology, Croatian Natural History Museum (Zagreb), under inventory numbers prefixed with 3L.

The following ammonoid taxa were identified: *Discoptychites megalodiscus* (Beyrich) (Figs. 9a–c), *Discoptychites* cf. *domatus* (Hauer) (Figs. 9d–f), *Flexoptychites*

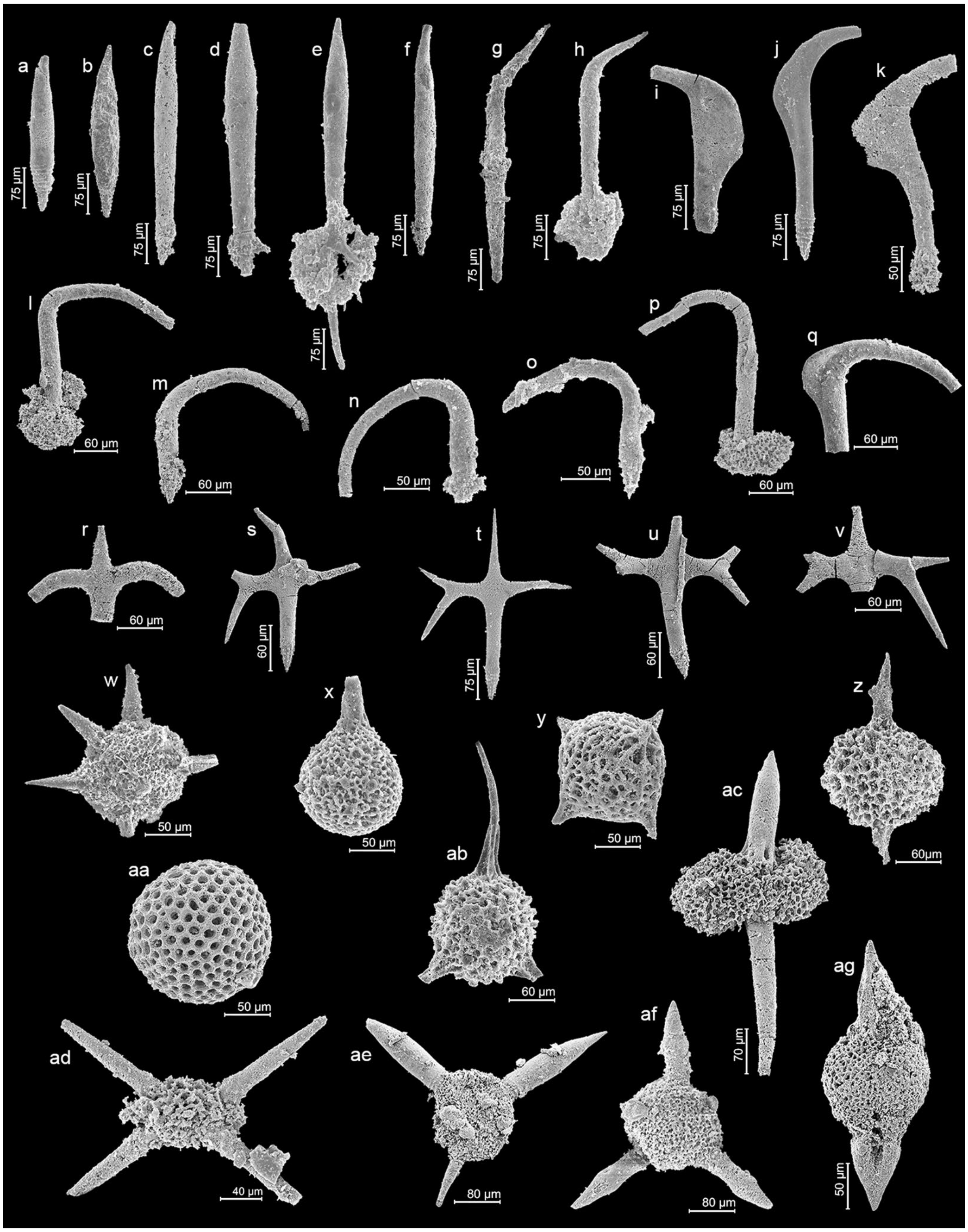


**Fig. 6** Late Anisian to early Ladinian radiolarians from radiolarian cherts in investigated sections. For each illustration, the sample number and scanning electron micrograph number are indicated. Taxonomic remarks are provided when necessary. The rock samples, residues and the illustrated specimens are stored at the Croatian Geological Survey, Zagreb. **a**, **b** *Paroertlispongus*? sp. 1 sensu Dumitrica (1999); **a** BRII-11,70_0013; **b** KGIII-1,60_19. **c**, **d** *Paroertlispongus* sp.; **c** BR-17,40_0043; **d** KGIV-3_0008. **e** *Paroertlispongus multispinosus* Kozur and Mostler; KGIV-4_0012. **f–h** *Paroertlispongus weddigei* (Lahm); **f** GK-23,30_0018; **g** KGIII-1,60_0020; **h** KGIV-4_16. Spines with variously bent short distal part are included. **i**, **k** *Falcispongus falciformis* Dumitrica; **i** KGIII-1,60_24; **j** KGIV-3_0010; **k** BR-17,40_0049. **l–p** *Oertlispongus inaequispinosus* Dumitrica, Kozur and Mostler; **l** GK-23,30_0013; **m** GK-23,30_0012; **n** DKXI-1,20_0007; **o** DKXI-1,20_0008; **p** BR-17,40_0044. **q** *Falcispongus calcaneum* Dumitrica; GKII-23,30_0044. **r** *Baumgartneria retrospina* Dumitrica; KGIII-1,60_0027. **s–v** *Baumgartenria bifurcata* Dumitrica; **s** GKII-23,30_0023; **t** KGIV-4_010; **u** GKII-23,30_0026; **v** GKII-23,30_0021. **w** *Astrocentrus pulcher* (Kozur and Mostler); KGIV-3_0027. **x** *Monospongella rotunda* Kozur and Mostler; KGIV-3_0019. **y** *Pentactinocapsa quadripes* Dumitrica; KGIV-4_0019. **z** *Amphisphaera*? *mesotriassica Dumitrica*, Kozur and Mostler; KGIII-1,60_0037. **aa** *Archaeocenosphaera* sp.; BR-17,40_0021. **ab** *Tripocyclia* sp. A sensu Nakaseko and Nishimura (1979); KGIV-4_0032; **ac** *Pararchaeospongoprunum* sp.; BR-17,40_0018. **ad** *Tetrapaurinella* cf. *discoidalis* Kozur and Mostler; BR-17, 40_33. **ae** *Neopaurinella* sp.; GKII-23.30_0029. **af** *Paurinella latispinosa* Kozur and Mostler; BRII-11,70; 0007. **ag** *Spongopallium* sp.; GKII-23,30_0011

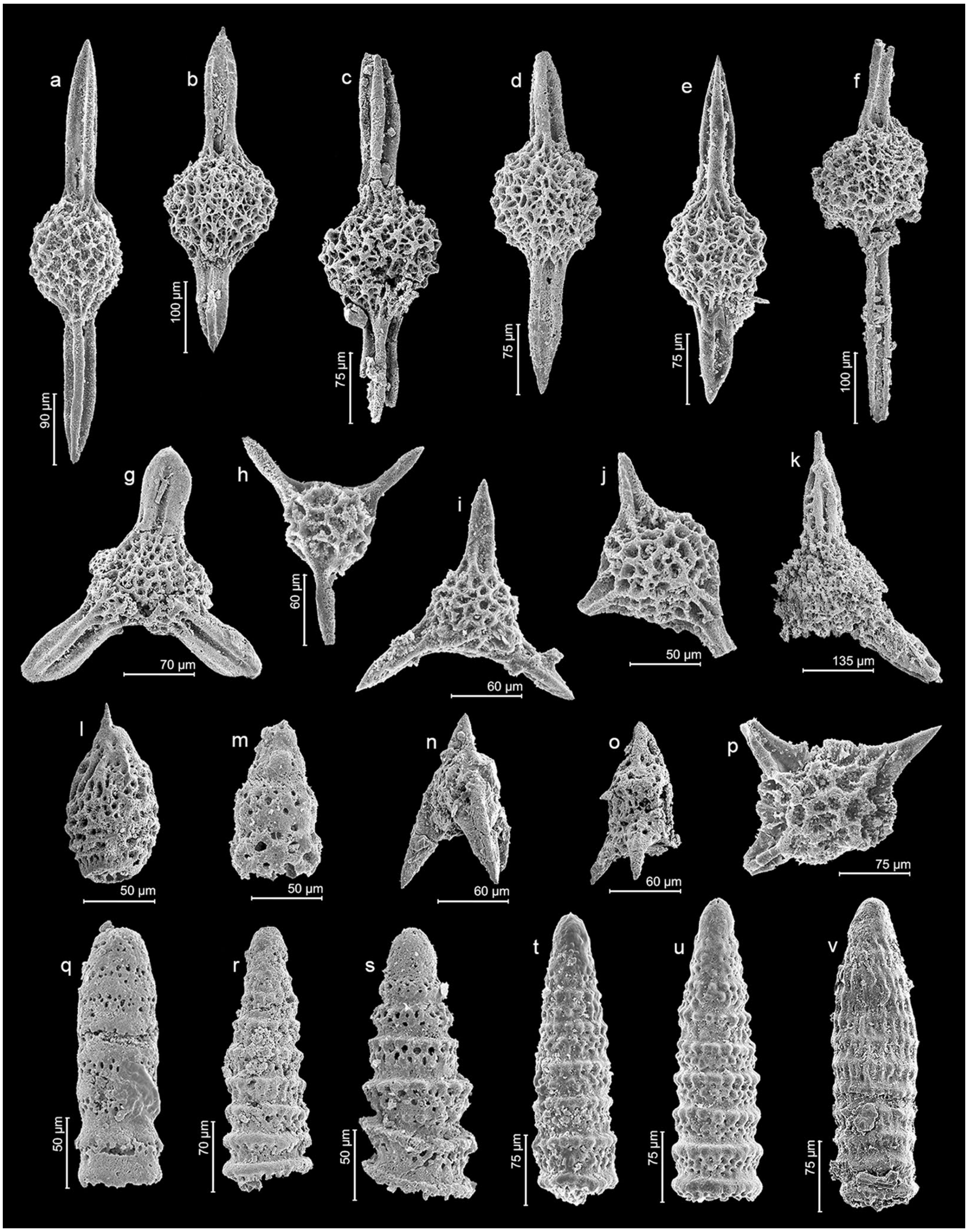


**Fig. 7** Late Anisian to early Ladinian radiolarians from radiolarian cherts in investigated sections in NW Croatia. For each illustration, the sample number and scanning electron micrograph number are indicated. Taxonomic remarks are provided when necessary. The rock samples, residues and illustrated specimens are stored at the Croatian Geological Survey, Zagreb. **a** *Pseudostylosphaera coccostyla* (Rüst); KGIV-4_0006. **b** *Pseudostylosphaera* aff. *japonica* KGIII-1,60_0012. The illustrated specimen differs from the type material by having polar spines of unequal lengths. **c** *Pseudostylosphaera postjaponica* Kozur and Mostler; GKII-23,30_004. **d**, **e** *Pseudostylosphaera acrior* (Bragin); **d** BR-17,40_0004; **e** KGIV-3_0007. **f** *Pseudostylosphaera longispinosa* Kozur and Mostler; KGIII-1,60_0014. **g** *Triassistephanidium laticornis* Dumitrica; BR-17,40_0015. **h** *Spongostephanidium spongiosum* Dumitrica; KGIV-4_0022. **i** *Cryptostephanidium cornigerum* Dumitrica; KGIV-3_0016. **j** *Cryptostephanidium* sp.; BR-17,40_0020. **k** *Eptingium manfredi* Dumitrica; KGIII-1,60_0017. **l** *Conospongocyrtis* sp.; GKII-23,30_35. **m** *Celluronta conica* Sugiyama; BR-17,40_0027. **n** *Hozmadia* sp.; GKII-23,30_0029. **o** *Hinedorcus* sp.; GKII-23,30_0049; **p** *Tiborella* cf. *anisica* Kozur and Mostler; KGIV-3_0026. **q** *Triassocampe cylindrica* Kozur and Mostler; BR-17,40_0008. **r** *Triassocampe* cf. *coronata* Bragin; BR-17,40_0002.s *Triassocampe deweveri* (Nakaseko and Nishimura); BR-17.40_0010. **t**, **u** *Triassocampe scalaris* Dumitrica, Kozur and Mostler; **t** KGIV-3_0003; **u** KGIV-3_0001. **v** *Striatotriassocampe nodosoannulata* Kozur and Mostler; GKII_23,30_0004

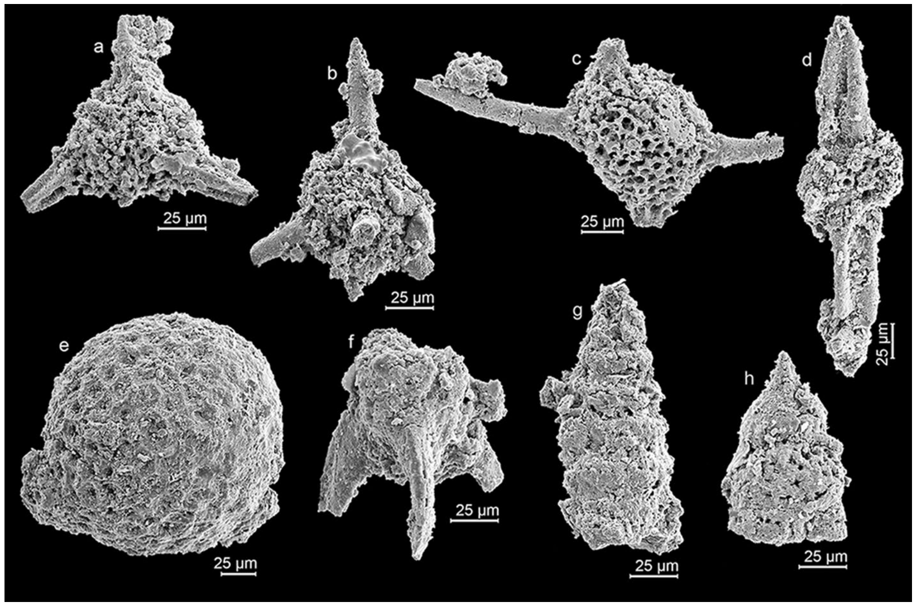


**Fig. 8** Radiolarian assemblage from sample SEK-48,35. For each illustration, the scanning electron micrograph number is indicated. The rock samples, residues and illustrated specimens are stored at the Croatian Geological Survey, Zagreb. **a** *Eptingium* sp.; SEK-48,35_0004; **b** *Tetrapaurinella tetrahedrica* Kozur and Mostler; SEK-48,35_0002; **c** *Tetrapaurinella discoidalis* Kozur and Mostler; SEK-48,35_0023; **d** *Spongoxystris hadra* Sugiyama; SEK-48,35_0006; **e** *Archaeocenosphaera* sp.; SEK-48,35_0017; **f** *Poulpus* sp.; SEK-48,35_0014; **g** *Triassocampe*? sp.; SEK-48,35_0001; **h** *Conospongocyrtis*? sp.; SEK-48,35_0025

*flexuosus* (Mojsisovics) (Figs. 9a–c, i–j), *Flexoptychites* cf. *acutus* (Mojsisovic) (Figs. 10d, e), *Flexoptychites studeri* (Mojsisovic) (Figs. 10f-h), *Gymnites madjereki* Gorjanović-Kramberger (Fig. 10k), *Flexoptychites*? sp. (Fig. 11a), *Procladiscites* cf. *brancoi* Mojsisovics (Figs. 11b–e, i-k), *Proarcestes* sp. (Figs. 11f, g), *Bulogites*? sp. (Fig. 11h), *Monophyllites* sp. (Figs. 11l, m), and *Leiophyllites* sp.

The genus *Flexopthychites* Spath is the only genus found in the section below the oncoid grainstone layer containing benthic foraminifers. This genus first appears in the Illyrian *Paraceratites trinodosus* Zone and ranges to the lower part of the *Nevadites secedensis* Zone (Brack and Reiber 1986, 1993; Vörös 2014, 2018).

Genus *Bulogites* Arthaber has the shortest stratigraphic range of all determined taxa, limited to the Pelsonian *Balaonites balatonicus* Zone (Vörös 2003, 2014, 2018; Brack et al. 2005; Monnet et al. 2008). The genus *Discoptychites* Diener also appears in the *Balatonites balatonicus* Zone (Vörös 2003, 2014), but its range extends to the Illyrian *Nevadites secedensis* Zone (Vörös 2014). The genus *Proarcestes* Mojsisovics is known from the *Paraceratites trinodosus* Zone and *Reitziites reitzi* Zone (Vörös 2010). Occurrences of the genera *Procladiscites* Mojsisovics, *Monophyllites* Mojsisovics and *Leiophyllites* Diener are well documented throughout the Anisian (e.g., Gaetani et al. 1992; Ballini 1994; Germani 1997; Vörös 2014).

Ammonoid assemblages from the Middle Triassic volcano-sedimentary successions were reported only in several other localities in Croatia. Assemblages similar to that from the Kuna gora IV section have previously been described from the eastern part of Kuna gora Mt. (Gorjanović-Kramberger 1896; Salopek 1918b, 1919) and from the Lika area (Japundžić et al. 2015). Additionally, in the Lika area, a different Illyrian ammonoid assemblage characteristic of the upper *Paraceratites trinodosus* and *Reitziites reitzi* Ammonoid Zones, which includes the marker species *Reitziiets reitzi* (Böckh), has been described from the succession of carbonate and pyroclastic rocks (Salopek 1914; Smirčić et al. 2020). The pelagic succession on Samoborsko gorje Mts., correlative to those described in this paper, contains middle Illyrian to early Longobardian assemblages (Salopek 1912, 1918c, 1936; Goričan et al. 2005).

Further south in the areas of the Dinarides, the ammonoid assemblages in volcano-sedimentary successions range in age from lower Illyrian to lower Carnian (Salopek 1918a; Jelaska et al. 2003; Balini et al. 2006; Smirčić et al. 2018).

## Benthic foraminifera

A relatively rich assemblage of benthic foraminifera was found in the oncoid grainstone sample (GT-209) in the Kuna gora IV section, between reddish micritic limestone and radiolarian cherts (Fig. 2). *Meandrospira dinarica* Kochansky-Devidé and Pantić (Figs. 12a-d), *Pilammina densa* Pantić (Figs. 12h–m), *Pilamminella semiplana* Kochansky-Devidé and Pantić (Figs. 12e–g), *Pilamminela* cf. *kuthani* (Salaj) (Figs. 12n–o), and *Endoteba* sp. (Figs. 12p, q) were identified as well as foraminifera from the Duostominids and Frondicularia groups.

The first appearance of *Meandrospira dinarica* Kochansky-Devidé and Pantić is at the base of the Anisian (Rettori 1995; Altiner et al. 2021). According to Rettori (1995), the last appearance of this species is in the Pelsonian. However, according to Salaj et al. (1983), the range should be extended to the Illyrian, below the base of the *Reitziiets reitzi*

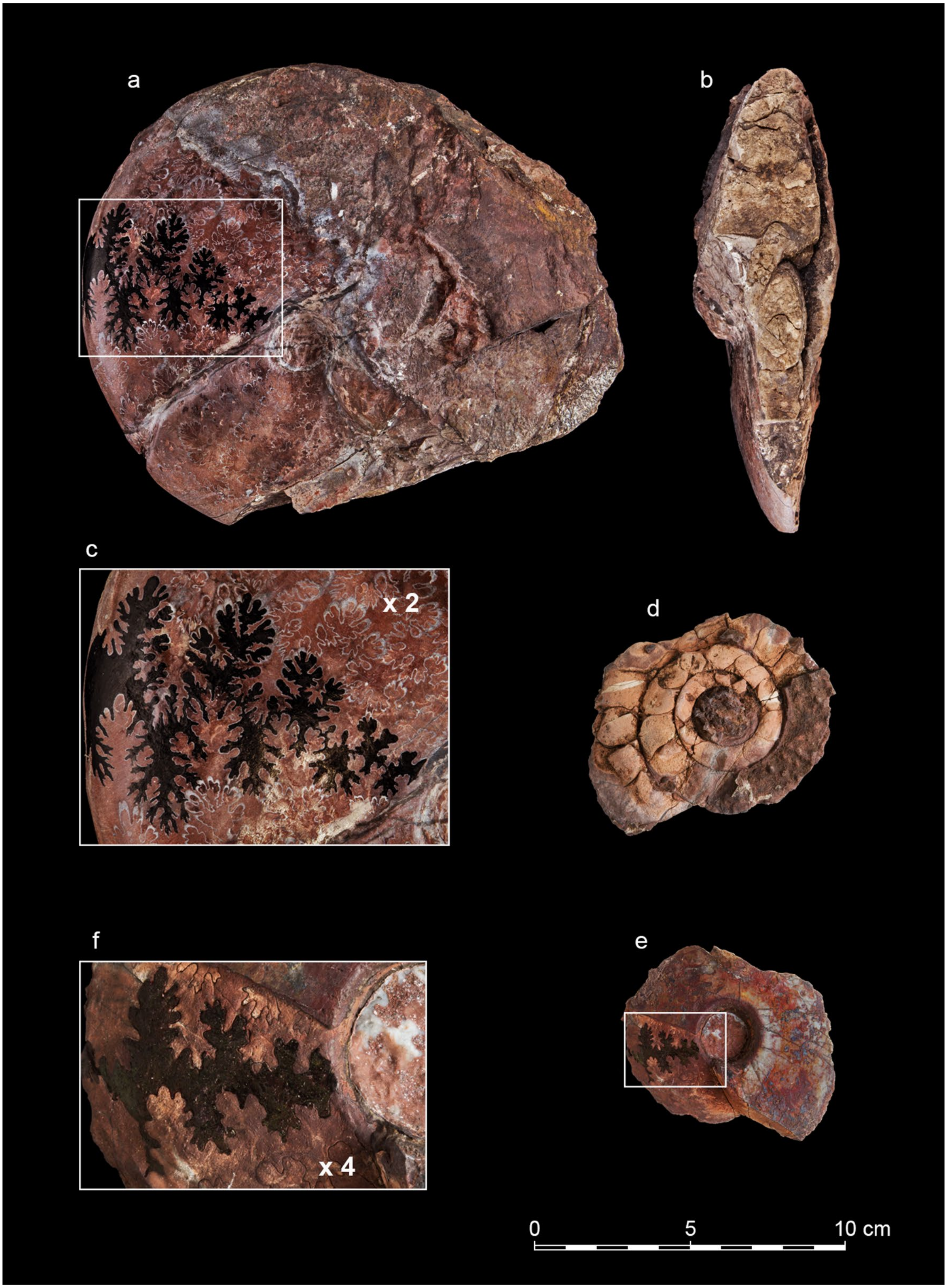


**Fig. 9** Ammonites from the Kuna gora IV section. **a–c** *Discoptychites megalodiscus* (Beyrich); 3L-741, lateral view (**a**), ventral view, (**b**) and suture line increased (**c**); secondary sample. **d–f** *Discoptychites* cf. *domatus* (Hauer); 3L-754, lateral views (**d**, **e**) and suture line increased (**f**); secondary sample

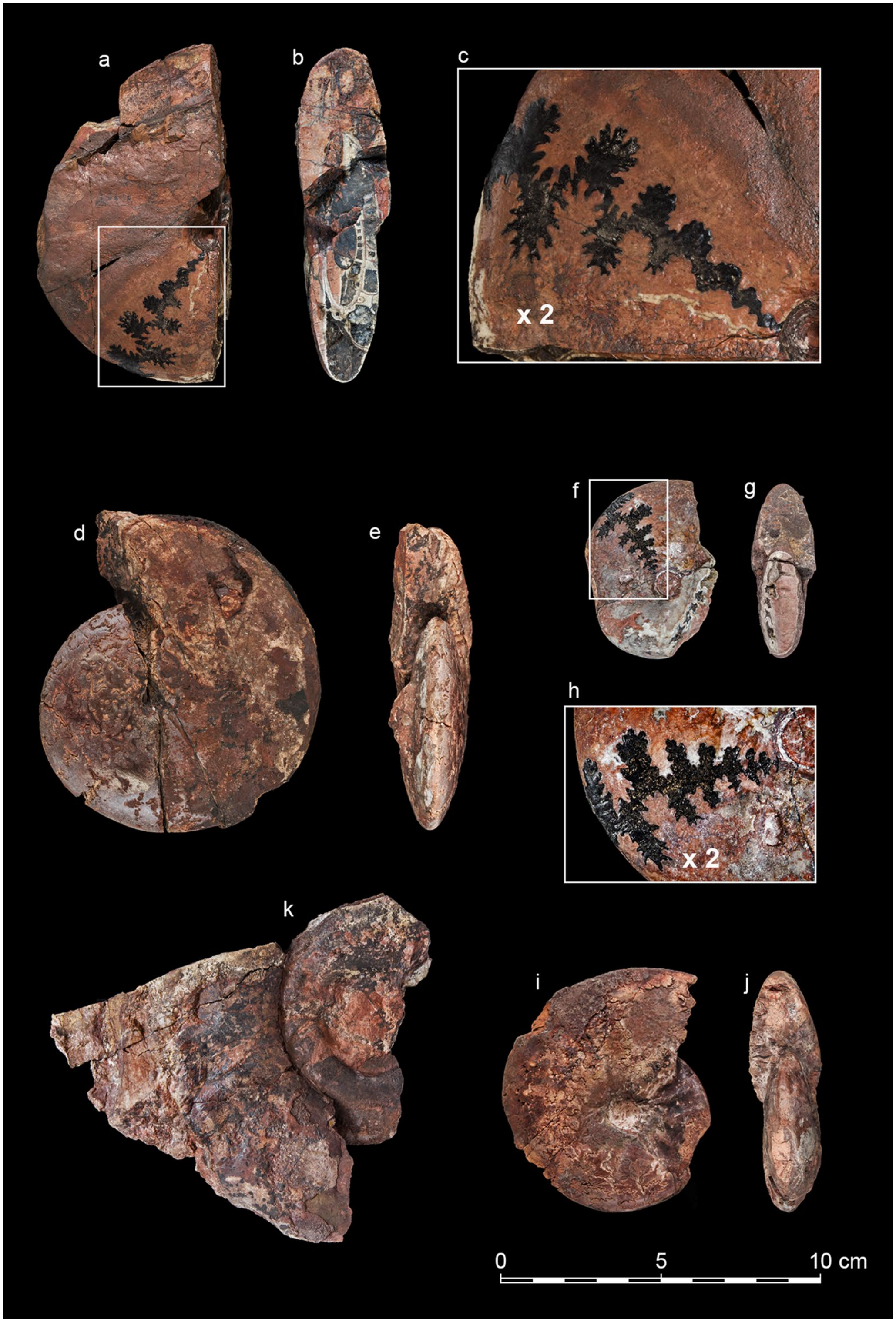


**Fig. 10** Ammonites from the Kuna gora IV section. **a–c** *Flexoptychites flexuosus* (Mojsisovics); 3L-743, lateral view (**a**), ventral view (**b**) and suture line increased (**c**); primary sample. **d**, **e** *Flexoptychites* cf. *acutus* (Mojsisovics); 3L-744, lateral view (**d**), ventral view (**e**); primary sample. **f–h** *Flexoptychites studeri* (Mojsisovics); 3L-743, lateral view (**f**), ventral view (**g**) and suture line increased (**h**); primary sample. **i, j** *Flexoptychites flexuosus* (Mojsisovics); 3L-748, lateral view (**i**), ventral view (**j**); primary sample. **k** *Gymnites madjereki* Gorjanović-Kramberger; 3L-742, lateral view; secondary sample

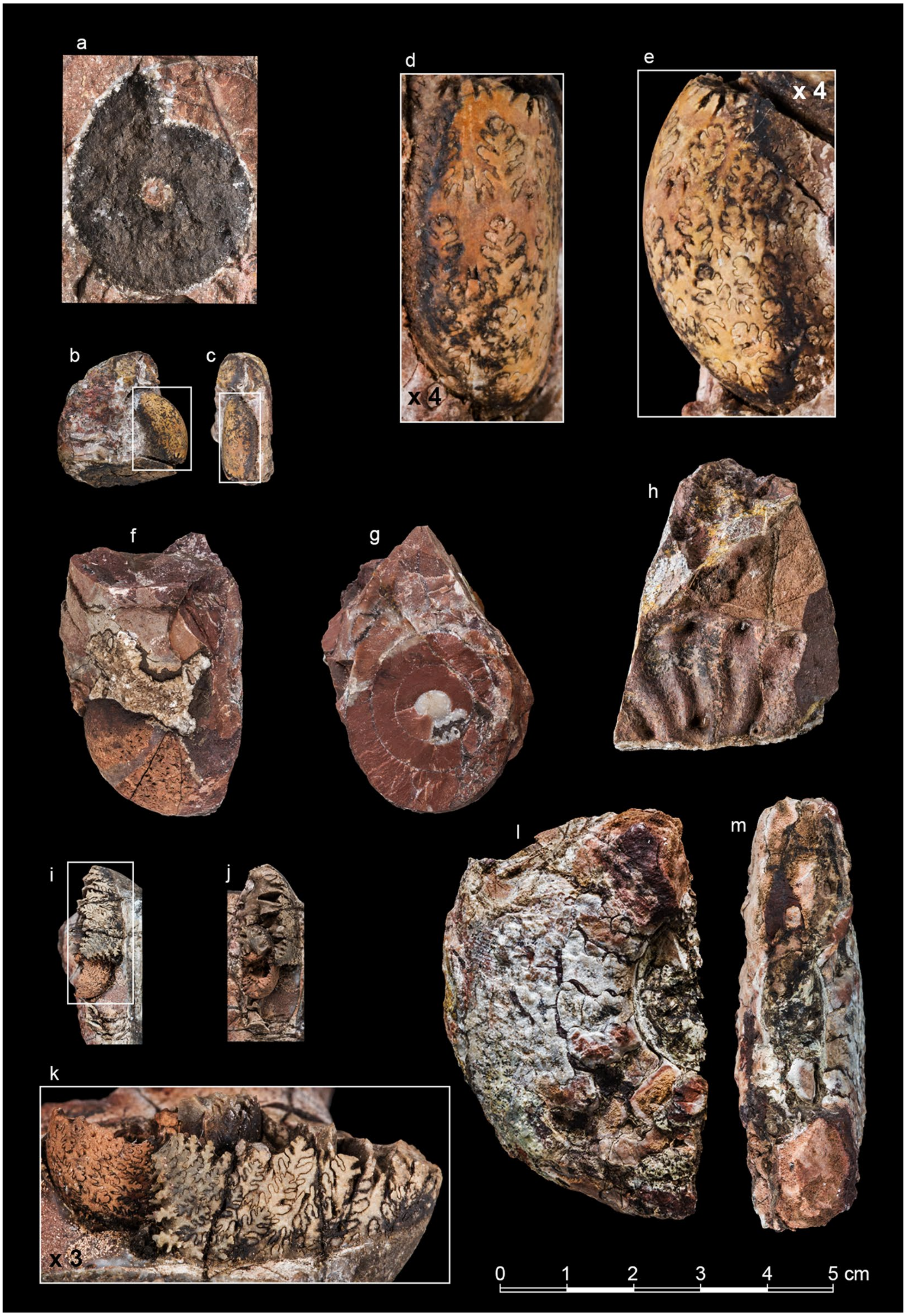


**Fig. 11** Ammonites from the Kuna gora IV section. **a** *Flexoptychites*? sp. (Mojsisovics); 3L-749, lateral view; primary sample. **b–e** *Procladiscites* cf. *brancoi* Mojsisovics; 3L-754, lateral view (**b**), ventral view (**c**) and suture line increased (**d**, **e**); secondary sample. **f, g** *Proarcestes* sp. (Mojsisovics); 3L-754, lateral view (**f**), ventral view (**g**); primary sample. **h** *Bulogites*? sp. Arthaber; 3L-756, lateral view; secondary sample. **i–k** *Procladiscites* cf. *brancoi* Mojsisovics; 3L-755, lateral view (**i**), ventral view (**j**) and suture line increased (**k**); secondary sample. **l**, **m** *Monophyllites* sp. Mojsisovics; 3L-757, lateral view (**l**), ventral view (**m**); secondary sample

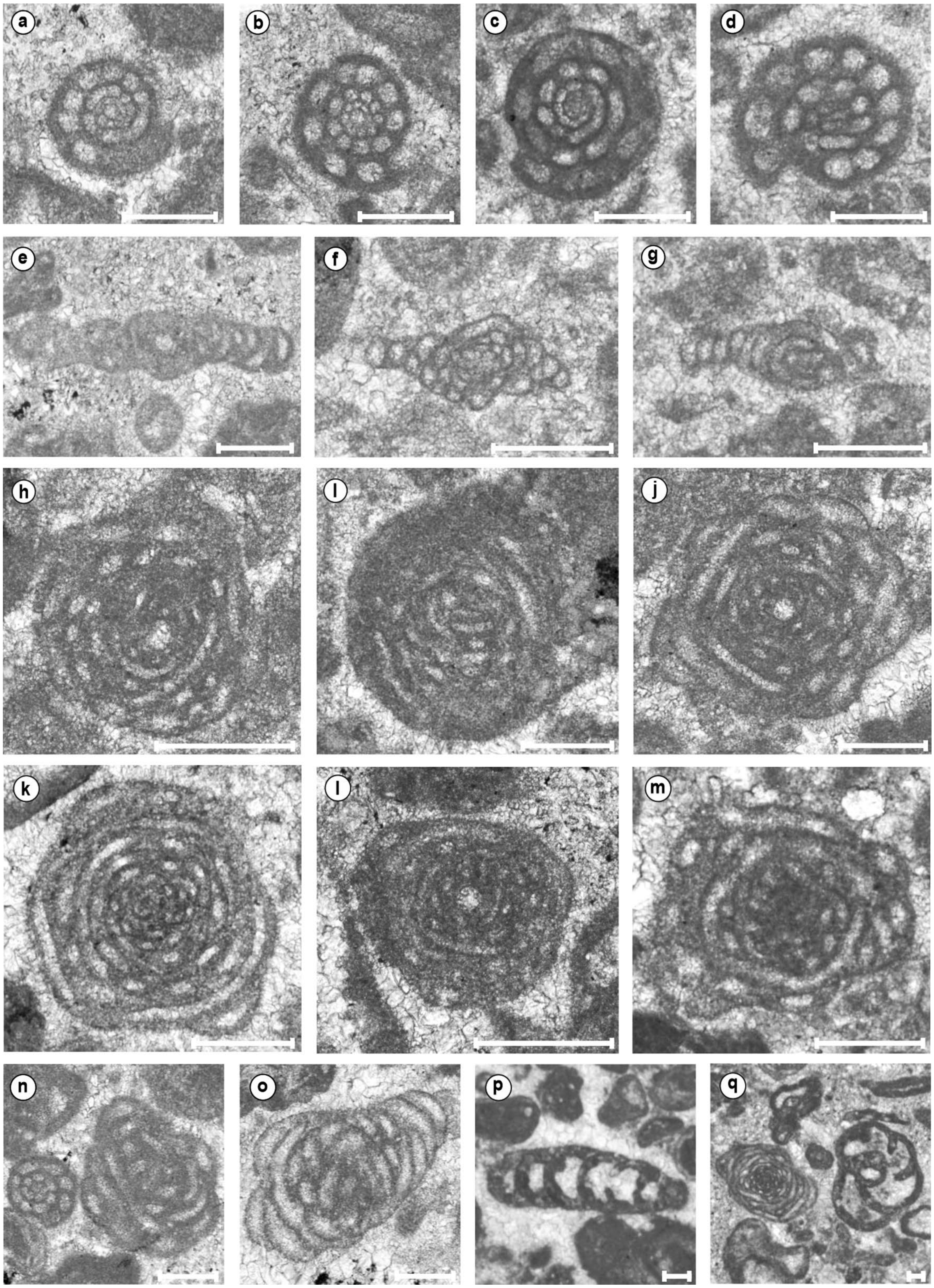


**Fig. 12** Foraminiferal assemblage from sample GT209 (Kuna gora IV section). The scale bar for all microphotographs is 100 μm: **a–d** *Meandrospira dinarica* Kochansky-Devidé and Pantić; **e–g** *Pilamminella semiplana* Kochansky-Devidé and Pantić; **h–m** *Pilammina densa* Pantić; **n**, **o** *Pilamminela* cf. *kuthani* (Salaj); **p**, **q** *Endotheba* sp. (**a**, **b**, **f**, **g**, **k**, **n**, **o** thin-section GT 209–1; **c**, **p** thin-section GT 209-2; **h**–**j** thin-section GT-209-3; **m**, **q** thin-section GT 209-4; **d**, **l** thin-section GT 209–5; **e** thin-section GT 209-6)

Ammonoid Zone. The early Illyrian age for this species is also shown by Sudar (1986) and Muttoni et al. (1998) based on co-occurrences with conodonts. *Meandrospira dinarica* is also found in a correlative succession in the Belski dol, Ivanščica Mt., together with dasycladal algae (Goričan et al. 2005; Grgasović 2022). *Pilamina densa*, often found in association with *Meandrospira dinarica,* has a somewhat shorter range since it first appears around the base of the Bithynian (Rettori 1995; Altiner et al. 2021). *Pilamminella semiplana* has the same range as *Meandrospira dinarica* (Rettori 1995). *Pilamminela* cf. *kuthani* is a relatively rare species described from the Carnian strata of the Slovakian Karst. Our specimens have some similarities with those illustrated by Salaj et al. (1983), but they are younger in age.

Therefore, the range of identified taxa is from the base of the Anisian to early Illyrian. However, because ammonites of early Illyrian age are found in the section below sample GT-109, this sample is also assigned an early Illyrian age.

### Conodonts

Two limestone samples (GKI-7,00; GKI-7,10) from the Gornji Kamenečki I section were collected for conodont extraction, which was carried out at the Geological Survey of Slovenia. Rock samples, with an approximate weight of 1 kg, were processed with the use of diluted acetic acid (7–10%). The insoluble residues were sieved, separated and handpicked under a binocular microscope.

Both analysed samples produced conodonts, however, only of fragmentary preservation. The poor state of preservation enabled the identification of the genus *Gladigondolella* in association with rare partially preserved specimens that have certain similarities to *Paragondolella trammeri* (Kozur). The identified conodont elements and their abundance are presented in Table 2. The two taxa are abundantly represented in the open-marine Tethys (Chen et al. 2015), and *Paragondolella trammeri* is stratigraphically significant. The fauna of the *trammeri* Zone (Illyrian-Fassanian) has been reported from many sections in the Dinarides (Smirčić et al. 2018; Kolar-Jurkovšek and Jurkovšek 2019). The age of the obtained conodont fauna from the Gornji Kamenečki I section does not permit confidential stratigraphic assignment due to their inadequate preservation.

**Table 2** Numerical distribution of conodonts in the Gornji Kamenečki I section

| Conodonts | Samples | |
|---|---|---|
| | GKI-7.00 | GKI-7.10 |
| *Gladigondolella* sp. | 3 | 5 |
| ? *Paragondolella trammeri* | 1 | 3 |
| Indeterminated fragments | 4 | 3 |

The recovered conodont fragments are black to grey in colour, with a CAI (colour alteration index) value of 5–6, which corresponds to the temperature ranges of 300–480 °C to 360–550 °C (Epstein et al. 1977; Rejebian et al. 1987).

## Discussion

### Age and depositional environment

The volcano-sedimentary deposits of NW Croatia studied in this paper represent a part of the larger passive continental margin of the western Neotethys preserved in the Southern Alps and the Dinarides (e.g., Schmid et al. 2008, 2020; van Hinsbergen et al. 2020). In this study, these continental margin successions are juxtaposed with formations derived from the oceanic realms of the Neotethys (Babić et al. 2002; Goričan et al. 2005; Slovenec et al. 2011; Belak et al. 2022). We propose a palaeogeographic name, the Northwestern Croatian Triassic Rift Basin (NCTRB), for the part of the continental margin where these volcano-sedimentary successions were deposited. During the late Anisian and early Ladinian, complex horst-and-graben topography caused by extensional tectonics largely controlled sedimentation processes at the continental margin (e.g., Goričan et al. 2005; Budai and Vörös 2006; Kovács et al. 2011; Gawlick et al. 2012, 2021; Celarc et al. 2013; Fig. 13). The onset of pelagic sedimentation on subsided blocks with shallow-marine carbonates was previously recorded in the Pelsonian (Goričan et al. 2005). The presence of stromatolite laminations in the dolostone in the Brezovica I section indicates formation in intratidal environments that contain cyanobacterial activity. However, the age of these deposits could not be determined. Deposition of micritic limestones containing the ammonoid genus *Flexopthychites* in the Kuna gora IV section below the radiolarian cherts confirms the existence of pelagic sedimentation in the NTCRB in the Illyrian *Paraceratites trinodosus* Zone. Pelagic conditions are also indicated in the Pelsonian *Balatonites balatonicus* Zone based on the occurrence of the genus *Bulogites* Arthaber as a secondary sample. Lower Illyrian benthic foraminifers prove the existence of a coeval shallow-water environment that provided carbonate detritus to the deeper parts of the basin. Limestones with “filaments” (thin-shelled bivalves) and radiolarians found in contact with trachy-basalts in the Gornji Kamenički I section are characteristic of open shelf or basin environments (Flügel 2010). Radiolarian cherts represent pelagic deposits deposited in periods of abating volcanic activity. Rare thin beds of pelagic limestones are found intercalated with pyroclastites in the Gornji Kamenečki I, Brezovica II and Kuna gora

III sections. Subsided blocks with pelagic sedimentation likely did not reach depths exceeding a few hundred metres (Goričan et al. 2005). In general, pelagic limestones, not radiolarites, are the predominant pelagic facies in the Middle Triassic rift basins of this region (e.g., Gianolla et al. 1998; Kovács et al. 2011). The prevalence of radiolarites over pelagic limestones in the investigated sections may indicate greater subsidence and a more distal position on the continental margin. Radiolarites from all sections contain Illyrian fauna (i.e., *Spongosilicarmiger italicus* Radiolarian Zone).

The extrusions of trachy-basalts found in the lower part of the Gornji Kamenečki I section were probably controlled by deep-rooted normal faults caused by extension (Fig. 13). Their contact with pelagic limestones indicates submarine extrusion and accumulation. The hyaloclastites present in the lower part of the Brezovica II section were formed by the quenching of magma that came into contact with cold sea water and by the subsequent resedimentation of the newly formed basaltic fragments (Staudigel and Schmincke 1984; Smith and Batiza 1989; Bergh and Sigvaldason 1991; McPhie et al. 1993). The relatively small thickness of these deposits, clast size (ash to lapilli), and their shape (mostly rounded) indicate that the source area could have been located distally; thus, the resedimentation processes could have modified the primary volcanic clasts. The Pietra Verde deposits were deposited in a pelagic environment by different gravitational mechanisms. The presence of X, Y and even bubble-wall shaped shards and rounded quartz crystalloclasts with oval cavities indicate that the material for these deposits came from volcanic eruptions that were enriched in volatiles. The volcanic material was likely deposited in a marine environment as pyroclastic density current deposits (Di Capua and Groppelli 2016, 2018), showing similarities to turbidites in the siliciclastic sense (Carey and Schneider 2011). Water-settled air fall mechanisms might have also played a role. Normal grading with a crystal-rich base, observed in some layers, supports the gravitational character of these deposits. The intercalation of Pietra Verde deposits and radiolarian cherts indicates episodic eruptions and deposition of pyroclastic material. Differences in the thickness of these deposits suggest that reworking of unconsolidated previously deposited volcanic material from topographic heights to deeper parts of the basin also occurred. The age span of the Pietra Verde deposits cannot be precisely determined. Because explosive volcanic eruptions produce a large volume of material available for sedimentation almost instantaneously, thick volcanic deposits can be deposited in pelagic environments within a short period of time. Illyrian age can

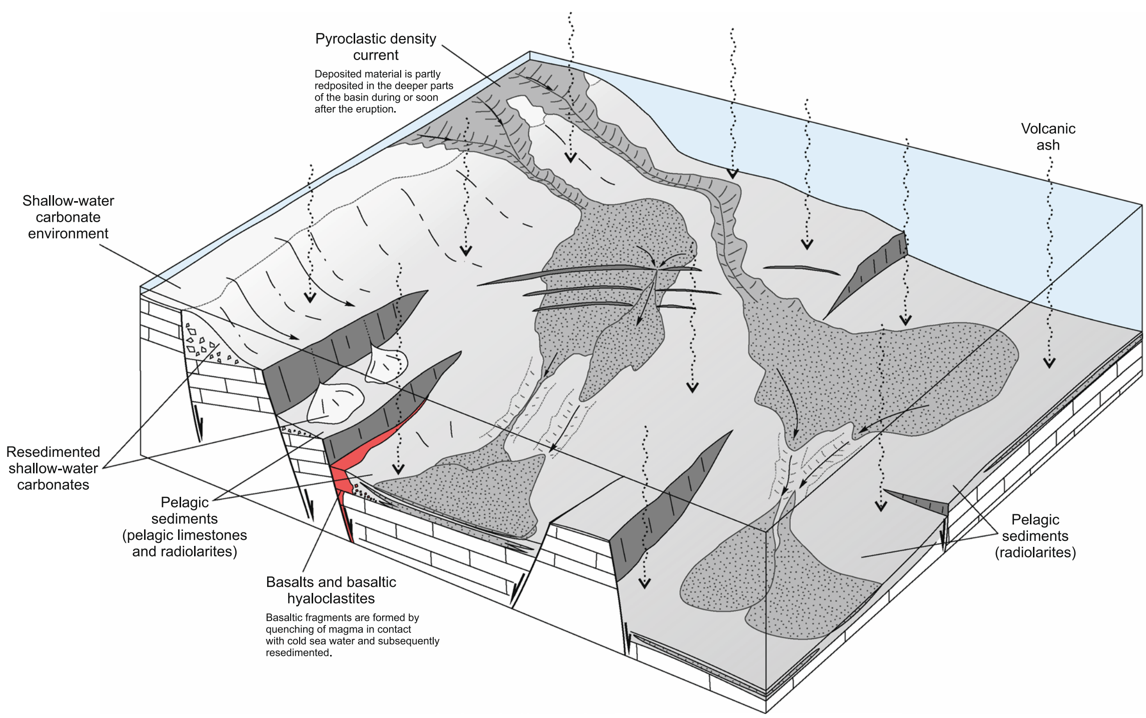


**Fig. 13** Interpretation of depositional environments at the rifted continental margin during the Middle Triassic (not to scale). See the text for discussion

be inferred from the radiolarites intercalated or in contact with volcaniclastics. Regional correlations (see below) indicate that volcanic activity started in the early Ilyirian (*Paraceratites trinodosus* Ammonoid Zone) and persisted through most of the Ladinian (e.g., Wotzlaw et al. 2018; Storck et al. 2018, 2020 and references therein).

Horizontal lamination and normal grading, together with grain size (silt and sand) as well as the mixing of volcanic and pelagic material, indicate that secondary volcaniclastic deposits found on top of Kuna gora IV, Gornji Kamenečki II and Sekolje sections were deposited as medium- to fine-grained turbidites (Stow 1979; Stow and Bowen 1980; Stow and Smillie 2020) with material provided by the reworking of unconsolidated pyroclastic detritus (Di Capua and Groppelli 2018; Di Capua et al. 2021a, b). Radiolarians obtained from these deposits in the Sekolje section are not preserved well enough to place precise age constraints but indicate a late Anisian age. Local and regional correlations (see below) suggest a Late Ladinian age for this facies and a possible significant stratigraphic gap in the investigated successions. In this case, it is likely that radiolarians found in the turbidites were resedimented from the substratum. Resedimentation by turbidites is also indicated by the concentration of radiolarians in the coarser intervals of the medium- to fine-grained turbidites. The stratigraphic gap in succession can be explained by the complex topography of the continental margin and the prevailing sedimentation mechanisms. Pyroclastic density currents have great erosive capacity and can play an important role in the redistribution of material in the sedimentary system (Di Capua and Groppelli 2018). Turbidites and strong bottom currents are also capable of reworking sediments deposited earlier and/or preventing deposition causing hiatuses in the sedimentary record (Stow and Smillie 2020).

## Local correlation

Correlative volcano-sedimentary successions from NW Croatia were previously described from Mt. Žumberak (Goričan et al. 2005) and Mt. Ivanščica (Goričan et al. 2005; Slovenec et al. 2020). These successions are also considered a part of the NCTRB. On Mt. Ivanščica, a platform-to-basin succession from the Belski dol quarry is composed of slope-derived breccia with overlying pelecypod limestones and intermediate to acidic pyroclastic rocks and radiolarites (Goričan et al. 2005). Breccia boulders and clasts were dated as Pelsonian—Illyrian based on benthic association and conodonts, while the breccia matrix contains Illyrian as well as some Fassanian conodont elements. The radiolarians above the breccia were dated as early Ladinian (Fassanian) at that time (Goričan et al. 2005). Following the ratification of the Anisian—Ladinian boundary by IUGS (Brack et al. 2005), the described Fassanian assemblages correspond to the upper Anisian. This succession is correlative to one found in the Kuna gora sections. The absence of coarse-grained breccia on Kuna gora may indicate a more distal position in relation to the shallow-water source of the material. The radiolarian assemblage contains the same age-diagnostic taxa in both successions. Resedimented Illyrian fossiliferous reefal limestones were also found on Mt. Ivanščica in a brecciated layer overlying metabasalts in the Očura quarry (Goričan et al. 2005). However, these assemblages are slightly younger than those found on Kuna gora. In our study, basaltic outflows were found only in the Gornji Kamenički I section overlain by pelagic limestones. Pelagic deposits from Mt. Žumberak, where clastic sequences directly overlie dolomites, include pelagic limestones, cherts and acidic pyroclastic rocks (Goričan et al. 2005). Radiolarian assemblages from these sequences are early Illyrian in age and thus slightly older than those on Mt. Ivanščica or in this study. Citing earlier studies on cephalopods from the Gregurić brijeg locality on Mt. Žumberak (Salopek 1912, 1936), in which the author described early Ladinian ("Buchenstein") and late Ladinian ("Wengen") ammonite species, Goričan et al. (2005) assumed that this locality represents the time span from the Illyrian to the Longobardian. If so, condensed sedimentation and/or stratigraphic gaps, such as those assumed for the sections in this study, can also be assumed for this succession.

In general, pyroclastic deposits intercalated in the pelagic successions of NW Croatia are intermediate to acidic (Goričan et al. 2005). However, a succession of andesitic and basaltic tuffs overlain by Illyrian (i.e., *Reitziites reitzi* Ammonoid Zone) radiolarites has been described from the Cerina locality on the northern slope of Mt. Ivanščica (Slovenec et al. 2020). However, on Kuna gora, andesite-basalt lavas and associated pyroclastic ash-flow tuff were dated by the K–Ar method (on separated K-feldspar) at 241.1 ± 5.2 Ma (Slovenec and Šegvić 2021). In this study, trachy-basaltic rocks were documented at the base of the Gornji Kamenički I section, and trachy-basaltic/andesitic tuff was documented only at the base of the Brezovica II section. Basaltic/andesitic rocks described by Slovenec and Šegvić (2021) are found below the volcano-sedimentary succession described in this study, which could indicate a middle Anisian age.

## Regional correlation

Middle Triassic volcaniclastites interbedded in pelagic sediments have been extensively reported from the Alpine–Carpathian region, including the Dinarides (e.g., Aubouin et al. 1970; Pamić 1984; Brack and Rieber 1986; Obenholzner 1991; Gianolla et al. 1998; Brack et al. 1999, 2005, 2007; Pálfy et al. 2003; Goričan et al. 2005; Budai and Vörös 2006; Velledits 2006; Brühwiler et al. 2007; Vörös et al. 2008; Kovács et al. 2011; Velledits et al. 2011; Gawlick et al.

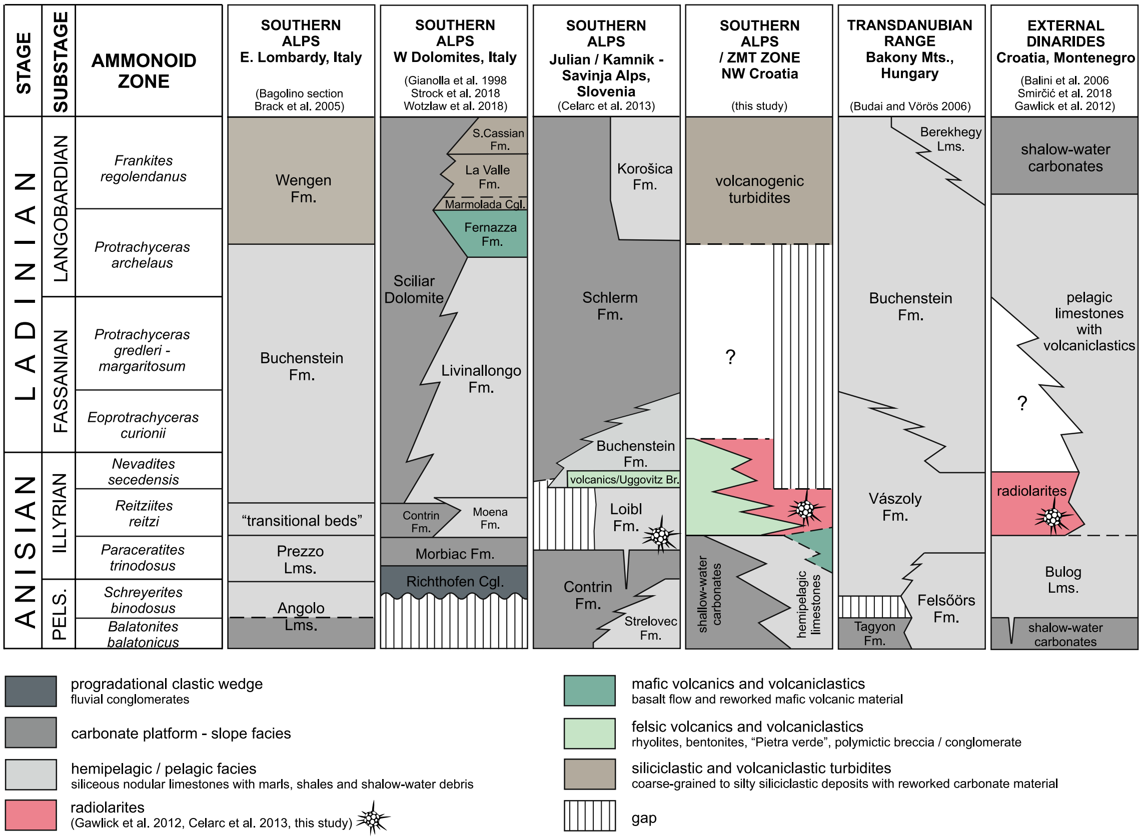


**Fig. 14** Correlation of the Northwestern Croatian Triassic Rift Basin successions with the Middle Triassic formations of the Southern Alps: Lombardian Alps (Brack et al. 2007), Dolomites (Gianolla et al. 1998, Strock et al. 2018, Wotzlaw et al. 2018), Julian and Kamnik-Savinja Alps (Celarc et al. 2013), Transdanubian range (Budai and Vörös 2006) and Dinarides (Balini et al. 2006; Gawlick et al. 2012; Smirčić et al. 2018). See Discussion section for more details

2012, 2021; Sudar et al. 2013; Smirčić et al. 2018, 2020; Slovenec et al. 2020; Karádi et al. 2022). These deposits present a regional marker for the extensional tectonics that created the complex patterns of sedimentary environments on the continental margin. Correlations of the volcano-sedimentary successions from the NCTRB, with selected successions from the Southern Alps, Transdanubian range and Dinarides, are shown in Fig. 14.

In the Dolomites and Lombardian Alps (Southern Alps, Italy), volcano-sedimentary successions reflect irregular patterns of carbonate platforms and deep-water basins that existed in this area during the late Anisian – early Ladinian (Bosellini 1984; Maurer 2000; Bosellini et al. 2003; Brack et al. 2007). In the western Dolomites, shallow-water carbonates of the Contrin Formation were replaced by pelagic carbonates with intercalated pyroclastics of the Buchenstein/Livinallongo Formation in the Illyrian *Reitziites reitzi* Ammonoid zone (Gianolla et al. 1998; Brack and Muttoni 2000; Brack et al. 2007). Shallow-water-derived turbidites and breccias are intercalated within pelagic sediments of the Buchenstein Formation in areas close to prograding carbonate slopes (Gianolla et al. 1998; Brack et al. 2007). Heterogeneous volcanic and volcanically derived rocks of the Fernazza Formation and siliciclastic deposits of the Wengen/La Valle Formation were deposited above the Buchenstein Formation in the late Ladinian (Brack and Reiber 1993; Gianolla et al. 1998; Brack et al. 2005, 2007). On the referent Bagolino section in eastern Lombardy, the onset of pelagic conditions was recorded earlier in the Anisian (*Balatonites balatonicus* Ammonoid Zone; Brack et al. 2005, 2007; Monnet et al. 2008; Storck et al. 2018). The pelagic Prezzo Limestone consists of limestone-shale alternations with the occurrence of the first volcaniclastic layers. The volcaniclastic Pietra Verde deposits intercalated within the Prezzo Limestone and the overlying succession consisting of "transitional beds" and siliceous nodular limestones of the Buchnstein Formation are very well constrained radiometrically between 242.6 and 238.6 Ma and correlate with other sections of this region (Mundil et al. 1996; Brack et al. 2005, 2007; Wotzlaw et al. 2018; Storck et al. 2018). The oldest dated volcaniclastic layers correspond to the Anisian *Paraceratites trinodosus* Ammonoid Zone (Storck et al. 2018). The transition from the Buchenstein Formation to the overlying turbidites of the Wengen Formation is constrained to the Longobardian *Protrachyceras archelaus* Ammoid Zone (Mundil et al. 1996; Storck et al. 2018). This succession is also well constrained biostratigraphically and includes ammonites and thin-shelled bivalves from the genus *Daonella* (Brack and Reiber 1993 and references therein; Brack et al. 2005). The onset of pelagic sedimentation recorded in the investigated sections of the NCTRB correlates well with that recorded in this region. Pelsonian carbonate platform break-up is marked by the deposition of the platform margin or slope facies on Kuna gora, as well as on Ivanščica Mt. (Goričan et al. 2005). The existence of Illyrian carbonate platform deposits correlative to the Contrin Formation is missing. Pelagic sedimentation with deposition of pyroclastic deposits in the *Reitziites reitzi* Ammonoid zone is well documented. A notable difference is the predominance of radiolarian cherts over pelagic limestones. There is also a noticeable difference in the thickness of the pyroclastic deposits, which can be explained by different sedimentation mechanisms. The individual Pietra Verde layers in the Dolomites were originally airborne deposits and redeposition occurred only in more subsided parts (Brack and Muttoni 2000). The gravitational nature of sedimentation, including the instantaneous redeposition of volcanic debris, is inferred to be a major depositional mechanism for the Pietra Verde deposits of NW Croatia. The secondary volcaniclastic deposits that are present on top of the investigated sections in the NCTRB are comparable to siliciclastic deposits of the Wengen Formation. These deposits are devoid of fossil assemblages, except for radiolarians, which are likely resedimented. However, the cephalopod "Wengen" fauna was described from correlative succession in NW Croatia recognized here as a part of the NTCRB earlier (Goričan et al. 2005 and references therein); thus, a Longobardian age can be assumed.

Successions correlative to those described in this study were described from central and western Slovenia (Jurkovšek 1984; Goričan and Buser 1988; Šmuc and Čar 2002). These successions were deposited in the southern part of the Slovenian Basin adjacent to the Adriatic Carbonate Platform (Dinaric Carbonate Platform in the Slovenian literature). Pelagic sedimentation in this area spanned from the late Anisian to the late Ladinian-Carnian, when progradation of the carbonate platform was recorded (Šmuc and Čar 2002), which is analogous to the developments documented in the studied area of the NCTRB (Goričan et al. 2005). Jurkovšek (1984) described pelagic succession consisting of grey nodular cherty limestone, chert, light green tuff (correlative to the Buchenstein Formation) and brown tuffaceous sandstone with black slate at the top (correlative to the Wengen Formation). The Illyrian age was determined by conodonts from the limestone at the base of the succession. Radiolarian assemblages from the cherty limestones intercalated within the pyroclastics contain the same age-diagnostic taxa as those from our described assemblages (Goričan and Buser 1988). These assemblages were previously dated as late Illyrian-Fassanian but now correspond to the late Illyrian after the ratification of the Anisian–Ladinian boundary by the IUGS (Brack et al. 2005). The siliciclastic deposits present on top of the section were dated with Daonellas as Longobardian (Jurkovšek 1984). In western Slovenia, similar Ladinian turbiditic deposits containing volcanoclastic interlayers were dated with Daonellas (Šmuc and Čar 2002 with references). These turbidites are correlative to the secondary volcaniclastic deposits found on top of the successions described from the NCTRB in this study, so the late Ladinian age of these deposits is additionally indicated by this correlation.

In the Southern Alps of Slovenia (Julian Alps and Kamnik-Savinja Alps), pelagic successions recorded the existence of a short-lived Anisian-Ladinian basin (Celarc et al. 2013). Here, drowning of the carbonate platform (Contrin Formation) occurred in the early Anisian *Paraceratites trinodosus* Ammonoid Zone. It is marked by the deposition of red nodular limestone of the Loibl Formation and dated with radiolarians and conodonts. Pyroclastic and felsic volcanic rocks along with carbonate breccia overlie the Loibl Formation, followed by pelagic limestones and marls of the Buchenstein Formation. The massive, partly dolomitized limestones of the Schlern Formation above the Buchenstein Formation record the filling of the basin from the adjacent carbonate platform. The described radiolarian fauna from the pelagic limestones of the Loibl Formation is assigned to the *Spongosilicarmiger transitus* Zone and is thus only slightly older than those found in NW Croatia. Another significant difference is the existence of rhyolite lavas in this succession, whereas only rhyolitic pyroclastites were found in NW Croatia.

The existence of Middle Triassic sedimentary basins formed by extensional tectonics is well documented in the Transdanubian range (Budai and Vörös 2006; Karádi et al. 2022) and Bükk Mountains (Velledits 2006). In the Transdanubian range, the Felsőörs Basin formed on the subsided block of the Tagyon platform in the Pelsonian *Balatonites balatonicus* Zone (Budai and Vörös 2006). The pelagic Felsőörs Formation consists of nodular cherty limestones, marly limestones and bituminous laminites. Tuffite intercalations occur in the upper part of the formation. The overlying Vászoly Formation consists mainly of volcaniclastics and siliceous limestones and gradually passes into the Buchenstein Formation. The radiometric age of this succession (Pálfy et al. 2003; Dunkl et al. 2019; Karádi et al. 2022) shows a good correlation with the data obtained from the Dolomites (e.g., Storck et al. 2018; Wotzlaw et al. 2018). In the Bükk Mountains, rapid subsidence in the Late Anisian-Early Ladinian was preceded by emersion marked by deposition of terrestrial sediments on top of shallow-water carbonates (Velledits 2006). As in other areas affected by rifting, the pelagic sedimentation onwards reflects horst-and-graben topography caused by extensional tectonics.

In the Dinarides, drowning of the carbonate ramp occurred in the Pelsonian. This event is well documented biostratigraphically with conodonts (Gawlick et al. 2012; Sudar et al. 2013; Smirčić et al. 2018). Red nodular Bulog Limestone was deposited above shallow-water carbonates (Dimitrijević and Dimitrijević 1991; Dimitrijević 1997; Gawlick et al. 2012; Sudar et al. 2013; Smirčić et al. 2018, 2020). In places, mixed siliciclastic and carbonate turbidites occur (Dimitrijavić 1997; Smirčić et al. 2018). The succession consisting of approximately six metres of radiolarites above the Bulog Limestone in the High Karst Zone of Montenegro was dated as late Anisian (Gawlick et al. 2012). Thin layers of volcanic ash are also locally present in the radiolarites. These radiolarites are comparable in thickness and age to those found in the NCTRB. They are also assigned to the *Spongosilicarminger italicus* Zone based on the same age-diagnostic species, although the youngest dated sample could be somewhat younger but is still likely Anisian (Gawlick et al. 2012).

Elsewhere in the Dinarides, pelagic limestones intercalated with volcaniclastic deposits were deposited throughout the Anisian and Ladinian (Balini et al. 2006; Missoni et al. 2012; Smirčić et al. 2018, 2020) and extending to the Carnian (Jelaska et al. 2003). In places, the Pietra Verde deposits reach significant thicknesses similar to those in the NCTRB, indicating that material redeposition was one of the main sedimentation mechanisms (Smirčić et al. 2018 and references therein). In places, hyaloclastites comparable to those found in the Brezovica II section occur with peperitic rocks, indicating underwater extrusions (Smirčić et al. 2016). Characteristic upper lower Ladinian (*Protrachyceras gredleri* Ammonoid Zone) radiolarian fauna indicates deposition in a restricted intraplatform basin (Goričan et al. 2015).

## Conclusions

Volcano-sedimentary successions of the NW Croatian mountains, defined as the Northwestern Croatian Triassic Rift Basin, were deposited on a relatively distal part of the continental margin with uneven topography. Pyroclastic deposits were generated from explosive, rift-related volcanism and deposited in a deep-marine environment by gravitational mechanisms, including pyroclastic density currents and resedimentation of unconsolidated, previously deposited volcanic material during multiple explosive phases. Ammonoid fauna indicates the onset of pelagic sedimentation in the Pelsonian with the existence of a coeval shallow-marine carbonate environment that provided carbonate detritus to the deeper parts of the basin. Deposition of radiolarian cherts and intercalated pyroclastic rocks is confined to the late Illyrian and possibly early Fassanian. Secondary volcaniclastic deposits, found higher in the sections, were deposited as medium- to fine-grained turbidites that eroded the substratum. A Longobardian age is assumed for these deposits based on local and regional correlations, indicating condensed sedimentation and/or the existence of a significant stratigraphic gap.

**Acknowledgements** This work was supported by the Croatian Science Foundation under the project "Revealing the Middle Triassic Paleotethyan Geodynamics Recorded in the Volcano-Sedimentary Successions of NW Croatia" (IP-2019-04-3824). The authors would like to thank the staff at the Ivan Rakovec Institute of Palaeontology ZRC SAZU, Ljubljana, for their hospitality and the use of their SEM. Careful review and constructive comments by Andera Di Capua and Péter Ozsvárt helped improve the manuscript. We also thank Professor Ulrich Riller for editorial work and constructive comments.

**Authors contributions** All authors contributed to study conception and design. Material preparation, data collection and analysis were performed by DK, DS, TG, MH, MB, DJ, TK-J, BŠ, LB, MV and DS. The first draft of the manuscript was written by Duje Kukoč and Duje Smirčić, and all authors provided comments for the revision of the manuscript. All authors read and approved the final manuscript.

**Funding** This work was supported by the Croatian Science Foundation under the project "Revealing the Middle Triassic Paleotethyan Geodynamics Recorded in the Volcano-Sedimentary Successions of NW Croatia" (IP-2019–04-3824).

**Data availability** All data generated or analysed during this study are included in this article.

**Code availability** Not applicable.

## Declarations

**Conflict of interest** The authors declare no conflicts of interest/competing interests.

## References

Altiner D, Payne JL, Lehrmann DJ, Özkan-Altiner S, Kelley BM, Summers MM, Yu M (2021) Triassic Foraminifera from the Great Bank of Guizhou, Nanpanjiang Basin, south China: taxonomic account, biostratigraphy, and implications for recovery from end-Permian mass extinction. J Paleontol 95(S84):1–53. https://doi.org/10.1017/jpa.2021.10

Aničić B, Juriša M (1984) Osnovna geološka karta SFRJ 1:100 000. List Rogatec L 33–68. Zvezni geološki zavod Beograd

Aničić B, Juriša M (1985) Osnovna geološka karta SFRJ 1:100 000. Tolmač za list Rogatec L 33–68. Zvezni geološki zavod Beograd

Aubouin J, Blanchet R, Cadet J-P, Celet P, Charvet J, Chorowitz J, Cousin M, Rampnoux J-P (1970) Essai sur la géologie des Dinarides. Bull Soc Géol Fr 12(6):1060–1095. https://doi.org/10.2113/gssgfbull.S7-XII.6.1060

Babić Lj (1976) Stratigrafski slijed i paleogeografska evolucija Ivanščice od gornjeg trijasa do sredine krede (Sedimentary sequence and paleogeographic evolution of Mt. Ivanščica (northern Croatia) from the Upper Triassic to the Middle of Cretaceous. In: Buser S, Drobne K (eds) 8. Jugoslovenski geološki kongres, 1–5 oktober 1974, Bled, 2. dio, Paleontologija, sedimentologija, stratigrafija, pp 53–62

Babić Lj, Hochuli PA, Zupanič J (2002) The Jurassic ophiolitic mélange in the NE Dinarides: Dating, internal structure and geotectonic implications. Eclogae Geol Helv 95:263–275. https://doi.org/10.5169/seals-168959

Babić Lj, Zupanič J (1978) Mlađi mezozoik Ivanščice. In: Babić Lj, Jelaska V (eds) Vodić ekskurzije 3. skupa sedimentologa Jugoslavije, Zagreb, pp 11–23

Ballini M (1994) Middle Triassic Ceratitides (Ammonoidea) collected by C. Renz from Hydra (Greece). Riv It Paleont Strat 100(3):351–364. https://doi.org/10.13130/2039-4942/8606

Balini M, Jurkovšek B, Kolar-Jurkovšek T (2006) New Ladinian ammonoids from Mt. Svilaja (External Dinarides, Croatia). Riv It Paleontol Strat 112(3):383–395. https://doi.org/10.13130/2039-4942/6348

Belak M, Slovenec D, Kolar-Jurkovšek T, Garašić V, Pécskay Z, Tibljaš D, Mišur I (2022) Low-grade metamorphic rocks of the Tethys subduction-collision zone in Medvednica Mt. (NW Croatia). Geol Carpath 73(3):207–229. https://doi.org/10.31577/GeolCarp.73.3.3

Bergh SG, Sigvaldason GE (1991) Pleistocene mass-flow deposits of basaltic hyaloclastite on a shallow submarine shelf, South Iceland. Bull Volcanol 53:597–611. https://doi.org/10.1007/BF00493688

Bosellini A (1984) Progradation geometries of carbonate platforms: example from the Triassic of the Dolomites, northern Italy. Sedimentology 31(1):1–24. https://doi.org/10.1111/j.1365-3091.1984.tb00720.x

Bosellini A, Gianolla P, Stefani M (2003) Geology of the Dolomites. Episodes 26(3):181–185. https://doi.org/10.18814/epiiugs/2003/v26i3/005

Brack P, Muttoni G (2000) High-resolution magnetostratigraphic and lithostratigraphic correlations in Middle Triassic pelagic carbonates from the Dolomites (northern Italy). Palaeogeogr Palaeoclim Palaeoecol 161(3–4):361–380. https://doi.org/10.1016/S0031-0182(00)00081-X

Brack P, Reiber H (1986) Stratigraphy and Ammonoids of the lower Buchenstein Beds of the Brescian Prealps and Giudicarie and their significance for the Anisian/Ladinian boundary. Eclogae Geol Helv 79(1):181–225

Brack P, Reiber H (1993) Towards a better definition of the Anisian/Ladinian boundary: New biostatigraphic data and correlations of boundary sections from the Southern Alps. Eclogae Geol Helv 86(2):415–527

Brack P, Reiber H, Urlichs M (1999) Pelagic successions in the Southern Alps and their correlation with the Germanic Middle Triassic. Zbl Geol Paläont I 7–8:853–876

Brack P, Reiber H, Nicora A, Mundil R (2005) The Global boundary Stratotype Section and Point (GSSP) of the Ladinian Stage (Middle Triassic) at Bagolino (Southern Alps, Northern Italy) and its implications for the Triassic time scale. Episodes 28(4):233–244. https://doi.org/10.18814/epiiugs/2005/v28i4/001

Brack P, Reiber H, Mundil R, Blendinger W, Maurer F (2007) Geometry and chronology of growth and drowning of Middle Triassic carbonate platforms (Cernera and Bivera/Clapsavon) in the Southern Alps (Northern Italy). Swiss J Geosci 100:327–347. https://doi.org/10.1007/s00015-007-1229-x

Brühwiler T, Houchuli PA, Mundil R, Schatz W, Brack P (2007) Bio- and chronostratigraphy of the Middle Triassic Reifling Formation of the westernmost Northern Calcareous Alps. Swiss J Geosci 100:443–455. https://doi.org/10.1007/s00015-007-1240-2

Budai T, Vörös T (2006) Middle Triassic platform and basin evolution of the Southern Bakony Mountains (Transdanubian range, Hungary). Riv It Paleontol Stratigr 112(3):359–371. https://doi.org/10.13130/2039-4942/6346

Carey SN, Schneider J-L (2011) Volcaniclastic processes and deposition in the deep-sea. In: Hüneke H, Mulder T (eds) Deep-sea sediments. Developments in sedimentology 63. Elsevier, Amsterdam, pp 457–515. https://doi.org/10.1016/B978-0-444-53000-4.00007-X

Castellarin A, Lucchini F, Rossi PL, Selli L, Simboli G (1988) The middle triassic magmatic-tectonic arc development in the Southern Alps. Tectonophysics 146(1–4):79–89. https://doi.org/10.1016/0040-1951(88)90083-2

Celarc B, Goričan Š, Kolar-Jurkovšek T (2013) Middle Triassic carbonate-platform break-up and formation of small-scale half-grabens (Julian and Kamnik-Savinja Alps, Slovenia). Facies 59:583–610. https://doi.org/10.1007/s10347-012-0326-0

Chen YL, Krystyn L, Orchard MJ, Lai XL, Richoz S (2015) A review of the evolution, biostratigraphy, provincialism and diversity of Middle and early Late Triassic conodonts. Pap Palaeontol 2(2):235–263. https://doi.org/10.1002/spp2.1038

Csontos L, Vörös A (2004) Mesozoic plate tectonic reconstruction of the Charpatian region. Palaeogeogr Palaeoclim Palaeoecol 210(1):1–56. https://doi.org/10.1016/j.palaeo.2004.02.033

De Zanche V, Gianolla P, Mietto P, Siorpas C, Vail PR (1993) Triassic Sequence Stratigraphy in the Dolomites (Italy). Mem Sci Geol 45:1–27

Di Capua A, Groppelli G (2016) Emplacement of pyroclastic density currents (PDCs) in a deep-sea water environment: the Val d'Aveto Formation case (Northern Apennines, Italy). J Volcanol Geotherm Res 328:1–8. https://doi.org/10.1016/j.jvolgeores.2016.08.003

Di Capua A, Gropelli G (2018) The riddle of volcaniclastic sedimentation in ancient deep-water basin: a discusion. Sediment Geol 378:52–60. https://doi.org/10.1016/j.sedgeo.2018.05.008

Di Capua A, Barilaro F, Groppelli G (2021a) Volcanism and Volcanogenic submarine sedimentation in Paleogene forland basins of the Alps: reassesing the source-to-sink system with an actualistic view. Geosciences 11(1):23. https://doi.org/10.3390/geosciences11010023

Di Capua A, Barilaro F, Szepesi J, Lukács R, Gál P, Norini G, Sulpizio R, Soós I, Harangi S, Groppelli G (2021b) Correlating volcanic dynamics and the construction of a submarine volcanogenic apron: An example from the Badenian (Middle Miocene) of North-Eastern Hungary. Mar Pet Geol 126:104944. https://doi.org/10.1016/j.marpetgeo.2021.104944

Di Capua A, De Rosa R, Kereszturi G, Le Pera E, Rosi M, Watt SFL (2022) Volcanically derived deposits and sequences: a unified terminological scheme for application in modern and ancient environments. Geol Soc Spec Publ. https://doi.org/10.1144/SP520-2021-201

Dimitrijavić MD (1997) Geology of Yugoslavia. Geological Institut GEMINI Special Publication, Beograd

Dimitrijević MN, Dimitrijević MD (1991) Triassic carbonate platform of the Drina-Ivanjica element (Dinarides). Acta Geol Hung 34(1–2):15–44

Dumitrica P (1999) The Oertlispongidae (Radiolaria) from the Middle Triassic of Masirah Island (Oman). Rev Micropaléontol 42:33–42. https://doi.org/10.1016/S0035-1598(99)90164-2

Dumitrica P (2017) On the status of the Triassic Nassellarian radiolarian family Tetraspinocyrtiidae Kozur and Mostler and description of some erlated taxa. Rev Micropaléontol 60(1):33–85. https://doi.org/10.1016/j.revmic.2017.01.001

Dunkl I, Farics É, Józsa S, Lukács R, Haas J, Budai T (2019) Traces of Carnian volcanic activity in the Transdanubian Range, Hungary. Int J Earth Sci (geol Rundsch) 108:1451–1466. https://doi.org/10.1007/s00531-019-01714-w

Epstein AG, Epstein JB, Harris LD (1977) Conodont Color Alteration—an Index to organic Metamorphism. Geol Surv Prof Pap 995:1–27. https://doi.org/10.3133/pp995

Ewart A (1982) The mineralogy and petrology of Tertiary-Recent orogenic volcanic rocks: with special reference to the andesitic-basaltic compositional range. In: Thorpe RS (ed) Andesites: orogenic andesites and related rocks. Wiley, New York, pp 25–95

Ferriere J, Baumgartner PO, Chanier F (2016) The Maliac Ocean: the origin of the Tethyan Hellenic ophiolites. Int J Earth Sci (geol Rundsch) 105:1941–1962. https://doi.org/10.1007/s00531-016-1303-6

Flügel E (2010) Microfacies of carbonate rocks. Springer, Berlin

Gawlick H-J, Firch W, Hoxa L, Dumitrica P, Krystin L, Lein R, Missoni S, Schlagintweit F (2008) Mirdita Zone ophiolites and associated sediments in Albania reveal Neotethys Ocean origin. Int J Earth Sci (geol Rundsch) 97:865–881. https://doi.org/10.1007/s00531-007-0193-z

Gawlick H-J, Goričan Š, Missoni S, Lein R (2012) Late Anisian platform drowning and radiolarite deposition as a consequence of the opening of the Neotethys ocean (High Karst nappe, Montenegro). Bull Soc Géol France 183(4):349–358. https://doi.org/10.2113/gssgfbull.183.4.349

Gawlick H-J, Lein R, Bucur II (2021) Precursor extension to the final Neo-Tethys break-up: flooding events and their significance for the correlation of shallow-water and deep marine organisms (Anisian, Eastern Alps, Austria). Int J Earth Sci (geol Rundsch) 110:419–446. https://doi.org/10.1007/s00531-020-01959-w

Gaetani M, Jacobshagen V, Nicora A, Kaufmann G, Tselepides V, Fantini-Sestini N, Mertmann D, Skourtsis-Coroneu V (1992) The Early-Middle Triassic Boundary at Chios (Greece). Riv It Paleontol Strat 98(2):181–204. https://doi.org/10.13130/2039-4942/8934

Germani D (1997) New data on ammonoids and biostratigraphy of the classical Spathian Kçira section (Lower Triassic, Albania). Riv It Paleontol Strat 103(3):267–292. https://doi.org/10.13130/2039-4942/7041

Gianolla P, De Zanche V, Mietto P (1998) Triassic sequence stratigraphy in the Southern Alps (Northern Italy): definition of sequence and basin evolution. In: de Graciansky PC, Hardenbol J, Jaquin T, Vail PR (eds) Mesozoic and Cenozoic sequence stratigraphy of European basins. SEPM Spec Publ 60:719–747. https://doi.org/10.2110/pec.98.02.0719

Golub Lj, Brajdić V (1970) Eruptivi i piroklastiti iz područja Vudelja i potoka Bistrice na sjevernim padinama Ivančice (Eruptive and pyroclastic rocks from Vudelja and from the Bistrica brook on the northern slopes of Mt. Ivanščica (Hrvatsko Zagorje, Yugoslavia). Zbornik radova Rudarsko-geološko-naftnog fakulteta 30. god. rada (1939–1969), Zagreb, pp 123–127

Golub Lj, Brajdić V, Šebečić B (1969) Eruptivne i piroklastične stijene Strahinšćice (Eruptive and pyroclastic rocks from Mt. Strahinjščica, Croatan Zagorje. Geol Vjesnik 23:205–217

Goričan Š, Buser S (1988) Middle Triassic radiolarians from Slovenia (Yugoslavia). Geologija 31:133–197

Goričan Š, Halamić J, Grgasović T, Kolar-Jurkovšek T (2005) Stratigraphic evolution of Triassic arc-back arc system in northwestern Croatia. Bull Soc Géol France 176(1):3–22. https://doi.org/10.2113/176.1.3

Goričan Š, Kolar-Jurkovšek T, Jurkovšek B (2015) Palaeoecology of Middle Triassic Low Diversity Radiolarian Fauna from Mt. Svilaja (External Dinarides, Croatia). In: Tekin UK, Tuncer A (eds) Abstract book of the 14th Interrad: An International Conference on Fossils and Recent Radiolarians, Antalya, Turkey, Radiolaria 35, pp 142–143

Goričan Š, O'Dogherty L, Baumgartner PO, Carter ES (2018) Mesozoic radiolarian biocronology – current status and future directions. Rev Micropaléontol 61(3–4):165–189. https://doi.org/10.1016/j.revmic.2018.08.001

Gorjanović-Kramberger D (1896) Die Fauna des Muschelkalkes der Kuna Gora in Croatien. Verhandlungen Der Kaiserlich-Königlichen Geologishen Reichsanstalt 15:201–205

Grgasović T (1997) Upper Triassic biostratigraphy and algae from Žumberak (Croatia). Geol Croat 50(2):201–214. https://doi.org/10.4154/GC.1997.28

Grgasović T (2022) Taxonomy of the fossil calcareous algae: Revision of genera *Physoporella* Steinmann and *Oligoporella* Pia (Dasycladales). Carnets Geol 22(7):171–310. https://doi.org/10.2110/carnets.2022.2207

Haas J, Budai T (1995) Upper Permian-Triassic Facis Zones in the Transdanubian Range. Riv It Paleontol Strat 101(3):249–266. https://doi.org/10.13130/2039-4942/8587

Haas J, Mioč P, Pamić J, Tomljenović B, Árkai P, Bérczi-Makk A, Koroknai B, Kovács S, Felgenhauer ER (2000) Complex structural pattern of the Alpine–Dinaridic–Pannonian triple junction. Int J Earth Sci (geol Rundsch) 89:377–389. https://doi.org/10.1007/s005310000093

Halamić J, Slovenec D, Kolar-Jurkovšek T (1998) Triassic Pelagic Limestones in Pillow Lavas in the Orešje Quarry near Gornja Bistra, Medvednica Mt. (Northwest Croatia). Geol Croat 51:33–45. https://doi.org/10.4154/GC.1998.06

Harangi SZ, Szabó CS, Józsa S, Szoldán ZS, Árva-Sós E, Balla M, Kubovics I (1996) Mesozoic igneous suites in Hungary: implications for genesis and tectonic setting in the northwestern part of Tethys. Int Geol Rev 38(4):336–360. https://doi.org/10.1080/00206819709465339

Japundžić D, Prlj Šimić N, Krizmanić K, Cuković Z (2015) Nova pelsonijska (srednji anizik) cefalopodna fauna s područja „Triplex Confinium" (Poštak, Gologlav, Orlovica), južna Hrvatska (New Pelsonian (Middle Anisian) cephalopod fauna from „Triplex Confinium" (Poštak, Gologlav Orlovica), south Croatia). In: Horvat M, Wacha L (eds) 5th Croatian Geological Congress with international participation, Abstracts book, Hrvatsko geološko društvo, Zagreb, pp 119–120

Jelaska V, Kolar-Jurkovšek T, Jurkovšek B, Gušić I (2003) Triassic beds in the basement of the Adriatic-Dinaric Carbonate Platform of the Svilaja Mt. (Croatia). Geologija 46(2):225–230. https://doi.org/10.5474/geologija.2003.019

Jurkovšek B (1984) Langobardian beds with daonaellas and posidonias in Slovenia. Geologija 27:41–95

Karádi V, Budai T, Haas J, Vörös A, Piros O, Dunkl I, Tóth E (2022) Change from shallow to deep-water environment on an isolated carbonate platform in the Middle Triassic of the Transdanubian Range (Hungary). Palaeogeogr Palaeoclimat Palaeoecol 587:110793. https://doi.org/10.1016/j.palaeo.2021.110793

Kolar-Jurkovšek T, Jurkovšek B (2019) Konodonti Slovenije (Conodonts of Slovenia). Geološki zavod Slovenije, Ljubljana

Kovács S, Sudar M, Grădinaru E, Gawlick H-J, Karamata S, Haas J, Péró C, Gaetani M, Mello J, Polák M, Aljinović D, Ogorelec B, Kolar-Jurkovšek T, Jurkovšek B, Buder S (2011) Triassic evolution of the tectonostratigraphic units of the Circum-Pannonian Region. Jb Geol B-A 151(3–4):199–280

Kozur HW (2003) Integrated ammonoid, conodont and radiolarian zonation of the Triassic. Hallesches Jahrb Geowiss 25:49–79

Kozur H, Mostler H (1994) Anisian to Middle Carnian radiolarian-zonation and description of some stratigraphically important radiolari-ans. Geol Paläont Mitt Innsbr Sonderband 3:39–255

Kozur HW, Krainer K, Mostler H (1996) Radiolarians and facies of the Middle Triassic Loibl Formation, South Alpine Karawanken

Mountains (Carinthia, Austria). Geol Paläont Mitt Innsbr Sonderband 4:195–269
Lužar-Oberiter B, Mikes T, von Eynatten H, Lj B (2009) Ophiolitic detritus in Cretaceous clastic formations of the Dinarides (NW Croatia): evidence from Cr–spinel chemistry. Int J Earth Sci (geol Rundsch) 98:1097–1108. https://doi.org/10.1007/s00531-008-0306-3
Lužar-Oberiter B, Mikes T, Dunkl I, Lj B, von Eynatten H (2012) Provenance of Cretaceous synorogenic sediments from NW Dinarides (Croatia). Swiss J Geosci 105:377–399. https://doi.org/10.1007/s00015-012-0107-3
Marci V, Ščavničar S, Sijarić G (1984) Novi podaci o vulkanskim stijenama Ivanščice (sliv potoka Železnice). Geol Vjesnik 37:97–104
Maurer F (2000) Growth mode of Middle Triassic carbonate platforms in the Western Dolomites (Southern Alps, Italy). Sediment Geol 134(3–4):275–286. https://doi.org/10.1016/S0037-0738(00)00049-X
McPhie J, Doyle M, Allen R (1993) Volcanic textures—a guide to the interpretation of textures in volcanic rocks. Centre for Ore Deposit and Exploration Studies, University of Tasmania
Missoni S, Gawlick H-J, Sudar MN, Jovanović D, Lein R (2012) Onset and demise of the Wetterstein Carbonate Platform in the mélange areas of the Zlatibor Mountain (Sirogojno, SW Serbia). Facies 58:95–111. https://doi.org/10.1007/s10347-011-0274-0
Monnet C, Brack P, Bucher H, Reiber H (2008) Ammonoids of the middle/late Anisian boundary (Middle Triassic) and the transgression of the Prezzo Limestone in eastern Lombardy-Giudicarie (Italy). Swiss J Geosci 101:61–84. https://doi.org/10.1007/s00015-008-1251-7
Mundil R, Brack MM, Rieber H, Oberli F (1996) High Resolution U-Pb Dating of Middle Triassic Volcaniclastics: Time-Scale Calibration and Verification for Tuning Parameters for Carbonate Sedimentation. Earth Planet Sci Lett 141(1–4):137–151. https://doi.org/10.1016/0012-821X(96)00057-X
Mundil R, Zühlke R, Bechstädt T, Peterhänsel A, Egenhoff SO, Oberli F, Meier M, Brack P, Reiber H (2003) Cyclicities in Triassic platform carbonates: synchronizing radio-isotopic and orbital clocks. Terra Nova 15:81–87. https://doi.org/10.1046/j.1365-3121.2003.00475.x
Mundil R, Pálfy J, Renne PE, Brack P (2010) The Triassic timescale: new constraints and a review of geochronological data. In: Lucas SG (ed) The Triassic Timescale. Geol Soc Spec Publ 334:41–60. https://doi.org/10.1144/SP334.3
Muttoni G, Kent DV, Meço S, Balini M, Nicora A, Rettori R, Gaetani M, Krystyn L (1998) Towards a better definition of the Middle Triassic magnetostratigraphy and biostratigraphy in the Tethyan Realm. Earth Planet Sci Lett 164(1–2):285–302. https://doi.org/10.1016/S0012-821X(98)00215-5
Nakaseko K, Nishimura A (1979) Upper Triassic Radiolaria from Southwest Japan. Sci Rep Col Gen Educ Osaka Univ 28(2):61–109
Obenholzner JH (1991) Triassic Volcanogenic Sediments from the Southern Alps (Italy, Austria, Yugoslavia). A Contribution to the “Pietra Verde” Problem. Sediment Geol 74(1–4):157–171. https://doi.org/10.1016/0037-0738(91)90038-F
O’Dogherty L, Carter ES, Dumitrica P, Goričan Š, De Wever P, Hungerbühler A, Bandini AN, Takemura A (2009) Catalogue of Mesozoicradiolarian genera. Part 1: Triassic. Geodiversitas 31(2):213–270. https://doi.org/10.5252/g2009n2a3
O’Dogherty L, Carter ES, Goričan Š, Dumitrica P (2010) Triassic radiolarian biostratigraphy. In: Lucas SG (ed) The Triassic Timescale. Geol Soc Spec Publ 334 (1):163–200. https://doi.org/10.1144/SP334.8
Pálfy J, Parrish RR, David K, Vörös A (2003) Mid-Triassic integrated U-Pb geochronology and ammonoid biochronology from the Balaton Highland (Hungary). J Geol Soc London 160(2):271–284. https://doi.org/10.1144/0016-764902-029
Pamić J (1984) Triassic magmatism of the Dinarides in Yugoslavia. Tectonophysics 109(3–4):273–307. https://doi.org/10.1016/0040-1951(84)90145-8
Pamić J, Tomljenović B (1998) Basic geological data on the Croatian part of the Mid-Transdanubian Zone as exemplified by Mt. Medvednica located along the Zagreb-Zemplen Fault Zone. Acta Geol Hung 41(4):389–400
Pamić J, Tomljenović B, Balen D (2002) Geodynamic ad petrogenetic evolution of Alpine ophiolites from the central and NW Dinarides: an overview. Lithos 65(1–2):113–142. https://doi.org/10.1016/S0024-4937(02)00162-7
Peccerillo R, Taylor SR (1976) Geochemistry of Eocene calc-alkaline volcanic rocks from the Kastamonu area, Northern Turkey. Contr Miner Pet 58:63–81. https://doi.org/10.1007/BF00384745
Rejebian VA, Harris AG, Huebner JS (1987) Conodont color and textural alteration: An index to regional metamorphism, contact metamorphism, and hydrothermal alteration. Geol Soc Am Bull 99(4):471–479. https://doi.org/10.1130/0016-7606(1987)99%3c471:CCATAA%3e2.0.CO;2
Rettori R (1995) Foraminiferi del Trias inferiore e medio della Tetide: Revisione tassonomica, stratigrafia ed interpretazione filogenetica. Université de Genève, Publications du Département de Géologie et Paléontologie 18
Salaj J, Borza K, Samuel O (1983) Triassic foraminifers of the west Carpathians. Geologický Ustav Dionýza Stúra, Bratislava
Salopek M (1912) O srednjem trijasu Gregurić brijega u Samoborskoj gori i o njegovoj fauni (On the Middle Triassic of Gregurić brijeg in Samoborska gora Mt. and its fauna). Djela Jugoslavenske Akademije Znanosti i Umjetnosti 20:1–34
Salopek M (1914) O naslagama s okaminama kod Kunovac vrela u Lici (On fossil deposits near Kunovac spring in Lika). Prirodoslovna Istraživanja Jugoslavenske Akademije Znanosti i Umjetnosti 4:1–23
Salopek M (1918a) O ladiničkim škriljevcima kod Donjeg Pazarišta (On Ladin slates near Donje Pazarište). Prirodoslovna Istraživanja Jugoslavenske Akademije Znanosti i Umjetnosti 13:3–20
Salopek M (1918b) Monografija trijadičke faune Kuna-gore (Monograph of the Triassic fauna of Kuna Gora). Prirodoslovna Istraživanja Jugoslavenske Akademije Znanosti i Umjetnosti 13:21–27
Salopek M (1918c) O naslagama s Daonellama u Hrvatskoj (On deposits with Daonellas in Croatia - in Croatian). Prirodoslovna Istraživanja Jugoslavenske Akademije Znanosti i Umjetnosti 13:28–33
Salopek M (1919) Monografija trijadičke faune Kuna-gore II (Monograph of the Triassic fauna of Kuna Gora II). Prirodoslovna Istraživanja Jugoslavenske Akademije Znanosti i Umjetnosti 14:165–184
Salopek M (1936) O cefalopodnim vapnencima Gregurić-brijega u Samoborskoj gori (On the cephalopod limestones of Gregurić-brijeg in Samoborska gora Mt). Prirodoslovna Istraživanja Jugoslavenske Akademije Znanosti i Umjetnosti 20:201–228
Schmid SM, Bernoulli D, Fügenschuh B, Matenco L, Scheffer S, Schuster R, Tischler M, Ustaszewski K (2008) The Alpine-Carpathian-Dinaridic orogenic system: correlation and evolution of tectonic units. Swiss J Geosci 101:139–183. https://doi.org/10.1007/s00015-008-1247-3
Schmid SM, Fügenschuh B, Kounov A, Matenco L, Nievergelt P, Oberhänsli R, Pleuger J, Schefer S, Schuster R, Tomljenović B, Ustaszewski K, van Hinsbergen DJJ (2020) Tectonic units of the Alpine collision zone between Eastern Alps and western Turkey. Gondwana Res 78:308–374. https://doi.org/10.1016/j.gr.2019.07.005

Slovenec D, Šegvić B (2021) Middle Triassic high-K calc-alkaline effusive and pyroclastic rocks from the Zagorje-Mid-Transdanubian Zone (Mt. Kuna Gora; NW Croatia): mineralogy, petrology, geochemistry and tectono-magmatic affinity. Geol Acta 19(2):1–23. https://doi.org/10.1344/GeologicaActa2021.19.2

Slovenec D, Lugović B, Meyer H-P, Garapić Šiftar G (2011) A tectono-magmatic correlation of basaltic rocks from ophiolite mélanges at the north-eastern tip of the Saa-Vardar suture zone, Northern Croatia, constrained by geochemistry and petrology. Ofioliti 36(1):77–100. https://doi.org/10.4454/ofioliti.v36i1.395

Slovenec D, Šegvić B, Halamić J, Goričan Š, Zanoni G (2020) An ensialic volcanic arc along the northwestern edge of Palaeotethys-Insights from the Mid-Triassic volcanosedimentary succession of Ivanščica Mt. (northwestern Croatia). Geol J 55(6):4324–4351. https://doi.org/10.1002/gj.3664

Slovenec D, Horvat M, Smirčić D, Belak M, Badurina L, Kukoč D, Grgasović T, Byerly K, Vukovski M, Šegvić B (2023) On the evolution of Middle Triassic passive margins of the Greater Adria Plate: inferences from the study of calc-alkaline and shoshonitic tuffs from NW Croatia. Ofioliti 58(1):31–46. https://doi.org/10.4454/ofioliti.v48i1.560

Smirčić D, Lugović B, Aljinović D, Hrvatović H, Kolar-Jurkovšek T, Jurkovšek B, Gajšak F (2016) Middle Triassic autoclastic deposits in the vicinity of Bosansko Grahovo (SW Bosnia and Herzegovina). Rud Geol Naft Zb 31(2):1–12. https://doi.org/10.17794/rgn.2016.2.1

Smirčić D, Kolar-Jurkovšek T, Aljinović D, Barudžija U, Jurkovšek B, Hrvatović H (2018) Stratigraphic definition and correlation of the Middle Triassic volcaniclastic facies in the External Dinarides: Croatia and Bosnia and Herzegovina. J Earth Sci 29:864–878. https://doi.org/10.1007/s12583-018-0789-1

Smirčić D, Japundžić D, Gaberšek N, Aljinović D, Prlj-Šimić N, Borčić N, Krizmanić K, Pavić I, Barudžija U (2020) First record of the upper Illyrian ammonoid subzone marker *Reitziites reitzi* in the Karst Dinarides. Rud Geol Naft Zb 35(2):75–84. https://doi.org/10.17794/rgn.2020.2.7

Smith TL, Batiza R (1989) New field and laboratory evidence for the origin of hyaloclastite flows on seamount summits. Bull Volcanol 51:96–114. https://doi.org/10.1007/BF01081979

Stampfli GM, Borel GD (2002) A plate tectonic model for the Paleozoic and Mesozoic constrained by dynamic plate boundaries and restored synthetic ocean isochrons. Earth Planet Sci Lett 196(1–2):17–33. https://doi.org/10.1016/S0012-821X(01)00588-X

Staudigel H, Schmincke H-U (1984) The Pliocene seamount series of La Palma, Canary Islands. J Geophys Res Solid Earth 89(B13):11195–11215. https://doi.org/10.1029/JB089iB13p11195

Stockar R, Dumitrica P, Baumgartner PO (2012) Early Ladinian radiolarian fauna from the Monte San Giorgio (Southern Alps, Switzerland): systematics, biostratigraphy and paleo(bio)geograhic implicatios. Riv It Paleontol Strat 118(3):375–437. https://doi.org/10.13130/2039-4942/6012

Storck J-K, Brack P, Wotzlaw JF, Ulmer P (2018) Timing an evolution of Middle Triassic magmatism in the Southern Alps (northern Italy). J Geol Soc Lond 176(2):253–268. https://doi.org/10.1144/jgs2018-123

Storck J-K, Wotzlaw J-F, Karakas Ö, Brack P, Gerdes A, Ulmer P (2020) Hafnium isotopic record of mantle-crust interaction in an evolving continental magmatic system. Earth Planet Sci Lett 535:116100. https://doi.org/10.1016/j.epsl.2020.116100

Stow DAV (1979) Distinguishing between fine-grained turbidites and contourites on the Nova Scotian deep water margin. Sedimentology 26(3):371–387. https://doi.org/10.1111/j.1365-3091.1979.tb00915.x

Stow DAV, Bowen AJ (1980) A physical model for the transport and sorting of fine-grained sediment by turbidity currents. Sedimentology 27(1):31–46. https://doi.org/10.1111/j.1365-3091.1980.tb01156.x

Stow D, Smillie Z (2020) Distinguishing between deep-water sediment facies: Turbidites, Conturites and Hemipelagites. Geosciences 10(2):68. https://doi.org/10.3390/geosciences10020068

Sudar M (1986) Triassic microfossils and biostratigraphy of the Inner Dinarides between Gučevo and Ljubišnja mts., Yugoslavija (Mikrofosili i biostratigrafija trijasa unutrašnjih Dinarida Jugoslavije između Gučeva i Ljubišnje). Geološki Anali Balkanskoga Poluostrva 50:151–394

Sudar M, Gawlick H-J, Lein R, Missoni S, Kovács S, Jovanović D (2013) Depositional environment, age and facies of the Middle Triassic Bulog and Rid Formations in the Inner Dinarides (Zlatobor Mountain, SW Serbia): evidence for the Anisian break-up of the Neotethys Ocean. N Jb Geol Paläont Abh 269(3):291–320. https://doi.org/10.1127/0077-7749/2013/0352

Šćavinčar B, Sćavinčar S, Šušnjara A (1984) Vulkanogeno-sedimentni srednji trijas u području potoka Suvaja (Svilaja pl., Vanjski Dinariai (The volcanic-sedimentary Middle Triassic in the Suvaja Brook Area (Mt. Svilaja, Outer Dinarides). Acta Geologica 14(2):35–82

Šimunić Al, Šimunić An (1979) Petrografski sastav i geneza trijaskih naslaga Ivanščice, Kalnika i Ravne gore (Hrvatsko zagorje) (Petrographic composition and genesis of Triassic deposits of Ivanščica, Kalnik and Ravna gora Mountain). Geol Vjesnik 32:243–253

Šimunić Al, Šimunić An (1997) Triassic deposits of Hrvatsko Zagorje. Geol Croat 50(2):243–250. https://doi.org/10.4154/GC.1997.32

Šimunić An, Pikija M, Hećimović I, Šimunić Al (1981) Osnovna geološka karta SFRJ 1:100,000. Tumač za list Varaždin L 33–69 (Basic Geological Map of SFRY 1:10000, Geology of the sheet Varaždin L 33–69). Geološki zavod Zagreb, Savezni geološki zavod Beograd

Šimunić An, Pikija M, Hećimović I (1983) Osnovna geološka karta SFRJ 1:100,000. List Varaždin L 33–69. Savezni geološki zavod Beograd

Šmuc A, Čar J (2002) Upper Ladinian to Lower Carnian Sedimentary Evolution in the Idrija-Cerkno Region, Western Slovenia. Facies 46:205–216. https://doi.org/10.1007/BF02668081

Tomljenović B, Csontos L (2001) Neogene-Quaternary structures in the border zone between Alps, Dinarides and Pannonian Basin (Hrvatsko zagorje and Karlovac Basins, Croatia). Int J Earth Sci (geol Rundsch) 90:560–578. https://doi.org/10.1007/s005310000176

Tomljenović B, Csontos L, Márton E, Márton P (2008) Tectonic evolution of the northwestern Internal Dinarides as constrained by structures and rotation of Medvednica Mountains, North Croatia. Geol Soc Spec Publ 298(1):145–167. https://doi.org/10.1144/SP298.8

Trubelja F, Burgath KP, Marchig V (2004) Triassic magmatism in the area of the Central Dinarides (Bosnia and Herzegovina): geochemical resolving of tectonic setting. Geol Croat 57(2):159–170. https://doi.org/10.4154/GC.2004.13

van Gelder IE, Matenco L, Willingshofer E, Tomljnović B, Andriessen PAM, Ducea MN, Beniest A, Gruić A (2015) The tectonic evolution of a critical segment of the Dinarides-Alps connection: Kinematic and geochronological inferences from the Medvednica Mountains, NE Croatia. Tectonics 34(9):1952–1978. https://doi.org/10.1002/2015TC003937

van Hinsbergen DJJ, Torsvik TH, Schmid SM, Maţenco LC, Maffione M, Vissers RLM, Gürer D, Spakman W (2020) Orogenic architecture of the Mediterranean region and kinematic reconstruction of its tectonic evolution since the Triassic. Gondwana Res 81:79–229. https://doi.org/10.1016/j.gr.2019.07.009

Velledits F (2006) Evolution of the Bükk Mountains (NE Hungary) during the Middle-Late Triassic asymetric rifting of the

Vardar-Meliata branch of the Neotethys Ocean. Int J Earth Sci (geol Rundsch) 95:395–412. https://doi.org/10.1007/s00531-005-0041-y
Velledits F, Péró CS, Blau J, Senowbari-Daryan B, Kovács S, Piros O, Pocsai T, Szügyi-Simon H, Dumitrică P, Pálfy J (2011) The oldest Triassic platform margin reef from the Alpine-Carpathian Triassic, Aggtelek, NE Hungary. Riv It Paleontol Strat 117(2):221–268. https://doi.org/10.13130/2039-4942/5973
Vörös A (2003) The Pelsonian ammonoid fauna of the Balaton Highland. In: Vörös A (ed) The Pelsonian Substage on the Balaton Highland (Middle Triassic, Hungary). Geologica Hungarica, Series Palaeontologica, vol 55, pp 71–121
Vörös A (2010) Late Anisian Ammonoidea from Szár-hegy (Rudabánya Mts); a Dinaric-type fauna from North Hungary. Fragm Palaeont Hung 28:1–20
Vörös A (2014) Ammonoid diversification in the Middle Triassic: examples from the Tethys (Eastern Lombardy, Balaton Highland) and the Pacific (Nevada). Cent Eur Geol 57(4):319–343. https://doi.org/10.1556/ceugeol.57.2014.4.1
Vörös A (2018) The Upper Anisian ammonoids of the Balaton Highland (Middle Triassic, Hungary). Geol Hung Palaeontol 60:1–241
Vörös A, Budai T, Szabó I (2008) The base of the Curionii Zone (Ladinian, Triassic) in Felsőörs (Hungary): improved correlation with the Global Stratotype Section. Cent Eur Geol 51(4):325–339. https://doi.org/10.1556/ceugeol.51.2008.4.3
Wotzlaw J-F, Brack P, Strock J-C (2018) High-resolution stratigraphy and zircon U-Pb geochronology of the Middle Triassic Buchenstein Formation (Dolomites, northern Italy): precession-forcing of hemipelagic carbonate sedimentation and calibration of the Anisian-Ladinian boundary interval. J Geol Soc 175(1):71–85. https://doi.org/10.1144/jgs2017-052

# 3. EVOLUTION OF EASTERN PASSIVE MARGIN OF ADRIA RECORDED IN SHALLOW- TO DEEP-WATER SUCCESSIONS OF THE TRANSITION ZONE BETWEEN THE ALPS AND THE DINARIDES (IVANŠČICA MT., NW CROATIA)

By

**Matija Vukovski**, Duje Kukoč, Tonći Grgasović, Ladislav Fuček & Damir Slovenec

*Published in Facies*

*DOI: https://doi.org/10.1007/s10347-023-00674-7*

Facies (2023) 69:18
https://doi.org/10.1007/s10347-023-00674-7

ORIGINAL ARTICLE

# Evolution of eastern passive margin of Adria recorded in shallow- to deep-water successions of the transition zone between the Alps and the Dinarides (Ivanščica Mt., NW Croatia)

Matija Vukovski[1] · Duje Kukoč[1] · Tonći Grgasović[1] · Ladislav Fuček[1] · Damir Slovenec[1]

Received: 24 May 2023 / Accepted: 4 September 2023


**Abstract**
Upper Triassic to Lower Cretaceous stratigraphic successions deposited on the passive continental margin of Adria microplate facing the Neotethys Ocean were investigated on Ivanščica Mt. (NW Croatia). This area represents a transitional area between the Alps and the Dinarides. After a short Middle Triassic pelagic episode related to the rifting of the Neotethys, progradation of the carbonate platform over newly formed grabens resulted in formation of stable shallow-water depositional environment during the Late Triassic. Tectonically induced subsidence pulse at the Triassic/Jurassic boundary affected SE part of the investigated area resulting in the deposition of pelagic limestones, shale, marls, and calcarenites above Upper Triassic platform carbonates. At the same time, NW part of the investigated area was still characterized by shallow-water sedimentation until the Pliensbachian. This second subsidence phase was manifested by formation of neptunian dykes within Lower Jurassic platform limestones and deposition of the Middle Jurassic pelagic limestones. These two Early Jurassic subsidence events are likely related to the rifting of the Alpine Tethys. Radiolarian cherts were deposited in both areas in the late Middle and Late Jurassic. Radiolarians from the SW Ivanščica Mt. indicate late Bathonian to Early Tithonian age of the radiolarian cherts. Uppermost Jurassic to Lower Cretaceous Aptychus limestone is found across the entire investigated area. These limestones were deposited from the Late Tithonian to the Valanginian when synorogenic mixed carbonate–siliciclastic turbidites started to fill the basin indicating a prominent compressional tectonic phase widely recorded in the Alps and the Dinarides.

**Keywords** Mesozoic · Platform drowning · Calcareous algae · Foraminifera · Radiolaria

## Introduction

In the transitional area between two orogens, the Alps and the Dinarides, in NW Croatia (Fig. 1a), Mesozoic formations, including stratigraphic successions derived from the passive continental margin of Adria microplate, are exposed from beneath thick sedimentary cover of the Pannonian Basin in several chain-forming mountains. This area was formed by complex, polyphase Mesozoic and Cenozoic tectonic history, mainly related to the evolution of Neotethys Ocean (Schmid et al. 2008, 2020; Tomljenović et al. 2008; van Gelder et al. 2015) and Pannonian Basin System (Tomljenović and Csontos 2001; Horváth et al. 2006; Balázs et al. 2016; Fodor et al. 2021). Middle Triassic and Early Jurassic rifting events related to opening of the Neotethys and the Alpine Tethys shaped the margin and formed rugged topography with deep-water basins and isolated morphological highs (e.g., Goričan et al. 2012, 2022). Shallow-water carbonate sedimentation persisted on these heights until final subsidence in the Early Jurassic (Šmuc 2005; Goričan et al. 2012; Rožič et al. 2017). Consequently, since the Toarcian onwards, Adriatic Carbonate Platform (AdCP, sensu Vlahović et al. 2005) remained the only carbonate platform in the area, rimmed by deep-water basins of the passive margin. In the Middle Jurassic, intraoceanic subduction started in the Neotethys, with Adria becoming the subducting plate (Schmid et al. 2008, 2020; Bortolotti et al. 2013) and trench-like basins formed in front of the advancing nappes (Gawlick and Missoni 2019). Obduction of ophiolites on the passive margin started in the Late Jurassic and lasted until the Early Cretaceous (Schmid et al. 2008,

✉ Duje Kukoč
dkukoc@hgi-cgs.hr

[1] Department of Geology, Croatian Geological Survey, Sachsova 2, 10000 Zagreb, Croatia

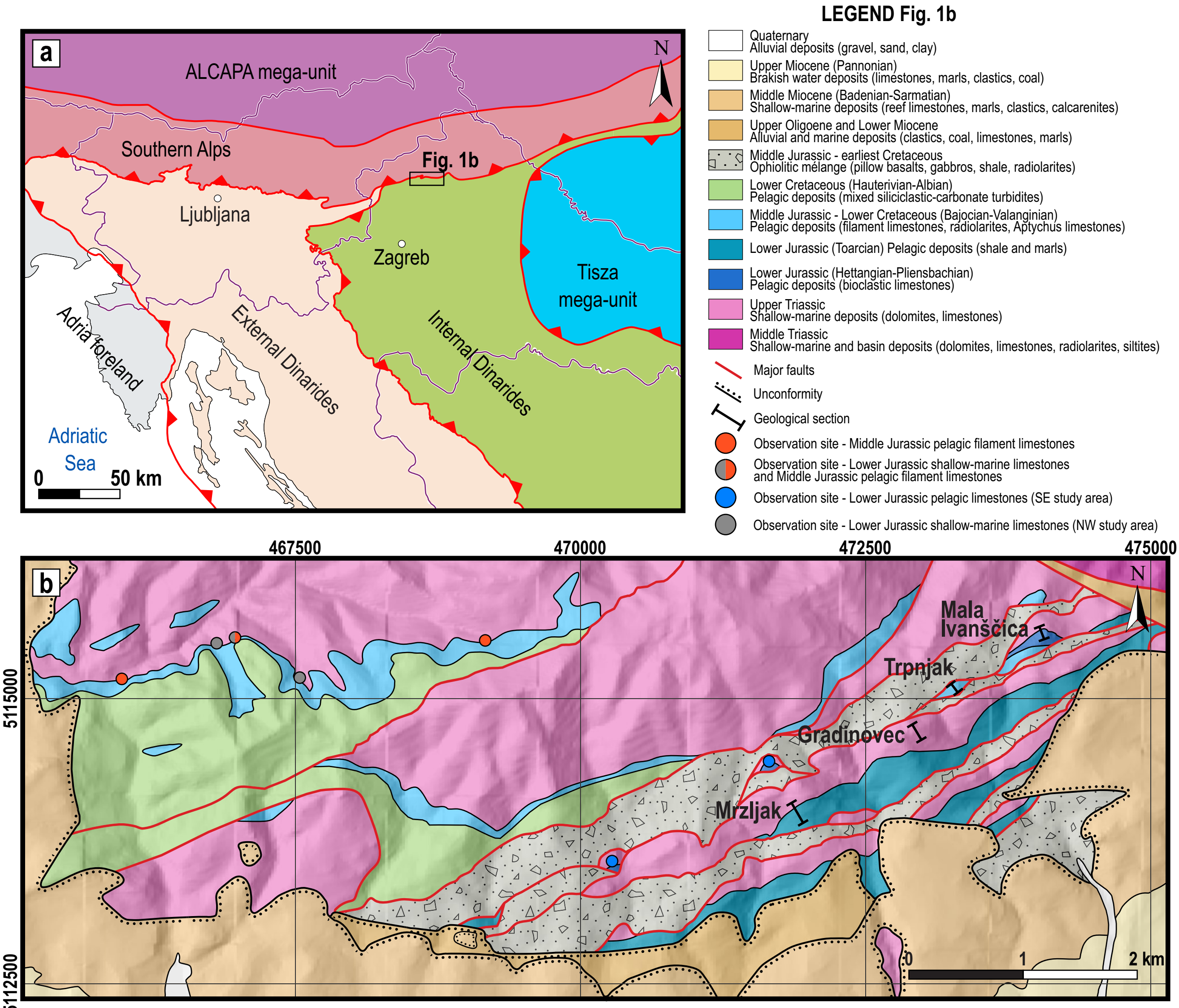


**Fig. 1** **a** Simplified tectonic map of the Dinaride–Alpine–Pannonian region (modified after Schmid et al. 2020). **b** Simplified geological map of the study area (position marked in (**a**) showing the spatial distribution of studied deposits, recorded sections, and important observation sites (modified after Šimunić et al. 1982)

2020). Synorogenic sediments, including thick flysch-type deposits, are deposited in the foredeep basin developed on the passive margin at this time (e.g., Zupanič et al. 1981; Lužar-Oberiter et al. 2012; Goričan et al. 2018).

The time of the final closure of the Neotethys is still debated; however, the related compressional tectonics resulted in emplacement of composite southwest-verging nappes of the Internal Dinarides, which were, in the study area, later overthrust by south-verging nappe of the Southern Alps (Gelder et al. 2015; Schmid et al. 2020; Fig. 1a). The formations preserved in both tectonic domains, however, share the same paleogeographic origin—eastern passive margin of the Adria microplate (Schmid et al. 2008; van Hinsbergen et al. 2020).

The evolution of the Adriatic passive margin is well documented in the Southern Alps (e.g., Goričan et al. 2012, 2018) and Northern Calcareous Alps (e.g., Missoni and Gawlick 2011a, b); however, less so in the Dinarides. In the study area, the complete Mesozoic succession derived from the Adriatic passive margin has never been described. When studied in the 1970s (Babić and Zupanič 1973, 1978; Babić 1974a, b, 1975; Šimunić et al. 1976, 1979), authors failed to reach a consensus about the depositional history of this area, with different concepts emerging regarding the Jurassic period. Since then, studies have concentrated on the Middle Triassic synrift part of the succession (Goričan et al. 2005; Slovenec et al. 2020, 2023; Kukoč et al. 2023), or Lower Cretaceous synorogenic formations (Zupanič et al.

1981; Lužar-Oberiter et al. 2009, 2012) with the Jurassic remaining unsolved. The aim of this study is to present for the first time the complete successions of the passive margin of Adria preserved in the mountains of NW Croatia. Detailed facies description and biostratigraphic data based on shallow-water and pelagic organisms from the newly discovered outcrops enable reconstruction of the evolution of this part of the margin as well as regional correlations. New data will provide a basis for a better understanding of the tectonic evolution of the area where the two orogens meet. Finally, evolution of the eastern Adriatic margin is discussed in the wider regional context showing bioproductivity as a primary factor controlling sedimentation on deeply submerged continental margins.

## Geological setting

The studied successions are located on Ivanščica Mt. in Hrvatsko zagorje region of NW Croatia. In this area, composite nappes of the Internal Dinarides are overthrust by south-verging nappes of the Southern Alps (van Gelder et al. 2015; Schmid et al. 2020; Fig. 1a), so part of the area can be assigned to the Southern Alps and part to the Dinarides. In the mountains of this region, including Ivanščica Mt., Upper Paleozoic–Mesozoic basement formations are uplifted from surrounding Neogene to Quaternary sediments of the SW Pannonian Basin and exposed at the surface (Fig. 1b). The complete Upper Paleozoic to Lower Cretaceous succession is found only on Ivanščica Mt. where it is in tectonic contact with the ophiolitic mélange (Babić et al. 2002; Slovenec et al. 2011; Lugović et al. 2015).

The oldest rocks on Ivanščica Mt. are Upper Paleozoic low-grade to non-metamorphic mostly clastic sediments (Šimunić et al. 1976, 1979; Šimunić 1992). Lower Triassic sedimentary formations exhibit gradual transition from shallow-water siliciclastic to carbonate sedimentation (Šimunić et al. 1979; Šimunić et al. 1982; Šimunić and Šimunić 1997). In the Anisian, extensional tectonics related to initial rifting and opening of the Meliata-Maliac branch of the Neotethys Ocean formed short-lived basins filled with pelagic and pyroclastic deposits (Goričan et al. 2005; Slovenec et al. 2020, 2023; Kukoč et al. 2023). These basins were filled by prograding carbonate platform in the Late Ladinian, resulting in deposition of thick succession of Upper Triassic carbonates regionally known as the Main Dolomite ("Hauptdolomit" in German or "Dolomia Principale" in Italian literature) and overlaying Dachstein Limestone (Šimunić et al. 1979; Šimunić et al. 1982; Šimunić and Šimunić 1997; Goričan et al. 2005).

Different interpretations exist about the Jurassic depositional history of Ivanščica Mt. According to Šimunić et al. (1976, 1979) and Šimunić et al. (1982) shallow-water conditions persisted until the Middle Jurassic emersion, which lasted until the Late Jurassic when sedimentation of the pelagic Aptychus limestone begun. By contrast, Babić (1974a, 1975) assumed completely pelagic Jurassic succession consisting of Early and Middle Jurassic condensed limestone with Fe–Mn mineralization and Upper Jurassic radiolarian cherts, which were overlain by the pelagic Aptychus limestone. Sedimentation of Aptychus limestone started in Late Tithonian and lasted until the end of the Valanginian when mixed carbonate–siliciclastic turbidites of the Oštrc Formation started to deposit (Babić et al. 1979; Babić and Zupanič 1973, 1978; Šimunić et al. 1982). These flysch-type deposits are interpreted as deposited in a clastic wedge in front of the obducting nappes containing ophiolites and distal Adriatic basement units (Zupanič et al. 1981; Lužar-Oberiter et al. 2009, 2012) and are recognized as regionally present synorogenic deposits (Goričan et al. 2018).

## Materials and methods

Geological mapping on the scale of 1:25 000 was done at the area of Ivanščica Mt. Mapped area of approximately 27 km$^2$ is densely forested and hilly with characteristic chained peaks intersected by deep and often very steep gorges. Four sections have been recorded in the southeastern part of Ivanščica Mt. (Figs. 1b and 2). Several important observation sites on the northern part of the mountain have been described (Fig. 1b); however, continuous sections could not be recorded at these localities due to poor exposure. Together, 72 samples were taken, from which 151 thin sections were made for microfacies analyses and calcareous microfossils determination. A total of 54 rock samples were taken from the sections of which 60 thin sections were made. Additional 11 chert and pelagic limestone samples were collected for radiolarian extraction. Microfacies types are named using terminology of Dunham (1962), while standard microfacies types and facies zones were determined according to Flügel (2010). Radiolarians were extracted from chert samples using diluted (5%) hydrofluoric acid. Selected radiolarians were photographed using JEOL JSM-IT 100 scanning electron microscope. Identified assemblages were dated using the zonation of Baumgartner et al. (1995b) based on unitary associations. Taxonomic determination follows the Catalogue of Mesozoic radiolarian genera (O'Dogherty et al. 2009) as well as recent revision of some Middle to Late Jurassic genera (O'Dogherty et al. 2017).

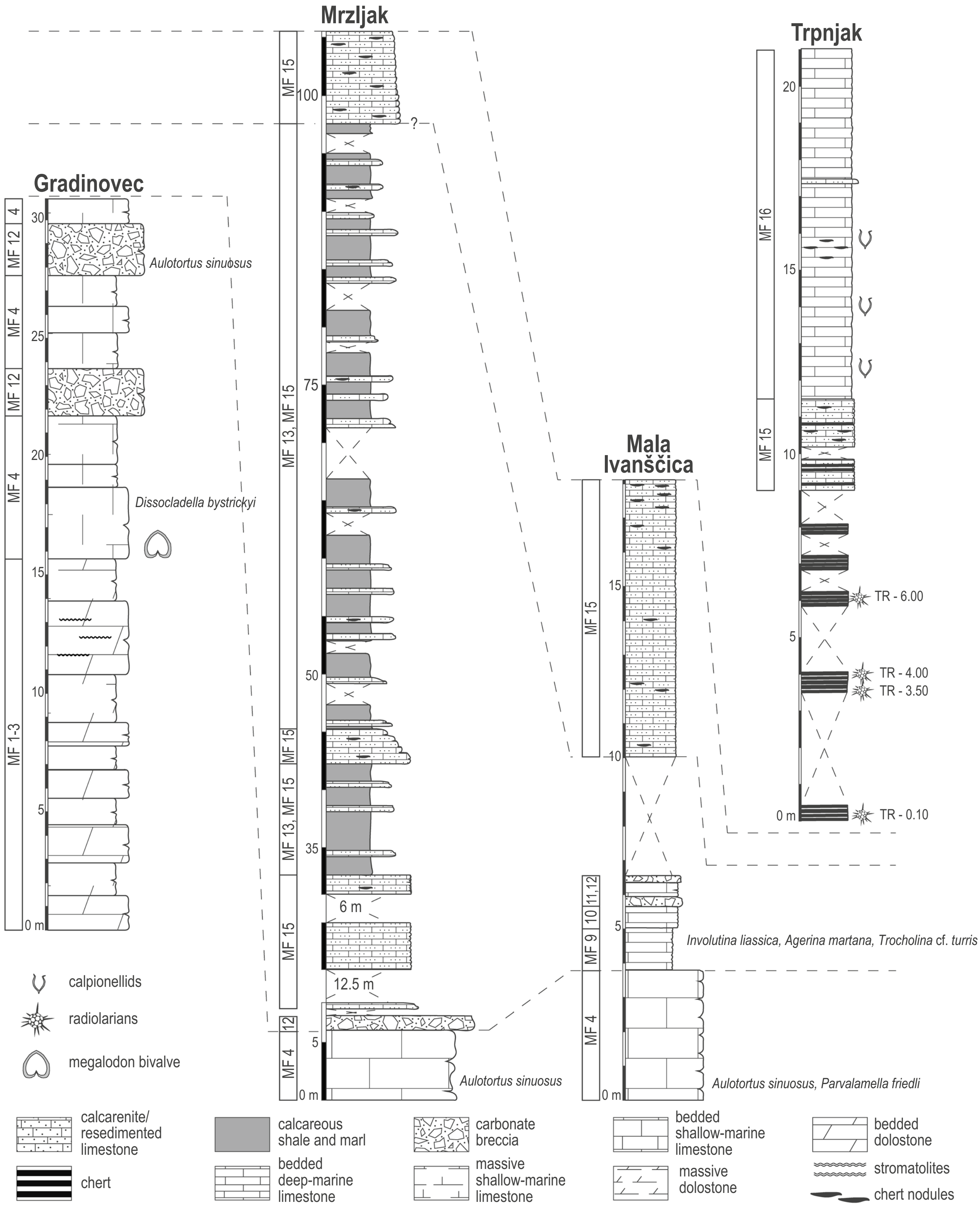


**Fig. 2** Detailed lithostratigraphic sections of studied Upper Triassic to Lowermost Cretaceous deposits from Ivanščica Mountain. Section localities are shown in Fig. 1b

## Description of sections

A summarized description of microfacies types (MF), fossil content, interpretation of depositional environments, and age assignments are given in Table 1.

### Section Gradinovec

Section Gradinovec consists of dolostones overlain by shallow-water limestone (Fig. 2). In the lower 1.4 m, dark grey dolomudstone alternates with light grey fenestral dolomudstone (MF 1). Overlaying 14 m interval of dolostone is characterized by regular rhythms of fenestral dolomudstone and crystalline dolostone (MF 2) with less common stromatolite dolobindstone (MF 3). Fenestrae are laminoid and more frequently irregular in shape, completely or partially filled with grey silt and/or sparite. Crystalline dolostone is likely formed out of dolomudstone in diagenesis by crystal growth. Dolostone is continuously overlain by limestone. The first 3 m are characterized by massive intraclastic–bioclastic packstone, followed by 12 m of irregular alteration of massive, occasionally horizontally laminated grey intraclastic–bioclastic packstone with intraclastic–peloidal packstone and rare peloidal–intraclastic packstone to wackestone (MF 4). Most carbonate grains are cortoids (coated grains) made of micritized and recrystallized skeletal grains, intraclasts, and peloids. Fabric is usually grain supported with micrite and fine peloids/intraclasts infilling. Although subordinately, irregular washed pockets of grainstones are present. Paleokarst features including cave systems and voids mainly filled with ancient speleothems and fine crystal silt are common characteristic of described limestone. In two levels of the section, coarse-grained matrix- to clast-supported unsorted intraformational limestone breccia appears.

### Section Mala Ivanščica

Mala Ivanščica section (Fig. 2) is characterized by densely packed, well-bedded intraclastic–peloidal–skeletal packstone to washed grainstone (MF 4) with occasional intercalations of oncolites. Most grains are sorted peloids or micritized intraclasts, both smoothly recrystallized. Skeletal grains are strongly recrystallized and exhibit micrite envelopes representing cortoids. Irregular fenestrae occur very rarely. Oncolites consist of millimeter-sized oncoids within unsorted peloidal packstone to grainstone matrix. Both lithofacies exhibit paleokarst features. Limestones of MF 4 type are overlain by light red thin to indistinctly bedded, rarely nodular bioclastic wackestone to packstone (MF 9). This bioclastic limestone (MF 9) is dominantly composed of echinoderm fragments as well as juvenile ammonites, gastropods, sponge spicules, ostracods, and benthic foraminifera within carbonate mud matrix (Fig. 3e, f). Thin bed well-sorted and moderately packed recrystallized rudstone containing fragments of echinoderms and thick-shelled bivalves is present within bioclastic limestones. Bioclastic limestone is continuously overlain by clear, unrecrystallized and loosely packed fine-grained intraclastic–bioclastic packstone (MF 10), composed of echinoderm fragments, abundant benthic foraminifera, and intraclasts within mud matrix (Fig. 3g). Last meter of this interval is characterized by thin-bedded poorly sorted ooid grainstone (MF 11) with breccia intercalations (MF 12). Grainstone is composed of irregularly shaped ooids and less abundant echinoderm fragments and benthic foraminifera (Fig. 3h). Poorly preserved cortoid grains occur only locally. Breccia is poorly sorted, loosely to moderately packed with rounded mudstone and cortoid grainstone clasts embedded in intraclastic–bioclastic packstone matrix. Higher in the section, well-bedded grey monotonous calcarenite is present (MF 15). Calcarenite consists of abundant echinoderm plates, intraclasts and peloids (Fig. 4c). Grains are densely packed, well sorted, ranging in size from coarse to very fine sand. Finning upward trend at the interval scale is notable, but overall, with very homogenous texture. Chert lenses and nodules occur in the whole interval but become gradually more abundant toward the top.

### Section Mrzljak

The lowermost part of Mrzljak section consists of medium-bedded grey limestone (Fig. 2) characterized by monotonous vertical and horizontal alteration of peloidal intraclastic grainstones and packstones (MF 4). These lithotypes consist mostly of unsorted to poorly sorted rounded peloids and micritized intraclasts within very fine peloidal matrix or sparite. Cortoids appear subordinately. Irregular fenestrae without any infilling are relatively abundant but decreasing toward the top. Carbonate breccia overlay described limestones. Breccia clasts are made of subangular packstone, grainstone, and mudstone of MF type 4 and 6 within calcarenite matrix equal to calcarenites found higher in the section (see below) Entire interval is characterized by paleokarst features. In the following interval, normally graded and well-sorted, thin-bedded, medium to very fine sand-sized calcarenite (MF 15) predominate over marly limestone (MF 13). The whole interval represents a general fining-upward sequence with occurrences of chert nodules in the upper part. Grains are exclusively made of various shallow-water carbonate lithoclasts and bioclasts with abundant echinoderm plates (Fig. 4c). The following 65 m interval consists mostly of thin-bedded brownish marl and clay-rich calcareous shale (MF 13). Centimeter-sized sequences are characterized by normal gradation and parallel lamination (Fig. 4a, b). Cross-lamination occurs rarely. Abundant concentrations

**Table 1** Studied carbonate lithofacies units and description of their microfacies, interpretation of depositional environments, list of most important biota and biostratigraphic age

| **Lithofacies unit** (section; see Fig. 1b for locations) and microfacies description | Depositional environment | Biota | Age |
|---|---|---|---|
| **Aptychus limestone** (Trpnjak): thin to medium-bedded (2–30 cm) light gray to white mudstones to wackestones (MF 16); occasional parallel lamination manifested in alternation of laminae more and less abundant in radiolarians and sponge spicules | Deep open shelf | Radiolarians, sponge spicules, calpionellids | Latest Tithonian–Valanginian (Babić and Zupanič 1973) |
| **Calcarenites** | Lower slope to deep open shelf | | |
| (Trpnjak): gray thin-bedded (5–15 cm) calcarenites (MF 15) consist of medium to fine sand-sized shallow-water intraclasts, peloids, bioclasts (echinoderms) and clasts of radiolarian cherts; chert nodules occur; poorly expressed fining-upward | | Valvulaminidae, Echinoderms | Tithonian |
| (Mrzljak, Mala Ivanščica): gray well-bedded (5–10 cm) calcarenites (MF 15) consist of medium sand-sized shallow-water peloids, intraclasts and bioclasts (echinoderms); chert nodules occur; fining upward | | Valvulinidae, Echinoderms | Aalenian –Callovian (?) |
| **Filament limestone** (observation sites only): indistinctly bedded light gray skeletal wackestones to packstones (MF 14) with abundant filaments and planktonic foraminifera | Deep open shelf | ? *Globuligerina oxfordiana,* protoglobigerinids, pelagic bivalve shells (*Bositra* sp.), sponge spicules, juvenile ammonites | Bajocian—callovian (?) |
| **Calcareous shale and marls** (Mrzljak): thin-bedded (5–10 cm) brownish marls and clay-rich calcareous shale (MF 13); common centimeter-size sequences characterized by normal grading and parallel-lamination; rare cross-lamination; coarse laminae abundant in calcified radiolarians | Deep open shelf | Radiolarians | Toarcian (?) |
| **Breccias** | Slope to deep shelf | | |
| (Mala Ivanščica): poorly sorted, loosely to moderately packed breccia (MF 12) with rounded clasts of mudstones (MF 6?) and cortoid grainstones (MF 4) embedded in intraclastic–bioclastic packstone matrix (MF 10) | | | Pliensbachian (?) |
| (Mrzljak): poorly sorted, densely packed breccia (MF 12) with subangular clasts of cortoid packstones to grainstones (MF 4) and mudstones (MF 6) separated from micritic matrix by microstylolites | | | Latest Triassic–Earliest Jurassic |
| (Gradinovec): unsorted, coarse-grained matrix- to clast-supported intraformational carbonate breccia (MF 12) with predominantly angular clasts of cortoid packstones and grainstones (MF 4) and fenestral mudstones (MF 6) embedded in intraclastic–peloidal–bioclastic packstone (MF 4) | Open lagoon to platform margin | | Rhaetian |
| **Grainstones** (Mala Ivanščica): thin-bedded (5–10 cm) poorly sorted ooid grainstone (MF 11); ooids are irregular in shape and non-spherical; other grains are echinoderm and foraminifera bioclasts and rare cortoids | Lower slope to deep shelf | Trocholinid foraminifera, echinoderms | Pliensbachian (?) |
| **Bioclastic limestone** (Mala Ivanščica): thin-bedded (< 10 cm) to indistinctly bedded, sometimes poorly nodular light red bioclastic packstones to wackestones (MF 9) with open marine biota; loose fine-grained intraclastic–bioclastic packstone (MF 10) with open marine biota | Lower slope to deep shelf | *Involutina liassica*, *Agerina martana, Trocholina* sp. cf. *T. Turris,* lagenids, juvenile ammonites, echinoderms, sponge spicules, ostracod shells, gastropods | Hettangian—Pliensbachian |
| **Grainy limestones** (observation sites only (see Fig. 1b)): massive to indistinctly bedded intraclastic–peloidal packstones (MF 7); oncoid floatstone (MF 8); both microfacies show less or no recrystallization compared to the Triassic cortoid limestones; very common fenestrae | Intertidal to subtidal | *Palaeodasycladus mediterraneus, Thaumatoporella parvovesiculifera, Duotaxis* sp. cf. *D. metula, Siphovalvulina gibraltarensis, Siphovalvulina variabilis, Siphovalvulina* sp. cf. *S. colomi, Textulariopsis sinemurensis* | Hettangian—Pliensbachian |
| **Cortoid limestone** (Gradinovec, Mrzljak, Mala Ivanščica): alternation of massive to bedded (20–60 cm) intraclastic–peloidal–bioclastic packstones, in places washed grainstones (MF 4); most carbonate grains are cortoids; irregular fenestrae occur rarely; rare occurrences of well-bedded laminated fenestral stromatolite bindstone (MF 5) and fenestral mudstones (MF 6); overall high degree of recrystallization; common paleokarst features | Moderate water energy open lagoon to platform margin, subintertidal | *Dissocladella bystricky, Triasina hantkeni, Aulotortus sinuosus, Aulotortus* sp., *Parvalamella friedli, Glomospirela* sp. cf. *G. grandis, Duotaxis* sp., *Permocalculus* sp., miliolid foraminifera | Rhaetian |
| **Dolostones** (Gradinovec): alternation of massive to poorly bedded (10–50 cm) dolomudstone (MF 1) and laminated stromatolite dolobindstone (MF 3); common highly crystalline dolostone (MF 2); fenestrae are very common, laminoid and irregular, partly filled with gray silt and/or sparite; overall high degree of recrystallization | Restricted lagoon, shallow subtidal and tidal flat | | Norian—Rhaetian |

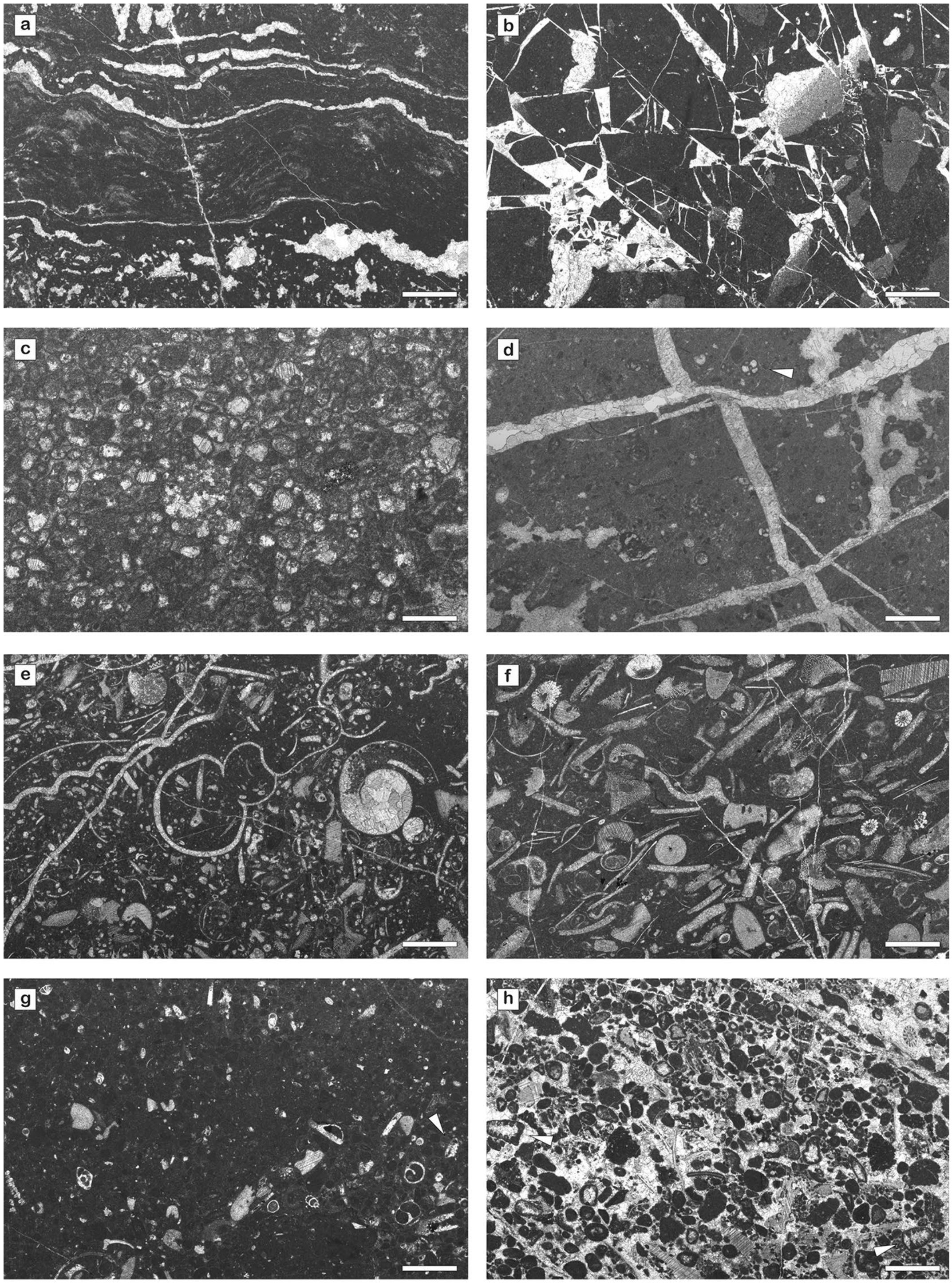


**Fig. 3** Photomicrographs of the investigated carbonate sedimentary deposits showing their characteristic microfacies (MF). **a** Fenestral laminated stromatolite dolobindstone (MF 2), sample GV-308B. **b** Fenestral dolomudstone (MF 1), sample GR-1. **c** Intraclastic–peloidal–bioclastic (cortoid) packstone (MF 4), sample GV-1532. **d** Fenestral intraclastic–peloidal packstone (MF 7) with *Siphovalvulina* sp. cf. *S. gibraltarensis* marked with arrow, sample VŽ-11534. **e** Bioclastic packstone to wackestone (MF 9) with juvenile ammonites, sponge spicules and echinoderms, sample GV-1600B. **f** Bioclastic packstone to wackestone (MF 9) with echinoderms, thin-shelled bivalves and juvenile ammonites, sample MI-4.0. **g** Loose fine-grained intraclastic–bioclastic packstone (MF 10) with *Involutina liassica* (white arrow), sample MI-4.8. **h** Ooid grainstone (MF 11) with *Trocholina* sp. cf. *T. elongata* (white arrows), sample MI-6.0. Scale bar is 0.5 mm

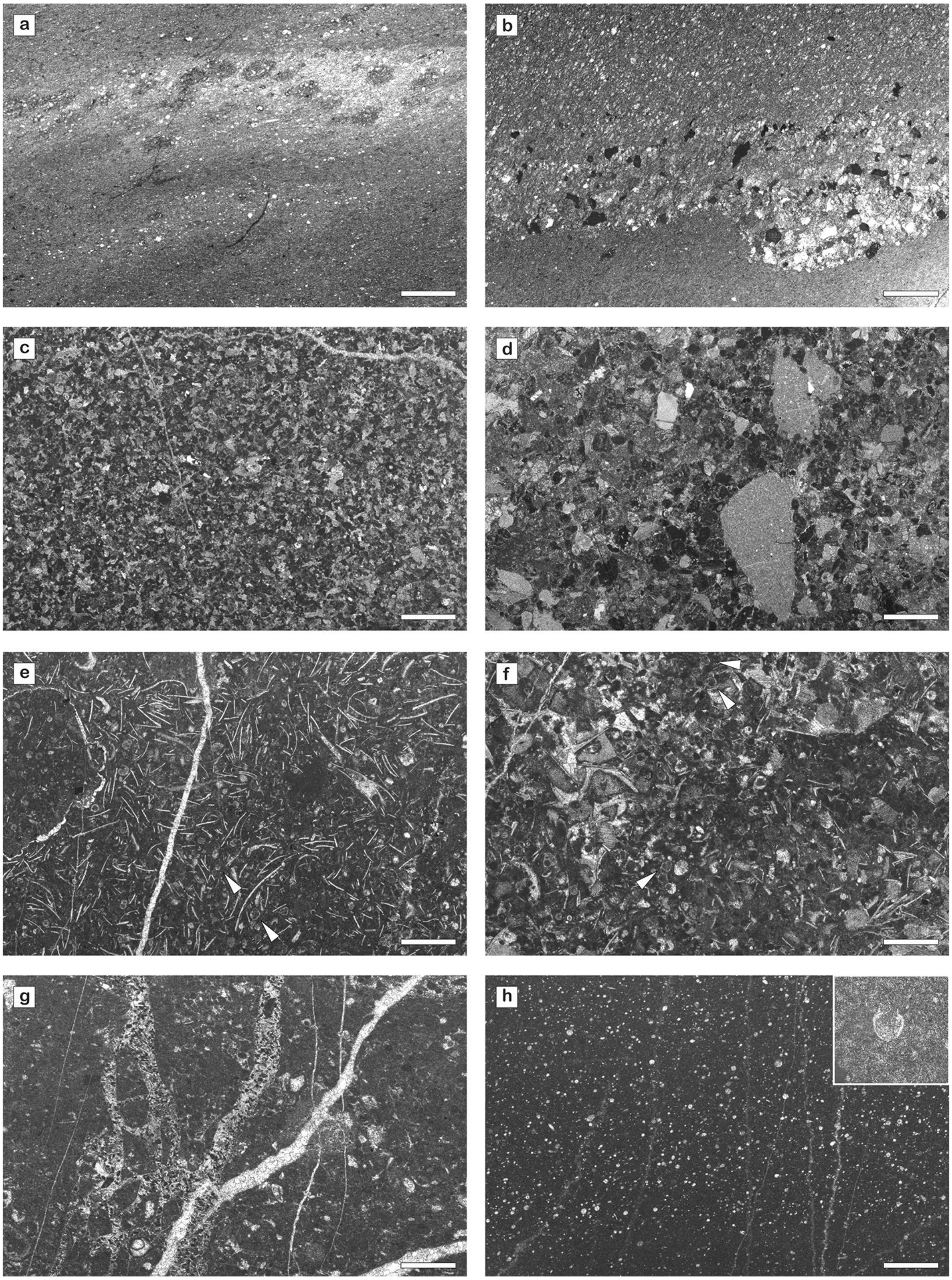


**Fig. 4** Photomicrographs of the investigated carbonate sedimentary deposits showing their characteristic microfacies (MF). **a** Clay-rich horizontally laminated calcareous shale (MF 13) with radiolarians, sample MR-50,3. **b** Fine- to very-fine-grained calcarenite with deformed bed base due to differential loading (MF 13), sample GV-1478. **c** Very-fine-grained calcarenite (MF 15) with echinoderms, sample MR-7.35. **d** Fine-grained calcarenite (MF 15) with echinoderms and volcanic ash clasts. **e** Skeletal wackestone (MF 14) with protoglobigerinids (white arrows) and *Bositra*-shell filaments, sample GV-150C. **f** Skeletal packstone (MF 14) with echinoderms, protoglobigerinids (white arrows) and *Bositra*-shell filaments, sample GV-150B. **g** Neptunian dike filled with skeletal packstone (MF 14) with *Bositra*-shell filaments and intraclasts cutting through oncoid floatstone (MF 8), sample TL-6B. **h** Bioclastic wackestone (MF 16) with radiolarians, sponge spicules and calpionellids, sample TR-14.0. Calpionellid *Calpionella alpina* Lorenz in upper right corner (scale bar 0.1 mm), sample TR-21.0

of calcified radiolarians are found in coarse-grained bottom intervals (Fig. 4b). Erosional marks are occasionally present at the bottom surface of each sequence. Thin-bedded calcarenites composed of medium to very fine sand-sized clasts are intercalated within marls of this interval. Their grains are well-sorted predominantly shallow-water intraclasts and peloids within clay-rich micrite. Chert nodules occur equally throughout whole interval, generally in calcarenite layers. The uppermost part of the section consists of prominent grey well bedded and well sorted dominantly medium sand-sized calcarenite (MF 15; Fig. 4c). A thinning upward and poorly expressed fining-upward trend is observed within this interval, while content of chert nodules seems to be constant through the interval. Grains are densely packed peloids, intraclasts, and bioclasts, exclusively derived from shallow-water carbonate platform with abundant echinoderm plates.

### Section Trpnjak

The lowermost part of Trpnjak section (Fig. 2) comprises well-bedded red radiolarian chert. However, large part of this interval is covered and the contact with underling lithologies is not exposed. Radiolarian cherts are overlain by 2.5 m of thin-bedded medium to fine sand-sized calcarenite (MF 15). In the lower part of this interval, calcarenite alternates with weathered radiolarian chert while irregular chert nodules occur in the calcarenite in the upper part of the interval. Calcarenite consists predominantly of bioclasts, intraclasts, and peloids (Fig. 4d). Clasts of vitriclastic tuff are common and generally more abundant in the lower part of the interval (Fig. 4d). The uppermost part of the section comprises thin- to medium-bedded light grey to white limestone which conformably overlie calcarenites. Microfacies of the limestone is mudstone to wackestone (MF 16) containing calcified radiolarians, calpionellids, and sponge spicules (Fig. 4h). Parallel lamination which manifests as alternation of laminae more and less abundant in fossils is present in some layers. Irregular chert nodules and discontinuous beds of dark grey chert are present only in the middle part of the interval. A bed of normally graded 15 cm thick calcarenite is noticed in the upper part.

### NW Ivanščica Mountain

In the NW part of Ivanščica Mt. (Fig. 1b), massive to indistinctly bedded grey limestone occurring atop of Upper Triassic dolostone (MF 1–3) and limestone (MF 4–6) was recorded. Oncoid floatstone (MF 8) and intraclastic peloidal packstone (MF 7) were determined. Packstone is very similar to those from sections Gradinovec, Mala Ivanščica, and Mrzljak but is significantly less recrystallized, does not contain cortoids and differ in fossil assemblage (Fig. 3d). Oncoid floatstone consists of calcareous algae and skeletal fragments dispersed within fine-grained intraclastic packstone matrix. Both microfacies exhibit sparfilled irregular fenestrae. Rare centimeter-sized fissures interpreted as Neptunian dykes are found in oncoid floatstones. Dykes are filled with bioclastic–intraclastic packstone to wackestone abundant in fragments of thin-shelled bivalves (Fig. 4g). Limestone with Neptunian dykes is overlain by massive to indistinctly bedded light grey “filament” limestone. This facies is characterized by light grey bioclastic–intraclastic wackestone to packstone with abundant filaments and pelagic biota (MF 14; Fig. 4e, f). Although direct contact has never been observed in an outcrop, many observation sites in the NW part of Ivanščica Mountain indicate deposition of red and yellow radiolarian chert atop filament limestone. This radiolarian chert is overlain by Aptychus limestone (MF 16).

## Biostratigraphy

### Algae and foraminifera

#### Triassic calcareous algae

Only one, recrystallized, longitudinal-oblique cross-section of dasycladal algae was found in the limestone in the middle part of Gradinovec section (Fig. 5a). This is likely a cross-section of *Dissocladella bystrickyi* Sokač and Grgasović, described from the Upper Triassic Main Dolomite on Medvednica Mt. (Sokač and Grgasović 1995). Norian-Rhaetian age of this species is based on correlation with the neighboring Žumberak Mts. (Grgasović 1997).

In the sample GV-53 laterally from the section, several cross-sections of previously unknown gymnocodiacean algae, likely belonging to the genus *Permocalculus* were found (Figs. 2 and 5b–e). This genus has a wide stratigraphic range from the Permian to the Miocene (Schlagintweit 1991). Since this genus has been found within the Triassic deposits only in the Carnian strata of the island of Hydra in Greece (Schäfer and Senowbari-Daryan 1983), our finding is likely an undescribed species. The related gymnocodiacean alga *Asterocalculus heraki* Sokač and Grgasović is described from the Rhaetian of the Main Dolomite of the Žumberak Mts. (Sokač and Grgasović 1998).

#### Triassic foraminifera

In the limestone sample GV-53, sampled laterally from Mrzljak section, recrystallized cross-sections of benthic foraminifera *Triasina hantkeni* Majzon were found (Figs. 2 and 5f–i). Although only the outer part of the test is visible, the characteristic structure of the genus *Triassina* can be recognized. This foraminifera is widespread and is considered the index fossil for the Rhaetian Stage (Gale et al. 2012

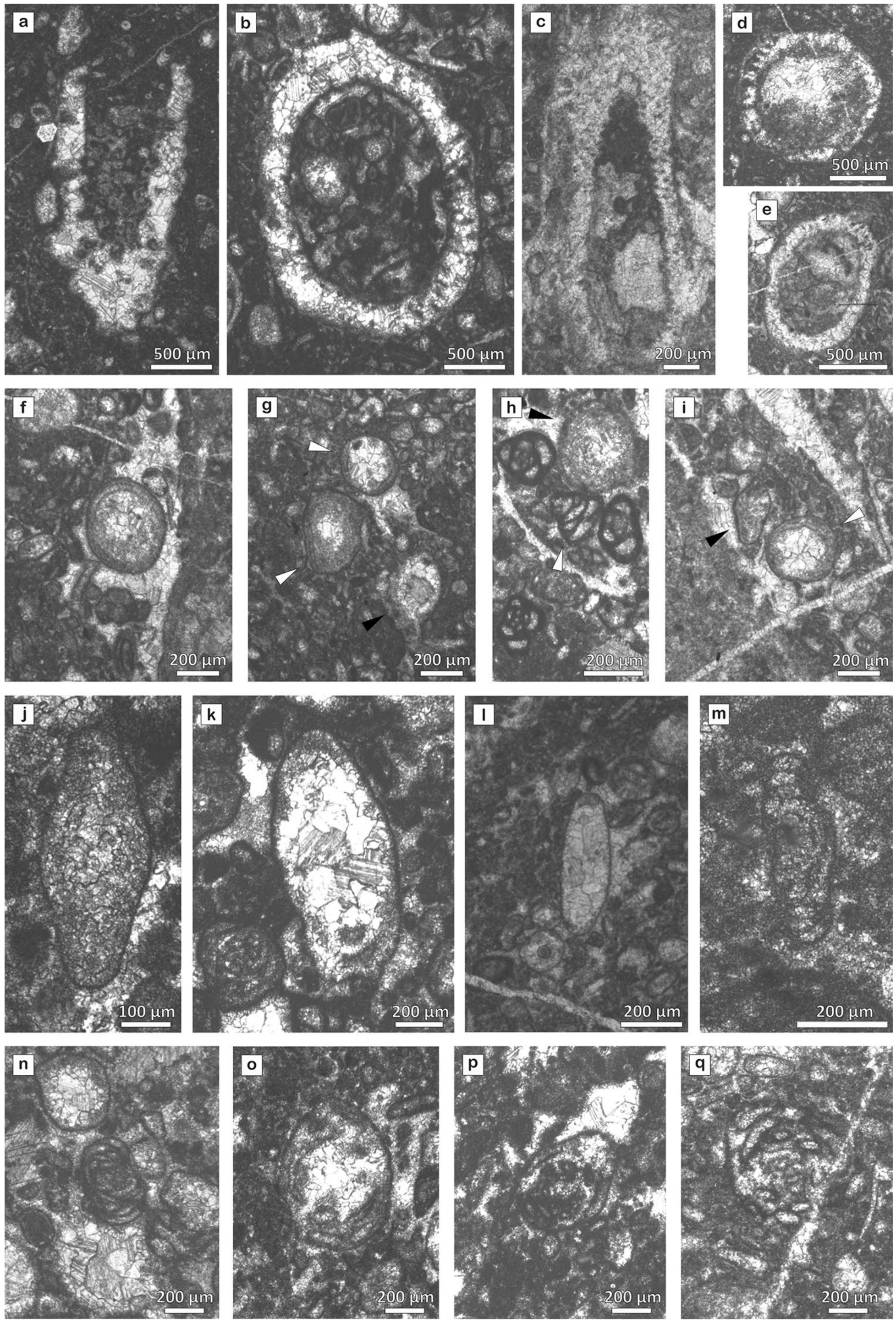


**Fig. 5** Photomicrographs of most important Triassic microfossils from investigated carbonate deposits. **a** *Dissocladella bystrickyi* Sokač and Grgasović, sample GR-4. **b–e** *Permocalculus* sp. samples GV-53A, GV-53B. **f** *Triasina hantkeni* Majzon, sample GV-53A. **g** *Triasina hantkeni* Majzon (white arrows) and *Aulotortus* sp. (black arrow), sample GV-53A. **h** *Triasina hantkeni* Majzon (black arrow) and *Duotaxis* sp. (white arrow) and miliolid foraminifera, sample GV-53B. **i** *Triasina hantkeni* Majzon (white arrow) and *Aulotortus sinuosus* Weynschenk (black arrow), sample GV-53B. **j–l** *Aulotortus sinuosus* Weynschenk, samples GR-8, GV-53A, MR-6; m–n) *Glomospirella* cf. *grandis* (Salaj), samples GV-52, GV-53B. **o–q** *Parvalamella friedli* (Kristan-Tollmann), samples GV-53A, GV-53B

and references therein), confirming the similar conclusions of Grgasović (2003) and Velić (2007). In the upper part of Gradinovec section, lowermost parts of Mrzljak and Mala Ivanščica sections, as well as in samples sampled laterally from recorded sections relatively numerous but poorly preserved cross-sections of *Aulotortus sinuosus* Weynschenk were found (Fig. 5i–l). This species is very common and has a fairly wide stratigraphic range from the Anisian to the Rhaetian (Piller 1978; Grgasović 1997; Gale 2012).

Several poorly preserved cross-sections of foraminifera *Parvalamella friedli* (Kristan-Tollmann) (former *Aulotortus friedli*, see Rigaud et al. 2012) were found in the lowermost part of the Mala Ivanščica section (Figs. 2 and 5o–q). The stratigraphic range of this species is from the Carnian to the Rhaetian (Chablais et al. 2010; Gale 2012). Also,

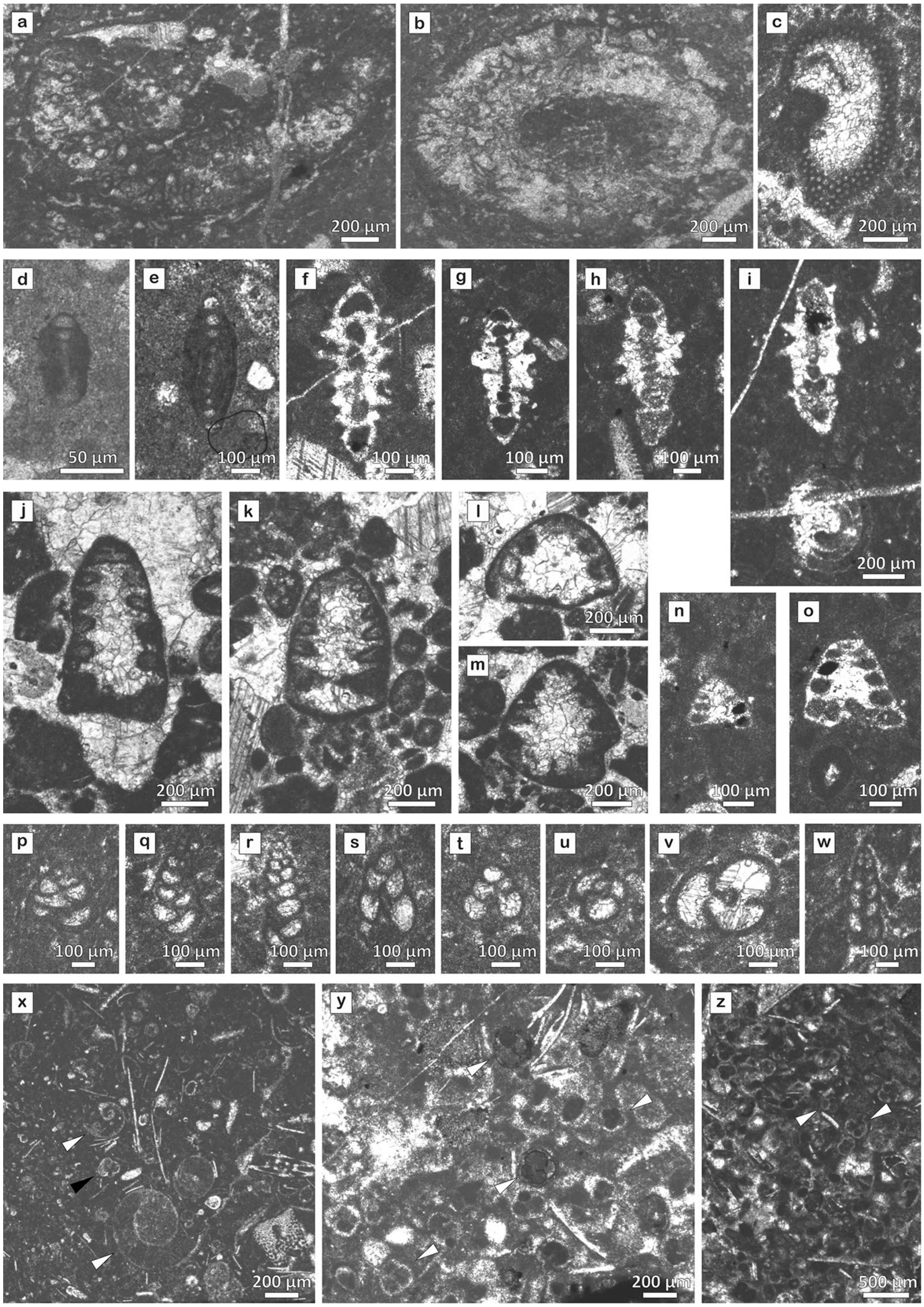


**Fig. 6** Photomicrographs of most important Jurassic microfossils from investigated carbonate deposits. **a**–**b** *Palaeodasycladus mediterraneus* (Pia), samples TL-6A, TL-6B. **c** *Thaumatoporella parvovesiculifera* (Raineri), sample TL-6A. **d**–**e** *Agerina martana* Farinacci, samples MI-4.8, GV-1600B. **f**–**i** *Involutina liassica* (Jones), samples MI-4.8, GV-1600B. **j**–**k** ? *Trocholina* sp., elongated test, samples MI-5.25, MI-6.0. **l**–**m** ? *Trocholina* sp. low conical test, samples MI-5.25, MI-6.0. **n**–**o** *Trocholina* sp. cf. *T. turris* Frentzen, sample MI-4.8. **p** *Duotaxis* sp. cf. *D. metula* Kristan, samples TL-6A, TL-6C. **q**–**r** *Textulariopsis sinemurensis* BouDagher-Fadel and Bosence, samples TL-6A, TL-6C. **s** *Siphovalvulina variabilis* Septfontaine, sample TL-6A. **t**–**v** *Siphovalvulina gibraltarensis* BouDagher-Fadel et al., samples TL-6A, TL-6C. **w** *Siphovalvulina* cf. *colomi* BouDagher-Fadel et al., sample TL-6B. **x** Pelagic biomicrite with filaments, juvenile ammonites (white arrows) and planktonic foraminifera (black arrow), sample GV-150A. **y**–**z** Pelagic biomicrite with numerous sections of planktonic foraminifera (white arrows), tentatively assigned to *Globuligerina oxfordiana* (Grigelis), sample GV-150B

*Glomospirella* sp. cf. *G. grandis* (Salaj) has been found in the same sample GV-53 located laterally from the recorded sections (Fig. 5m, n).

We can conclude that the microfossil assemblages from the limestones of Gradinovec section and lowermost parts of Mrzljak and Mala Ivanščica sections belong to the Late Triassic. This age constraint can be further limited to the Rhaetian with the occurrences of *T. hantkeni* found laterally from recorded sections.

### Jurassic calcareous algae

In the limestone samples from the NW part of investigated area, cross-sections of dasycladal alga *Palaeodasycladus mediterraneus* (Pia) were found (Fig. 6a, b). Although cross-sections are poorly preserved, in some places, the characteristic structure of this alga with a large number of branches located in three rows can be recognized. On one specimen, branching of a second-order branch into two third-order branches is observed (Fig. 6a). After Sokač (2001), the stratigraphic range of the species corresponds to the lower and middle part of the Early Jurassic. Rychliński et al. (2018) described this species from the Hettangian to Early Pliensbachian (Carixian) of the southern part of the Western Tethys. Rare specimens of problematic alga *Thaumatoporella parvovesiculifera* (Raineri) occur in the same sample (Fig. 6c).

### Jurassic foraminifera

In samples from the NW part of the investigated area, together with *P. mediterraneus,* very rare sections of three morphotypes of the genus *Siphovalvulina* have been determined: *S. gibraltarensis* (Fig. 6t–v), *S. variabilis* Septfontaine (Fig. 6s) and *Siphovalvulina* sp. cf. *S. colomi* (BouDagher-Fadel et al. 2001; Fig. 6w). The range of this genus according to Velić (2007) is from the Sinemurian to the Toarcian, although BouDagher-Fadel and Bosence (2007) indicated shorter range from the Sinemurian to the Pliensbachian. In addition, Gale et al. (2018) concluded that the range of *Siphovalvulina* is from the Sinemurian (or possibly Hettangian) to the Early Cretaceous. *Textulariopsis sinemurensis* BouDagher-Fadel and Bosence (Fig. 6q, r), also characteristic of the Sinemurian and the Pliensbachian is found in the same sample. *Duotaxis* sp. cf. *D. metula* Kristan (Fig. 6p), which first appears in Norian/Rhaetian and ranges through the Early Jurassic (Gale 2012 and references therein), was also found.

In the middle part of Mala Ivanščica section (Fig. 6f–i) numerous cross-sections of foraminiferal species *Involutina liassica* (Jones) were found. It is characteristic of almost the entire Lower Jurassic (Velić 2007) and is paleoambietally related to marginal parts of the carbonate platform and the slope. In the same sample, *Trocholina* sp. cf. *T. turris* Frentzen (Fig. 6n, o) has been found. This species ranges from the Rhaetian to the Early Jurassic (Gale et al. 2012). One specimen of the foraminifera *Agerina martana* Farinacci (former *Vidalina martana*, see Farinacci 1991) was also found in the same sample (Mala Ivanščica section; Fig. 6d) and in samples sampled laterally from the section (Fig. 6e). This species first appears in Late Sinemurian and ranges to the Toarcian (Velić 2007); however, earlier occurrences cannot be excluded (Rožić et al. 2017).

Above this level at Mala Ivanščica section, different cross-sections of trocholinid benthic foraminifera (thin-sections MI-4.8, MI-5.25 and MI-6.0) have been found, some of them elongated (Fig. 6j, k) and some low conical (Fig. 6l–n). Due to poor preservation, specific determination has not been possible.

We can conclude that the age of part of the studied limestones from the NW area is Hettangian to Pliensbachian. The lower middle part of Mala Ivanščica section is of Early Jurassic age, since it lies conformly on the Rhaetian limestone and contains fossils of Hettangian to Toarcian age.

Planktonic foraminifera have been found in several samples of limestone from the NW part of Ivanščica Mt. In sample TL-5, recrystallized tests of planktonic foraminifera belonging to the family Conoglobigerinidae are clearly seen in the micritic matrix with filaments and sponge spicules, and some cross-sections with four more clearly visible ventricles in the posterior bend correspond to species of the genus *Globuligerina*. A more diverse assemblage of planktonic foraminifera was found in the sample GV-150 (Fig. 6x–z) and GV-574. These thin sections are also dominated by mostly recrystallized, but also somewhat better-preserved sections from the family Conoglobigerinidae, tentatively assigned to *Globuligerina oxfordiana* (Grigelis) in thin-sections GV-150A and possibly GV-574. The occurrence of this species would indicate a stratigraphic range from the Bajocian to the Oxfordian.

## Radiolarians

Four productive chert samples from Trpnjak section yielded moderately well preserved radiolarians. The identified radiolarian species are listed in Table 2 and illustrated in Figs. 7 and 8. The stratigraphic position of samples is shown in Fig. 2.

In total, 59 radiolarian species were determined, of which 10 are in open nomenclature. In all samples, nassellarians are more abundant than spumellarians and rare sponge spicules are present. The assemblages were dated with the zonation of Baumgartner et al. (1995b) with ranges of the species indicated in Table 2. Following species, however, have longer ranges than established by Baumgartner et al. (1995b). The range of *Zhamoidellum ovum* Dumitrica has been extended from UAZ 6–7 (Šmuc and Goričan 2005) to the Berriasian (Matsuoka 1998). *Hemicryptocapsa carpathica* (Dumitrica) also ranges up to the Berriasian (Matsuoka 1998). The range of *Mizukidella kamoensis* (Mizutani and Kido) has been extended to middle/late Oxfordian (Auer et al. 2009) and the range of *Gongylothorax favosus oviformis* Suzuki and Gawlick has been extended to include the entire Oxfordian (Matsuoka 1992; Auer et al. 2009). For the range of *Hexasaturnalis nakasekoi* (Dumitrica and Dumitrica-Jud) and *H. minor* (Baumgartner) see Dumitrica and Dumitrica-Jud (2005).

Sample TR-0.10 is assigned a relatively broad range from UAZone 7 (late Bathonian-early Callovian) to UAZone 10 (late Oxfordian-early Kimmeridgian) based on co-occurrences of *Cinguloturris carpatica* Dumitrica, *Loopus primitivus* (Matsuoka and Yao), *Hemicryptocapsa carpathica* (Dumitrica), *Parahsuum carpaticum* Widz and DeWever and *Protunuma japonicus* Matsuoka and Yao, who all first appear in UAZone 7, with *Paronaella broennimanni* Pessagno and *Transhsuum maxwelli* (Pessagno), who last appear in UAZone10. Because of its stratigraphic position below samples dated as Oxfordian (see below), this sample is likely not younger than early Oxfordian.

Sample TR-3.50 is assigned to UAZone 9 (middle-late Oxfordian)–UAZone 10 (late Oxfordian-early Kimmeridgian) based on the first occurrence of *Archaeodictyomitra minoensis* (Mizutani) and the last occurrences of *Eucyrtidiellum nodosum* Wakita and *Tritrabs casmaliaensis* (Pessagno).

The maximum range of sample TR-4.00 is from UAZone 7 (late Bathonian-early Callovian) to UAZone 11 (late Kimmeridgian-early Tithonian) based on co-occurrences of several species that first appear in UAZone 7, including *Gongylothorax favosus oviformis* Suzuki and Gawlick, *Hemicryptocapsa carpathica* (Dumitrica), *Loopus primitivus* (Matsuoka and Yao), *Pantanellium riedeli* Pessagno, *Protunuma japonicus* Matsuoka and Yao and *Ristola altissima altissima* (Rüst) with *Eucyrtidiellum ptyctum* (Riedel and Sanfilippo) and *Transhsuum brevicostatum* (Ožvoldová) who last appear in UAZone 11. However, because sample TR-4.00 is stratigraphically above sample TR-3.50 (UAZ 9–10), this sample cannot be older than UAZone 9. In addition, the presence of *Gongylothorax favosus oviformis* Suzuki and Gawlick in this sample means that the sample is not younger than the late Oxfordian; therefore, we assign both samples to middle to late Oxfordian.

Sample TR-6.00 is assigned to UAZone 9 (middle-late Oxfordian)–UAZone 11 (late Kimmeridgian-early Tithonian) based on co-occurrences of *Archaeodictyomitra minoensis* (Mizutani) who first appear in UAZone 9 and several species which last appear in UAZone 11 including *Cinguloturris carpathica* Dumitrica, *Eucyrtidiellum ptyctum* (Riedel and Sanfilippo), *Transhsuum okamurai* (Mizutani), and *Tritrabs exotica* (Pessagno).

## Discussion

### Stratigraphic evolution

The described successions from Ivanščica Mt. were a part of the eastern passive margin of Adria microplate, formed after the Middle Triassic rifting related to the opening of the Neotethys (Ferriere et al. 2016; Schmid et al. 2008, 2020). Subsequently, the rifting of the Alpine Tethys in the Early Jurassic to the west (Masini et al. 2013) caused further subsidence and onset of pelagic sedimentation in newly subsided blocks (e.g., Goričan et al. 2012 and references therein). From the Pliensbachian onwards, Adriatic Carbonate Platform (AdCP sensu Vlahović et al. 2005) was the only domain with shallow-water carbonate production in the area. The two successions described in this paper originated from two subsided blocks located to the east or the northeast of the AdCP (Fig. 9). Together with tectonically induced subsidence, plankton productivity and carbonate production on the platform played an important role in the sedimentation control in the neighboring basins on the passive margin.

Middle Triassic rift basin preserved on Ivanščica Mt. was short lived and shallow-water carbonate sedimentation was reestablished in the Ladinian (Goričan et al. 2005). Shallow-water conditions were recorded in the studied sections throughout the Late Triassic (Fig. 2). Fenestrae and stromatolite laminae in dolostone of Gradinovec section indicate deposition in subtidal to intertidal/supratidal environment, while microfacies of overlaying limestone (MF 4–6) recorded in Gradinovec, Mala Ivanščica, and Mrzljak sections indicates shallow-water sedimentation near the platform margin. The age of these deposits is determined based on dasycladal algae found in dolostone and benthic foraminifera from the limestone. Paleokarst features found in limestone (MF 6) indicate occasional subaerial exposure.

In the SE part of the study area, deepening of the depositional environment around the Triassic/Jurassic boundary is marked by the deposition of breccia on Mrzljak section and light red bioclastic wackestone to packstone with open marine fauna (MF 9–10) atop of Upper Triassic shallow-water limestone in Mala Ivanščica section (Figs. 2 and 9b). Benthic foraminifera indicate Early Jurassic age for these deposits. This accelerated subsidence pulse around the Triassic/Jurassic boundary has previously been recorded regionally (e.g., Rožič et al. 2017). Calcareous shale and marls containing radiolarians, recorded in Mrzljak section, represents deep-marine facies. Occasional intercalations of calciturbidites represent redeposited material from adjacent shallow-water

**Table 2** Occurrence of radiolarian species in chert samples from Trpnjak section. Zonal ranges of the species according to zonation of Baumgartner et al. (1995b) are given in the second column; the arrows indicate that the ranges have been subsequently extended (see text for additional references). The zonal assignment of each sample is given in the bottom row

| Radiolarians | UAZs (Baumgartner et al. 1995b) | Samples | | | |
|---|---|---|---|---|---|
| | | TR – 0.10 | TR – 3.50 | TR – 4.00 | TR – 6.00 |
| *Angulobracchia* sp. | – | • | | | |
| *Archaeodictyomitra apiarium* (Rüst) | 8–22 | | • | | |
| *Archaeodictyomitra minoensis* (Mizutani) | 9–12 | | • | | • |
| *Archaeodictyomitra rigida* Pessagno | – | cf | | | |
| *Archaeodictyomitra spelae* Chiari, Cortese and Marcucci | – | | • | | |
| *Archaeodictyomitra* spp. | – | | | • | • |
| *Archaespongoprunum elegans* Wu | – | • | | • | |
| *Archaespongoprunum imlayi* Pessagno | – | | • | | cf |
| *Archicapsa* (?) *guttiformis* Tan | – | | | • | |
| *Campanomitra* (?) *galera* (Suzuki) | – | | | • | |
| *Campanomitra* (?) *umenokiensis* (Suzuki) | – | | | • | • |
| *Campanomitra tuscanica* (Chiari, Cortese, and Marcucci) | – | | • | • | • |
| *Campanomitra* (?) sp. | – | | | | • |
| *Cinguloturris carpatica* Dumitrica | 7–11 | • | • | cf | • |
| *Crococapsa hexagona* (Hori) | – | • | | | cf |
| *Crococapsa subcrassitestata* (Aita) | – | | | | cf |
| *Crococapsa* sp. | – | | | | • |
| *Doliocapsa matsuokai* (Yeh) | – | | | | • |
| *Doliocapsa stecki* (O'Dogherty, Goričan and Dumitrica) | – | | • | • | |
| *Eoxitus dhimenaensis* (Baumgartner) | 3–11 | • | | | |
| *Eucyrtidiellum* (?) sp. aff. *E.* (?) *circumperforatum* Chiari, Marcucci and Prela | – | | • | | |
| *Eucyrtidiellum nodosum* Wakita | 3–10 | | • | | |
| *Eucyrtidiellum ptyctum* (Riedel and Sanfilippo) | 5–11 | • | • | • | • |
| *Gongylothorax favosus oviformis* Suzuki and Gawlick (was *Gongylothorax* sp. aff. *G. favosus* Dumitrica in Baumgartner et al. 1995a) | 7–8 → | | | • | cf |
| *Gongylothorax marmoris* Kiessling and Zeiss | – | | • | | |
| *Gongylothorax* sp. aff. *G. marmoris* Kiessling and Zeiss | | | • | | |
| *Hemicryptocapsa carpathica* (Dumitrica) | 7–11 → | • | | • | |
| *Hemicryptocapsa yaoi* (Kozur) | – | | | cf | |
| *Hexasaturnalis minor* (Baumgartner) | – | | | • | |
| *Hexasaturnalis nakasekoi* Dumitrica and Dumitrica-Jud | – | | • | | |
| *Loopus martae* Beccaro | – | | | • | |
| *Loopus primitivus* (Matsuoka and Yao) | 7–12 | cf | • | • | |
| *Mirifusus dianae* (Karrer) | 7–20 | | cf | | cf |
| *Mizukidella kamoensis* (Mizutani and Kido) | 3–7 → | | • | cf | |
| *Mizukidella mokaensis* O'Dogherty, Goričan and Gawlick | – | | • | | |
| *Pantanellium riedeli* Pessagno | 7–12 | cf | | cf | |
| *Parahsuum carpaticum* Widz and DeWever (was *Parahsuum* sp. S in Baumgartner et al. 1995a) | 7–11 | • | | | |
| *Parahsuum* sp. | – | | • | | |
| *Paronaella broennimanni* Pessagno | 3–10 | • | | | |
| *Parvicingula veghae* (Grill and Kozur) | – | | • | | |
| *Parvicingula* (?) sp. | – | • | | | |
| *Parvimitrella* sp. | – | | | • | |
| *Praeconocaryomma* sp. | – | | | | • |
| *Praeparvicingula sodaensis* (Pessagno & Whalen) | – | | | | • |

**Table 2** (continued)

| Radiolarians | UAZs (Baumgartner et al. 1995b) | Samples | | | |
|---|---|---|---|---|---|
| | | TR – 0.10 | TR – 3.50 | TR – 4.00 | TR – 6.00 |
| *Protunuma japonicus* Matsuoka and Yao | 7–12 | • | • | • | • |
| *Pseudoeucyrtis* sp. B sensu Widz 1991 | – | | | | • |
| *Ristola altissima altissima* (Rüst) | 7–12 | | | • | |
| *Spinosicapsa spinosa* (Ožvoldová) | 8–13 | | | | • |
| *Spinosicapsa triacantha* (Fischli) | – | | • | cf | • |
| *Thanarla patricki* gr. (Kocher) | – | • | | | • |
| *Transhsuum brevicostatum* (Ožvoldová) | 3–11 | • | | • | |
| *Transhsuum maxwelli* (Pessagno) | 3–10 | • | | | |
| *Transhsuum okamurai* (Mizutani) | 7–11 | | • | | • |
| *Triactoma blakei* (Pessagno) | 4–11 | | • | | |
| *Tritrabs casmaliaensis* (Pessagno) | 4–10 | | • | | |
| *Tritrabs exotica* (Pessagno) | 4–11 | | cf | | • |
| *Tritrabs rhododactylus* Baumgartner | 3–13 | | | | cf |
| *Xitomitra annibill* (Kocher) | – | | • | | |
| *Zhamoidellum ovum* Dumitrica | ← 9–11 → | • | • | • | • |
| Age assignments of samples (UAZs of Baumgartner et al. 1995b) | | 7–10 | 9–10 | 7–11 | 9–11 |

environments. Absence of coarse-grained deposits indicates a relatively distal position in regard to source of material. Because no fossils were obtained from these deposits, their Toarcian age is assumed based on regional correlation (Jenkyns and Clayton 1986; Vórós and Galàcz 1998; Goričan et al. 2003; Šmuc and Goričan 2005; Rožič 2009). Pelagic limestone from Mala Ivanščica section, as well as shale and marls from Mrzljak section are both overlain by calcarenites (Fig. 2). Their shallow-water carbonate grains were most likely redeposited as turbidites from the AdCP. Besides material deposited by turbidites, a large proportion of carbonate mud in deep-sea sediments during the Early Jurassic represents lime mud shed from carbonate platforms (Schlager and James 1978; Bernoulli and Kälin 1984; Flügel 2010). Although present at this time, calcareous nannoplankton and planktonic foraminifera were not important components of pelagic limestones until the Late Jurassic and early Late Cretaceous, respectively.

In the NW part of the study area, outcrops of fenestral intraclastic packstone containing dasycladal algae and benthic foraminifera indicate shallow-water conditions here persisted at latest until the late Pliensbachian (Figs. 2, 9b). Neptunian dykes in these Lower Jurassic platform limestone were formed either by deformation due to extension (Lehner 1991) or by gravity sliding on tilted blocks formed during the Early Jurassic rifting phase (Winterer et al. 1991). Deposition of filament wackestone to packstone containing open-marine biota on top of shallow-water limestone marks the deepening of the depositional environment. This limestone also fills the neptunian dykes in the platform limestone. The age of these pelagic limestone is constrained to Middle Jurassic based on planktonic foraminifera and assumed age of overlying radiolarian chert. Neptunian dykes filled with the Middle Jurassic pelagic limestone within Lower Jurassic carbonate rocks are well known from the Southern Alps (Winterer et al. 1991; Črne et al. 2007).

Radiolarian cherts, found in both SE and NW parts of the investigated area (Figs. 9b and 10), represent typical pelagic facies in deep-water basins of the western Tethys, with the shift from carbonate to siliceous deposition usually occurring around the Early Bajocian (Baumgartner 2013). This shift is linked to changes in surface fertility of the ocean attributed to paleoclimatic changes (Bartolini et al. 1999; Baumgartner 2013). The oldest radiolarian sample in this study has been assigned to the Late Bathonian–Early Callovian to Early Oxfordian. We note that contact with underlying deposits has not been found (Fig. 2), and therefore the entire thickness and age span of the radiolarian cherts could not be precisely determined.

Siliceous sedimentation persisted in the study area until the Tithonian when the character of sedimentation changed again to carbonate with the deposition of the Aptychus limestone as observed in Trpnjak section (Figs. 2 and 9). This deep-marine

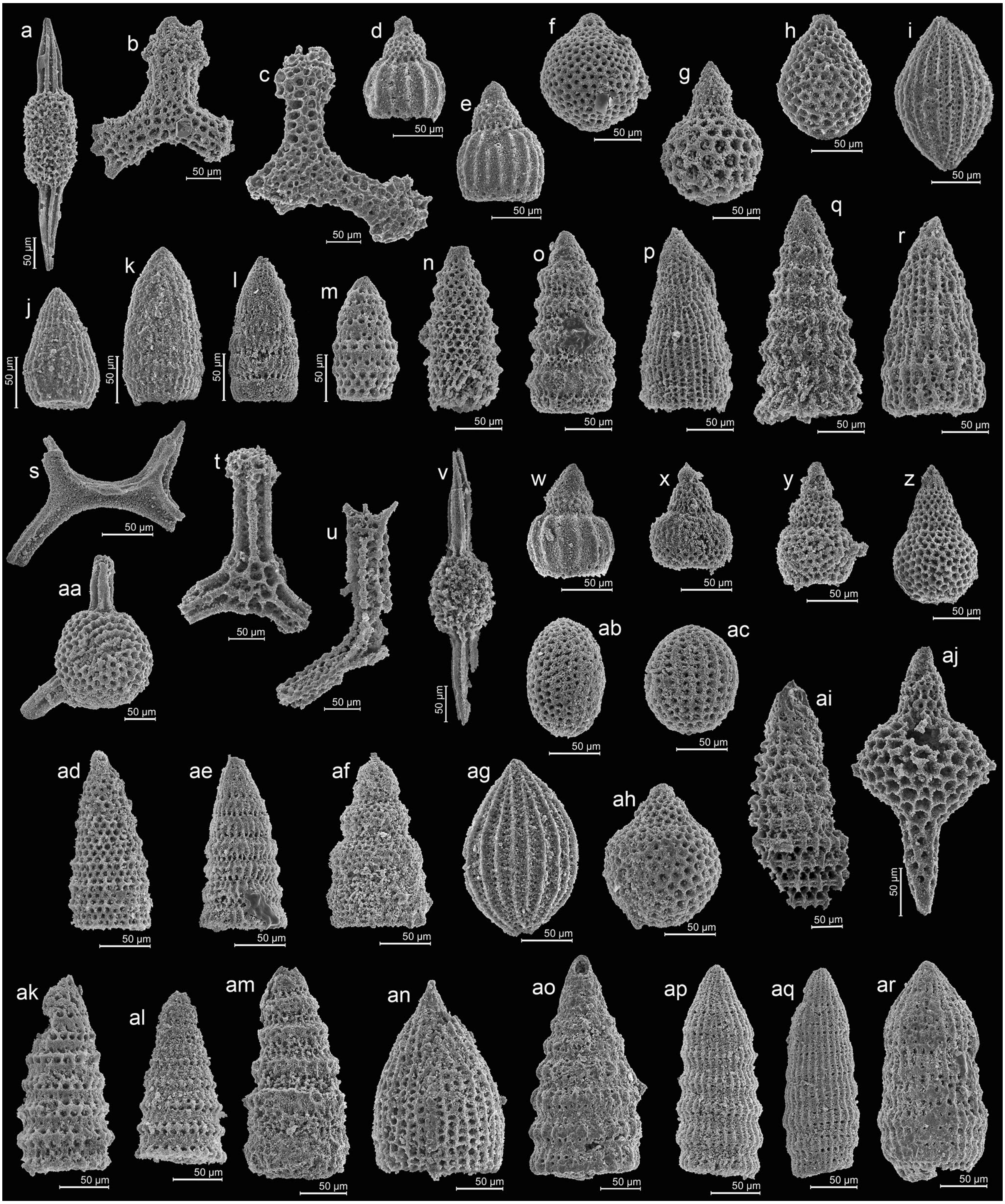


limestone (known regionally as Maiolica or Biancone) is characteristic of uppermost Jurassic to Lower Cretaceous successions of all deep-water paleogeographic domains of the Alpine–Dinaric realm (Weissert 1981; Goričan et al. 2012, 2022; Fig. 10). This change from siliceous to carbonate sedimentation is attributed to a rapid diversification of calcareous nannoplankton in the Tithonian (Bronemann et al. 2003). On Ivanščica Mt., this change has been dated with calpionellids

◂**Fig. 7** Middle to Late Jurassic radiolarians from Trpnjak section. For each illustration, the scanning electron micrograph number is indicated. Taxonomical remarks are given when needed. Figs. a–r: radiolarians from sample TR-0.10. **a** *Archaespongoprunum elegans* Wu, TR-0.10_0061; **b** *Paronaella broennimanni* Pessagno, TR-0.10_0047; **c** *Angulobracchia* sp., TR-0.10_0036; **d, e** *Eucyrtidiellum ptyctum* (Riedel and Sanfilippo), d TR-0.10_0006; e TR-0.10_0004; **f** *Hemicryptocapsa carpathica* (Dumitrica), TR-0.10_0059; **g** *Crococapsa hexagona* (Hori), TR-0.10_0048; **h** *Zhamoidellum ovum* Dumitrica, TR-0.10_0015; **i** *Protunuma japonicus* Matsuoka and Yao, TR-0.10_0008; **j** *Thanarla patricki* gr. (Kocher), TR-0.10_0021; **k** *Archaeodictyomitra* sp. cf. *A. rigida* Pessagno, TR-0.10_0050; **l** *Loopus* sp. cf. *L. primitivus* (Matsuoka and Yao), TR-0.10_0054; **m** *Parvicingula* (?) sp., TR-0.10_0014; **n** *Eoxitus dhimenaensis* (Baumgartner), TR-0.10_0052; **o** *Cinguloturris carpatica* Dumitrica, TR-0.10_0056; **p** *Parahsuum carpaticum* Widz and DeWever, TR-0.10_0051; **q** *Transhsuum brevicostatum* (Ožvoldová), TR-0.10_0001; **r** *Transhsuum maxwelli* (Pessagno), TR-0.10_0057. Figs. s–ar: radiolarians from sample TR-3.50. **s** *Hexasaturnalis nakasekoi* Dumitrica and Dumitrica-Jud, TR-3.50_0010; **t** *Tritrabs* sp. cf. *T. exotica* (Pessagno), TR-3.50_0026; **u** *Tritrabs casmaliaensis* (Pessagno), TR-3.50_0029; **v** *Archaespongoprunum imlayi* Pessagno, TR-3.50_0057; **w** *Eucyrtidiellum ptyctum* (Riedel and Sanfilippo), TR-3.50_0011; **x** *Eucyrtidiellum nodosum* Wakita, TR-3.50_0012; **y** *Eucyrtidiellum* (?) sp. aff. *E.* (?) *circumperforatum* Chiari, Marcucci and Prela, TR-3.50_0013, illustrated morphotype has more inflated abdomen and more pronounced strictures between segments then the holotype; **z** *Doliocapsa stecki* (O'Dogherty, Goričan and Dumitrica), TR-3.50_0038; **aa** *Triactoma blakei* (Pessagno), TR-3.50_0047; **ab** *Gongylothorax* sp. aff. *G. marmoris* Kiessling and Zeiss, TR-3.50_0014, illustrated morphotype differs from the holotype by overall more elongated shape.**;** **ac** *Gongylothorax marmoris* Kiessling and Zeiss, TR-3.50_0023; **ad** *Parvicingula veghae* (Grill and Kozur), TR-3.50_0003; **ae** *Loopus primitivus* (Matsuoka and Yao), TR-3.50_0059; **af** *Xitomitra annibill* (Kocher), TR-3.50_0046; **ag** *Protunuma japonicus* Matsuoka and Yao, TR-3.50_0008; **ah** *Zhamoidellum ovum* Dumitrica, TR-3.50_0020; **ai** *Mirifusus* sp. cf. *M. dianae* (Karrer), TR-3.50_0041; **aj** *Spinosicapsa triacantha* (Fischli), TR-3.50_0034; **ak** *Mizukidella mokaensis* O'Dogherty, Goričan and Gawlick, TR-3.50_0044; **al** *Mizukidella kamoensis* (Mizutani and Kido), TR-3.50_0051; **am** *Cinguloturris carpatica* Dumitrica, TR-3.50_0053; **an** *Parahsuum* sp., TR-3.50_0050; **ao** *Transhsuum okamurai* (Mizutani), TR-3.50_0002; **ap** *Archaeodictyomitra minoensis* (Mizutani), TR-3.50; 0005; **aq** *Archaeodictyomitra spelae* Chiari, Cortese and Marcucci, TR-3.50_0001; **ar** *Archaeodictyomitra apiarium* (Rüst), TR-3.50_0006

as Late Tithonian (Babić and Zupanič 1973). Late Tithonian age was also determined for calcarenite at the base of pelagic limestone succession (Šikić and Grimani 1965; Babić and Zupanič 1973). Shallow-water carbonate material was deposited as distal turbidites and likely originated from the AdCP together with the lithoclasts of tuff, which is common in Upper Jurassic successions of the AdCP (Velić et al. 2002; Blažeković-Smojić et al. 2009). The deposition of the Aptychus limestone continued until the Valanginian (Babić and Zupanič 1973) on Ivanščica Mt. Similar ages have recently been obtained from the neighboring Rudnica Mt. (Reháková and Rožič 2019). The mixed siliciclastic–carbonate turbidites of the Oštrc Formation, which overly the Aptychus limestone, are recognized as synorogenic sediments, deposited in front of obducting ophiolite nappes (Zupanič et al. 1981; Lužar-Oberiter et al. 2009, 2012). Genetically related successions are well known from the Alps and the Dinarides (Mikes et al 2008; Missoni and Gawlick 2011a; Goričan et al. 2018). The oldest synorogenic deposits in the Dinarides are dated in the Bosnian Basin as Tithonian (Mikes et al. 2008 and references therein). On Ivanščica Mt., deposition of Aptychus limestone lasted until the Valanginian and synorogenic deposits are dated as Hauterivian to Albian, indicating that Ivanščica Mt. occupied a more proximal position on the Adriatic margin in relation to the AdCP.

## Stratigraphic correlations

During the Mesozoic, vast areas of shallow water and pelagic sedimentation formed the eastern passive margin of Adria microplate (Fig. 9a). Stratigraphic successions attributed to the margin, preserved today in the Alps and the Dinarides, reflect complex topography formed during the Middle Triassic rifting (e.g., Goričan et al. 2012, 2022 and references therein). Pelagic conditions were recorded in some areas from the Middle Triassic onwards, while in other areas, shallow-water carbonate sedimentation persisted until they were drowned as a result of tectonically induced subsidence during the latest Triassic or Early Jurassic (Figs. 9 and 10). From the Middle Jurassic, pelagic conditions were recorded in all subsided areas of the eastern Adriatic margin (Fig. 10). In latest Jurassic–Early Cretaceous, synorogenic sediments, related to the emplacement of the Neotethyan ophiolites, were deposited in foredeep basins formed on the passive margin (e.g., Blanchet et al. 1969; Faupl and Wagreich 2000; Mikes et al. 2008; Lužar-Oberiter et al. 2009, 2012; Goričan et al. 2018; Fig. 10). Oštrc Formation on Mt. Ivanščica has long been recognized as one of these synorogenic formations (Zupanič et al. 1981; Lužar-Oberiter et al. 2009; 2012) together with the Vranduk Formation in the Dinarides, Studor Formation in the Southern Alps, and Rossfeld Formation in the Northern Calcareous Alps. The correlation of these formations and underlying successions indicates that synorogenic sediments represent a time-transgressive unit deposited over distal pelagic successions in the Tithonian to Berriasian while reaching drowned areas of the Late Triassic shallow-water lagoons around Hauterrivian–Barremian (Goričan et al. 2018). The purpose of this chapter is to correlate the newly described Upper Triassic–Jurassic successions underling the Oštrc Formation with similar successions of the eastern Adriatic margin (Fig. 10).

In the neighboring Žumberak Mts. (Fig. 9a), shallow- to deep-water succession correlative to those on Mt. Ivanščica

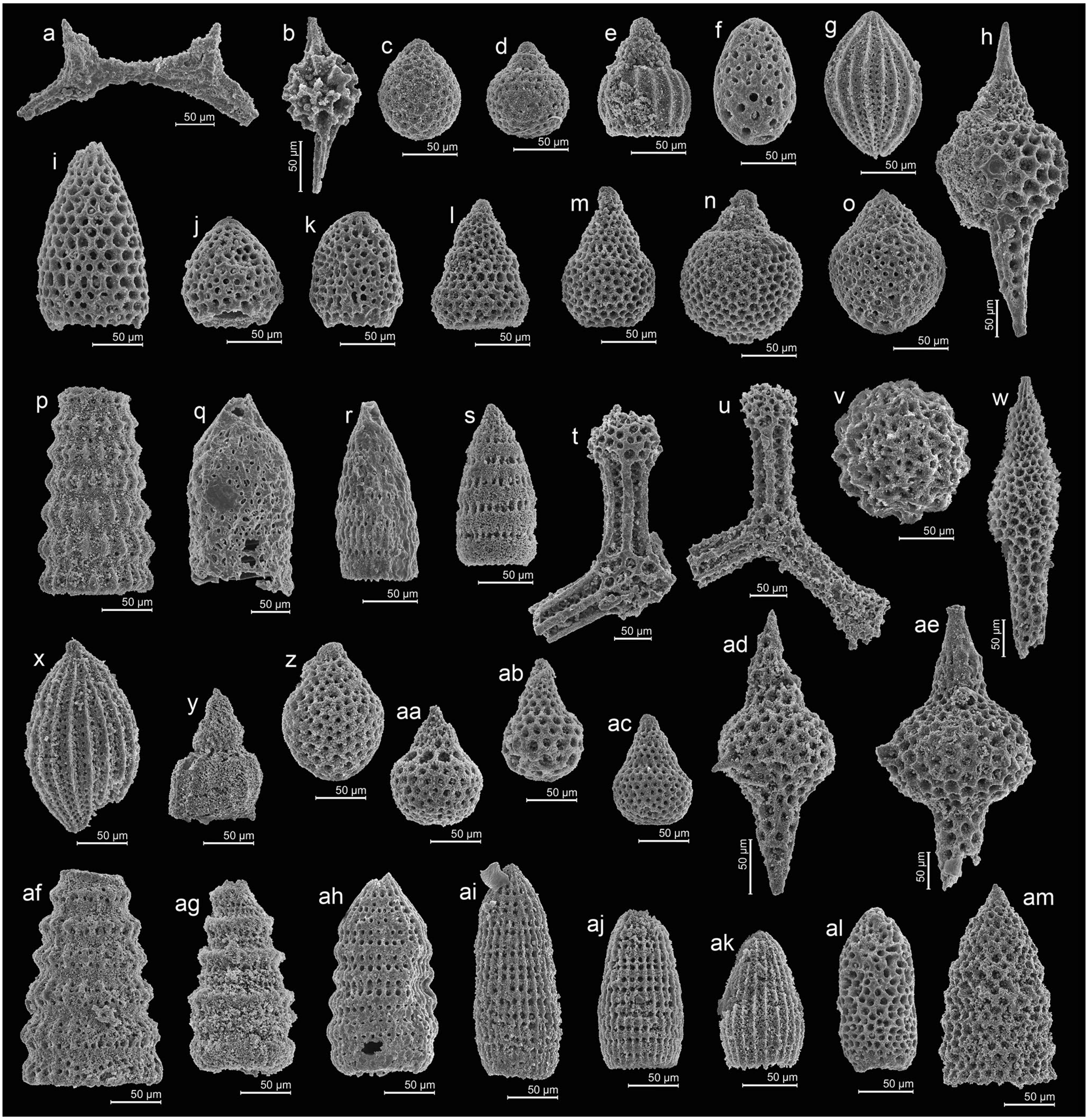


was described. This succession, attributed to the AdCP margin, starts with Upper Triassic dolostone and limestone identical to the Hauptdolomit and Dachstein Limestone from Ivanščica Mt. (Grgasović 1997). Lower Jurassic shallow-water limestone is overlain by upper Lower Jurassic slope limestone (Dragičević and Velić 2002) followed by Middle to Upper Jurassic pelagic limestone rich in *Bositra*-shell filaments and protoglobigerinids (Gušić and Babić 1970). These pelagic limestone in places contain resedimented shallow-water material including foraminifera indicative of early Late Jurassic age (Bucković et al. 2004). Uppermost Tithonian to Lower Cretaceous Aptychus limestone (Gušić and Babić 1970; Babić 1973, 1976; Bucković et al. 2004) is overlain by carbonate–siliciclastic turbidites of the Lower Cretaceous Kravljak Formation (Babić 1974b; Lužar-Obertier et al. 2009, 2012).

◂**Fig. 8** Late Jurassic radiolarians from Trpnjak section. For each illustration, the scanning electron micrograph number is indicated. Figs. a–s: radiolarians from sample TR-4.00. **a** *Hexasaturnalis minor* (Baumgartner), TR-4.00_0001; **b** *Pantanellium* sp. cf. *P. riedeli* Pessagno, TR-4.00_0002; **c** *Gongylothorax favosus oviformis* Suzuki and Gawlick, TR-4.00_0041; **d** *Hemicryptocapsa* sp. cf. *H. yaoi* (Kozur), TR-4.00_0043; **e** *Eucyrtidiellum ptyctum* (Riedel and Sanfilippo), TR-4.00_0018; **f** *Archicapsa* (?) *guttiformis* Tan, TR-4.00_0009; **g** *Protunuma japonicus* Matsuoka and Yao, TR-4.00_0014; **h** *Spinosicapsa* sp. cf. *S. triacantha* (Fischli), TR-4.00_0024; **i** *Campanomitra tuscanica* (Chiari, Cortese, and Marcucci), TR-4.00_0006; **j** *Campanomitra* (?) *umenokiensis* (Suzuki), TR-4.00_0017; **k** *Campanamitra* (?) *galera* (Suzuki), TR-4.00_0019; **l** *Parvimitrella* sp., TR-4.00_0025; **m** *Doliocapsa stecki* (O'Dogherty, Goričan and Dumitrica), TR-4.00_0030; **n** *Hemicryptocapsa carpathica* (Dumitrica), TR-4.00_0039; **o** *Zhamoidellum ovum* Dumitrica, TR-4.00_0028; **p** *Transhsuum brevicostatum* (Ožvoldová), TR-4.00_0005; **q** *Ristola altissima altissima* (Rüst), TR-4.00_0035; **r** *Loopus primitivus* (Matsuoka and Yao), TR-4.00_0003; **s** *Loopus martae* Beccaro, TR-4.00_0008. Figs. t–am: radiolarians from sample TR-6.00. **t** *Tritrabs exotica* (Pessagno), TR-6.00_0066; **u** *Tritrabs* sp. cf. *T. rhododactylus* Baumgartner, TR-6.00_0063; **v** *Praeconocaryomma* sp., TR-6.00_0041; **w** *Pseudoeucyrtis* sp. B sensu Widz 1991, TR-6.00_0060; **x** *Protunuma japonicus* Matsuoka and Yao; TR-6.00_0006; **y** *Eucyrtidiellum ptyctum* (Riedel and Sanfilippo), TR-6.00_0023; **z** *Zhamoidellum ovum* Dumitrica; TR-6.00_0021; **aa** *Crococapsa* sp. cf. *C. subcrassitestata* (Aita), TR-6.00_0050; **ab** *Crococapsa* sp., TR-6.00_0047; **ac** *Doliocapsa matsuokai* (Yeh), TR-6.00_0034; **ad** *Spinosicapsa triacantha* (Fischli), TR-6.00_0059; **ae** *Spinosicapsa spinosa* (Ožvoldová), TR-6.00_0059; **af** *Transhsuum okamurai* (Mizutani), TR-6.00_0027; **ag** *Cinguloturris carpatica* Dumitrica, TR-6.00_0008; **ah** *Archaeodictyomitra minoensis* (Mizutani), TR-6.00_0002; **ai, aj** *Archaeodictyomitra* spp., ai TR-6.00_0003, aj TR-6.00_0036; **ak** *Thanarla patricki* gr. (Kocher), TR-6.00_0049; **al** *Campanomitra* (?) sp., TR-6.00_0001; **am** *Praeparvicingula sodaensis* (Pessagno & Whalen), TR-6.00_0025

In the Bosnian Zone of the central Dinarides ('Zone Bosniaque' of Aubouin et al. 1970; Fig. 9a), two stratigraphic successions are described, both including Lower Cretaceous flysch-type deposits of the Vranduk Formation (Fig. 10). The first succession, representing central part of the Bosnian Zone, is entirely deep water. Middle Triassic to Lower Jurassic limestone is overlain by Middle to Upper Jurassic cherts and Berriasian to Cenomanian flysch-type deposits (Cadet 1978). The second succession, representing the external part of the Bosnian Zone, consists of massive dolostone of possibly Early Jurassic age overlain by bedded limestone, black chert and Tithonian–Berriasian breccia. Here, flysch-type deposits are dated with foraminifera as Barremian–Aptian to Cenomanian (Cadet 1978). This succession of the external Bosnian Zone correlates well with the successions on Ivanščica Mt.

In the Julian Alps, several paleogeographic units containing deep-water successions originating from the passive margin of Adria are preserved (Fig. 9a). The successions of the Bled Basin and eastern Julian High differ from other successions by containing Lower Cretaceous flysch-type deposits (Cousin 1981; Kukoč et al. 2012; Goričan et al. 2018). These two successions correlate well with successions of Ivanščica Mt. and Bosnian Zone (Goričan et al. 2018; Fig. 10) indicating the same paleogeographic origin. The onset of flysch-type sedimentation in the other basins of the Julian Alps occurred in the Campanian–Maastrichtian, which is one of the argument used to position the Bled Basin on the outer margin of the Adriatic plate (Goričan et al. 2012 and references therein; Fig. 9a).

The Bled Basin succession is characterized by pelagic sedimentation from the Middle Triassic onwards (Cousin 1981; Kukoč et al. 2012; Goričan et al. 2018; Gale et al. 2019, 2021) and is correlative to the central Bosnian Zone (Fig. 10). Upper Triassic–Lower Jurassic carbonates are overlain by the Pliensbachian coarse-grained breccia, Middle to Upper Jurassic radiolarian cherts, and uppermost Jurassic Biancone limestone. Lowermost Cretaceous carbonate gravity-flow deposits overlying the Biancone limestone contain shallow-water debris as well as grains of basalt and provide evidence of a carbonate platform which existed in the internal zones but is not preserved today (Kukoč et al. 2012). Overlying turbidites of the Studor Formation correspond to the Vranduk Formation in the Bosnian Zone (Cousin 1981; Kukoč et al. 2012; Goričan et al. 2018).

The succession of the east Julian High originated from the drowned block of the Julian Carbonate Platform (Goričan et al. 2018) located to the north of the AdCP (Fig. 9a) and consists of Upper Triassic–Lower Jurassic Dachstein Limestone capped by the Lower Jurassic pelagic limestone (Fig. 10). In this succession, radiolarian cherts have not been found. Instead, pelagic Biancone limestone directly overlies Lower Jurassic crinoidal limestone. Flysch-type deposits of the Studor Formation are dated as Barremian in this succession (Goričan et al. 2018). This succession is correlative to the ones of the external Bosnian Zone and Ivanščica Mt. with notable differences being the absence of radiolarian cherts as well as paleogeographic origin.

Correlative succession to those on Ivanščica Mt. can also be found in the Tirolic Nappes of the Northern Calcareous Alps (Fig. 10). In this area, transition from the Dachstein carbonate platform to the open shelf is described (e.g., Missoni and Gawlick 2011a, b and references therein). Unlike in the Southern Alps and the Dinarides, synorogenic deposits in the Northern Calcareous Alps occur only in pelagic successions deposited on top of Upper Triassic shallow-water carbonates (e.g., Missoni and Gawlick 2011a, b). The Late Triassic evolution of both areas is identical. Carbonate deposits, including Hauptdolomite and bedded lagoonal Dachstein Limestone, were deposited until the end of the Triassic. Condensed Adnet Group and Klauss Formation

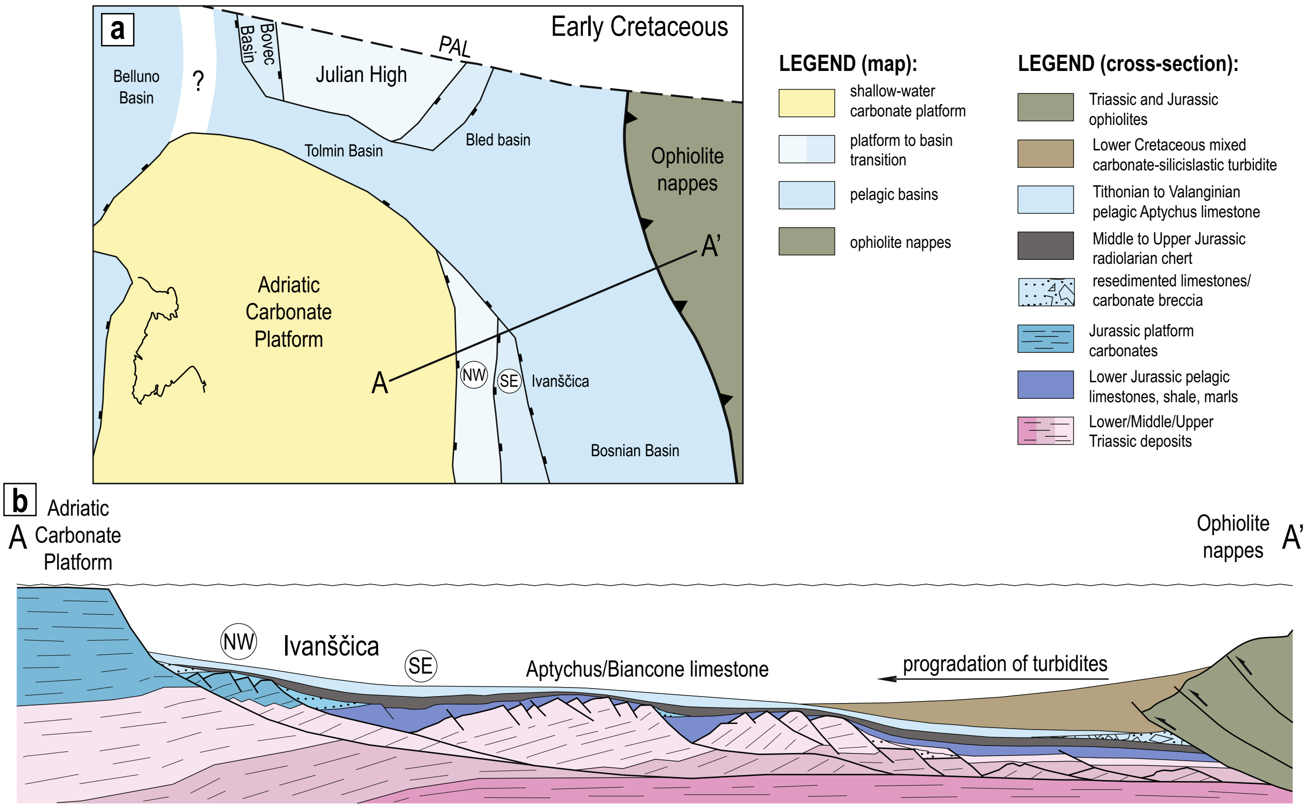


**Fig. 9** **a** Schematic paleogeographical map (not in scale) showing distribution of various depositional environments in the wider study area during Early Cretaceous times. Paleogeographical units to the north are displaced along the Periadriatic lineament (PAL) and nowadays can be found in the Transdanubian range. Modified after Goričan et al. (2018). **b** Conceptual cross-section across eastern Adriatic passive continental margin and investigated area showing the distribution of various depositional environments as a result of polyphase rift-related tectonics. Different timing of platform drowning is documented by different age of prerift and synrift deposits preserved in different faulted blocks. Block representing SE Ivanščica Mt. exhibits Upper Triassic and older prerift deposits overlain by Lower Jurassic synrift deposits while in the same time, block representing NW Ivanščica Mt. retained shallow-marine deposition and was not influenced by faulting and subsidence until the Pliensbachian. Middle Jurassic to Lowermost Cretaceous radiolarian cherts and pelagic limestones representing postrift deposits, onlapping over Lower Jurassic synrift deposits and older prerift deposits representing seafloor of the residual topographies. Progradation of synorogenic turbidites from the distal domains reached the study area in the Hauterivian

(Böhm 2003; Gawlick et al. 2009) were deposited on top of drowned shallow-water carbonates in the Early and Middle Jurassic. Reddish pelagic limestone of the lower Adnet Formation was deposited on top of drowned Rhaetian reefs. Marly limestone, breccia, and marl with intercalated limestone beds of the upper Adnet Formation form a sequence of increasingly pelagic sedimentation (Böhm 2003). This succession of the Adnet Formation corresponds well with the succession of SW Ivanščica Mt. The notable difference is the absence of breccias and predominance of calcarenites on Mt. Ivanščica. Limestone of the Klaus Formation, often found as fissure filling, contain protoglobigerinas and *Bositra*-shells among other pelagic fossils (Gawlick et al. 2009). Comparable limestone is found in neptunian dykes on NW Ivanščica.

The change from carbonate to siliceous sedimentations occurred around the Bathonian/Callovian boundary in the Northern Calcareous Alps (Gawlick and Frisch 2003; Fig. 10). Radiolarites, interstratified by thick mass-flow deposits, were deposited in trench-like basins in front of propagating thrust belt (Missoni and Gawlick 2011b). Radiolarian cherts on Ivanščica Mt. are devoted of significant mass-flow deposits indicating deposition away from the thrust front. Pelagic limestone of the Oberalm Formation deposited in the Northern Calcareous Alps from the late Tithonian to Berriasian intercalated with gravity-flow deposits (Barmstein limestone). Short-lived, isolated carbonate platforms, which formed on top of newly formed nappe stack, provided shallow-water material for these gravity-flow deposits (Missoni and Gawlick 2011a, b). Correlative

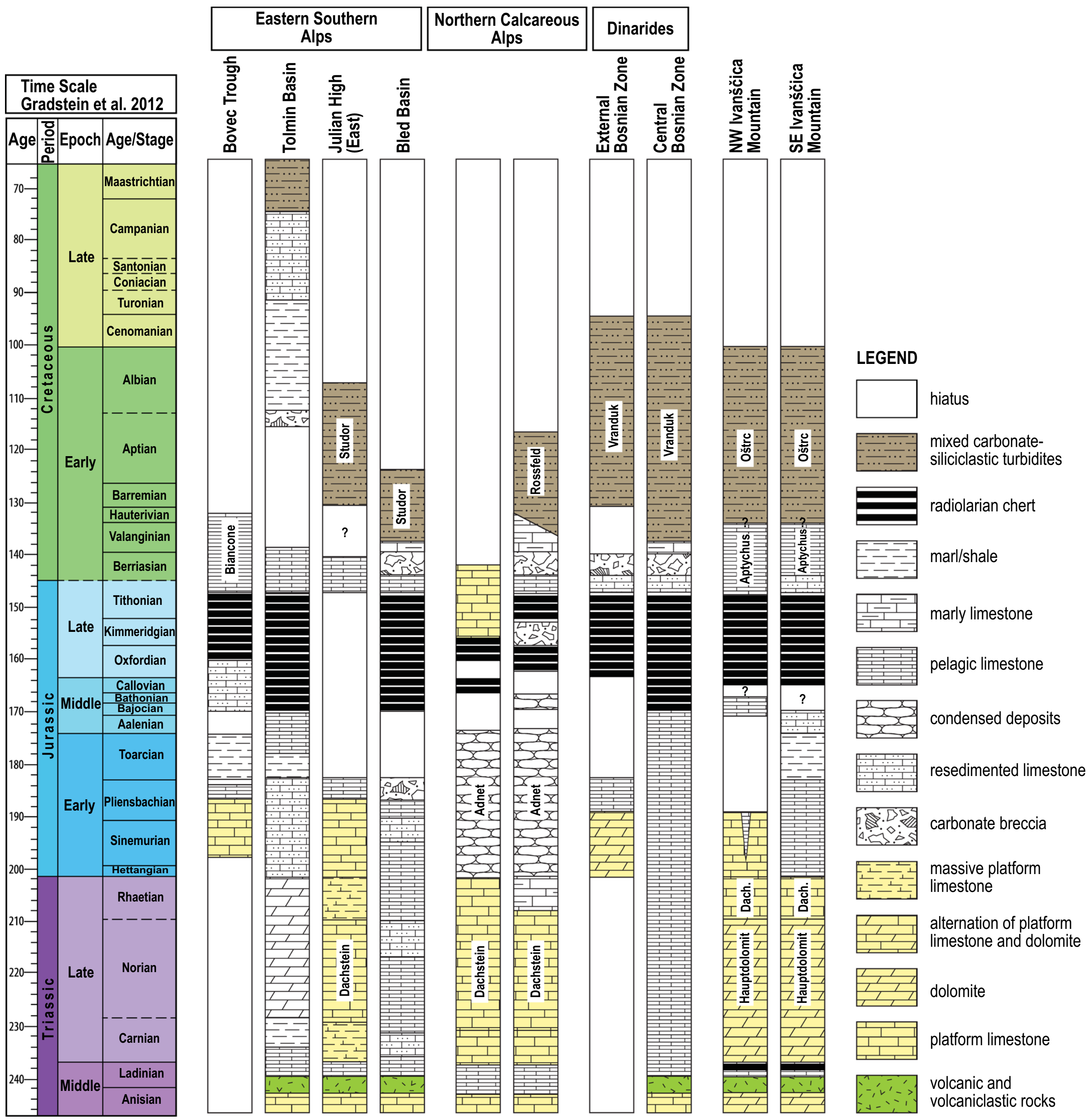


**Fig. 10** Chronostratigraphic overview of selected Middle Triassic to Cretaceous successions of the Adriatic passive continental margin and their correlation with studied Ivanščica successions. Ivanščica succession is compiled after Babić and Zupanič (1973, 1978), Šimunić et al. (1982), Kukoč et al. 2023 and the results of this study. Bovec Basin is compiled according to Goričan et al. (2003) and Šmuc and Goričan (2005). Other sections are adopted from Goričan et al. (2018)

Aptychus limestone on Mt. Ivanščica is significantly less thick than the Oberlam Formation and only has thin calcarenite beds at its base. Shallow-water material for these calcarenites likely originated from the AdCP. Finally, Valanginian to Aptian Rossfeld Formation (Faupl and Wagreich 2000; Missoni and Gawlick 2011a) corresponds to the turbidites of the Oštrc Formation on Mt. Ivanščica.

Besides described paleogeographic units, deposits of Adriatic passive margin can be found in the Transdanubian Central Range. In that area, Upper Triassic Dachstein Limestone is overlain by Hettangian oncoidal-ooidal Kardosrét limestone and Hettangian to Sinemurian foraminiferal and crinoidal micritic Pisznice limestone (Görög 1994; Vörös and Galàcz 1998) which correlates with Lower Jurassic bioclastic limestone of SE Ivanščica Mt. Lower and Middle Jurassic deposits are represented mostly by various condensed limestones which are continuously overlain by Middle to Upper Jurassic Lókút Radiolarite Formation and Uppermost Jurassic to Lower Cretaceous Biancone limestone (Vórós and Galàcz 1998) which is in agreement with other pelagic successions from the Adriatic passive margin. By contrast to paleographically more external succession of Bakony Mountains, succession of Gerecse Mountains in the NE Transdanubian Central Range recorded the onset of Lower Cretaceous turbidities (Császár and Árgyelán 1994; Vórós and Galàcz 1998). This indicates a more internal paleogeographic position of the NE Transdanubian Central Range, similar to one of Ivanščica Mt.

## Correlation with deep-water basins of the Adria plate

The Jurassic evolution of the eastern Adriatic margin recorded on Ivanščica Mt. is comparable with evolutions of other Mesozoic deep-water basins that existed on deeply submerged parts of the Adriatic plate. Remnants of the western margin of Adria with several deep-water basins and plateaus are preserved in the Southern Alps (Winterer and Bosellini 1981; Bertotti et al. 1993; Berra et al. 2009). The complex topography of this part of the margin is a result of the latest Triassic and Early Jurassic extension related to the opening of the Alpine Tethys (Winterer and Bosellini 1981; Bertotti et al. 1993). Pelagic sedimentation characterized deeply submerged Lombardian and Belluno basins from the Early Jurassic, while shallow-water carbonate sedimentation persisted on the Trento Plateau until the end of the Early Jurassic (Winterer and Bosellini 1981; Baumgartner et al. 1995c; Berra et al. 2009; Baumgartner 2013). Furthermore, intraplatform Budva Basin, preserved in the External Dinarides, was formed during the Middle Triassic rifting episode, and was characterized by pelagic sedimentation until the end of Cretaceous (Goričan 1994; Goričan et al. 2022). Another basin attributed to the Adriatic margin characterized by pelagic sedimentation during this period is the Lagonegro Basin preserved in the southern Apennines (De Wever and Miconnet 1985; Bertinelli et al. 2005).

The proximal parts of these submerged margins were influenced by active carbonate platforms, which, in time of high carbonate production, supplied the basins with peri-platform ooze and resedimented shallow-water material. Sedimentation in the distal parts, however, seems to be controlled mainly by fluctuations in sea-surface fertility, which in-turn is controlled by climatic factors (De Wever et al. 2014; Baumgartner 2013). Generally high carbonate production in the Early Jurassic is reflected in the deposition of pelagic and resedimented limestones in deep-water basins. In the Lombardian and Belluno basins, hemipelagic and resedimented limestones of Moltrasio and Soverzene formations were deposited, followed by marly limestone of the Sogno and Igne formations (Winterer and Bosellini 1981; Baumgartner et al. 1995c; Gaetani 2010; Baumgartner 2013). Redeposited oolites of Concesio Formation and condensed limestone of Rosso Ammonitico Lombardo are also present in the Toarcian in the Lombardian Basin (Baumgartner et al. 1995c; Gaetani 2010). In the Budva Basin, the pelagic bar limestone contains carbonate gravity-flow deposits (Goričan 1994; Goričan et al. 2022). Lower Jurassic pelagic limestones are recorded also in the Lagonegro Basin (Bertinelli et al. 2005). On Ivanščica Mt., pelagic limestone with resedimented carbonate material is deposited above the Upper Triassic shallow-water carbonates.

In the Middle Jurassic, the character of the sedimentation changed from carbonate to siliceous throughout the western Tethys (Baumgartner 2013). Historically, deposition of radiolarites has been explained by subsidence of the distal margins below the CCD (e.g., Bosellini and Winterer 1975); however, in recent years, radiolarites have been interpreted as high bioproductivity deposits (e.g., Bernoulli and Jenkyns 2009; Baumgartner 2013). The Middle Jurassic onset of radiolarite deposition in the western Tethys coincides with the positive shift in $\delta^{13}C$, which may indicate eutrophic conditions and the demise of carbonate production (Bartollini et al. 1999; Baumgartner 2013). Baumgartner (2013) attributes this change in sea-surface fertility to input of nutrients from big rivers, while other authors envision high-productivity upwelling systems brought by monsoonal climate regime (De Wever et al. 2014; Ikeda et al. 2017). During the Middle and Late Jurassic, radiolarites were deposited in the Lombardian Basin (Chiari et al. 2007; Baumgartner 2013), Budva Basin (Goričan 1994, Goričan et al. 2022), and Lagonegro Basin (Bertinelli et al. 2005), with onset of radiolarite sedimentation generally occurring around the Bajocian. Now submerged Trento Plateau was characterized by deposition of condensed Rosso Ammonitico limestone (Baumgartner et al. 1995c; Martire et al. 2006) and pelagic limestone of Fonzaso Formation, which was also deposited in the Belluno Basin (Baumgartner et al. 1995c; Beccaro et al. 2002, 2008). The onset of radiolarian sedimentation on Ivanščica Mt. could not be dated since the lower part of the radiolarite succession is not exposed; however, deposition of radiolarites is recorded from possibly Late Bathonian–early Callovian to the Tithonian.

The end of radiolarite deposition in the Tithonian is probably related to gradual decrease of nutrient availability during the Late Jurassic and diversification of oligotrophic nannoplankton (Bronneman et al. 2003; Baumgartner 2013). Aptychus limestone deposited on Ivanščica Mt. is regionally recognized facies, also referred to as Biancone or Maiolica, and is deposited in all basins of the Southern Alps (Weissert

1981; Jud 1994; Bumgartner et al. 1995c; Chiari et al. 2007; Lukender 2010; Baumgartner 2013). In the Budva Basin, Tithonian to Hauterrivian–Barremian Praevalis limestone is correlative to the Biancone/Maiolica facies (Goričan 1994; Goričan et al. 2022).

## Conclusion

Two described stratigraphic successions represent the continuous Upper Triassic to Lower Cretaceous shallow water to pelagic succession of the eastern passive margin of the Adria microplate. Upper Triassic dolostones and limestones indicate shallow-water deposition within mostly restricted parts of carbonate platform. In the SE Ivanščica Mt., rapid subsidence is documented at the Triassic/Jurassic boundary by deposition of Lower Jurassic pelagic bioclastic limestone and overlying shale and marls directly atop of Upper Triassic platform carbonates. In the NW Ivanščica Mt., shallow-water conditions persisted until the Pliensbachian. This is inferred from the findings of Hettangian to Pliensbachian shallow-water limestone with Neptunian dykes, overlain by Middle Jurassic pelagic limestone. Middle Jurassic change from calcareous to siliceous sedimentation is recorded in the Ivanščica Mt. succession by the deposition of radiolarian chert which overlay Lower to Middle Jurassic successions in both SE and NW study area. Radiolarians from the SW Ivanščica Mt. indicate late Bathonian to early Tithonian age of radiolarian cherts. In the late Tithonian to Valanginian, pelagic Aptychus limestone was deposited on top of radiolarian cherts overlain by Hauterivian to Albian synorogenic deposits. Documented stratigraphic evolution of the Ivanščica Mt. is in good accordance with the passive margin successions originating from the Adria plate, preserved today in the Alps, Apennines, and the Dinarides.

**Acknowledgements** We are thankful to laboratory staff at the Croatian Geological Survey for preparing the thin sections. We would also like to thank the staff at the Ivan Rakovec Institute of Palaeontology ZRC SAZU, Ljubljana, for their warm hospitality and the use of their SEM. We are grateful to Marco Chiari (Firenze) and one anonymous reviewer for their careful review and constructive comments. We would also like to thank Facies editor Wolfgang Kiessling for editorial work and suggestions that helped improve the manuscript.

**Author contributions** MV: field work, conceptualization, methodology, analysis (microfacies), investigation, writing (original draft, review, and editing); DK: field work, conceptualization, methodology, analysis (radiolarians), writing (original draft, review, and editing); TG: field work, analysis (algae and foraminifera), writing (original draft, review, and editing); LF: analysis (algae and foraminifera), writing (review and editing); DS: writing (review and editing).

**Funding** This research was supported by the Croatian Science Foundation under the project "Revealing the Middle Triassic Paleotethyan Geodynamics Recorded in the Volcano-Sedimentary Successions of NW Croatia" (IP-2019–04-3824).

**Data availability** All the material, thin-sections and radiolarian samples are housed in the Croatian Geological Survey, Department of Geology.

## Declarations

**Conflict of interest** The authors have no competing interests to declare that are relevant to the content of this article.

## References

Aubouin J, Blanchet R, Cadet JP, Celet P, Charvet J, Chorowicz J, Cousin M, Rampnoux JP (1970) Essai sur la geologie des Dinarides. Bull Soc Géol Fr 12(7):1060–1095

Auer M, Gawlick HJ, Suzuki H, Schlagintweit F (2009) Spatial and temporal development of siliceous basin and shallo-water carboates sedimentation in Oxfordian Northern Calcareous Alps. Facies 55:63–87. https://doi.org/10.1007/s10347-008-0155-3

Babić Lj (1973) Upper Tithonian to Valanginian basinal sediments west of Bregana. Geol Vjesn 26:11–27

Babić Lj (1974a) Jurassic-Cretaceous sequence of Mt. Ivanščica (Northern Croatia). Bull Sci Cons Acad Yugosl (A) 19(7–8):181–182

Babić Lj (1974b) Hauterivian to Cenomanian time in the region of Žumberak, Northwestern Croatia: stratigraphy, sediments, paleogeographic and paleotectonic evolution. Geol Vjesn 27:11–33

Babić Lj (1975) Condensed Liassic sedimentation on Mt. Medvednica and Mt. Ivanščica (Northern Croatia) and its significance for the interpretation of the paleogeographic evolution of the Inner Dinaric Belt. Geol Vjesn 28:11–28

Babić Lj (1976) Pomak granice između unutrašnje i vanjske Dinarske regije, primjer šireg područja Žumberka (Migration of the boundary between inner and outer Dinaric zones). 8. Jugoslovanski geološki kongres, Slovensko geološko društvo, Ljubljana, pp 45–51

Babić Lj, Zupanič J (1973) Uppermost Jurassic and Early Cretaceous deposits on Mt. Ivanščica – northern Croatia. Geol Vjesn 26:267–272

Babić Lj, Zupanič J (1978) Mlađi mezozoik Ivanščice. In: Babić Lj, Jelaska V (ed) Vodič ekskurzije 3. Skupa sedimentologa Jugoslavije. Croatian Geological Society, Zagreb, pp 11–23

Babić Lj, Zupanič J, Crnjaković M (1979) The recognition of the two units in the "Clastic Formation with ophiolites" of Mt. Ivanščica and the role of a magmatic belt and an active continental margin. Proceedings of 4th Meeting of the Section for geology geophysics and geochemistry Scientific. Council for oil, Zagreb, pp 115–123

Babić Lj, Hochuli PA, Zupanič J (2002) The Jurassic ophiolitic mélange in the NE Dinarides: dating, internal structure and geotectonic implications. Eclogae Geol Helv 95:263–275

Balázs A, Matenco L, Magyar I, Horváth F, Cloetingh S (2016) The link between tectonics and sedimentation in back-arc basins: new genetic constraints from the analysis of the Pannonian Basin. Tectonics 35:1526–1559. https://doi.org/10.1002/2015TC004109

Bartolini A, Baumgartner PO, Guex J (1999) Middle and Late Jurassic radiolarian palaeoecology versus carbon-isotope stratigraphy. Palaeogeogr Palaeoclimatol Palaeoecol 145:43–60. https://doi.org/10.1016/S0031-0182(98)00097-2

Baumgartner PO (2013) Mesozoic radiolarites – accumulation as a function of sea surface fertility on Tethyan margins and in ocean basins. Sedimentology 60:292–318. https://doi.org/10.1111/sed.12022

Baumgartner PO, O'Dogherty L, Goričan Š, Dumitrica-Jud R, Dumitrica P, Pillevuit A, Urquhart E, Matsuoka A, Danelian

T, Bartolini A, Carter ES, De Wever P, Kito N, Marcucci M, Steiger T (1995a) Radiolarian catalogue and systematics of Middle Jurassic to Early Cretaceous Tethyan genera and species. In: Baumgartner PO, O'Dogherty L, Goričan Š, Urquhart E, Pillevuit A, De Wever P (eds) Middle jurassic to lower cretaceous radiolaria of tethys: occurrences, Systematics, Biochronology. Mémoires de Géologie, vol 23. Lausanne pp 37–685

Baumgartner PO, Bartolini A, Carter ES, Conti M, Cortese G, Danelian T, De Wever P, Dumitrica P, Dumitrica-Jud R, Goričan Š, Guex J, Hull DM, Kito N, Marcucci M, Matsuoka A, Murchey B, O'Dogherty L, Savary J, Vishnevskaya V, Widz D, Yao A (1995b) Middle Jurassic to Early Cretaceous radiolarian biochronology of Tethys based on unitary associations. Mémoires de Géologie, vol. 23, Lausanne, pp 1013–1048

Baumgartner PO, Martire L, Goričan Š, O'Dogherty L, Erba E, Pillevuit A (1995c) New middle and upper jurassic radiolarian assemblages co-occurring with ammonites and nannofossils from the Southern Alps (Northern Italy). In: Baumgartner PO, O'Dogherty L, Goričan Š, Urquhart E, Pillevuit A, De Wever P (eds) Middle Jurassic to Lower Cretaceous Radiolaria of Tethys: Occurrences, Systematics, Biochronology. Mémoires de Géologie, vol. 23, Lausanne, pp 737–749

Beccaro P, Baumgartner PO, Martire L (2002) Radiolarian biostratigraphy of the Fonzaso Formation, Middle-Upper Jurassic, Southern Alps, Italy. Micropaleontology 48(suppl 1):43–60

Beccaro P, Diserens M-O, Goričan Š, Martire L (2008) Callovian radiolarians from the lowermost calcare Selcifero di Fonzaso at Ponte Serra (Trento Plateau, Souther Alps, Italy). Riv It Paleontol Strat 114:489–504. https://doi.org/10.13130/2039-4942/5913

Bernoulli D, Kälin O (1984) Jurassic sediments. Site 547, northwest African margin: remarks on stratigraphy, facies and diagenesis, and comparison with some Tethyan equivalents. Init Rep DSDP 79:437–448

Bernoulli D, Jenkyns HC (2009) Ancient oceans and continental margins of the Alpine-Mediterranean Tethys: deciphering clues from Mesozoic pelagic sediments and ophiolites. Sedimentology 56:149–190. https://doi.org/10.1111/j.1365-3091.2008.01017.x

Berra F, Galli MT, Reghellini F, Torricelli S, Fantoni R (2009) Stratigraphic evolution of theTriassic-Jurassic succession in the Western Southern Alps (Italy): the record of the two-stage rifting on the distal passive margin of Adria. Basin Res 21:335–353. https://doi.org/10.1111/j.1365-2117.2008.00384.x

Bertinelli A, Ciarapica G, De Zanche V, Marcucci M, Mietto P, Passeri L, Rigo M, Roghi G (2005) Stratigraphic evolution of the Triassic-Jurassic Sasso di Castalda succession (Lagonegro Basin, Southern Apennines, Italy). Boll Soc Geol It 124(1):161–175

Bertotti G, Picotti V, Bernoulli D, Castellarin A (1993) From rifting to drifting: tectonic evolution of the South Alpine upper crust from Triassic to early Cretaceous. Sedim Geol 86:53–76. https://doi.org/10.1016/0037-0738(93)90133-P

Blanchet R, Cadet JP, Charvet J, Rampnoux JP (1969) Sur l'existence d'un important domaine de flysch tithonique—crétacé inférieur en Yougoslavie: l'unité du flysch bosniaque. Bull Soc Géol Fr 7(11):871–880

Blažeković-Smojić S, Smajlović J, Koch G, Bulić J, Trutin M, Oreški E, Alajbeg A, Veseli V (2009) Source potential and palynofacies of Late Jurassic ''Lemeš facies'', Croatia. Org Geochem 40:833–845. https://doi.org/10.1016/j.orggeochem.2009.05.005

Böhm F (2003) Lithostratigraphy of the Adnet Group (Lower to Middle Jurassic, Salzburg, Austria). In: Piller WE (ed) Stratigraphia Austriaca – Österr Akad Wiss Schriftenr Erdwiss Komm, vol 16. VÖAW, Vienna, pp 231–268

Bortolotti V, Chiari M, Marroni M, Pandolfi L, Principi G, Saccani E (2013) Geodynamic evolution of ophiolites from Albania and Greece (Dinaric-Hellenic belt): one, two, or more oceanic basins? Int J Earth Sci 102:783–811. https://doi.org/10.1007/s00531-012-0835-7

Bosellini A, Winterer EL (1975) Pelagic limestone and radiolarite of the Tethyan Mesozoic: a genetic model. Geology 3(5):279–282. https://doi.org/10.1130/0091-7613(1975)3%3c279:PLAROT%3e2.0.CO;2

BouDagher-Fadel MK, Bosence DWJ (2007) Early Jurassic benthic foraminiferal diversification and biozones in shallow-marine carbonates of western Tethys. Senckenb Lethaea 87(1):1–39. https://doi.org/10.1007/BF03043906

BouDagher-Fadel MK, Rose EPF, Bosence DWJ, Lord AR (2001) Lower jurassic foraminifera and calcified microflora from Gibraltar, Western Mediterranean. Palaeontol 44:601–621. https://doi.org/10.1111/1475-4983.00193

Bronemann A, Aschwer U, Mutterlose J (2003) The impact of calcareous nannofossils on the pelagic carbonate accumulation across the Jurassic-Cretaceous boundary. Palaeogeogr Palaeoclimatol Palaeoecol 199:187–228. https://doi.org/10.1016/S0031-0182(03)00507-8

Bucković D, Cvetko Tešović B, Gušić I (2004) Late Jurassic paleoenvironmental evolution of the western Dinarides (Croatia). Geol Carpath 55:3–18

Cadet JP (1978) Essai sur l'évolution alpine d'une paléomarge continentale: les confins de la Bosnie-Herzégovine et du Monténégro (Yougoslavie). Mém De La Soc Géol De Fr (nouvelle Série) 133:1–83

Chablais J, Martini R, Onoue T (2010) Aulotortus friedli from the Upper Triassic gravitational flow deposits of the Kumagawa River (Kyushu, Southwest Japan). Paleo Res 14(2):151–160. https://doi.org/10.2517/1342-8144-14.2.151

Chiari M, Cobianchi M, Picotti V (2007) Integrated stratigraphy (radiolarians and calcareous nannofossils) of the Middle to Upper Jurassic Alpine radiolarites (Lombardian Basin, Italy): Constraints to their genetic interpretation. Palaeogeogr Palaeoclimatol Palaeoecol 249:233–270. https://doi.org/10.1016/j.palaeo.2007.02.001

Cousin M (1981) Les rapports Alpes-Dinarides. Les confins de l'Italie et de la Yougoslavie. Soc géol du Nord, Publ 5, 1:1–521, Annexe 2:1–52

Črne AE, Šmuc A, Skaberne D (2007) Jurassic neptunian dikes at Mt Mangart (Julian Alps, NW Slovenia). Facies 53:249–265. https://doi.org/10.1007/s10347-007-0102-8

Császár G, Árgyelán GB (1994) Stratigraphic and micromineralogic investigations on Cretaceous Formations of the Gerecse Mountains, Hungary and their palaeogeographic implications. Cretac Res 15(4):417–434. https://doi.org/10.1006/cres.1994.1024

De Wever P, Miconnet P (1985) Datations directes des radiolarites du bassin du Lagonegro (Lucanie, Italie méridionale). Implications Et Conséquences. Rev Es Micropaleontol 17(3):373–402

De Wever P, O'Dogherty L, Goričan Š (2014) Monsoon as a cause of radiolarite in the Tethyan realm. C R Geosci 346:287–297. https://doi.org/10.1016/j.crte.2014.10.001

Dragičević I, Velić I (2002) The northeastern margin of the Adriatic Carbonate Platform. Geol Croat 55(2):185–232. https://doi.org/10.4154/GC.2002.16

Dumitrica P, Dumitrica-Jud R (2005) *Hexasaturnalis nakasekoi* nov. sp., a Jurassic saturnalid radiolarian species frequently confounded with *Hexasaturnalis suboblongus* (Yao). Rev Micropaléontol 48:159–168. https://doi.org/10.1016/j.revmic.2005.03.001

Dunham R (1962) Classification of carbonate rocks according to depositional texture. In: Ham W (ed) Classification of carbonate rocks. AAPG Tulsa, Tulsa, pp 108–121

Farinacci A (1991) Emendation of Vidalina Schlumberger and the new genus Agerina (Foraminifera). Paleopelagos 1:5–16

Faupl P, Wagreich M (2000) Late Jurassic to Eocene palaeogeography and geodynamic evolution of the Eastern Alps. Mitt Österreichischen Geol Ges 92:79–94

Ferriere J, Baumgartner PO, Chanier F (2016) The Maliac Ocean: the origin of the Tethyan Hellenic ophiolites. Int J Earth Sci 105:1941–1963. https://doi.org/10.1007/s00531-016-1303-6

Flügel E (2010) Microfacies of carbonate rocks: analysis, interpretation and application, 2nd edn. Springer, Heidelberg

Fodor L, Balázs A, Csillag G, Dunkl I, Héja G, Jelen B, Kelemen P, Kövér S, Németh A, Nyíri D, Selmeczi I, Trajanova M, Ma V, Mi V (2021) Crustal exhumation and depocenter migration from the Alpine orogenic margin towards the Pannonian extensional back-arc basin controlled by inheritance. Glob Planet Change. https://doi.org/10.1016/j.gloplacha.2021.103475103475

Gaetani M (2010) From Permian to Cretaceous: Adria as pivotal between extensions and rotations of Tethys and Atlantic Oceans. J Virtual Explor 36. https://doi.org/10.3809/jvirtex.2010.00235.

Gale L (2012) Rhaetian foraminiferal assemblage from the Dachstein Limestone of Mt. Begunjščica (Košuta Unit, eastern Southern Alps). Geologija 55:17–44. https://doi.org/10.5474/geologija.2012.002

Gale L, Kolar-Jurkovšek T, Šmuc A, Rožič B (2012) Integrated Rhaetian foraminiferal and conodont biostratigraphy from the Slovenian Basin, eastern Southern Alps. Swiss J Geosci 105:435–462. https://doi.org/10.1007/s00015-012-0117-1

Gale L, Barattolo F, Rettori R (2018) Morphometric approach of Lower Jurassic siphovalvulinid foraminifera. Riv It Paleontol Strat 124:265–282. https://doi.org/10.13130/2039-4942/9984

Gale L, Kolar-Jurkovšek T, Karničnik B, Celarc B, Goričan Š, Rožič B (2019) Triassic deep-water sedimentation in the Bled Basin, eastern Julian Alps. Slovenia. Geologija 62(2):153–173. https://doi.org/10.5474/geologija.2019.007

Gale L, Kukoč D, Rožič B, Vidervol A (2021) Sedimentological and paleontological analysis of the Lower Jurassic part of the Zatrnik Formation on the Pokljuka plateau. Slovenia. Geologija 64(2):173–188. https://doi.org/10.5474/geologija.2021.010

Gawlick HJ, Frisch W (2003) The Middle to Late Jurassic carbonate clastic radiolaritic flysch sediments in the Northern Calcareous Alps: sedimentology, basin evolution, and tectonics - an overview. N Jb Geol Palaon Abh 230:163–213. https://doi.org/10.1127/njgpa/230/2003/163

Gawlick HJ, Missoni S (2019) Middle-Late Jurassic sedimentary mélange formation related to ophiolite obduction in the Alpine-Carpathian-Dinaridic Mountain Range. Gondwana Res 74:144–172. https://doi.org/10.1016/j.gr.2019.03.003

Gawlick HJ, Missoni S, Schlagintweit F, Suzuki H, Frisch W, Krystyn L, Blau J, Lein R (2009) Jurassic tectonostratigraphy of the austroalpine domain. J Alp Geol 50:1–152. https://doi.org/10.5038/1937-8602.55.1.7

Goričan Š (1994) Jurassic and Cretaceous radiolarian biostratigraphy and sedimentary evolution of the Budva Zone (Dinarides, Montenegro). Mém Géol (Lausanne) 18:1–177

Goričan Š, Šmuc A, Baumgartner PO (2003) Toarcian Radiolaria from Mt. Mangart (Slovenian–Italian border) and their paleoecological implications. Mar Micropaleontol 49:275–301. https://doi.org/10.1016/S0377-8398(03)00034-3

Goričan Š, Halamić J, Grgasović T, Kolar-Jurkovšek T (2005) Stratigraphic evolution of Triassic arc-backarc system in northwestern Croatia. Bull Soc Geol Fr 176(1):3–22. https://doi.org/10.2113/176.1.3

Goričan Š, Košir A, Rožič B, Šmuc A, Gale L, Kukoč D, Celarc B, Črne AE, Kolar-Jurkovšek T, Placer L, Skaberne D (2012) Mesozoic deep-water basins of the eastern Southern Alps (NW Slovenia). J Alp Geol 54:101–143

Goričan Š, Žibret L, Košir A, Kukoč D, Horvat A (2018) Stratigraphic correlation and structural position of Lower Cretaceous flysch-type deposits in the eastern Southern Alps (NW Slovenia). Int J Earth Sci 107:2933–2953. https://doi.org/10.1007/s00531-018-1636-4

Goričan Š, Đaković M, Baumgartner PO, Gawlick HJ, Cifer T, Djerić N, Horvat A, Kocjančić A, Kukoč D, Mrdak M (2022) Mesozoic basins on the Adriatic continental margin – a cross-section through the Dinarides in Montenegro. Folia Biologica et Geologica 63(2):85–150. https://doi.org/10.3986/fbg0099

Görög Á (1994) Early Jurassic Planktonic Foraminifera from Hungary. Micropaleontology 40(3):255–260

Gradstein FM, Ogg JG, Schmitz MD, Ogg GM (2012) The geological time scale 2012. Elsevier, Amsterdam

Grgasović T (1997) Upper Triassic biostratigraphy and algae from Žumberak (Croatia). Geol Croat 50(2):201–214. https://doi.org/10.4154/GC.1997.28

Grgasović T (2003) Revizija rodova Physoporella Steinmann i Oligoporella Pia (Dasycladales). Dissertation, University of Zagreb

Gušić I, Babić Lj (1970) Neke biostratigrafske i litogenetske osobine jure Žumberka. Geol Vjesn 23:39–49

Horváth F, Bada G, Szafián P, Tari G, Ádám A, Cloetingh S (2006) Formation and deformation of the Pannonian Basin: constraints from observational data. Geol Soc London Mem 32(1):191–206. https://doi.org/10.1144/GSL.MEM.2006.032.01.11

Ikeda M, Tada R, Ozaki K (2017) Astronomical pacing of the global silica cycle recorded in Mesozoic bedded cherts. Nat Commun 8:15532. https://doi.org/10.1038/ncomms15532

Jenkyns HC, Clayton CJ (1986) Black shales and carbon isotopes in pelagic sediments from the Tethyan Lower Jurassic. Sedimentology 33(1):87–106

Jud R (1994) Biochronology and Systematics of Early Cretaceous Radiolaria of the Western Tethys. Mém Géol (Lausanne) 19:1–147

Kukoč D, Goričan Š, Košir A (2012) Lower Cretaceous carbonate gravity-flow deposits from the Bohinj area (NW Slovenia): evidence of a lost carbonate platform in the internal dinarides. Bull Soc Géol Fr 183(4):383–392. https://doi.org/10.2113/gssgfbull.183.4.383

Kukoč D, Smirčić D, Grgasović T, Horvat M, Belak M, Japundžić D, Kolar-Jurkovšek T, Šegvić B, Badurina L, Vukovski M, Slovenec D (2023) Biostratigraphy and facies description of Middle triassic rift-related volcano-sedimentary successions at the junction of the Southern Alps and the Dinarides (NW Croatia). Int J Earth Sci 112:1175–1291. https://doi.org/10.1007/s00531-023-02301-w

Lehner BL (1991) Neptunian dykes along a drowned carbonate platform margin: an indication for recurrent extensional tectonic activity? Terra Nova 3:593–602

Lugović B, Slovenec D, Schuster R, Schwarz W, Horvat M (2015) Petrology, geochemistry and tectono-magmatic affinity of gabbroic olistoliths from the ophiolite mélange in the NW Dinaric-Vardar ophiolite zone (Mts. Kalnik and Ivanščica, North Croatia). Geol Croat 68:25–49. https://doi.org/10.4154/gc.2015.03

Lukender A (2010) The biancone and rosso ammonitico facies of the northern Trento plateau (Dolomites, Southern Alps, Italy). Ann Naturhist Mus Wien, Serie A 113:9–33

Lužar-Oberiter B, Mikes T, von Eynatten H, Babić Lj (2009) Ophiolitic detritus in Cretaceous clastic formations of the Dinarides (NW Croatia): evidence from Cr-spinel chemistry. Int J Earth Sci 98:1097–1108. https://doi.org/10.1007/s00531-008-0306-3

Lužar-Oberiter B, Mikes T, Dunkl I, Babić Lj, von Eynatten H (2012) Provenance of cretaceous synorogenic sediments from the NW Dinarides (Croatia). Swiss J Geosci 105:377–399. https://doi.org/10.1007/s00015-012-0107-3

Martire L, Clari P, Lozar F, Pavia G (2006) The rosso ammonitico Veronese (Middle-Upper Jurassic of the Trento Plateau): a

proposal of lithostratigraphic ordering and formalization. Riv It Paleontol Strat 112:227–250. https://doi.org/10.13130/2039-4942/6338
Masini E, Manatschal G, Mohn G (2013) The Alpine Tethys rifted margins: reconciling old and new ideas to understand the stratigraphic architecture of magma-poor rifted margins. Sedimentology 60:174–196. https://doi.org/10.1111/sed.12017
Matsuoka A (1992) Jurassic and early createceous radiolarians from Leg 129, Sites 800 and 801, western Pacific Ocean. Proceedings of the Ocean Drillin Program, Scientific Results – College Station, TX (Ocean Drilling Program), 129: 203–220. https://doi.org/10.2973/odp.proc.sr.129.121.1992
Matsuoka A (1998) Faunal composition of earliest Cretaceous (Berriasian) radiolaria from the Mariana Trench in the western Pacific. Proceedings of the Sixth Radiolarian Symposium. News of Osaka Micropaleontol, Spec Vol 11:165–187
Mikes T, Christ D, Petri R, Dunkl I, Frei D, Báldi-Beke M, Reitner J, Wemmer K, Hrvatović H, von Eynatten H (2008) Provenance of the Bosnian Flysch. Swiss J Geosci 101:31–54. https://doi.org/10.1007/s00015-008-1291-z
Missoni S, Gawlick HJ (2011a) Jurassic mountain building and Mesozoic– Cenozoic geodynamic evolution of the Northern Calcareous Alps as proven in the Berchtesgaden Alps (Germany). Facies 57:137–186. https://doi.org/10.1007/s10347-010-0225-1
Missoni S, Gawlick HJ (2011b) Evidence for Jurassic subduction from the Northern Calcareous Alps (Berchtesgaden; Austroalpine, Germany). Int J Earth Sci 100:1605–1631. https://doi.org/10.1007/s00531-010-0552-z
O'Dogherty L, Carter ES, Dumitrica P, Goričan Š, De Wever P, Bandini AN, Baumgartner PO, Matsuoka A (2009) Catalogue of Mesozoic radiolarian genera. Part 2: Jurassic – Cretaceous. Geodiversitas 31:271–356. https://doi.org/10.5252/g2009n2a4
O'Dogherty L, Goričan Š, Gawlick HJ (2017) Middle and Late Jurassic radiolarians from the Neotethys suture in the Eastern Alps. J Paleontol 91(1):25–72. https://doi.org/10.1017/jpa.2016.96
Piller W (1978) Involutinacea (Foraminifera) der Trias und des Lias. Beitr Paläont Österr 5:1–164
Reháková D, Rožič B (2019) Calpionellid biostratigraphy and sedimentation of the Biancone limestone from the Rudnica Anticline (Sava Folds, eastern Slovenia). Geologija 62(1):89–101. https://doi.org/10.5474/geologija.2019.004
Rigaud S, Martini R, Rettori R (2012) Parvalamellinae, a new subfamily for Triassic glomospiroid involutinidae. J Foraminifer Res 42(3):245–256. https://doi.org/10.2113/gsjfr.42.3.245
Rožič B (2009) Perbla and tolmin formations: revised toarcian to tithonian stratigraphy of the tolmin Basin (NW Slovenia) and regional correlations. Bull Soc Géol Fr 180:411–430. https://doi.org/10.2113/gssgfbull.180.5.411
Rožič B, Kolar-Jurkovšek T, Žvar-Rožič P, Gale L (2017) Sedimentary record of subsidence pulse at the Triassic/Jurassic boundary interval in the Slovenian Basin (eastern Southern Alps). Geol Carpath 68(6):543–561. https://doi.org/10.1515/geoca-2017-0036
Rychliński T, Gaździcki A, Uchman A (2018) Dasycladacean alga palaeodasycladus in the northern Tethys (West Carpathians, Poland) and its new palaeogeographic range during the Early Jurassic. Swiss J Geosci 111:305–315. https://doi.org/10.1007/s00015-018-0301-z
Schäfer P, Senowbari-Daryan B (1983) Die kalkalgen aus der obertrias von Hydra, Griechenland. Paleontographica 185:83–142
Schlager W, James NP (1978) Low-magnesium calcite limestone forming at the deep-sea floor, tongue of the Ocean, Bahamas. Sedimentol 25:675–702
Schlagintweit F (1991) On the occurrence of the genus permocalculus ELLIOTT, 1955 (Calcareous algae, Gymnocodiaceae) in the upper cretaceous of the northern calcareous alps (Branderfleck Formation, Gosau Formation) with the description of permocalculus gosaviense n. sp. Revue De Paleobiologie 10:37–46
Schmid SM, Bernoulli D, Fügenschuh B, Matenco L, Schefer S, Schuster R, Tischler M, Ustaszewski K (2008) The Alpine–Carpathian–Dinaridic orogenic system: correlation and evolution of tectonic units. Swiss J Geosci 101:139–183. https://doi.org/10.1007/s00015-008-1247-3
Schmid S, Fügenschuh B, Kounov A, Matenco L, Nievergelt P, Oberhänsli R, Pleuger J, Schefer S, Schuster R, Tomljenović B, Ustaszewski K (2020) Tectonic units of the Alpine collision zone between Eastern Alps and western Turkey. Gondwana Res 78:308–374. https://doi.org/10.1016/j.gr.2019.07.005
Šikić K, Grimani M (1965) Prvi nalaz jure u srednjoj i sjeverozapadnoj Hrvatskoj i rasprostranjenost dijabazno-rožnjačkih naslaga u Baniji i Kordunu. Acta Geol 5:397–405
Šimunić A (1992) Geol odnosi središnjeg dijela Hrvatskog Zagorja. Dissertation, University of Zagreb
Šimunić An, Šimunić Al (1997) Triassic deposits of Hrvatsko Zagorje. Geol Croat 50(2):243–250. https://doi.org/10.4154/GC.1997.32
Šimunić An, Pikija M, Šimunić Al, Šikić L, Milanović M (1976) Stratigrafsko-tektonski odnosi centralnog i istočnog dijela Ivanšćice. 8. Jugoslovanski geološki kongres. Slovensko geološko društvo, Ljubljana, pp 303–314
Šimunić An, Šimunić Al, Milanović M (1979) Geološka građa Ivanšćice i Ravne gore. Geol Vjesn 31:157–174
Šimunić A, Pikija M, Hećimović I (1982) Basic geological map of SFRJ 1:100.000. Sheet Varaždin L33-69. Federal Geological Institute Belgrade
Slovenec D, Lugović B, Meyer H, Garapić Šiftar G (2011) A Tectonomagmatic correlation of basaltic rocks from ophiolite mélanges at the North-Eastern tip of the Sava-Vardar suture Zone, Northern Croatia, constrained by geochemistry and petrology. Ofioliti 36(1):77–100. https://doi.org/10.4454/ofioliti.v36i1.395
Slovenec D, Šegvić B, Halamić J, Goričan Š, Zanoni G (2020) An ensialic volcanic arc along the northwestern edge of paleotethys—insights from the Mid-Triassic volcano-sedimentary succession of Ivanščica Mt. (northwestern Croatia). Geol J 55:4324–4351. https://doi.org/10.1002/gj.3664
Slovenec D, Horvat M, Smirčić D, Belak M, Badurina L, Kukoč D, Grgasović T, Byerly K, Vukovski M, Šegvić B (2023) On the evolution of Middle Triassic passive margins of the Greater Adria Plate: inferences from the study of calc-alkaline and shoshonitic tuffs from NW Croatia. Ofioliti 48(1):31–46. https://doi.org/10.4454/ofioliti.v48i1.560
Šmuc A (2005) Jurassic and cretaceous stratigraphy and sedimentary evolution of the Julian Alps, NW Slovenia. Založba ZRC/ZRC Publishing, Ljubljana. https://doi.org/10.3986/9789612545147
Šmuc A, Goričan Š (2005) Jurassic sedimentary evolution of a carbonate platform into a deep-water basin, Mt Mangart (Slovenian–Italian border). Riv Ital Paleontol Strat 111:45–70. https://doi.org/10.13130/2039-4942/62690
Sokač B (2001) Lower and Middle Liassic calcareous algae (Dasycladales) from Mt. Velebit (Croatia) and Trnovski Gozd (Slovenia) with particular reference to genus Palaeodasycladus (PIA, 1920) 1927 and its species. Geol Croat 54:133–257. https://doi.org/10.4154/GC.2001.07
Sokač B, Grgasović T (1995) Dissocladella bystrickyi n. sp., a new calcareous alga (Dasycladaceae) from upper triassic dolomites of Mt. Medvednica (Northern Croatia). Geol Croat 48:1–7. https://doi.org/10.4154/GC.1995.01
Sokač B, Grgasović T (1998) Asterocalculus heraki n. gen., n. sp., a new calcareous alga (Gymnocodiaceae) from the upper triassic hauptdolomite of Žumberak, North Croatia. Facies 38:197–206. https://doi.org/10.1007/BF02537365

Tomljenović B, Csontos L (2001) Neogene-quaternary structures in the border zone between Alps, Dinarides and Pannonian Basin (Hrvatsko Zagorje and Karlovac Basins, Croatia). Int J Earth Sci 90(3):560–578. https://doi.org/10.1007/s005310000176

Tomljenović B, Csontos L, Márton E, Márton P (2008) Tectonic evolution of the northwestern Internal Dinarides as constrained by structures and rotation of Medvednica mountains, North Croatia. Geol Soc London Sp Publ 298:145–167. https://doi.org/10.1144/SP298.8

van Gelder IE, Matenco L, Willingshofer E, Tomljenović B, Andriessen PAM, Ducea MN, Beniest A, Gruić A (2015) The tectonic evolution of a critical segment of the Dinarides-Alps connection: kinematic and geochronological inferences from the Medvednica Mountains. NE Croatia. Tectonics 34(9):1952–1978. https://doi.org/10.1002/2015TC003937

van Hinsbergen DJJ, Torsvik TH, Schmid SM, Maţenco L, Maffione M, Vissers RLM, Gürer D, Spakman W (2020) Orogenic architecture of the Mediterranean region and kinematic reconstruction of its tectonic evolution since the Triassic. Gondwana Res 81:79–229. https://doi.org/10.1016/j.gr.2019.07.009

Velić I (2007) Stratigraphy and palaeobiology of Mesozoic benthic foraminifera of the Karst Dinarides (SE Europe). Geol Croat 60(1):1–113. https://doi.org/10.4154/GC.2007.01a

Velić I, Tišljar J, Vlahović I, Velić J, Koch G, Matičec D (2002) Palaeogeographic variability and depositional environments of the upper jurassic carbonate rocks of velika kapela Mt. (Gorski Kotar Area, Adriatic Carbonate Platform, Croatia). Geol Croat 55:121–138. https://doi.org/10.4154/GC.2002.13

Vlahović I, Tišljar J, Velić I, Matičec D (2005) Evolution of the Adriatic carbonate platform: palaeogeography, main events and depositional dynamics. Palaeogeogr Palaeoclimatol Palaeoecol 220:333–360. https://doi.org/10.1016/j.palaeo.2005.01.011

Vörös A, Galácz A (1998) Jurassic palaeogeography of the transdanubian central range (Hungary). Riv Ital Paleontol Stratigr 104:69–84. https://doi.org/10.13130/2039-4942/6112

Weissert H (1981) Depositional processes in an ancient pelagic environment: the lower cretaceous Maiolica of the Southern Alps. Ecol Geol Helv 74:339–352

Widz D (1991) Les radiolaires du Jurassique supérieur des radiolarites de la Zone des Klippes de Pieniny (Carpathes occidentales, Pologne). Rev Micropaléontol 34:231–260

Winterer EL, Bosellini A (1981) Subsidence and sedimentation on a Jurassic passive continental margin, Southern Alps (Italy). Am Assoc Petroleum Geol Bull 65:394–421. https://doi.org/10.1306/2F9197E2-16CE-11D7-8645000102C1865D

Winterer EL, Metzler CV, Sarti M (1991) Neptunian dykes and associated breccias (Southern Alps, Italy and Switzerland): role of gravity sliding in open and closed systems. Sedimentology 38:381–404

Zupanič J, Babić Lj, Crnjaković M (1981) Lower Cretaceous basinal clastics (Oštrc Formation) in the Mt. Ivanščica (Northwestern Croatia). Acta Geologica 11(1):1–44

## 4. THE EARLY HISTORY OF THE NEOTETHYS ARCHIVED IN THE OPHIOLITIC MÉLANGE OF NORTHWESTERN CROATIA

By

Duje Kukoč, Damir Slovenec, Branimir Šegvić, **Matija Vukovski**, Mirko Belak, Tonći Grgasović, Marija Horvat & Duje Smirčić

*Published in Journal of the Geological Society*

*DOI: https://doi.org/10.1144/jgs2023-143*

Research article

JGS
*Journal of the Geological Society*

https://doi.org/10.1144/jgs2023-143 | Vol. 181 | 2023 | jgs2023-143

# The early history of the Neotethys archived in the ophiolitic mélange of northwestern Croatia

**Duje Kukoč[1], Damir Slovenec[1*], Branimir Šegvić[2], Matija Vukovski[1], Mirko Belak[1], Tonći Grgasović[1], Marija Horvat[1] and Duje Smirčić[3]**

[1] Croatian Geological Survey, Ulica Milana Sachsa 2, HR-10000 Zagreb, Croatia
[2] Department of Geosciences, Texas Tech University, 1200 Memorial Circle, Lubbock, TX 79409, USA
[3] Faculty of Mining, Geology and Petroleum Engineering, University of Zagreb, Pierottijeva 6, HR-10000 Zagreb, Croatia
DK, 0000-0002-7176-6770; DS, 0000-0003-3251-827X; BŠ, 0000-0002-3769-7249; MV, 0000-0002-9970-5849; TG, 0000-0001-8031-4293; MH, 0000-0002-2445-5283; DS, 0000-0002-6360-8203
* Correspondence: damir.slovenec@hgi-cgs.hr

**Abstract:** Ophiolite exposures in NW Croatia have been attributed to the Western Vardar Ophiolitic Unit and interpreted as derived from the Meliata–Maliac–Vardar branch of the Neotethys Ocean. Blocks within the ophiolitic mélange on Mt Ivanščica were investigated to determine the petrological and geochemical characteristics of the effusive rocks and to carry out radiolarian dating of the associated pelagic sedimentary rocks. The analysed effusive basic rocks represent chemostratigraphically uniform subalkaline high-Ti massive tholeiitic basalts characterized by an enriched composition typical of incompatible element-enriched mid-ocean ridge basalt (E-MORB). These basalts are compatible with *c.* 9–11% of partial melting of an enriched mantle source transitional between primitive and depleted MORB-type mantle and were formed in the non-subduction geotectonic setting of E-MORB-type rocks. This reflects an initial succession of oceanic protocrust formation and the onset of ocean spreading. Radiolarians from the chert and shale successions associated with the basalts indicate a Late Anisian–Early Ladinian age of initial ocean floor spreading, which continued into the Langobardian. The obtained data are correlative with reported blocks interpreted as remnants of the Triassic Neotethys crust from the ophiolitic mélange of the Western Vardar Ophiolitic Unit and reaffirm a common origin from a single ocean basin located east of the Adria microplate.

**Thematic collection:** This article is part of the Ophiolites, melanges and blueschists collection available at: https://www.lyellcollection.org/topic/collections/ophiolites-melanges-and-blueschists

**Received** 30 August 2023; **revised** 30 October 2023; **accepted** 8 November 2023

Ophiolite sequences, as remnants of the Earth's ancient oceanic lithosphere, offer unique insights into the evolution of ancient oceans. Although ophiolites can be preserved as large thrust sheets with a relatively undisturbed lithostratigraphy (e.g. Dilek and Furnes 2011, 2014), they are more often found as fragmented original sequences occurring as blocks within chaotic units commonly referred to as ophiolitic mélange (Gansser 1974). These chaotic units were formed through the interplay of tectonic and sedimentary processes during the subduction and emplacement of ophiolites onto continental margins (Festa *et al.* 2010*a*, *b*, 2022; Bortolotti *et al.* 2013). Lithologies found in an ophiolitic mélange may include rocks tectonically offscraped from the subducting plate as well as gravitationally emplaced olistoliths derived from the overthrust plate (Wakabayashi 2015; Festa *et al.* 2022). Strong deformation during the long-lasting and multi-stage geodynamic evolution of orogens results in the creation of polygenetic mélanges in which recognizing the prevailing generation mechanism (i.e. tectonic v. sedimentary) can be challenging (Wakabayashi 2015; Festa *et al.* 2022). Nevertheless, the investigation of ophiolitic mélanges represents an important tool in understanding and reconstructing the tectonic evolution of orogenic belts (Festa *et al.* 2022).

Ophiolites are a prominent feature of the Dinaridic–Hellenidic orogenic belt (Schmid *et al.* 2008, 2020; Robertson *et al.* 2009). These ophiolites represent remnants of an oceanic domain that existed between the Adria microplate and Eurasia during the Mesozoic (Schmid *et al.* 2008, 2020; van Hinsbergen *et al.* 2020). The exact number of oceanic branches is, however, still disputed (Robertson *et al.* 2009; Saccani *et al.* 2011; Ferrière *et al.* 2012; Robertson 2012; Bortolotti *et al.* 2013). Nevertheless, most researchers now favour a single-ocean geodynamic model (e.g. Bernoulli and Laubscher 1972; Baumgartner 1985; Pamić *et al.* 2002; Bortolotti *et al.* 2005, 2013; Gawlick *et al.* 2008; Schmid *et al.* 2008, 2020; Chiari *et al.* 2011; Gawlick and Missoni 2019; Stanković *et al.* 2023), in contrast with those researchers who interpret the ophiolites as have been derived from two oceans separated by a microcontinent (e.g. Robertson *et al.* 1991; Robertson and Shallo 2000; Dilek *et al.* 2005; Božović *et al.* 2013; Prelević *et al.* 2017).

This ocean, the Meliata–Maliac–Vardar branch of the Neotethys Ocean (*sensu* Schmid *et al.* 2008, 2020), opened during the Mid-Triassic and existed until the Cretaceous. As it was almost entirely consumed during the Mid- to Late Jurassic subduction, the early oceanic crust of the Neotethys Ocean is seldom preserved as a coherent ophiolite sheet (Ferrière *et al.* 2015, 2016) and is more often found in the form of fragments within the ophiolitic mélange (e.g. Chiari *et al.* 1996, 2011; Danelian and Robertson 2001; Bortolotti *et al.* 2006; Ozsvárt and Kovács 2012; Ozsvárt *et al.* 2012; Gawlick *et al.* 2016*a*, *b*). Studying the lithologies archived in ophiolitic mélange therefore has a crucial role in reconstructing the early history of the Neotethys Ocean. In the absence of other fossil groups in the pelagic sedimentary rocks associated with the preserved blocks of oceanic lithosphere, radiolarian biochronology has a vital role in investigating ophiolites.

Blocks of Triassic oceanic lithosphere have been reported (e.g. Slovenec *et al.* 2011) in the ophiolitic mélange of NW Croatia (Fig. 1a, b), which represents the northwesternmost segment of the Neotethys Ocean. However, fragments of undisturbed oceanic crust and the overlying pelagic sediments are rare (Goričan *et al.* 2005).

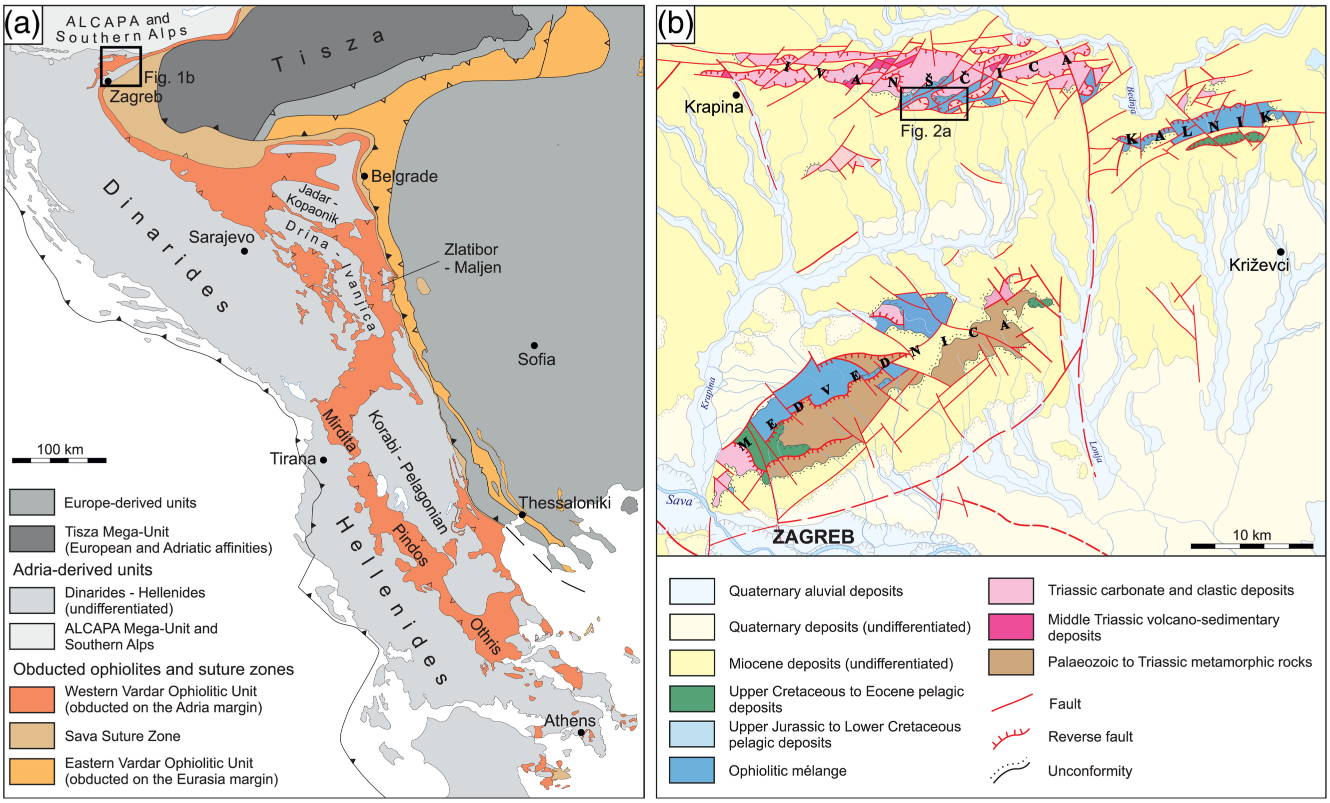


**Fig. 1.** (**a**) Map of ophiolite belts in the Dinaridic–Hellenidic orogenic system showing the location of the investigated area. (**b**) Simplified geological map of NW Croatia showing pre-Neogene formations exposed from beneath the Miocene–Quaternary sedimentary infill of the Pannonian basin and the study area on Mt Ivanščica. Source: Part (a) simplified after Schmid *et al.* (2020); part (b) from Croatian Geological Survey (2009).

This study presents new petrological and geochemical data for basalts and biostratigraphic data for the associated radiolarian cherts from the ophiolitic mélange of northwestern Croatia. These new data provide valuable information about the geotectonic setting, petrogenesis and geodynamic evolution of these rocks, enabling their spatial and temporal correlation across the wider Dinaridic–Hellenidic orogenic system and further advancing our understanding of the early evolution of the Neotethys Ocean.

## Geological setting

### Overview of the Dinaridic–Hellenidic ophiolites

Ophiolitic exposures in NW Croatia represent the northwesternmost exposures of Neotethyan ophiolites and are attributed to the Western Vardar Ophiolitic Unit (*sensu* Schmid *et al.* 2008, 2020; Fig. 1a). Further to the south in the Internal Dinarides, ophiolite exposures of this unit form two belts, in places separated by continental blocks: an external belt referred to as the Dinaridic ophiolite belt (Pamić *et al.* 2002; Karamata 2006) or the Central Dinaric Ophiolite Belt (Lugović *et al.* 1991) and an internal belt known as the Inner Dinaric Ophiolite Belt (Lugović *et al.* 1991), the Vardar Zone (Pamić *et al.* 2002), the Western Vardar ophiolites (Karamata 2006) or the External Vardar subzone (Dimitrijević 1997). In the one-ocean geodynamic model, both belts are regarded as a single ophiolitic thrust sheet obducted westwards onto the continental margin of Adria (e.g. Bortolotti *et al.* 2004*a*, 2013; Schmid *et al.* 2008, 2020). The two continental blocks – Drina–Ivanjica, which separates the two belts, and Jadar–Kopaonik, exposed within the internal belt (Spahić and Gaudenyi 2020) – represent exposed distal parts of the Adriatic margin (Schmid *et al.* 2008; Chiari *et al.* 2011). A similar distinction between the two belts can also be made in the Albanides and the Hellenides (Robertson and Shallo 2000; Bortolotti *et al.* 2005, 2013; Dilek *et al.* 2005; Saccani *et al.* 2011).

The ophiolites of the Western Vardar Ophiolitic Unit predominantly consist of ultramafic lithologies and include sequences generated in mid-ocean ridge and supra-subduction zone (SSZ) settings (Lugović *et al.* 1991; Beccaluva *et al.* 1994; Bortolotti *et al.* 1996, 2004*a*; Saccani *et al.* 2011). Effusive rocks with an SSZ geochemical signature are also present, in places associated with radiolarites ranging in age from Late Bajocian to Middle Callovian–Early Oxfordian (Marccuci *et al.* 1994; Prela *et al.* 2000; Chiari *et al.* 2004, 2023). At several locations in Albania and Greece, occurrences of mid-ocean ridge basalt (MORB)-type effusive rocks and associated pelagic sediments of a Late Anisian–Norian age have been interpreted as ophiolite nappes containing remnants of oceanic lithosphere (Bortolotti *et al.* 2008, 2013; Chiari *et al.* 2012; Ferrière *et al.* 2015).

The ophiolites of the Western Vardar Ophiolitic Unit are underlain by a metamorphic sole with radiometric ages corresponding to the Mid-Jurassic (Bortolotti *et al.* 2013; Šegvić *et al.* 2020) and by an ophiolitic mélange (e.g. Dimitrijević and Dimitrijević 1973; Bortolotti *et al.* 1996, 2013; Babić *et al.* 2002; Gawlick and Missoni 2019). The latter is known in the older regional literature as the Diabase-chert Formation (e.g. Dimitrijević and Dimitrijević 1973) and the Rubik Complex in Albania (Bortolotti *et al.* 1996, 2013), whereas in Greece there are several names for this unit, which occurs in different ophiolite complexes (for details, see Bortolotti *et al.* 2013).

The ophiolitic mélange contains a mixture of continental and ocean-derived lithologies and is interpreted as having formed by tectonic and sedimentary processes during the subduction and emplacement of nappes carrying ophiolites on the continental margin of Adria (e.g. Dimitrijević and Dimitrijević 1973; Robertson and Karamata 1994; Schmid *et al.* 2008; Robertson *et al.* 2009; Chiari *et al.* 2011; Saccani *et al.* 2011; Bortolotti *et al.* 2013; Gawlick *et al.* 2016*b*, 2017; Gawlick and Missoni 2019). Blocks of MORBs associated with radiolarites of Mid- to Late Triassic age have been widely reported from the ophiolitic mélange, providing evidence for continuous seafloor spreading along the entire length of this branch of the Neotethys Ocean from the Late Anisian to the Norian (e.g. Obradović and Goričan 1988; Chiari *et al.* 1996, 2011; Danelian and Robertson 2001; Goričan *et al.* 2005; Bortolotti *et al.* 2006; Gawlick *et al.* 2008, 2016*a*, *b*, 2017; Ozsvárt and Kovács 2012; Ozsvárt *et al.* 2012).

According to the majority of geodynamic models describing the origin of the Western Vardar ophiolites, the onset of seafloor spreading in the Meliata–Maliac Ocean occurred in the Late Anisian–Early Ladinian (e.g. Bortolotti *et al.* 2004*b*; Ferrière *et al.* 2015, 2016; Gawlick *et al.* 2016*a*). The transition into a convergent regime occurred in the Early–Mid-Jurassic with the onset of east-dipping intra-oceanic subduction and the formation of the supra-subduction crust of the Vardar Ocean (e.g. Bortolotti *et al.* 2013). Obduction of the ophiolites on the continental margin of Adria occurred from the Late Jurassic to the earliest Cretaceous (Schmid *et al.* 2008) or, according to some researchers, might have already started in the Mid-Jurassic (Gawlick and Missoni 2019).

## NW Croatia and the Repno Complex

In northwestern Croatia, the Mesozoic formations, including ophiolites, have limited exposure beneath the thick Neogene and Quaternary sediments of the Pannonian Basin (Fig. 1b). Ophiolitic mélange is exposed on the Ivanščica, Kalnik, Medvednica and Samoborska gora mountains (Fig. 1b). This is a tectonically complex area that represents the junction of the Dinarides, the Southern Alps and the Tisza Block (e.g. Haas *et al.* 2000; Schmid *et al.* 2008, 2020; Tomljenović *et al.* 2008). Similar to the Internal Dinarides, a long-lasting and complex Mesozoic and Cenozoic evolution created a complex nappe stack built of formations derived from the distal passive margin of Adria, including the ophiolitic mélange obducted on the continental margin during the Late

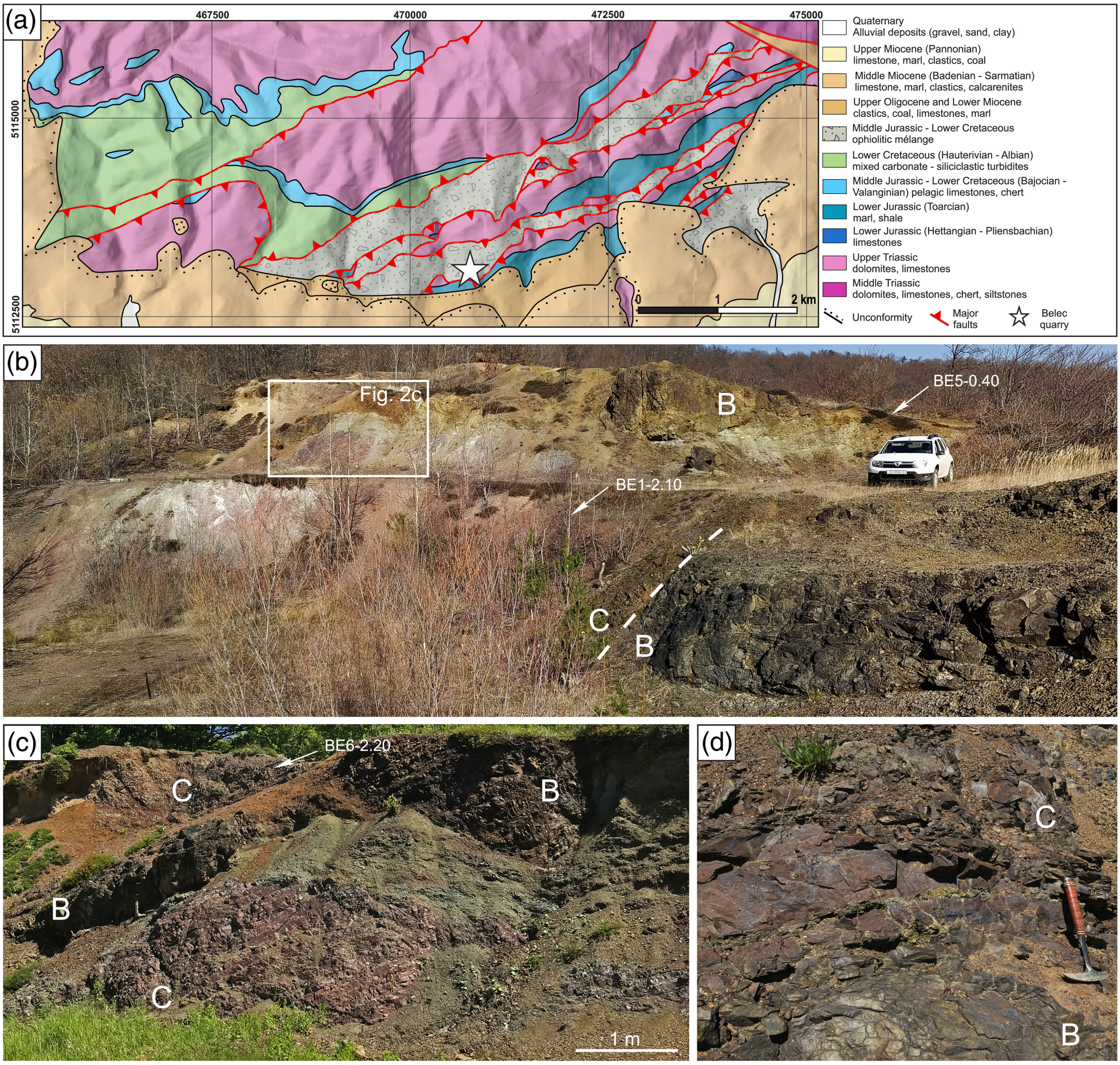


**Fig. 2.** (**a**) Geological map of the investigated area on Mt Ivanščica (for location, see Fig. 1b). (**b–d**) Field photographs of ophiolitic mélange in the investigated quarry. (**b**) Photograph of the quarry front with locations of radiolarian samples marked. (**c**) Upper part of the larger investigated block of chert with shale interbeds. (**d**) Block with stratigraphic contact of pillow basalt and chert. B, basalt; C, chert.

Jurassic–earliest Cretaceous obduction (Babić *et al.* 2002; Slovenec and Pamić 2002; Tomljenović *et al.* 2008; van Gelder *et al.* 2015; Mišur *et al.* 2023). The Dinaridic structures in this area have been overprinted by younger retro-wedge Alpine thrusting (van Gelder *et al.* 2015). Structural and palaeomagnetic data indicate that the block carrying the NW Croatian mountains experienced clockwise rotation and eastwards escape during the Late Paleogene and Neogene (Tomljenović *et al.* 2008), which resulted in the recent alignment of these mountains almost perpendicular to the overall NW–SE Dinaridic structural trend.

An ophiolite complex with preserved slivers of oceanic lithosphere, such as those in the Internal Dinarides, Albanides or the Hellenides, is not preserved in the study area. Instead, ophiolitic exposures are limited to the ophiolitic mélange, which has been named the Repno Complex (Babić and Zupanič 1978) and interpreted as the remnants of a distinct Repno Oceanic Domain (ROD; Babić *et al.* 2002). Here, we adopt the interpretation of the ROD as a part of a single oceanic domain neighbouring Adria – that is, the Maliac–Meliata–Vardar branch of the Neotethys Ocean (Babić *et al.* 2002; Schmid *et al.* 2008, 2020).

The mélange of the Repno Complex is built of millimetre- to kilometre-sized blocks of sandstone, chert, shale, basalt, gabbro and ultramafic rocks found in a pelitic to siliceous matrix that shows a characteristic scaly cleavage (Babić *et al.* 2002; Slovenec and Pamić 2002). The matrix contains Hettangian–Late Bajocian palynomorph assemblages, indicating that the mélange formed after the Late Bajocian (Babić *et al.* 2002). Blocks of basalt in stratigraphic contact with Middle to Upper Triassic chert and shale have been described, as well as basalts with enclosed Middle Triassic limestone (Halamić and Goričan 1995; Halamić *et al.* 1998; Goričan *et al.* 2005). Isolated uppermost Bajocian–Lower Callovian chert blocks have also been reported (Halamić *et al.* 1999). The geodynamic evolution of the ROD inferred from analyses of the mélange components includes intra-continental rifting during the Anisian, followed by the formation of a proto-oceanic crust and oceanic spreading, with the maximum widening of the oceanic domain around the Bajocian and the generation of an infant proto-arc crust in the Callovian–Oxfordian (Slovenec and Lugović 2009, 2012; Slovenec *et al.* 2010, 2011; Lugović *et al.* 2015).

## Description of the sampling area

Mt Ivanščica is largely built of Middle and Upper Triassic massive and bedded dolomites (Šimunić and Šimunić 1979, 1997; Šimunić *et al.* 1981, 1982; Aničić and Juriša 1985; Fig. 1b). Middle Triassic pelagic sedimentary rocks, together with volcanic and volcaniclastic lithologies ranging from basaltic to rhyolitic, are also present (Goričan *et al.* 2005; Slovenec *et al.* 2020, 2023; Kukoč *et al.* 2023). These deposits, originating from deep water basins formed during the initial rifting of the Neotethys Ocean, include upper Illyrian–lower Fassanian radiolarites intercalated with calc-alkaline rhyolitic tuffs, as well as basalts crystallized from high-K shoshonitic magma (Slovenec *et al.* 2020, 2023; Kukoč *et al.* 2023). Younger Mesozoic deposits on Mt Ivanščica include Upper Triassic–Lower Jurassic shallow marine carbonates and an overlying Lower Jurassic–Cretaceous pelagic succession attributed to the distal continental

**Table 1.** Occurrence of radiolarian species in analysed samples from Mt Ivanščica

| | Sample No. | | |
|---|---|---|---|
| Radiolarian species | BE1-2.10 | BE5-0.40 | BE6-2.20 |
| **Oertlispongidae** | | | |
| *Baumgartneria retrospina* Dumitrica | • | cf. | |
| *Falcispongus* (?) sp. | | • | |
| *Oertlispongus inaequispinosus* Dumitrica, Kozur and Mostler | • | • | |
| *Paroertlispongus multispinosus* Kozur and Mostler | • | • | |
| *Paroertlispongus* (?) sp. 1 *sensu* Dumitrica 1999 | • | • | |
| **Other Spumellaria** | | | |
| *Archaeocenosphaera* spp. | • | • | • |
| *Pentaspongodiscus discoides* Tekin | | | • |
| *Tetracapnuchosphaera truncata* Kozur and Mostler | | | cf. |
| **Entactinaria** | | | |
| *Cryptostephanidium cornigerum* Dumitrica | | | • |
| *Cryptostephanidium reticulospinosum* Dumitrica and Tekin | | | • |
| *Divatella* (?) sp. | | | • |
| *Eptingium manfredi* Dumitrica | • | • | |
| *Muelleritortis expansa* Kozur and Mostler | | | • |
| *Pseudostylosphaera canaliculata* (Bragin) | | • | |
| *Pseudostylosphaera gracilis* Kozur and Mock | | | cf. |
| *Pseudostylosphaera longispinosa* Kozur and Mostler | • | | |
| *Pseudostylosphaera nazarovi* (Kozur and Mostler) | | | • |
| *Pseudostylosphaera timorensis* Sashida and Kamata | • | | |
| *Pseudostylosphaera* sp. | | • | |
| *Spongostephanidium spongiosum* Dumitrica | cf. | cf. | |
| *Tiborella magnidentata* Dumitrica, Kozur and Mostler | | • | |
| *Triassistephanidium laticorne* Dumitrica | • | • | |
| *Tritortis dispiralis* (Bragin) | | | • |
| **Nassellaria** | | | |
| *Annulotriassocampe baldii* Kozur | | | • |
| *Annulotriassocampe sulovensis* (Kozur and Mock) | | | • |
| *Corum kraineri* Tekin | | | cf. |
| *Spinotriassocampe annulata* (Nakaseko and Nishimura) | cf. | | |
| *Striatotriassocampe* sp. | • | • | |
| *Triassocampe deweveri* (Nakaseko and Nishimura) | cf. | • | |

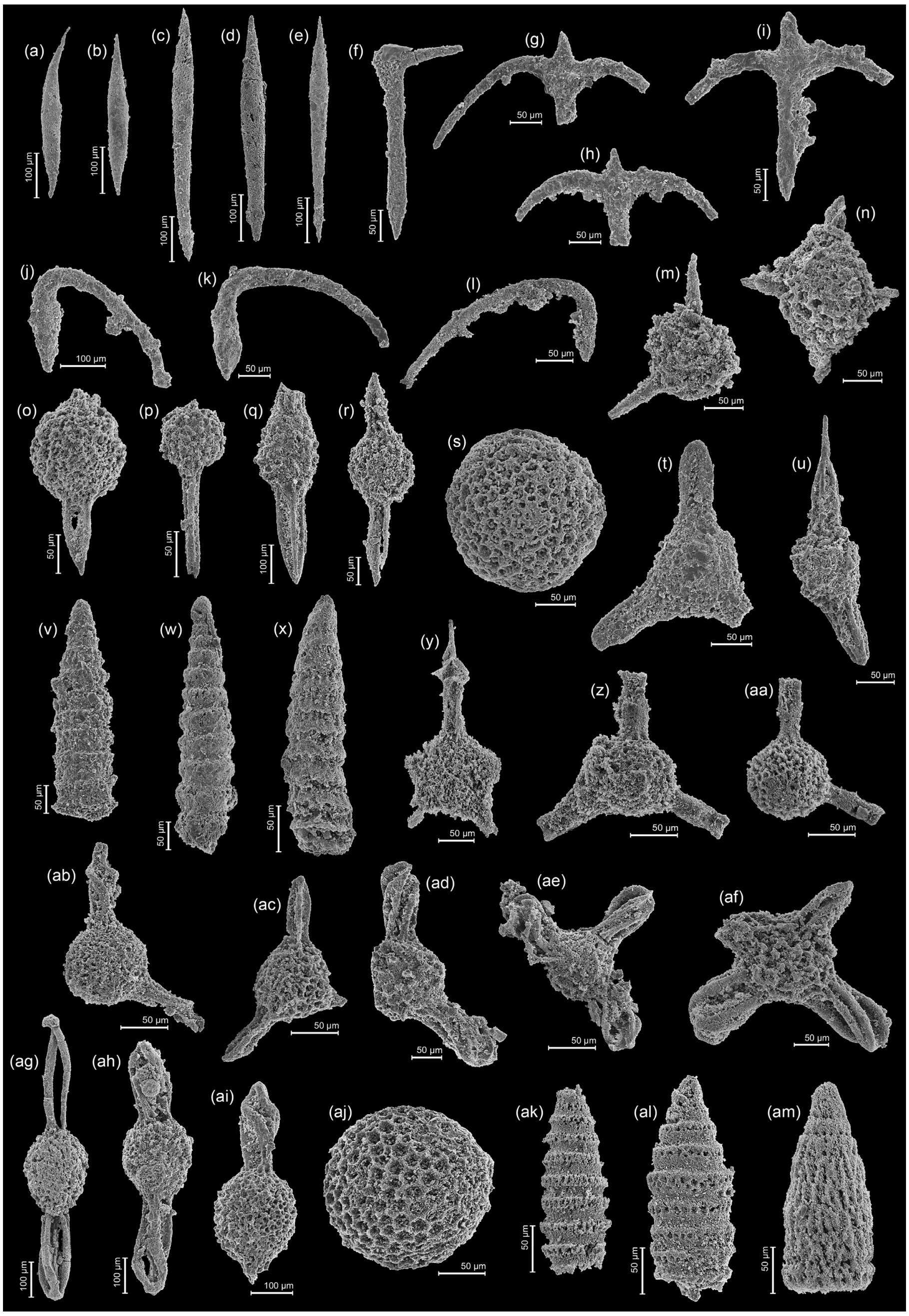

**Fig. 3.** Middle Triassic radiolarian taxa from chert–shale blocks from Belec quarry. The scanning electron micrograph number is indicated for each illustration. **(a–x)** Late Anisian–Early Ladinian radiolarians from samples BE1-2.10 and BE5-0.40. (**a**, **b**) *Paroertlispongus* (?) sp. 1 *sensu* Dumitrica 1999; (**a**) BE1-2.10_0018 and (**b**) BE5-0.40_0021. (**c–e**) *Paroertlispongus multispinosus* Kozur and Mostler; (**c**) BE1-2.10_0016, (**d**) BE1-2.10_0014 and (**e**) BE5-0.40_0018. (**f**) *Falcispongus* (?) sp., BE5-0.40_0016. (**g–i**) *Baumgartneria retrospina* Dumitrica; (**g**) BE1-2.10_0009, (**h**) BE1-2.10_0011 and (**i**) BE1-2.10_0013. (**j–l**) *Oertlispongus inaequispinosus* Dumitrica, Kozur and Mostler; (**j**) BE5-0.40_0011, (**k**) BE1-2.10_0008 and (**l**) BE1-2.10_0006. (**m**) *Spongostephanidium* sp. cf. *S. spongiosum* Dumitrica; BE1-2.10_0030. (**n**) *Tiborella magnidentata* Dumitrica, Kozur and Mostler; BE5-0.40_0027. (**o**) *Pseudostylosphaera* sp.; BE5-0.40_0037. (**p**) *Pseudostylosphaera longispinosa* Kozur and Mostler; BE1-2.10_0019. (**q**) *Pseudostylosphaera canaliculata* (Bragin); BE5-0.40_0034. (**r**) *Pseudostylosphaera timorensis* Sashida and Kamata; BU1-2.10_0021. (**s**) *Archaeocenosphaera* spp.; BE5-0.40_0039. (**t**) *Triassistephanidium laticorne* Dumitrica; BE5-0.40_0026. (**u**) *Eptingium manfredi* Dumitrica; BE1-2.10_0025. (**v**) *Triassocampe deweveri* (Nakaseko and Nishimura); BE5-0.40_0036. (**w**) *Spinotriassocampe* sp. cf. *S. annulata* (Nakaseko and Nishimura); BE1-2.10_0040. (**x**) *Striatotriassocampe* sp. BE1-2.10_0005. **(y–am)** Late Ladinian–earliest Carnian radiolarians from sample BE6-2.20. (**y**) *Pentaspongodiscus discoides* Tekin; BE6-2.20_0039. (**z**) *Tetracapnuchosphaera* sp. cf. *T. truncata* Kozur and Mostler; BE6-2.20_0042. (**aa**) *Divatella* (?) sp.; BE6-2.20_0045. (**ab**) *Cryptostephanidium reticulospinosum* Dumitrica and Tekin; BE6-2.20_0026. (**ac**) *Cryptostephanidium cornigerum* Dumitrica; BE6-2.20_0040. (**ad**) *Tritortis dispiralis* (Bragin); BE6-2.20_0023. (**ae**, **af**) *Muelleritortis expansa* Kozur and Mostler; (**ae**) BE6-2.20_0014 and (**af**) BE6-2.20_0015. (**ag, ah**) *Pseudostylosphaera nazarovi* (Kozur and Mostler); (**ag**) BE6-2.20_0028 and (**ah**) BE6-2.20_0029. (**ai**) *Pseudostylosphaera* sp. cf. *P. gracilis* Kozur and Mock; BE6-2.20_0030. (**aj**) *Archaeocenosphaera* spp.; BE6-2.20_0035. (**ak**) *Annulotriassocampe sulovensis* (Kozur and Mock); BE6-2.20_0004. (**al**) *Annulotriassocampe baldii* Kozur, BE6-2.20_0053. (**am**) *Corum* sp. cf. *C. kraineri* Tekin, BE6-2.20_0005.

margin of Adria (Babić 1976; Šimunić *et al.* 1981; Lužar–Oberiter *et al.* 2009, 2012; Vukovski *et al.* 2023).

Ophiolitic mélange crops out along the southern slopes of Mt Ivanščica (Fig. 1b) and occupies the structurally upper parts of imbricates that consist of stratigraphic successions of the distal continental margin of Adria (Fig. 2a). At the investigated locality, the mélange is characterized by a block-in-matrix structure with centimetre- to decametre-sized blocks of mostly sandstone (quartz

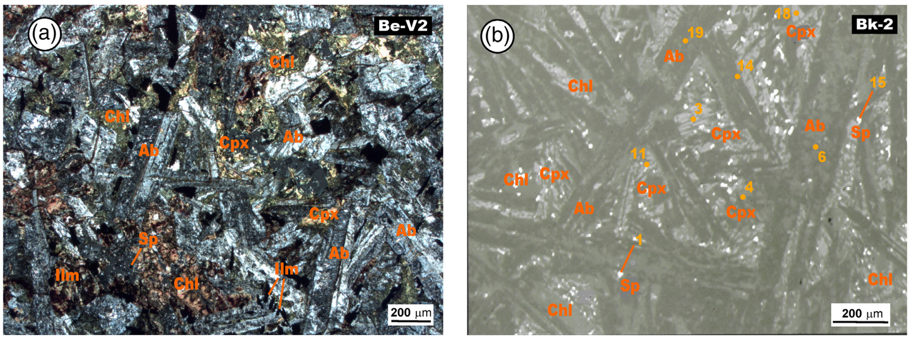


**Fig. 4.** (**a**) Microphotograph of thin section (crossed polars) and (**b**) back-scattered electron image of ophitic basalt from the ophiolitic mélange on Mt Ivanščica. Mineral abbreviations after Whitney and Evans (2010): Ab, albite; Chl, chlorite; Cpx, clinopyroxene; Ilm, ilmenite; Sp, spinel.

wacke and lithic arenite) and basalt, rarely chert and only sporadically gabbro within a shaly matrix. Composite blocks of basalt and chert are also present (Fig. 2b–d). The ratio of blocks and matrix varies in different outcrops. Well-developed kinematic indicators within the matrix indicate a splay in multiple shear directions, suggesting the influence of several tectonic events.

In an abandoned quarry near the village of Belec, several large blocks of basalt and associated chert and shale (Fig. 2b–d) were sampled for our petrological, geochemical and palaeontological investigations. Two chert blocks were sampled. The larger block consists of red chert showing clear stratification, with individual beds up to 15 cm thick and shale interlayers occurring in the middle part of the succession. The contact with the underlying basalt is tectonically disrupted. Higher in the succession, a *c.* 1 m thick interval of basalts is recorded in clear stratigraphic contact with the chert. The basalts are massive and show no pillow structure. Another smaller block of red chert was also sampled. This block has no contact with the basalts and the relationship with the previously described block is unclear. Because of the orientation of the beds in the larger block, it is possible that the smaller block is part of the same succession. A clear stratigraphic contact of pillow basalt and chert has been documented in another block within the quarry (Fig. 2d); however, no productive radiolarian sample was recovered from this block.

## Analytical techniques

Forty-four chert–shale samples were collected for the extraction of radiolarians. All the samples were treated with hydrofluoric acid (8%). Identifiable radiolarians were extracted from three samples and photographed using a JEOL JSM-IT 100 scanning electron microscope at the Ivan Rakovec Institute of Palaeontology (ZRC SAZU, Ljubljana, Slovenia). Fourteen thin sections of representative rock samples were analysed using an Olympus BH-2 polarization microscope at the Croatian Geological Survey (Zagreb, Croatia).

The chemical compositions of the mineral phases from a representative sample were determined at the Institute of Geosciences (University of Heidelberg, Germany) using a CAMECA SX51 electron microprobe equipped with five wavelength-dispersive spectrometers. Measurements were performed using an accelerating voltage of 15 kV, a beam current of 20 nA, a beam size of *c.* 1 µm (10 µm for feldspars) and a 10 s counting time for all elements. Natural minerals, oxides and silicates were used for calibration. The mineral formulas were calculated using the MINPET software package written by Linda R. Richard (Gatineau, Québec, Canada).

Six whole-rock samples were analysed for major elements by inductively coupled plasma optical emission spectrometry and for all trace elements by inductively coupled plasma mass spectrometry at Actlab Laboratories (Hamilton, Ontario, Canada). The major and trace element concentrations were measured using the US Geological Survey BHVO-2, W-2 and BIR-1 reference materials with an accuracy and precision better than ±1 and ±5%, respectively ($3\sigma$ at 10 times the detection limit). The detection limits were: $TiO_2$ and MnO, 0.001 wt%; $SiO_2$, $Al_2O_3$, $Fe_2O_3$, MgO, CaO, $Na_2O$, $K_2O$ and $P_2O_5$, 0.01 wt%; Lu, 0.002 ppm; Eu, 0.005 ppm; Ta, Pr, Sm, Gd, Ho, Er, Yb and U, 0.01 ppm; Th, La, Ce, Nd and Tm, 0.05 ppm; Cs and Hf, 0.1 ppm; Nb, 0.2 ppm; Y, 0.5 ppm; Sc, Rb and Zr, 1 ppm; Sr, 2 ppm; Ba, 3 ppm; V and Pb, 5 ppm; and Cr and Ni, 20 ppm. The quality of the measurements was checked by replicating the analysis on *c.* 12% of the samples.

X-ray diffraction (XRD) analyses were performed on the global fraction of a set of four representative samples. Sample preparation included an initial powdering of the material in an agate mortar prior to measurement. The measurements were undertaken at Texas Tech University's Geosciences Clay Laboratory (Lubbock, TX, USA) using a Bruker D8 Advance diffractometer. The measurements consisted of a step scan in the Bragg–Brentano geometry with CuKα radiation (40 kV, 40 mA). Sample mounts were scanned for 1.8 s per 0.02° from 3° to 70° $2\theta$. The XRD traces were interpreted using Bruker EVA software and comparison with the PDF4 database issued by the International Centre for Diffraction Data.

## Radiolarian dating

Identifiable radiolarians were extracted from three samples. Figure 2b, c shows the position of the sampled locations within the quarry. The radiolarians are rare and poorly preserved in all samples. The inventory of radiolarian species in the analysed samples is shown in Table 1 and the radiolarian taxa are illustrated in Figure 3.

The dating of samples BE1-2.10 and BE5-0.40 is based on the co-occurrence of *Oertlispongus inaequispinosus* Dumitrica, Kozur and Mostler (Fig. 3j–l), *Paroertlispongus multispinosus* Kozur and

**Table 2.** Distribution and relative abundance (determined by X-ray diffraction) of mineral phases in basalts from Mt Ivanščica

| Sample No.: | Be-V2 | Be-V4/1 | Be-V1/3 | Be-V1/1 |
|---|---|---|---|---|
| Qtz | | | ++ | ++ |
| Ab | ++ | ++ | + | ++ |
| Mg-Chl | ++ | | + | |
| Fe-Chl | | ++ | | ++ |
| Dol | + | | | |
| Cal | + | ++ | | + |
| Ana | + | | | |
| Ms | + | | + | |
| An | + | | | |
| Min | * | | | |

Abbreviations (after Whitney and Evans 2010): Qtz, quartz; Ab, albite; Chl, chlorite; Dol, dolomite; Cal, calcite; Ana, anatase; Ms, muscovite; An, anorthite; Min, minnesotaite; ++, major phases; +, minor phases; *, phases present, but not unequivocally confirmed by X-ray diffraction.

**Table 3.** Representative chemical compositions and calculated mineral formulas and modal fractions of plagioclase, clinopyroxene and spinel from basalts in the ophiolitic mélange on Mt Ivanščica

| Mineral: | Plagioclase | | | Clinopyroxene | | | | | | Spinel | | | |
|---|---|---|---|---|---|---|---|---|---|---|---|---|---|
| Sample No.: | Bk-2 | Bk-2 | Bk-2 | Bk-2 | Bk-2 | Bk-2 | Bk-2 | Bk-2 | Bk-2 | Bk-2 | Bk-2 | Bk-2 | Bk-2 |
| No. of analyses: | 6 | 14 | 19 | 3 | 4 | 11 | 18 | 22 | 24 | 1 | 15 | 20 | 21 |
| Site: | c | r | c | c | c | r | r | c | c | c | c | c | c |
| $SiO_2$ | 67.64 | 67.23 | 67.56 | 45.07 | 44.87 | 45.96 | 47.39 | 47.42 | 46.37 | 0.07 | 0.08 | 0.08 | 0.08 |
| $TiO_2$ | 0.00 | 0.00 | 0.00 | 3.49 | 3.77 | 2.61 | 2.33 | 2.30 | 2.59 | 1.08 | 1.82 | 0.43 | 0.46 |
| $Al_2O_3$ | 20.27 | 20.45 | 20.16 | 6.87 | 6.18 | 7.38 | 6.46 | 6.04 | 6.30 | 29.60 | 25.44 | 39.74 | 38.08 |
| $Cr_2O_3$ | 0.00 | 0.00 | 0.00 | 0.20 | 0.28 | 0.60 | 0.09 | 0.18 | 0.16 | 30.29 | 28.91 | 27.06 | 29.06 |
| FeO | 0.44 | 0.13 | 0.09 | 11.11 | 13.07 | 8.70 | 8.05 | 8.66 | 10.89 | 13.65 | 29.33 | 14.98 | 14.89 |
| MnO | 0.00 | 0.00 | 0.00 | 0.17 | 0.25 | 0.20 | 0.19 | 0.22 | 0.21 | 0.14 | 0.17 | 0.06 | 0.07 |
| NiO | 0.00 | 0.00 | 0.00 | 0.00 | 0.00 | 0.00 | 0.00 | 0.00 | 0.00 | 0.17 | 0.13 | 0.22 | 0.23 |
| MgO | 0.00 | 0.00 | 0.00 | 9.83 | 9.40 | 11.85 | 12.88 | 12.89 | 11.09 | 13.52 | 12.18 | 17.59 | 17.28 |
| CaO | 0.59 | 0.97 | 0.62 | 21.64 | 21.05 | 21.41 | 21.42 | 21.61 | 21.20 | 0.00 | 0.00 | 0.00 | 0.00 |
| $Na_2O$ | 11.43 | 11.40 | 11.44 | 0.44 | 0.44 | 0.49 | 0.43 | 0.38 | 0.40 | 0.00 | 0.00 | 0.00 | 0.00 |
| $K_2O$ | 0.08 | 0.02 | 0.04 | 0.05 | 0.12 | 0.02 | 0.00 | 0.00 | 0.10 | 0.00 | 0.00 | 0.00 | 0.00 |
| Total | 100.45 | 10.20 | 99.91 | 98.87 | 99.43 | 99.22 | 99.24 | 99.81 | 99.31 | 98.52 | 98.06 | 100.16 | 100.15 |
| Si | 2.953 | 2.942 | 2.960 | 1.731 | 1.727 | 1.732 | 1.777 | 1.772 | 1.761 | 0.002 | 0.002 | 0.002 | 0.002 |
| Ti | 0.000 | 0.000 | 0.000 | 0.101 | 0.109 | 0.074 | 0.066 | 0.065 | 0.074 | 0.024 | 0.042 | 0.009 | 0.010 |
| $Al_{tot}$ | 1.042 | 1.054 | 1.040 | 0.311 | 0.280 | 0.328 | 0.285 | 0.266 | 0.282 | 1.048 | 0.925 | 1.306 | 1.261 |
| $Al^{IV}$ | | | | 0.269 | 0.273 | 0.268 | 0.223 | 0.228 | 0.239 | | | | |
| $Al^{VI}$ | | | | 0.042 | 0.007 | 0.060 | 0.062 | 0.038 | 0.043 | | | | |
| Cr | 0.000 | 0.000 | 0.000 | 0.006 | 0.009 | 0.018 | 0.003 | 0.005 | 0.005 | 0.719 | 0.705 | 0.596 | 0.646 |
| $Fe^{3+}$ | | | | 0.053 | 0.077 | 0.077 | 0.058 | 0.082 | 0.076 | 0.180 | 0.280 | 0.075 | 0.069 |
| $Fe^{2+}$ | 0.016 | 0.005 | 0.003 | 0.304 | 0.344 | 0.197 | 0.194 | 0.189 | 0.270 | 0.414 | 0.477 | 0.274 | 0.281 |
| Mn | 0.000 | 0.000 | 0.000 | 0.006 | 0.008 | 0.006 | 0.006 | 0.007 | 0.007 | 0.004 | 0.004 | 0.001 | 0.002 |
| Ni | 0.000 | 0.000 | 0.000 | 0.000 | 0.000 | 0.000 | 0.000 | 0.000 | 0.000 | 0.004 | 0.003 | 0.005 | 0.005 |
| Mg | 0.000 | 0.000 | 0.000 | 0.563 | 0.539 | 0.666 | 0.720 | 0.718 | 0.628 | 0.605 | 0.560 | 0.731 | 0.724 |
| Ca | 0.028 | 0.045 | 0.029 | 0.891 | 0.868 | 0.865 | 0.860 | 0.865 | 0.863 | 0.000 | 0.000 | 0.000 | 0.000 |
| Na | 0.968 | 0.967 | 0.972 | 0.033 | 0.033 | 0.036 | 0.031 | 0.028 | 0.029 | 0.000 | 0.000 | 0.000 | 0.000 |
| K | 0.004 | 0.001 | 0.002 | 0.002 | 0.006 | 0.001 | 0.000 | 0.000 | 0.005 | 0.000 | 0.000 | 0.000 | 0.000 |
| Total | 5.011 | 5.014 | 5.006 | 3.998 | 3.994 | 4.000 | 4.000 | 4.000 | 3.995 | 3.000 | 3.000 | 3.000 | 3.000 |
| Cr# | | | | | | | | | | 40.7 | 43.3 | 31.4 | 33.9 |
| Mg# | | | | 64.9 | 61.0 | 77.2 | 78.8 | 79.2 | 69.9 | 59.4 | 54.0 | 72.7 | 72.0 |
| An | 2.80 | 4.44 | 2.89 | | | | | | | | | | |
| Ab | 96.80 | 95.46 | 96.91 | | | | | | | | | | |
| Or | 0.40 | 0.10 | 0.20 | | | | | | | | | | |
| Wo | | | | 49.04 | 47.27 | 47.74 | 46.79 | 46.50 | 46.80 | | | | |
| En | | | | 30.99 | 29.37 | 36.76 | 39.15 | 38.59 | 34.07 | | | | |
| Fs | | | | 19.96 | 23.35 | 15.50 | 14.06 | 14.91 | 19.13 | | | | |

Chemical compositions in wt%, mineral formulas in atoms per formula unit (a.p.f.u.) and modal fractions in mol.%. Formulas calculated on the basis of eight oxygens and total Fe as divalent for plagioclase; four cations and six oxygens for clinopyroxene; three cations and four oxygens for spinel. Cr# = 100*[Cr/(Cr + Al)]; Mg# = 100*[Mg/(Mg + $Fe^{2+}$)]; An = 100*Ca/(Ca + N + K); Wo = $Ca_2Si_2O_6$; En = $Mg_2Si_2O_6$; Fs = $Fe_2Si_2O_6$. c = core, r = rim.

Mostler (Fig. 3c–e) and *Eptingium manfredi* Dumitrica (Fig. 3u). The first appearance of *O. inaequispinosus* is in the *Spongosilicarmiger italicus* Radiolarian Zone (for compiled range, see Stockar *et al.* 2012), meaning that both samples are not older than the *S. italicus* Zone. This radiolarian zone corresponds to the lower part of the *Reitziites reitzi* Ammonoid Zone (Kozur 2003; Goričan *et al.* 2018). After the ratification of the Global Stratotype Section and Point (GSSP) for the base of the Ladinian stage by the International Union of Geological Sciences (Brack *et al.* 2005), the *R. reitzi* Zone is considered to be Anisian. The occurrence of *P. multispinosus* and *E. manfredi* in both samples indicate that the samples are not younger than the lower Fassanian unnamed radiolarian zone (Stockar *et al.* 2012), which is correlative to the upper part of the *Eoprotrachyceras curionii* Ammonoid Zone (Kozur 2003; Goričan *et al.* 2018).

The range of sample BE6-2.20 is based on the occurrence of *Muelleritortis expansa* Kozur and Mostler identified in the sample (Fig. 3ae, af). This species first occurs in the Upper Ladinian *Muelleritortis cochleata* Radiolarian Zone and ranges to the base of the lowermost Carnian *Tritortis kretaensis* Radiolarian Zone (Tekin 1999). In summary, the lower part of the chert–shale succession is dated as late Illyrian–early Fassanian and the upper part is assigned to the Langobardian–earliest Carnian.

## Mineralogy, petrography and phase chemistry of the effusive rocks

The effusive rocks are represented by massive medium- to coarse-grained basic lavas, characterized by irregular fracturing. The primary igneous textures are well preserved in all samples. All the samples are aphyric and show holocrystalline ophitic to rarely variolitic textures and isotropic structures (Fig. 4). The XRD mineralogy shows a uniform composition dominated by hydrothermal albite and chlorite, while the minor phases are dolomite, calcite, muscovite and anatase (Table 2). Some minor anorthite-rich plagioclase and an abundance of quartz in samples containing radiolarites have also been identified. Based on the intensity ratios of chlorite basal reflexes (003/005), a range of Fe/Mg octahedral occupancies has been documented (Brown and Brindley 1980). This

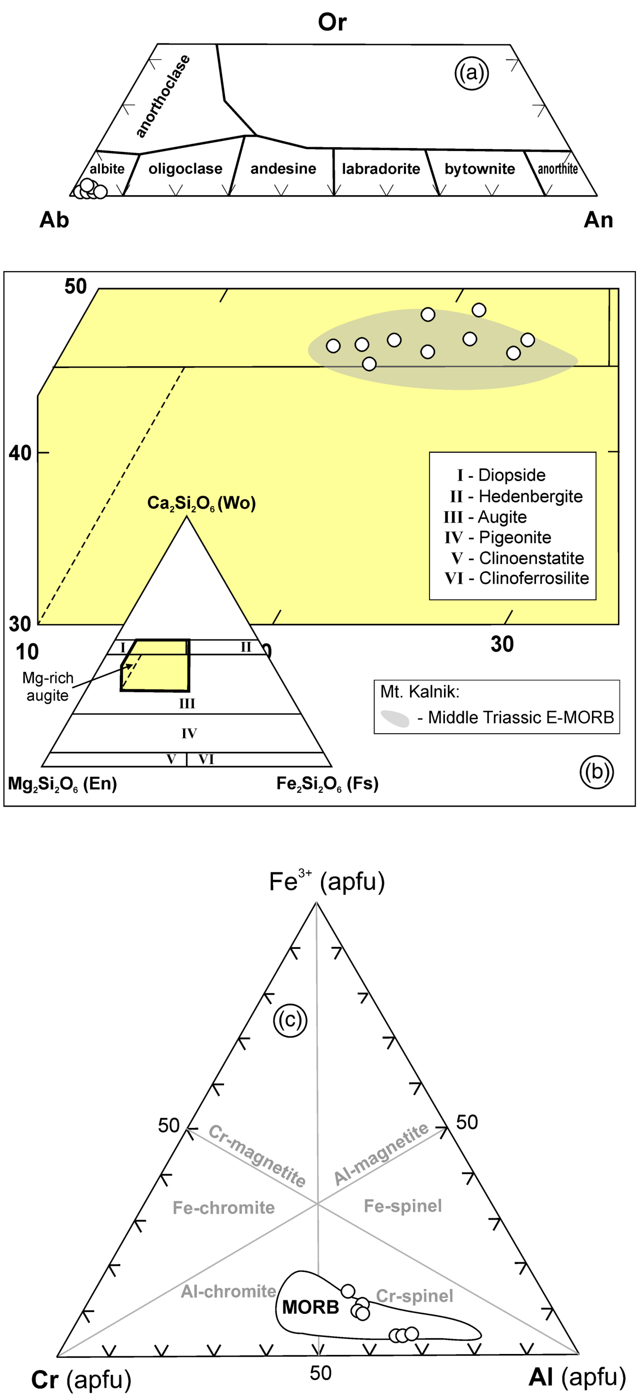


**Fig. 5.** Classification diagrams for (**a**) feldspar (Ab–An–Or plot; Deer *et al.* 1992; Dana *et al.* 1993), (**b**) pyroxene [En–Wo–Fs ($Mg_2Si_2O_6$–$Ca_2Si_2O_6$–$Fe_2Si_2O_6$) plot; Morimoto 1988] and (**c**) spinel (Cr–Al–$Fe^{3+}$ plot; Stevens 1944) for basalts from the ophiolitic mélange on Mt Ivanščica. The fields for spinel in the mid-ocean ridge basalt setting are from Saccani and Tassinari (2015 and references cited therein). The fields for clinopyroxene compositions from Middle Triassic incompatible element-enriched mid-ocean ridge basalt from the ophiolitic mélange on Mt Kalnik (Slovenec *et al.* 2011) are plotted for correlation constraints. E-MORB, incompatible element-enriched mid-ocean ridge basalt; MORB, mid-ocean ridge basalt.

is consistent with high-temperature metasomatism of the bedrock in the prehnite–pumpellyite and pumpellyite–actinolite facies, as inferred for Mesozoic ophiolite and non-ophiolite basalts–andesites and tuffs of the western Neotethys Ocean (Šegvić *et al.* 2023).

The petrographic evidence suggests the following order of crystallization: ±spinel → plagioclase → clinopyroxene ± Fe–Ti oxide. This order is typical of volcanic rocks formed at a mid-ocean ridge (Beccaluva *et al.* 1980). Selected plagioclase, clinopyroxene and spinel compositions are shown in Table 3. Acicular to plate-shaped plagioclase is commonly altered to albite and/or peristerite ($An_{2.8\text{-}4.4}$; Figs 4a, b and 5a) and partially sericitized or calcified. Grains of plagioclase may appear to be rather heterogeneous due to tiny inclusions of chlorite and epidote-like phases. Clinopyroxene is represented by intergranular columnar diopside ($Wo_{46.5\text{-}49.0}En_{29.4\text{-}39.2}Fs_{14.1\text{-}23.4}$; Figs 4a, 5b), which may be largely altered to chlorite. The diopside chemistry is characterized by a uniform CaO content (*c.* 21.40 wt%), high $TiO_2$ (up to 3.77 wt%) and moderate Mg# (61.0–79.2). A moderately high Ti/Al ratio (0.22–0.39) suggests a high cooling rate of crystallization (Tracy and Robinson 1977). The values of this ratio, as well as the $Al^{VI}/Al^{IV} \leq 0.22$ ratio, indicate low to intermediate crystallization pressures, which are largely consistent with those of MORBs (Beccaluva *et al.* 1989). The estimated maximum diopside crystallization temperatures and pressures vary between 1089 and 1104°C and 0.38 and 0.56 GPa, respectively (Neave and Putirka

**Table 4.** Chemical compositions of basalts from the ophiolitic mélange on Mt Ivanščica

| Sample No.: | Be-V1/1 | Be-V1/2 | Be-V2 | Be-V3 | Be-V4/2 | Bk-2 |
|---|---|---|---|---|---|---|
| $SiO_2$ | 45.62 | 44.81 | 49.04 | 46.83 | 47.55 | 47.06 |
| $TiO_2$ | 1.96 | 1.63 | 1.98 | 1.72 | 1.59 | 1.64 |
| $Al_2O_3$ | 16.23 | 14.83 | 16.51 | 16.02 | 15.98 | 15.99 |
| $Fe_2O_{3total}$ | 8.72 | 9.55 | 8.83 | 8.93 | 9.20 | 8.61 |
| MnO | 0.52 | 0.70 | 0.51 | 0.51 | 0.58 | 0.58 |
| MgO | 6.03 | 9.40 | 5.72 | 7.21 | 8.70 | 7.33 |
| CaO | 5.21 | 5.27 | 4.18 | 4.55 | 4.60 | 4.98 |
| $Na_2O$ | 4.92 | 3.31 | 5.03 | 4.56 | 3.68 | 3.89 |
| $K_2O$ | 0.69 | 0.22 | 0.52 | 0.44 | 0.38 | 0.32 |
| $P_2O_5$ | 0.21 | 0.19 | 0.25 | 0.20 | 0.20 | 0.22 |
| LOI | 10.05 | 9.84 | 7.36 | 8.92 | 7.70 | 9.30 |
| Total | 99.96 | 99.74 | 99.93 | 99.89 | 100.20 | 99.92 |
| Mg# | 60.6 | 67.7 | 59.3 | 61.6 | 65.9 | 65.1 |
| Cs | 0.8 | 0.6 | 0.7 | 1.2 | 1.3 | 0.9 |
| Rb | 9 | 6 | 10 | 8 | 10 | 11 |
| Ba | 166 | 40 | 259 | 105 | 85 | 92 |
| Th | 0.52 | 0.67 | 0.48 | 0.77 | 0.83 | 0.81 |
| Ta | 0.43 | 0.49 | 0.42 | 0.49 | 0.62 | 0.52 |
| Nb | 6.8 | 7.7 | 6.7 | 7.2 | 8.8 | 7.8 |
| Sr | 288 | 125 | 302 | 198 | 180 | 164 |
| Zr | 153 | 121 | 162 | 142 | 118 | 129 |
| Hf | 2.8 | 2.7 | 3.0 | 3.3 | 2.7 | 2.9 |
| Y | 30.1 | 27.5 | 32.5 | 29.5 | 20.0 | 22.7 |
| Sc | 39 | 37 | 40 | 38 | 37 | 40 |
| V | 315 | 235 | 312 | 306 | 270 | 298 |
| Cr | 290 | 580 | 280 | 320 | 400 | 340 |
| Ni | 80 | 200 | 60 | 90 | 120 | 110 |
| La | 8.02 | 8.21 | 8.51 | 8.21 | 7.37 | 8.48 |
| Ce | 19.8 | 21.4 | 22.3 | 20.5 | 19.1 | 22.1 |
| Pr | 2.62 | 2.98 | 3.37 | 3.03 | 2.55 | 3.26 |
| Nd | 11.9 | 15.0 | 16.5 | 12.6 | 11.8 | 16.1 |
| Sm | 3.29 | 3.91 | 4.36 | 3.62 | 3.15 | 4.22 |
| Eu | 1.19 | 1.15 | 1.64 | 1.32 | 1.06 | 1.44 |
| Gd | 3.63 | 4.77 | 5.59 | 4.03 | 3.51 | 5.32 |
| Tb | 0.62 | 0.81 | 0.97 | 0.72 | 0.58 | 0.89 |
| Dy | 3.84 | 5.15 | 5.89 | 4.59 | 3.74 | 5.24 |
| Ho | 0.81 | 1.00 | 1.19 | 0.97 | 0.76 | 1.08 |
| Er | 2.39 | 2.75 | 3.34 | 3.03 | 2.22 | 3.16 |
| Tm | 0.331 | 0.385 | 0.469 | 0.389 | 0.312 | 0.412 |
| Yb | 2.21 | 2.49 | 2.83 | 2.39 | 2.01 | 2.42 |
| Lu | 0.319 | 0.388 | 0.425 | 0.362 | 0.307 | 0.406 |

Chemical compositions of major oxides in wt%, trace element and rare earth elements in ppm. LOI = loss-on-ignition at 1100°C.Mg# = 100*molar [MgO/(MgO + $FeO_{total}$)].

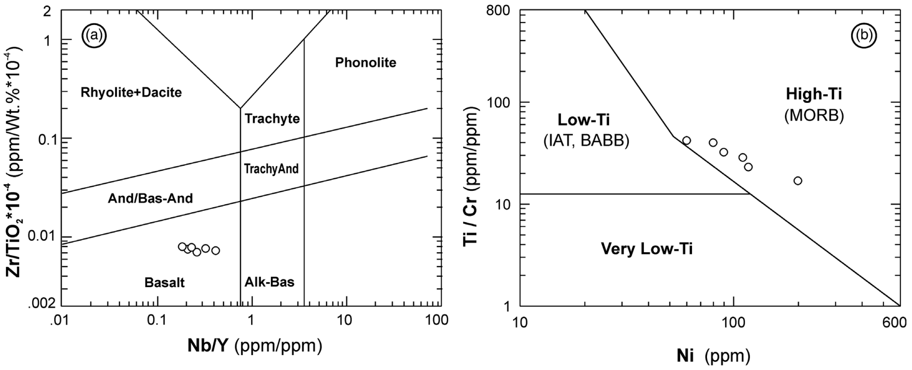


**Fig. 6.** (**a**) Nb/Y–$Zr/TiO_2*10^{-4}$ classification diagram (Winchester and Floyd 1977) and (**b**) Ni–Ti/Cr diagram (Beccaluva *et al.* 1983) for basalts from the ophiolitic mélange on Mt Ivanščica. BABB, back-arc basin basalt; IAT, island arc tholeiite; MORB, mid-ocean ridge basalt. And, andesite; Bas, basalt; TrachyAnd, trachyandesite; Alk-Bas, alkaline basalt.

2017). Slightly lower pressures (0.27–0.35 (±0.2) GPa) were calculated using the geobarometer of Nimis (1999) and Nimis and Ulmer (1998). The groundmass spinel has a composition typical of Cr-spinel (Figs 4b, 5c), characterized by a moderately high Cr# (3.4–43.3), Mg# (54.0–72.7) and a relatively wide range of $TiO_2$ contents (0.43–1.82 wt%). The Fe–Ti oxides (magnetite and ilmenite) and apatite are accessory minerals.

## Bulk rock chemistry of the effusive rocks

The chemical compositions of the analysed rocks are shown in Table 4. A high loss-on-ignition (up to 10.05 wt%) indicates severe seafloor hydrothermal alteration (Polat *et al.* 2002; Polat and Hofmann 2003), as has been reported for oceanic lithosphere from the study area (Šegvić *et al.* 2023). In contrast with the large ion lithophile elements (Cs, Rb, K and Ba), the concentrations of the high field strength elements (Th, Nb, Ta, Ti, Hf, Y) and rare earth elements (REEs) show good correlations with the Zr concentrations (not shown) as a differentiation index (Pearce 1975; Staudigel *et al.* 1996), indicating little mobilization. The concentrations of the high field strength elements and the REEs are therefore used to characterize the geochemical and petrogenetic characteristics of the studied rocks. In the Nb/Y v. $Zr/TiO_2 \times 0.0001$ classification diagram (Winchester and Floyd 1977), all the analysed rocks plot in the field of subalkaline tholeiitic basalts (Fig. 6a). They are characterized by a high-Ti affinity (Fig. 6b; Table 4) and moderately high Ti/V ratios (32.9–41.6), typical of mid-ocean ridge ophiolitic extrusive rocks (Beccaluva *et al.* 1983; Shervais 1982). The basalts crystallized from poorly to moderately evolved magmas (Mg# = 67.7–59.3; Ni = 60–200 ppm).

Figure 7a shows the normalized multi-element concentration patterns and Figure 7b shows the chondrite-normalized REE patterns. All the rocks show selective large ion lithophile element enrichment, consistent with their polyphase seafloor hydrothermal alteration, and a smooth pattern of a gradual decrease in enrichment from Th to Lu, which ranges from 7 to 0.7 times relative to normal-type mid-ocean ridge basalt (N-MORB). The rocks show a narrow range of Ta–Nb anomalies relative to La, from a barely noticeable negative to a very slight positive anomaly $[(Nb/La)_N = 0.84–1.28]$. The smooth and parallel normalized REE patterns show continuous weak enrichment of light REEs over heavy REEs $[La/Lu)_{CN}$ = 2.1–2.6] of 8–22 times relative to chondrite without a clearly expressed Eu anomaly. This shape of the multi-element and REE profile is ideally matched to that of incompatible element-enriched mid-ocean ridge basalts (E-MORBs) (Fig. 7a, b).

## Discussion

Successions composed of igneous basement representing the oceanic lithosphere and sedimentary rocks deposited on the ocean

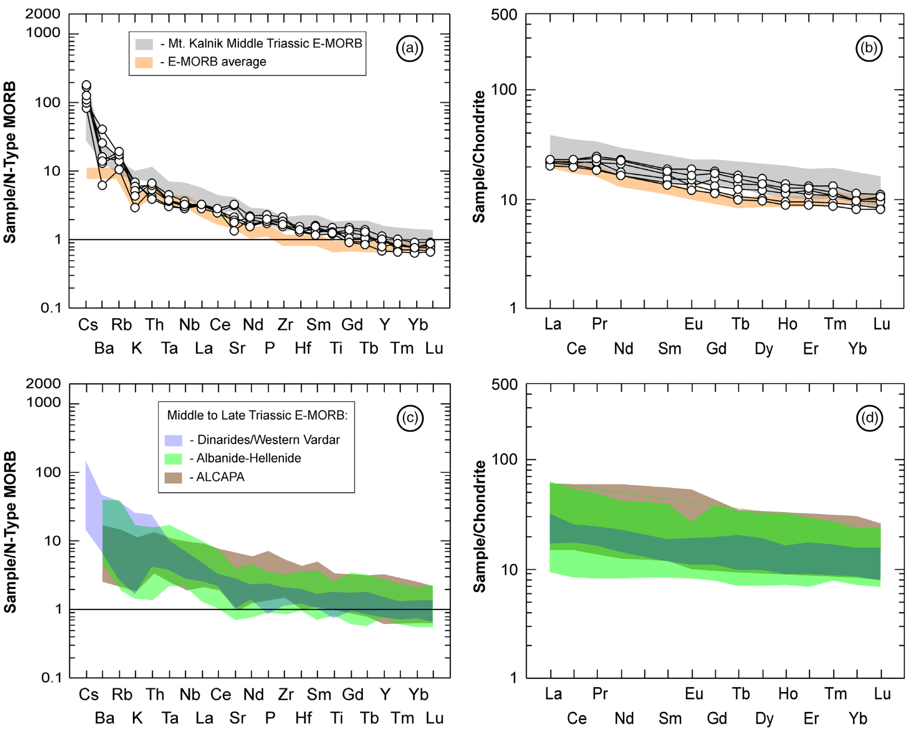


**Fig. 7.** (**a**, **c**) Normal-type mid-ocean ridge basalt-normalized (Sun and McDonough 1989) multi-element patterns and (**b**, **d**) rare earth element-normalized (Taylor and McLennan 1985) patterns for basalts from the ophiolitic mélange on Mt Ivanščica. The fields for incompatible element-enriched mid-ocean ridge basalts (E-MORBs) (Sun and McDonough 1989), Middle Triassic E-MORBs from the ophiolitic mélange on Mt Kalnik (Slovenec *et al.* 2011) and from the Inke–Tóalmás–Darnó Hill–Bódva valley in the ALCAPA Unit (Downes *et al.* 1990; Harangi *et al.* 1996), as well as Middle to Late Triassic E-MORBs from the Dinarides/Western Vardar belt (Majer 1993; Vishnevskaya *et al.* 2009; Kiss *et al.* 2012; Šuica *et al.* 2018 and unpublished data) and Middle to Late Triassic E-MORBs from the Albanides–Hellenides (Bortolotti *et al.* 2009; Saccani *et al.* 2011 and references cited therein; Chiari *et al.* 2012) are plotted for correlation constraints.

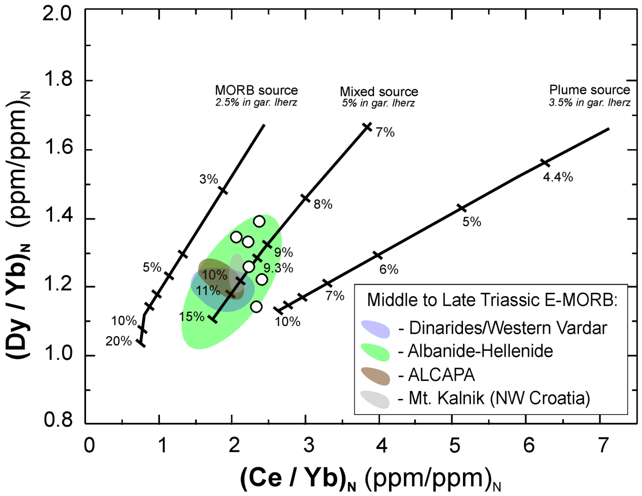


**Fig. 8.** $(Dy/Yb)_N$–$(Ce/Yb)_N$ diagram and partial melting model (Haase and Devey 1996) for the basalts from the ophiolitic mélange on Mt Ivanščica. The melt model for accumulated batch melting using 1% melt steps. Partition coefficients and mid-ocean ridge basalt source from McKenzie and O'Nions (1991). The plume source has 2.2 ppm Ce, 0.55 ppm Dy and 0.35 ppm Yb; the mixed source for enriched tholeites has 1.7 ppm Ce. Melting starts with residual garnet and continues in the spinel lherzolite field. The fields for Middle Triassic incompatible element-enriched mid-ocean ridge basalts (E-MORBs) from the ophiolitic mélange on Mt Kalnik (Slovenec *et al.* 2011) and from the Inke–Tóalmás–Darnó Hill–Bódva valley in the ALCAPA Unit (Downes *et al.* 1990; Harangi *et al.* 1996), as well as Middle to Late Triassic E-MORBs from the Dinarides/Western Vardar belt (Majer 1993; Vishnevskaya *et al.* 2009; Kiss *et al.* 2012; Šuica *et al.* 2018 and unpublished data) and Middle to Late Triassic E-MORBs from the Albanides–Hellenides (Bortolotti *et al.* 2009; Saccani *et al.* 2011 and references cited therein; Chiari *et al.* 2012) are plotted for correlation constraints.

floor represent the uppermost part of an ophiolitic sequence. These can be detached and offscraped from the subducting oceanic plate near the toe of an accretionary wedge (e.g. Matsuda and Isozaki 1991) or eroded from an ophiolitic nappe during its emplacement on the continental margin (e.g. Gawlick and Missoni 2019). Long-lasting and intense deformation during the evolution of accretional and subsequently collisional orogens leads to the dismemberment of coherent units and the incorporation of their fragments into mélanges, commonly accompanied by lithologies of different origins (e.g. Festa *et al.* 2022). Metre- to decametre-sized blocks of radiolarian chert and shale associated with basalt from mélange outcrops on Mt Ivanščica have been recognized as remnants of the oceanic crust of the western Neotethys branch (i.e. the Meliata–Maliac–Vardar branch of the Neotethys Ocean *sensu* Schmid *et al.* 2008, 2020).

The effusive basic rocks analysed in this study represent chemostratigraphically uniform subalkaline, high-Ti, massive tholeiitic basalts characterized by an enriched composition typical of E-MORBs (Fig. 7a, b). In the Ta/Yb v. Th/Yb diagram (Haase and Devey 1996), wherein three potential mantle sources are considered, the analysed basalts plot along melting curve for the mixed plume/MORB mantle source (Fig. 8). Accordingly, the Belec basalts are compatible with *c.* 9–11% partial melting of an enriched mantle source transitional between primitive and depleted MORB-type mantle (Haase and Devey 1996). Enriched oceanic crust produced during this magmatic stage was formed in the geotectonic setting of E-MORBs unrelated to subduction (Figs 7a, b and 9a, b). The same geotectonic setting is indicated by the chemical composition of the primary mineral phases (Figs 5c, 9c), as well as their order of crystallization, which includes the crystallization of plagioclase prior to clinopyroxene (Beccaluva *et al.* 1983). Basalts generated from this enriched magma clearly reflect an initial succession of oceanic protocrust formation and the onset of ocean spreading. The depth of crystallization of the analysed basaltic lavas is estimated to be 12–17 km based on the calculated crystallization pressures of diopside.

The E-MORB-type effusive rocks indicate the formation of oceanic crust at the spreading ridge in the Repno segment of the Neotethys Ocean (Fig. 10). Radiolarian assemblages from the associated radiolarian cherts indicate a late Illyrian to early Fassanian age for the oldest oceanic crust, with magmatic activity continuing in the Langobardian. This is in line with the biostratigraphic ages obtained from rift-related volcano-sedimentary successions from Mt Ivanščica and neighbouring mountains, which suggests that the initial rifting linked to the opening of this part of the Neotethys Ocean may have started in the Pelsonian (Kukoč *et al.* 2023). Extension related to rifting initially created deep water basins on the continental margin that accumulated pelagic sediments and volcaniclastic debris (Goričan *et al.* 2005; Slovenec *et al.* 2020, 2023; Kukoč *et al.* 2023), eventually leading to the formation of oceanic crust (Goričan *et al.* 2005; Fig. 10).

Earlier studies have shown that the newly formed ocean continued to spread until the latest Bajocian–Early Bathonian, when intra-oceanic subduction led to the formation of supra-subduction island arc tholeiite-type magmas and a metasomatized accretionary mantle wedge (Slovenec and Lugović 2009, 2012; Slovenec *et al.* 2011; Lugović *et al.* 2015; Fig. 10). A similar geodynamic evolution has been proposed for the Dinaridic ophiolites (Lugović *et al.* 1991; Trubelja *et al.* 1995; Babajić 2009; Šegvić *et al.* 2014) and for the whole Meliata–Maliac–Vardar oceanic system (e.g. Bortolotti *et al.* 2004*a*, 2013; Saccani and Photiades 2005; Saccani *et al.* 2011).

The origin of the ophiolitic mélange of the Dinarides–Hellenides orogenic belt is still a matter of debate, mainly focusing on the area where the mélange was formed and the age of its formation (e.g. Robertson *et al.* 2009; Gawlick *et al.* 2017). One group of researchers interprets the ophiolitic mélange as being formed in front of the advancing nappes during ophiolite obduction on the continental margin (Ferrière *et al.* 2015; Gawlick *et al.* 2016*b*; Gawlick and Missoni 2019). According to this interpretation, the obduction of the Western Vardar ophiolites on the continental margin of Adria may have already started in the Mid-Jurassic (e.g. Gawlick *et al.* 2008) and the mélange was mainly formed by sedimentary processes in deep water basins on the deformed continental margin. The material for the mélange was provided by the erosion of the advancing nappes, which included Triassic MORBs and their sedimentary cover (e.g. Ferrière *et al.* 2015; Gawlick *et al.* 2016*b*; Gawlick and Missoni 2019).

Other researchers consider the formation of the ophiolitic mélange to be a multi-stage process that started in the Mid-Jurassic with the inception of intra-oceanic subduction and the formation of an accretionary wedge and ended with the final emplacement of the ophiolites on the continental margin in the Late Jurassic–earliest Cretaceous (e.g. Robertson and Karamata 1994; Schmid *et al.* 2008; Saccani *et al.* 2011; Bortolotti *et al.* 2013). These researchers consider the mélange to be a tectono-sedimentary unit consisting of the lithologies scrapped off the subducting plate and accreted to the upper plate, as well as gravitationally emplaced olistoliths derived from the upper plate (e.g. Bortolotti *et al.* 1996; Saccani and Photiades 2005; Schmid *et al.* 2008; Chiari *et al.* 2011). It is widely accepted that the western Neotethys Ocean, including the ROD, was affected by intra-oceanic subduction starting in the Mid-Jurassic (e.g. Schmid *et al.* 2008; Saccani *et al.* 2011; Slovenec *et al.* 2011; Bortolotti *et al.* 2013; Fig. 10). The early emplacement of Triassic MORBs into an accretionary wedge likely occurred during this stage (Saccani and Photiades 2005; Saccani *et al.* 2011). Then, presumably in the Late Jurassic, an ophiolitic sheet built of newly formed Mid- to Late Jurassic intra-oceanic supra-subduction crust was thrust onto the accretionary wedge before being obducted

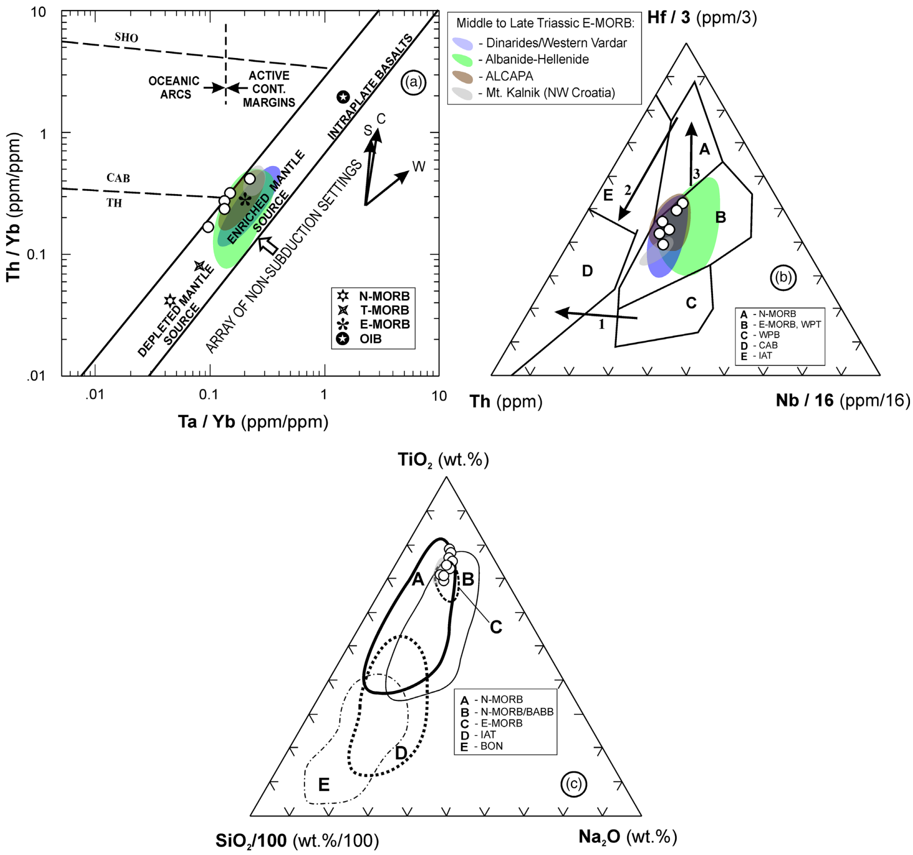


**Fig. 9.** Discrimination diagrams for the basalts from the ophiolitic mélange on Mt Ivanščica. (**a**) Ta/Yb–Th/Yb diagram (Pearce 1983). S, subduction zone enrichment; SHO, shosonites; C, crustal contamination; W, within-plate enrichment; CAB, calc-alkaline basalts; Th, tholeiites. Normal-type mid-ocean ridge basalt (N-MORB), incompatible element-enriched MORB (E-MORB) and ocean island basalt (OIB) compositions are from Sun and McDonough (1989). Transitional MORB (T-MORB) composition is from Geshi *et al.* (2007). (**b**) Th–Nb/16–Hf/3 diagram (Wood 1980). A, N-MORB; B, E-MORB and within-plate tholeiites (WPT); C, alkaline within-plate basalts (WPB); D, calc-alkali basalts (CAB); E, island arc tholeiites (IAT); 1, crustal contamination; 2, supra-subduction zone ophiolites trend; 3, MORB ophiolites trend. (**c**) $SiO_2$/100–$Na_2O$–$TiO_2$ diagram (simplified after Beccaluva *et al.* 1989) for clinopyroxene. BABB, back-arc basin basalts; BON, boninites. Field for Middle Triassic E-MORBs from the ophiolitic mélange on Mt Kalnik (Slovenec *et al.* 2011) and from the Inke–Tóalmás–Darnó Hill–Bódva valley in the ALCAPA Unit (Downes *et al.* 1990; Harangi *et al.* 1996), as well as Middle to Late Triassic E-MORBs from the Dinarides/Western Vardar belt (Majer 1993; Vishnevskaya *et al.* 2009; Kiss *et al.* 2012; Šuica *et al.* 2018 and unpublished data) and Middle to Late Triassic E-MORBs from the Albanides–Hellenides (Bortolotti *et al.* 2009; Saccani *et al.* 2011 and references cited therein; Chiari *et al.* 2012) are plotted for correlation constraints.

on the continental margin (Gaggero *et al.* 2009; Bortolotti *et al.* 2013; Fig. 10). The Triassic oceanic crust found in the ophiolitic mélange therefore represents a vestige of an ancient accretionary wedge incorporated in the mélange during the obduction of ophiolites on the continental margin.

## Correlation of Mid- to Late Triassic biostratigraphic ages from the ROD with similar occurrences throughout the ALCAPA–Dinaride–Hellenide area

Although Mid- to Late Triassic ophiolites are widespread in the Dinarides–Hellenides orogenic belt as a result of its consumption during subduction, remnants of the early crust of the Neotethys Ocean are relatively rare and almost exclusively known from fragments within ophiolitic mélange (e.g. Ferrière *et al.* 2015, 2016). In the neighbouring mountains in NW Croatia (Fig. 1b), Mid- to Late Triassic effusive rocks of comparable geochemical and petrological characteristics have been found in the ophiolitic mélange on Mt Kalnik (Slovenec *et al.* 2011; Figs 7c, d and 9a, b). Radiolarian assemblages from pelagic sediments in contact with MORBs on Mt Kalnik range from the Illyrian to the Norian (Halamić and Goričan 1995; Goričan *et al.* 2005).

The oldest radiolarian assemblage from the pelagic sediments associated with basalts is found at the Hrastov brijeg locality on Mt Kalnik (Goričan *et al.* 2005). This assemblage, correlative to those from samples BE1-2.10 and BE5-0.40 in this study, was dated to the late Fassanian at the time; however, after the ratification of the GSSP for the base of the Ladinian stage by the International Union of Geological Sciences (Brack *et al.* 2005), it is considered to be late Illyrian–Fassanian. A Late Ladinian assemblage, correlative to that from sample BE6-2.20 in this study, has been reported from the Hruškovec locality on Mt Kalnik (Goričan *et al.* 2005).

Correlative biostratigraphic ages, together with the comparable geochemical characteristics of effusive rocks from mélange outcrops in NW Croatia, indicate a common origin of these blocks as the fragmented oceanic crust of the ROD. Furthermore, combined biostratigraphic data indicate that seafloor spreading in the ROD may have started as early as the late Illyrian and continued until at least the Norian.

Further south, although relatively rarely represented, fragmented E-MORBs have been found in the ophiolitic mélange of the Internal Dinarides (Majer 1993; Vishnevskaya *et al.* 2009; Chiari *et al.* 2011; Kiss *et al.* 2012; Šuica *et al.* 2018; Figs 1a, 7c, d, 8 and 9a, b). Reported biostratigraphic ages for Triassic E-MORB-type oceanic crust (Figs 7c, d, 8 and 9a, b) are in good correlation with those from the ROD. The oldest radiolarite associated with basalts, dated as Late Anisian–Early Ladinian, is reported from the Zlatibor–Maljen area (Chiari *et al.* 2011), whereas other ages range from the Ladinian to the Norian (Obradović and Goričan 1988; Vishnevskaya *et al.* 2009; Chiari *et al.* 2011; Gawlick *et al.* 2016*b*).

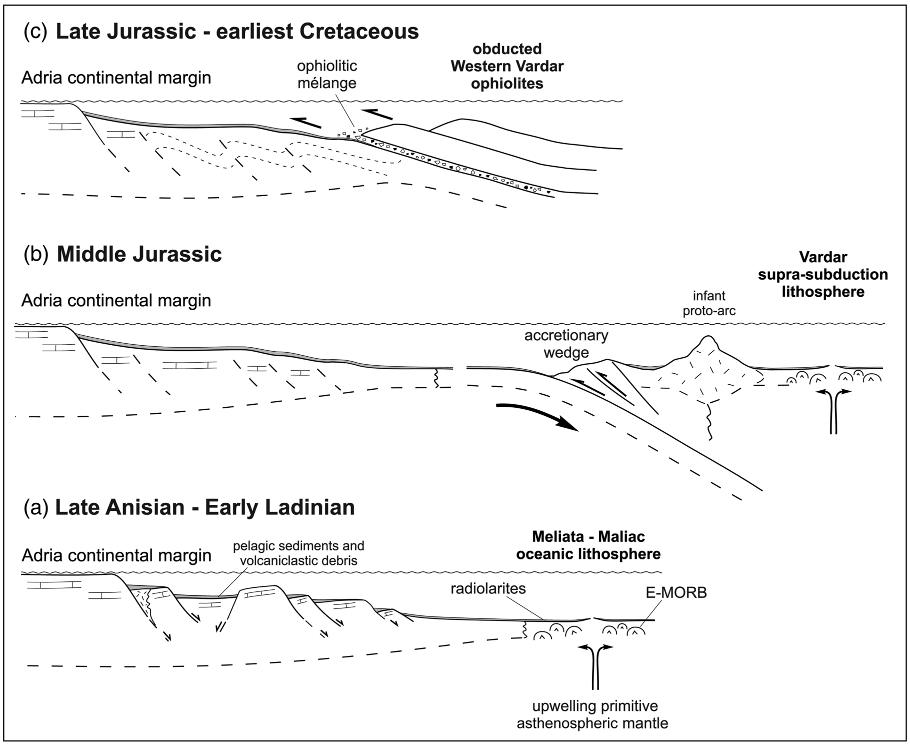


**Fig. 10.** Schematic geodynamic model for the evolution of the western part of the Repno Oceanic Domain and the eastern continental margin of Adria from the Mid-Triassic to the Late Jurassic (not to scale). (**a**) During the Mid-Triassic rifting phase, extensional tectonics produced a complex horst-and-graben topography on the continental margin. Pelagic sediments and volcaniclastic debris started accumulating in the newly formed deep water basins from the Mid- to Late Anisian (Goričan *et al.* 2005; Slovenec *et al.* 2020, 2023; Kukoč *et al.* 2023). Shortly afterwards, in the Late Anisian–Early Ladinian, the initial formation of a spreading ridge occurred in the Meliata–Maliac Ocean (Goričan *et al.* 2005; this study). (**b**) In the Mid-Jurassic, east-dipping intra-oceanic subduction led to the formation of an intra-oceanic accretionary prism and the formation of the supra-subduction oceanic lithosphere of the Vardar Ocean (Slovenec *et al.* 2011). Pieces of the Triassic ocean floor were likely incorporated into the accretionary prism at this time. (**c**) During obduction of the ophiolites on the continental margin of Adria in the Late Jurassic–earliest Cretaceous (Schmid *et al.* 2008), the ophiolitic mélange was formed in front of the advancing nappes incorporating the old accretionary prism.

E-MORBs are also common as blocks of massive and pillow lavas in ophiolitic mélanges in Albania and Greece (e.g. Saccani and Photiades 2005; Bortolotti *et al.* 2009, 2013; Saccani *et al.* 2011; Chiari *et al.* 2012; Figs 7c, d, 8 and 9a, b). In the Mirdita Zone in Albania (Fig. 1a), Illyrian radiolarites are found associated with basaltic–gabbroic rocks (Chiari *et al.* 1996; Bortolotti *et al.* 2006; Gawlick *et al.* 2008, 2016*a*). The oldest dated sample is assigned to the *Spongosilicarmiger transitus* Radiolarian Zone, which is correlative to the Illyrian *Kellnerites felsoeoersensis* Ammonoid Zone (Gawlick *et al.* 2016*a*). This is so far the oldest reported radiolarite occurrence associated with the oceanic crust reported from the Maliac–Meliata branch of the Neotethys Ocean. Other reported ages for Triassic oceanic crust in the Mirdita Zone range from the Illyrian (the *R. reitzi* Ammonid Zone) to the Norian (Kellici *et al.* 1994; Chiari *et al.* 1996; Bortolotti *et al.* 2004*a*, 2006; Gawlick *et al.* 2008, 2016*a*). The oldest oceanic crust in the Mirdita Zone is therefore only slightly older than that from the ROD, possibly indicating that seafloor spreading in the Meliata–Maliac Ocean propagated from SE to NW. We note that some of the occurrences of Triassic oceanic crust in Albania are interpreted by some researchers as blocks within the mélange, whereas other workers consider those assigned to the so-called Porava Unit to be a separate tectonic unit consisting of basalt with a preserved radiolarite cover (for details, see Bortolotti *et al.* 2013).

Much like in Albania, remnants of E-MORB-type Neotethys ocean floor (Figs 7c, d, 8 and 9a, b) are found both as blocks within ophiolitic mélange and as part of the ophiolitic sequence in ophiolitic complexes in Greece (Bortolotti *et al.* 2013; Ferrière *et al.* 2015, 2016; Fig. 1a). The reported Mid- to Late Triassic radiolarian ages for the sedimentary cover of the ocean floor are identical to those found in the rest of the Meliata–Maliac Ocean. The oldest obtained radiolarian ages correspond to the Illyrian–lower Fassanian and range up to the Norian (Bortolotti *et al.* 2003, 2008; Chiari *et al.* 2012; Ozsvárt *et al.* 2012; Ferrière *et al.* 2015).

To the north of the investigated area in NW Croatia, the remnants of E-MORB-type Neotethys crust have also been recognized in displaced fragments in the Darnó and Szarvaskö Complex (ALCAPA Unit; Fig. 1a) in NE Hungary (Downes *et al.* 1990; Harangi *et al.* 1996; Schmid *et al.* 2008; Figs 7c, d, 8 and 9a, b). Similar to other fragments of the Triassic ocean floor discussed earlier, the radiolarites in contact with basalts in the Darnó and Szarvaskö Complex contain Illyrian–Langobaridan and Carnian faunas (Ozsvárt and Kovács 2012 and references cited therein), indicating the same origin.

In summary, the geochemical characteristics of basalts from the Belec area, interpreted as originating from the ROD, and their age are well correlated with fragments of the oceanic crust and overlying pelagic sediments preserved in the ophiolitic mélange occurring from Hungary to Greece. This reaffirms the proposed geodynamic model that regards the ROD as a part of a single ocean, the Neotethys Ocean, located east of Adria (Babić *et al.* 2002; Schmid *et al.* 2008, 2020; Slovenec *et al.* 2011; Bortolotti *et al.* 2013). Furthermore, in conjunction with previously published data, our findings provide further evidence of continuous seafloor spreading in the Neotethys Ocean from the Late Anisian to the Norian.

## Conclusions

Decametre- to metre-sized blocks of effusive rocks in contact with radiolarian chert and shale from mélange on Mt Ivanščica are recognized as the uppermost part of the ophiolitic sequence. This sequence is interpreted as remnants of an early crust of the ROD, considered to be the northwesternmost segment of the Neotethys Ocean. The effusive rocks represent subalkaline, high-Ti, massive tholeiitic basalts characterized by an enriched composition typical of E-MORB and clearly reflect the initial succession of oceanic protocrust formation and the onset of an ocean spreading ridge. Radiolarians indicate a late Illyrian–early Fassanian to Langobardian age for the chert–shale succession associated with the basalts. Fragments of the Triassic oceanic crust with overlying sediments were incorporated into an accretionary wedge during the Mid- to Late Jurassic intra-oceanic subduction within the ROD and were subsequently included in the ophiolitic mélange during the obduction of the ophiolites on the continental margin of Adria, most likely in the Late Jurassic–earliest Cretaceous.

*Scientific editing by Edoardo Barbero*

**Acknowledgements** The authors thank their colleagues at the Ivan Rakovec Institute of Palaeontology ZRC SAZU, Ljubljana for their hospitality and the use of their scanning electron microscope. The authors are especially grateful to the late Boško Lugović (formerly of the University of Zagreb) and Hans-Peter Meyer (University of Heidelberg) for providing excellent microprobe data and Illona Fin (University of Heidelberg) for preparing the high-quality polished thin sections. The authors also thank Yildirim Dilek (Miami University, USA), Andrea Festa (University of Torino, Italy) and Edoardo Barbero (CNR National Research Council, Italy), the guest editors of this thematic collection, as well as Špela Goričan (ZRC SAZU, Ljubljana, Slovenia) and Emilio Saccani (University of Ferrara, Italy), whose careful reviews and constructive comments helped to improve our paper.

**Author contributions** **DK:** conceptualization (equal), investigation (equal), formal analysis (equal), writing – original draft (lead); **DS:** conceptualization (equal), formal analysis (equal), writing – original draft (equal); **BŠ:** formal analysis (equal), writing – original draft (supporting); **MV:** investigation (equal), writing – original draft (supporting); **MB:** investigations (equal), writing – review and editing (supporting); **TG:** investigations (equal), writing – review and editing (supporting); **MH:** writing – review and editing (supporting); **DS:** writing – review and editing (supporting).

**Funding** This work was supported by the Croatian Science Foundation under the project Revealing the Middle Triassic Paleotethyan Geodynamics Recorded in the Volcano-Sedimentary Successions of NW Croatia (IP-2019-04-3824).

**Competing interests** The authors declare that they have no known competing financial interests or personal relationships that could have appeared to influence the work reported in this paper.

**Data availability** All data generated or analysed during this study are included in this published article.

## References

Aničić, B. and Juriša, M. 1985. *Osnovna geološka karta SFRJ 1:100 000. Tolmač za list Rogatec L 33-68. [Basic Geological Map of SFRY 1:10000, Explanatory Notes for Sheet Rogatec L 33-68]*. Savezni geološki zavod, Beograd [in Slovenian].

Babajić, E. 2009. *Petrological and Geochemical Characteristic of Mafic Rocks from the Krivanja–Konjuh Ophiolitic Complex*. PhD thesis, University of Tuzla [in Bosnian with English summary].

Babić, Lj. 1976. Stratigrafski slijed i paleogeografska evolucija Ivanščice od gornjeg trijasa do sredine krede [Sedimentary sequence and paleogeographic evolution of Mt. Ivanščica (northern Croatia) from the Upper Triassic to the Middle of Cretaceous]. *In:* Buser, S. and Drobne, K. (eds) *8. Jugoslovenski geološki kongres, 1–5 oktober 1974, Bled, 2. dio, Paleontologija, sedimentologija, stratigrafija*. Slovensko geološko društvo (Slovenian Geological Society), Ljubljana, 53–62 [in Croatian with English summary].

Babić, Lj. and Zupanič, J. 1978. Mlađi mezozoik Ivanščice. *In:* Babić, L. and Jelaska, V. (eds) *Vodić ekskurzije 3. skupa sedimentologa Jugoslavije, Zagreb*. Hrvatsko geološko društvo (Croatian Geological Society), Zagreb, 11–23 [in Croatian].

Babić, Lj., Hochuli, P.A. and Zupanič, J. 2002. The Jurassic ophiolitic mélange in the NE Dinarides: dating, internal structure and geotectonic implications. *Eclogae Geologicae Helvetiae*, **95**, 263–275, https://doi.org/10.5169/seals-168959

Baumgartner, P.O. 1985. *Jurassic Sedimentary Evolution and Nappe Emplacement in the Argolis Peninsula (Peloponnesus; Greece)*. Mémoires de la Société Helvétique des Sciences Naturelles, **99**.

Beccaluva, L., Piccardo, G.B. and Serri, G. 1980. Petrology of northern Apennine ophiolites and comparison with other Tethyan ophiolites. *In:* Panayiotou, A. (ed.) *Ophiolites: Proceedings, International Ophiolite Symposium, 1–8 April 1979, Nicosia, Cyprus*. Republic of Cyprus Ministry of Agriculture and Natural Resources, Geological Survey Department, Nicosia, 314–331.

Beccaluva, L., Di Girolamo, P., Macciotta, G. and Morra, V. 1983. Magma affinities and fractionation trends in ophiolites. *Ofioliti*, **8**, 307–324.

Beccaluva, L., Macciotta, G., Piccardo, G.B. and Zeda, O. 1989. Clinopyroxene composition of ophiolite basalts as petrogenetic indicator. *Chemical Geology*, **77**, 165–182, https://doi.org/10.1016/0009-2541(89)90073-9

Beccaluva, L., Coltorti, M., Premti, I., Saccani, E., Siena, F. and Zeda, O. 1994. Mid-ocean ridge and suprasubduction affinities in the ophiolitic belts from Albania. *Ofioliti*, **19**, 77–96.

Bernoulli, D. and Laubscher, H. 1972. The palinspastic problem of the Hellenides. *Eclogae Geologicae Helvetiae*, **65**, 107–118, https://doi.org/10.5169/seals-164079

Bortolotti, V., Kodra, A., Marroni, M., Mustafa, F., Pandolfi, L., Principi, G. and Saccani, E. 1996. Geology and petrology of ophiolitic sequences in the Mirdita region (northern Albania). *Ofioliti*, **21**, 3–20.

Bortolotti, V., Carras, N., Chiari, M., Fazzuoli, M., Marcucci, M., Photiades, A. and Principi, G. 2003. The Argolis peninsula in the palaeogeographic and geodynamic frame of the Hellenides. *Ofioliti*, **28**, 79–94, https://www.ofioliti.it/index.php/ofioliti/article/view/196

Bortolotti, V., Chiari, M., Marcucci, M., Marroni, M., Pandolfi, L., Principi, G. and Saccani, E. 2004*a*. Comparison among the Albanian and Greek ophiolites: in search of constraints for the evolution of the Mesozoic Tethys Ocean. *Ofioliti*, **29**, 19–35, https://www.ofioliti.it/index.php/ofioliti/article/view/204

Bortolotti, V., Chiari, M., Kodra, A., Marcucci, M., Mustafa, F., Principi, G. and Saccani, E. 2004*b*. New evidences for Triassic MORB magmatism in the northern Mirdita Zone ophiolites (Albania). *Ofioliti*, **29**, 247–250, https://www.ofioliti.it/index.php/ofioliti/article/view/217

Bortolotti, V., Marroni, M., Pandolfi, L. and Principi, G. 2005. Mesozoic to Tertiary tectonic history of the Mirdita ophiolites, northern Albania. *Island Arc*, **14**, 471–492, https://doi.org/10.1111/j.1440-1738.2005.00479.x

Bortolotti, V., Chiari, M. *et al.* 2006. Triassic MORB magmatism in the southern Mirdita Zone (Albania). *Ofioliti*, **31**, 1–9, https://www.ofioliti.it/index.php/ofioliti/article/view/323

Bortolotti, V., Chiari, M., Marcucci, M., Photiades, A., Principi, G. and Saccani, E. 2008. New geochemical and age data on the ophiolites from Othrys area (Greece): implication for the Triassic evolution of the Vardar Ocean. *Ofioliti*, **33**, 135–151, https://www.ofioliti.it/index.php/ofioliti/article/view/365

Bortolotti, V., Carras, N. *et al.* 2009. The ophiolite-bearing mélange in the Early Tertiary Pindos Flysch of Etolia (central Greece). *Ofioliti*, **34**, 83–94, https://www.ofioliti.it/index.php/ofioliti/article/view/380

Bortolotti, V., Chiari, M., Marroni, M., Pandolfi, L., Principi, G. and Saccani, E. 2013. Geodynamic evolution of ophiolites from Albania and Greece (Dinaric–Hellenic belt): one, two, or more oceanic basins? *International Journal of Earth Sciences*, **102**, 783–811, https://doi.org/10.1007/s00531-012-0835-7

Božović, M., Prelević, D., Romer, R.L., Barth, M., Van den Bogaard, P. and Boev, B. 2013. The Demir Kapija Ophiolite, Macedonia (FYROM): a snapshot of subduction initiation within a back-arc. *Journal of Petrology*, **54**, 1427–1453, https://doi.org/10.1093/petrology/egt017

Brack, P., Reiber, H., Nicora, A. and Mundil, R. 2005. The Global Boundary Stratotype Section and Point (GSSP) of the Ladinian Stage (Middle Triassic) at Bagolino (southern Alps, northern Italy) and its implications for the Triassic time scale. *Episodes*, **28**, 233–244, https://doi.org/10.18814/epiiugs/2005/v28i4/001

Brown, G. and Brindley, G.W. 1980. X-ray diffraction procedures for clay mineral identification. *In:* Brindley, G.W. and Brown, G. (eds) *Crystal Structures of Clay Minerals and their X-ray Identification*. Mineralogical Society, London, 305–306.

Chiari, M., Marcucci, M., Cortese, G., Ondrejickova, A. and Kodra, A. 1996. Triassic radiolarian assemblages in the Rubik area and Cukali zone, Albania. *Ofioliti*, **21**, 77–84.

Chiari, M., Marcucci, M. and Prela, M. 2004. Radiolarian assemblages from the Jurassic cherts of Albania: new data. *Ofioliti*, **29**, 95–105, https://www.ofioliti.it/index.php/ofioliti/article/view/208

Chiari, M., Djerić, N. *et al.* 2011. The geology of the Zlatibor–Maljen area (western Serbia): a geotraverse across the ophiolites of the Dinaric–Hellenic collisional belt. *Ofioliti*, **36**, 139–166, https://ofioliti.it/index.php/ofioliti/article/view/399

Chiari, M., Bortolotti, V., Marcucci, M., Photiades, A., Principi, G. and Saccani, E. 2012. Radiolarian biostratigraphy and geochemistry of the Koziakas massif ophiolites (Greece). *Bulletin de la Societé géologique de France*, **183**, 287–306, https://doi.org/10.2113/gssgfbull.183.4.287

Chiari, M., Saccani, E., Prela, M., Bortolotti, V., Marcucci, M. and Matsuoka, A. 2023. Radiolarian biostratigraphy of the northern Albania ophiolites: new data from the sub-ophioliic mélange and eastern Mirdita ophiolites. *Ofioliti*, **48**, 137–151, https://doi.org/10.4454/ofioliti.v48i2.566

Croatian Geological Survey 2009. *Geological Map of Republic of Croatia, Scale 1:300.000*. Hrvatski geološki institut, Zagreb.

Dana, J.D., Klein, C. and Hurlbut, C.S. 1993. *Manual of Mineralogy*. Wiley, New York.

Danelian, T. and Robertson, A.H.F. 2001. Neotethyan evolution of eastern Greece (Pagondas Mélange, Evia Island) inferred from radiolarian biostratigraphy and the geochemistry of associated extrusive rocks. *Geological Magazine*, **138**, 345–363, https://doi.org/10.1017/S0016756801005337

Deer, W.A., Howie, R.A. and Zussman, J. 1992. *An Introduction to the Rock-Forming Minerals*. Longman, London.

Dilek, Y. and Furnes, H. 2011. Ophiolite genesis and global tectonics: geochemical and tectonic fingerprinting of ancient oceanic lithosphere. *GSA Bulletin*, **123**, 387–341, https://doi.org/10.1130/B30446.1

Dilek, Y. and Furnes, H. 2014. Ophiolites and their origins. *Elements*, **10**, 93–100, https://doi.org/10.2113/gselements.10.2.93

Dilek, Y., Shallo, M. and Furnes, H. 2005. Rift-drift, seafloor spreading, and subduction tectonics of Albanian ophiolites. *International Geology Review*, **47**, 147–176, https://doi.org/10.2747/0020-6814.47.2.147

Dimitrijević, M.D. 1997. *Geology of Yugoslavia*. Geological Institute, Belgrade, GEMINI Special Publications.

Dimitrijević, M.D. and Dimitrijević, M.N. 1973. Olistostrome mélange in the Yugoslavian Dinarides and Late Mesozoic plate tectonics. *The Journal of Geology*, **81**, 328–340, https://doi.org/10.1086/627874

Downes, H., Pantó, G.Y., Árkai, P. and Thirlwall, M.F. 1990. Petrology and geochemistry of Mesozoic igneous rocks, Bükk mountains, Hungary. *Lithos*, **24**, 201–215, https://doi.org/10.1016/0024-4937(90)90032-V

Dumitrica, P. 1999. The Oertlispongidae (Radiolaria) from the Middle Triassic of Masirah Island (Oman). *Revue de Micropaléontologie*, **42**, 33–42, https://doi.org/10.1016/S0035-1598(99)90164-2

Ferrière, J., Chanier, F. and Ditbanjong, P. 2012. The Hellenic ophiolites: eastward or westward obduction of the Maliac Ocean, a discussion. *International Journal of Earth Sciences*, **101**, 1559–1580, https://doi.org/10.1007/s00531-012-0797-9

Ferrière, J., Chanier, F. *et al.* 2015. The evolution of the Triassic–Jurassic Maliac oceanic lithosphere: insights from the supra-ophiolitic series of Othris (continental Greece). *Bulletin de la Société géologique de France*, **186**, 399–411, https://doi.org/10.2113/gssgfbull.186.6.399

Ferrière, J., Baumgartner, P.O. and Chanier, F. 2016. The Maliac Ocean: the origin of the Tethyan Hellenic ophiolites. *International Journal of Earth Sciences*, **105**, 1941–1962, https://doi.org/10.1007/s00531-016-1303-6

Festa, A., Pini, G.A., Dilek, Y. and Codegone, G. 2010*a*. Mélanges and mélange-forming processes: a historical overview and new concepts. *International Geology Review*, **52**, 1040–1105, https://doi.org/10.1080/00206810903557704

Festa, A., Pini, G.A. *et al.* 2010*b*. Peri-Adriatic mélanges and their evolution in the Tethyan realm. *International Geology Review*, **52**, 369–403, https://doi.org/10.1080/00206810902949886

Festa, A., Barbero, E., Remitti, F., Ogata, K. and Pini, G.A. 2022. Mélanges and chaotic rock units: implications for exhumed subduction complexes and orogenic belts. *Geosystems and Geoenvironment*, **1/2**, 100030, https://doi.org/10.1016/j.geogeo.2022.100030

Gaggero, L., Marroni, M., Pandolfi, L. and Buzzi, L. 2009. Modeling the oceanic lithosphere obduction: constraints from the metamorphic sole of Mirdita ophiolites (northern Albania). *Ofioliti*, **34**, 17–42, https://www.ofioliti.it/index.php/ofioliti/article/view/376

Gansser, A. 1974. The ophiolitic mélange, a world-wide problem on Tethyan examples. *Eclogae Geologicae Helvetiae*, **67**, 479–507, https://doi.org/10.5169/seals-164302

Gawlick, H.-J. and Missoni, S. 2019. Middle–Late Jurassic sedimentary mélange formation related to ophiolite obduction in the Alpine–Carpathian–Dinaridic mountain range. *Gondwana Research*, **74**, 144–172, https://doi.org/10.1016/j.gr.2019.03.003

Gawlick, H.-J., Frisch, W. *et al.* 2008. Mirdita Zone ophiolites and associated sediments in Albania reveal Neotethys Ocean origin. *International Journal of Earth Sciences*, **97**, 865–881, https://doi.org/10.1007/s00531-007-0193-z

Gawlick, H.-J., Goričan, Š., Missoni, S., Dumitrica, P., Lein, R., Frisch, W. and Hoxha, L. 2016*a*. Middle and Upper Triassic radiolarite components from the Kcira–Dushi–Komani ophiolitic mélange and their provenance (Mirdita Zone, Albania). *Revue de Micropaléontologie*, **59**, 359–380, https://doi.org/10.1016/j.revmic.2016.03.002

Gawlick, H.-J., Missoni, S., Suzuki, H., Sudar, M., Lein, R. and Jovanović, D. 2016*b*. Triassic radiolarite and carbonate components from a Jurassic ophiolitic mélange (Dinaridic ophiolite belt). *Swiss Journal of Geosciences*, **109**, 473–494, https://doi.org/10.1007/s00015-016-0232-5

Gawlick, H.-J., Djerić, N., Missoni, S., Bragin, N.Y., Lein, R., Sudar, M. and Jovanović, D. 2017. Age and microfacies of oceanic Upper Triassic radiolarite components from the Middle Jurassic ophiolitic mélange in the Zlatibor Mountains (Inner Dinarides, Serbia) and their provenance. *Geologica Carpathica*, **68**, 350–365, https://doi.org/10.1515/geoca-2017-0024

Geshi, N., Umino, S., Kumagai, H., Sinton, J.M., White, S.M., Kisimoto, K. and Hilde, T.W. 2007. Discrete plumbing systems and heterogeneous magma sources of a 24 $km^3$ off-axis lava field on the western flank of East Pacific Rise, 14° S. *Earth and Planetary Science Letters*, **258**, 61–72, https://doi.org/10.1016/j.epsl.2007.03.019

Goričan, Š., Halamić, J., Grgasović, T. and Kolar-Jurkovšek, T. 2005. Stratigraphic evolution of Triassic arc–backarc system in northwestern Croatia. *Bulletin de la Société géologique de France*, **176**, 3–22, https://doi.org/10.2113/176.1.3

Goričan, Š., O'Dogherty, L., Baumgartner, P.O. and Carter, E.S. 2018. Mesozoic radiolarian biochronology – current status and future directions. *Revue de Micropaléontologie*, **61**, 165–189, https://doi.org/10.1016/j.revmic.2018.08.001

Haas, J., Mioč, P. *et al.* 2000. Complex structural pattern of the Alpine–Dinaridic–Pannonian triple junction. *International Journal of Earth Sciences*, **89**, 377–389, https://doi.org/10.1007/s005310000093

Haase, K.M. and Devey, C.W. 1996. Geochemistry of lavas from the Ahu and Tupa volcanic felds, Easter Hotspot, southeast Pacific: implications for magma genesis near a spreading axis. *Earth and Planetary Science Letters*, **137**, 129–143, https://doi.org/10.1016/0012-821X(95)00217-Z

Halamić, J. and Goričan, Š. 1995. Triassic radiolarites from Mts. Kalnik and Medvednica (northwestern Croatia). *Geologia Croatica*, **48**, 129–146, http://www.geologia-croatica.hr/index.php/GC/article/view/GC.1995.10

Halamić, J., Slovenec, D. and Kolar-Jurkovšek, T. 1998. Triassic pelagic limestones in pillow lavas in the Orešje Quarry near Gornja Bistra, Medvednica Mt. (northwest Croatia). *Geologia Croatica*, **51**, 33–45, http://www.geologia-croatica.hr/index.php/GC/article/view/GC.1998.06

Halamić, J., Goričan, Š., Slovenec, D. and Kolar-Jurkovšek, T. 1999. A Middle Jurassic radiolarite–clastic succession from the Medvednica Mt. (NW Croatia). *Geologia Croatica*, **52**, 29–57, http://www.geologia-croatica.hr/index.php/GC/article/view/GC.1999.03

Harangi, S., Szabó, C., Józsa, S., Szoldán, Z., Árva-Sós, E., Balla, M. and Kubovics, I. 1996. Mesozoic igneous suites in Hungary: implications for genesis and tectonic setting in the northwestern part of Tethys. *International Geological Review*, **38**, 336–360, https://doi.org/10.1080/00206819709465339

Karamata, S. 2006. The geological development of the Balkan Peninsula related to the approach, collision and compression of Gondwanan and Eurasian units. *Geological Society, London, Special Publications*, **260**, 155–178, https://doi.org/10.1144/GSL.SP.2006.260.01.07

Kellici, I., De Wever, P. and Kodra, A. 1994. Mesozoic radiolarians from different sections of the Mirdita nappe, Albania. Paleontology and stratigraphy. *Revue de Micropaléontologie*, **37**, 209–222.

Kiss, G., Molnár, F., Palinkaš, L., Kovács, S. and Hrvatović, H. 2012. Correlation of Triassic advanced rifting-related Neotethyan submarine basaltic volcanism of the Darnó Unit (NE-Hungary) with some Dinaridic and Hellenidic occurrences on the basis of volcanological, fluid–rock interaction, and geochemical characteristics. *International Journal of Earth Sciences*, **101**, 1503–1521, https://doi.org/10.1007/s00531-011-0706-7

Kozur, H.W. 2003. Integrated ammonoid, conodont and radiolarian zonation of the Triassic. *Hallesches Jahrbuch für Geowissenschaften*, **25**, 49–79.

Kukoč, D., Smirčić, D. *et al.* 2023. Biostratigraphy and facies description of Middle Triassic rift-related volcano-sedimentary successions on the junction of the southern Alps and the Dinarides (NW Croatia). *International Journal of Earth Sciences*, **112**, 1175–1201, https://doi.org/10.1007/s00531-023-02301-w

Lugović, B., Altherr, R., Raczek, I., Hofmann, A.W. and Majer, V. 1991. Geochemistry of peridotites and mafic igneous rocks from the Central Dinaric ophiolite belt, Yugoslavia. *Contributions to Mineralogy and Petrology*, **106**, 201–216, https://doi.org/10.1007/BF00306434

Lugović, B., Slovenec, D., Schuster, R., Schwarz, W.H. and Horvat, M. 2015. Petrology, geochemistry and tectono-magmatic affinity of gabbroic olistoliths from the ophiolite mélange in the NW Dinaric–Vardar ophiolite zone (Mts. Kalnik and Ivanščica, North Croatia). *Geologia Croatica*, **68**, 25–49, https://doi.org/10.4154/GC.2015.03

Lužar-Oberiter, B., Mikes, T., von Eynatten, H. and Babić, L. 2009. Ophiolitic detritus in Cretaceous clastic formations of the Dinarides (NW Croatia): evidence from Cr-spinel chemistry. *International Journal of Earth Sciences*, **98**, 1097–1108, https://doi.org/10.1007/s00531-008-0306-3

Lužar-Oberiter, B., Mikes, T., Dunkl, I., Babić, L. and von Eynatten, H. 2012. Provenance of Cretaceous synorogenic sediments from NW Dinarides (Croatia). *Swiss Journal of Geosciences*, **105**, 377–399, https://doi.org/10.1007/s00015-012-0107-3

Majer, V. 1993. Ophiolite complex of the Banija and Pokuplje region in Croatia and Pastirevo in northwestern Bosnia. *Acta Geologica*, **23**, 39–84 [in Croatian, with an English summary].

Marccuci, M., Kodra, A., Pirdeni, A. and Gjata, T. 1994. Radiolarian assemblages in the Triassic and Jurassic cherts of Albania. *Ofioliti*, **19**, 105–115.

Matsuda, T. and Isozaki, Y. 1991. Well-documented travel history of Mesozoic pelagic chert in Japan: from remote ocean to subduction zone. *Tectonics*, **10**, 475–499, https://doi.org/10.1029/90TC02134

McKenzie, D.P. and O'Nions, R.K. 1991. Partial melt distributions from inversion of rare earth element concentrations. *Journal of Petrology*, **32**, 1027–1091, https://doi.org/10.1093/petrology/32.5.1021

Mišur, I., Balen, D., Klötzli, U., Belak, M., Massonne, H.-J., Brlek, M. and Brčić, V. 2023. Petrochronological study of chloritoid schist from Medvednica Mountain (Zagorje Mid-Transdanubian Zone, Croatia). *Geologia Croatica*, **76**, 13–36, https://doi.org/10.4154/gc.2023.02

Morimoto, N. 1988. Nomenclature of pyroxenes. *Schweizerische Mineralogische und Petrographische Mitteilungen*, **68**, 95–111.

Neave, D.A. and Putirka, K.D. 2017. A new clinopyroxene–liquid barometer, and implications for magma storage pressures under Icelandic rift zones. *American Mineralogist*, **102**, 777–794, https://doi.org/10.2138/am-2017-5968

Nimis, P. 1999. Clinopyroxene geobarometry of magmatic rocks. Part 2: structural geobarometers for basic to acid, tholeiitic and mildly alkaline magmatic systems. *Contributions to Mineralogy and Petrology*, **135**, 62–74, https://doi.org/10.1007/s004100050498

Nimis, P. and Ulmer, P. 1998. Clinopyroxene geobarometry of magmatic rocks. Part 1: an expanded structural geobarometer for anhydrous and hydrous, basic and ultrabasic systems. *Contributions to Mineralogy and Petrology*, **133**, 122–135, https://doi.org/10.1007/s004100050442

Obradović, J. and Goričan, Š. 1988. Siliceous deposits in Yugoslavia: occurrences, types, and ages. *In:* Hein, J. and Obradović, J. (eds) *Siliceous Deposits of the Tethys and Pacific Regions*. Springer, New York, 51–64.

Ozsvárt, P. and Kovács, S. 2012. Revised Middle and Late Triassic radiolarian ages for ophiolite mélanges: implications for the geodynamic evolution of the northern part of the early Mesozoic Neotethyan subbasins. *Bulletin de la Société géologique de France*, **183**, 273–286, https://doi.org/10.2113/gssgfbull.183.4.273

Ozsvárt, P., Dosztály, L., Migiros, G., Tselepidis, V. and Kovács, S. 2012. New radiolarian biostratigraphic age constraints on Middle Triassic basalts and radiolarites from the Inner Hellenides (northern Pindos and Othris Mountains, northern Greece) and their implications for the geodynamic evolution of the early Mesozoic Neotethys. *International Journal of Earth Sciences*, **101**, 1487–1501, https://doi.org/10.1007/s00531-010-0628-9

Pamić, J., Tomljenović, B. and Balen, D. 2002. Geodynamic and petrogenetic evolution of Alpine ophiolites from the central and NW Dinarides: an overview. *Lithos*, **65**, 113–142, https://doi.org/10.1016/S0024-4937(02)00162-7

Pearce, J.A. 1975. Basalt geochemistry used to investigate past tectonic environments on Cyprus. *Tectonophysics*, **25**, 41–67, https://doi.org/10.1016/0040-1951(75)90010-4

Pearce, J.A. 1983. Role of the sub-continental lithosphere in magma genesis at active continental margins. *In:* Hawkesworth, C.J. and Norry, M.J. (eds) *Continental Basalts and Mantle Xenoliths*. Shiva, Nantwich, 230–249.

Polat, A. and Hofmann, A.W. 2003. Alteration and geochemical patterns in the 3.7–3.8 Ga Isua greenstone belt, West Greenland. *Precambrian Research*, **126**, 197–218, https://doi.org/10.1016/S0301-9268(03)00095-0

Polat, A., Hofmann, A.W. and Rosing, M.T. 2002. Boninite-like volcanic rocks in the 3.7–3.8 Ga Isua greenstone belt, West Greenland: geochemical evidence for intra-oceanic subduction zone processes in the early Earth. *Chemical Geology*, **184**, 231–254, https://doi.org/10.1016/S0009-2541(01)00363-1

Prela, M., Chiari, M. and Marcucci, M. 2000. Jurassic radiolarian biostratigraphy of the sedimentary cover of ophiolites in the Mirdita Area, Albania: new data. *Ofioliti*, **25**, 55–62, https://www.ofioliti.it/index.php/ofioliti/article/view/114

Prelević, D., Wehrheim, S. *et al.* 2017. The Late Cretaceous Klepa basalts in Macedonia (FYROM)—constraints on the final stage of Tethys closure in the Balkans. *Terra Nova*, **29**, 145–153, https://doi.org/10.1111/ter.12264

Robertson, A.H.F. 2012. Late Palaeozoic–Cenozoic tectonic development of Greece and Albania in the context of alternative reconstructions of Tethys in the Eastern Mediterranean region. *International Geology Review*, **54**, 373–454, https://doi.org/10.1080/00206814.2010.543791

Robertson, A.H.F. and Karamata, S. 1994. The role of the subduction–accretion processes in the tectonic evolution of the Mesozoic Tethys in Serbia. *Tectonophysics*, **234**, 73–94, https://doi.org/10.1016/0040-1951(94)90205-4

Robertson, A.H.F. and Shallo, M. 2000. Mesozoic–Tertiary tectonic evolution of Albania in its regional Eastern Mediterranean context. *Tectonophysics*, **316**, 197–254, https://doi.org/10.1016/S0040-1951(99)00262-0

Robertson, A.H.F., Clift, P.D., Degnan, P.J. and Jones, G. 1991. Palaeogeographic and palaeotectonic evolution of the Eastern Mediterranean Neotethys. *Palaeogeography, Palaeoclimatology, Palaeoecology*, **87**, 289–343, https://doi.org/10.1016/0031-0182(91)90140-M

Robertson, A.H.F., Karamata, S. and Šarić, K. 2009. Overview of ophiolites and related units in the Late Palaeozoic–Early Cenozoic magmatic and tectonic development of Tethys in the northern part of the Balkan region. *Lithos*, **108**, 1–36, https://doi.org/10.1016/j.lithos.2008.09.007

Saccani, E. and Photiades, A. 2005. Petrogenesis and tectonomagmatic significance of volcanic and subvolcanic rocks in the Albanide–Hellenide ophiolitic mélanges. *Island Arc*, **14**, 494–516, https://doi.org/10.1111/j.1440-1738.2005.00480.x

Saccani, E. and Tassinari, R. 2015. The role of MORB and SSZ magma-types in the formation of Jurassic ultramafic cumulates in the Mirdita ophiolites (Albania) as deduced from chromian spinel and olivine chemistry. *Ofioliti*, **40**, 37–56, https://doi.org/10.4454/ofioliti.v40i1.434

Saccani, E., Beccaluva, L., Photiades, A. and Zeda, O. 2011. Petrogenesis and tectono-magmatic, significance of basalts and mantle peridotites from the Albanian–Greek ophiolites and sub-ophiolitic mélanges. New constraints for the Triassic–Jurassic evolution of the Neo-Tethys in the Dinaride sector. *Lithos*, **124**, 227–242, https://doi.org/10.1016/j.lithos.2010.10.009

Schmid, S.M., Bernoulli, D. *et al.* 2008. The Alpine–Carpathian–Dinaridic orogenic system: correlation and evolution of tectonic units. *Swiss Journal of Geosciences*, **101**, 139–183, https://doi.org/10.1007/s00015-008-1247-3

Schmid, S.M., Fügenschuh, B. *et al.* 2020. Tectonic units of the Alpine collision zone between Eastern Alps and western Turkey. *Gondwana Research*, **78**, 308–374, https://doi.org/10.1016/j.gr.2019.07.005

Šegvić, B., Kukoč, D. *et al.* 2014. New record of Middle Jurassic radiolarians and evidence of Neotethyan dynamics documented in a mélange from the Central Dinaridic Ophiolite Belt (CDOB, NE Bosnia and Herzegovina). *Ofioliti*, **39**, 33–43, https://doi.org/10.4454/ofioliti.v39i1.427

Šegvić, B., Slovenec, D., Schuster, R., Babajić, E., Badurina, L. and Lugović, B. 2020. Sm–Nd geochronology and petrologic investigation of a sub-ophiolite metamorphic sole from the Dinarides (Krivaja–Konjuh ophiolite complex, Bosnia and Herzegovina). *Geologia Croatica*, **73**, 1–11, https://doi.org/10.4154/gc.2020.09

Šegvić, B., Slovenec, D. and Badurina, L. 2023. Major and rare earth element mineral chemistry of low-grade assemblages inform dynamics of hydrothermal ocean-floor metamorphism in the Dinaridic Neotethys. *Geological Magazine*, **160**, 444–470, https://doi.org/10.1017/S0016756822001030

Shervais, J.W. 1982. Ti–V plots and petrogenesis of modern and ophiolitic lavas. *Earth and Planetary Science Letters*, **59**, 101–118, https://doi.org/10.1016/0012-821X(82)90120-0

Šimunić, A. and Šimunić, A. 1979. Petrografski sastav i geneza trijaskih naslaga Ivanščice, Kalnika i Ravne gore (Hrvatsko zagorje) [Petrographic composition and genesis of Triassic deposits of Ivanščica, Kalnik and Ravna gora Mountain]. *Geološki vjesnik*, **32**, 243–253 [in Croatian with English summary].

Šimunić, A. and Šimunić, A. 1997. Triassic deposits of Hrvatsko Zagorje. *Geologia Croatica*, **50**, 243–250, http://www.geologia-croatica.hr/index.php/GC/article/view/GC.1997.32

Šimunić, A., Pikija, M., Hećimović, I. and Šimunić, A. 1981. *Osnovna geološka karta SFRJ 1:100,000. Tumač za list Varaždin L 33-69 [Basic Geological Map of SFRY 1:10000, Explanatory Notes for Sheet Varaždin L 33-69]*. Savezni geološki zavod, Beograd [in Croatian].

Šimunić, A., Pikija, M. and Hećimović, I. 1982. *Osnovna geološka karta SFRJ 1:100000, list Varaždin L33-69 [Basic Geological Map of SFRY 1:100000. Varaždin Sheet]*. Savezni geološki zavod, Beograd [in Croatian].

Slovenec, D. and Lugović, B. 2009. Geochemistry and tectono-magmatic affinity of extrusive and dyke rocks from the ophiolite mélange in the SW Zagorje–Mid-Transdanubian Zone (Mt. Medvednica, Croatia). *Ofioliti*, **34**, 63–80, https://www.ofioliti.it/index.php/ofioliti/article/view/378

Slovenec, D. and Lugović, B. 2012. Evidence of the spreading culmination in the Eastern Tethyan Repno oceanic domain assessed by the petrology and geochemistry of N-MORB extrusive rocks from the Mt. Medvednica ophiolite mélange (NW Croatia). *Geologia Croatica*, **65**, 435–446, https://doi.org/10.4154/GC.2012.32

Slovenec, D. and Pamić, J. 2002. The Vardar Zone ophiolites of Mt. Medvednica located along the Zagreb–Zemplin line (NW Croatia). *Geologica Carpathica*, **53**, 53–59.

Slovenec, D., Lugović, B. and Vlahović, I. 2010. Geochemistry, petrology and tectonomagmatic significance of basaltic rocks from the ophiolite mélange at the NW External–Internal Dinarides junction (Croatia). *Geologica Carpathica*, **61**, 273–294, https://doi.org/10.2478/v10096-010-0016-1

Slovenec, D., Lugović, B., Meyer, H.-P. and Garapić-Šiftar, G. 2011. A tectono-magmatic correlation of basaltic rocks from ophiolite mélanges at the north-eastern tip of the Sava-Vardar suture Zone, northern Croatia, constrained by geochemistry and petrology. *Ofioliti*, **36**, 77–100, https://www.ofioliti.it/index.php/ofioliti/article/view/395

Slovenec, D., Šegvić, B., Halamić, J., Goričan, Š. and Zanoni, G. 2020. An ensialic volcanic arc along the northwestern edge of Palaeotethys – insights from the Mid-Triassic volcanosedimentary succession of Ivanščica Mt. (northwestern Croatia). *Geological Journal*, **55**, 4324–4351, https://doi.org/10.1002/gj.3664

Slovenec, D., Horvat, M. *et al.* 2023. On the evolution of Middle Triassic passive margins of the Greater Adria Plate: inferences from the study of calc-alkaline and shoshonitic tuffs from NW Croatia. *Ofioliti*, **58**, 31–46, https://doi.org/10.4454/ofioliti.v48i1.560

Spahić, D. and Gaudenyi, T. 2020. Reconsidering Paleozoic differences between the Jadar block and the Drina-Ivanjica unit. *Geoloski anali Balkanskoga Poluostrva*, **81**, 1–9, https://doi.org/10.2298/GABP191014002S

Stanković, N., Gerya, T., Cvetkov, V. and Cvetković, V. 2023. Did the Western and the Eastern Vardar ophiolites originate through a single intra-oceanic subduction? Insight from numerical modelling. *Gondwana Research*, **124**, 124–140, https://doi.org/10.1016/j.gr.2023.07.005

Staudigel, H., Plank, T., White, B. and Schmincke, H.U. 1996. Geochemical fluxes during sea floor alteration of the basaltic upper oceanic crust: DSDP Sites 417 and 418. *Geophysical Monograph Series*, **96**, 19–38, https://doi.org/10.1029/GM096p0019

Stevens, R.E. 1944. Composition of some chromites of the Western Hemisphere. *American Mineralogist*, **29**, 1–34.

Stockar, R., Dumitrica, P. and Baumgartner, P.O. 2012. Early Ladinian radiolarian fauna from the Monte San Giorgio (southern Alps, Switzerland): systematics, biostratigraphy and paleo(bio)geographic implications. *Rivista Italiana di Paleontologia e Stratigrafia*, **118**, 375–437, https://doi.org/10.13130/2039-4942/6012

Šuica, S., Lugović, B. and Kukoč, D. 2018. Tectono-magmatic significance of the pillow basalts from the ophiolitic mélange of the Dinarides. *Ofioliti*, **43**, 85–101, https://www.ofioliti.it/index.php/ofioliti/article/view/506

Sun, S.S. and McDonough, W.F. 1989. Chemical and isotopic systematics of oceanic basalts: implications for mantle composition and processes. *Geological Society, London, Special Publications*, **42**, 313–345, https://doi.org/10.1144/GSL.SP.1989.042.01.19

Taylor, S.R. and McLennan, S.M. 1985. *The Continental Crust: its Composition and Evolution*. Blackwell, Oxford.

Tekin, U.K. 1999. Biostratigraphy and systematics of Late Middle to Late Triassic radiolarians from the Taurus Mountains and Ankara region, Turkey. *Geologisch-Paläontologische Mitteilungen Innsbruck*, **5**, 1–296.

Tomljenović, B., Csontos, L., Márton, E. and Márton, P. 2008. Tectonic evolution of the northwestern Internal Dinarides as constrained by structures and rotation of Medvednica Mountains, North Croatia. *Geological Society, London, Special Publications*, **298**, 145–167, https://doi.org/10.1144/SP298.8

Tracy, R.J. and Robinson, P. 1977. Zoned titanium augite in alkali olivine basalt from Tahiti and the nature of titanium substitutions in augite. *American Mineralogist*, **62**, 634–645.

Trubelja, F., Marching, V., Burgath, K.-P. and Vujović, Ž. 1995. Origin of the Jurassic Tethyan ophiolites in Bosnia: a geochemical approach to tectonic setting. *Geologia Croatica*, **48**, 49–66, http://www.geologia-croatica.hr/index.php/GC/article/view/GC.1995.05

van Gelder, I.E., Matenco, L. *et al.* 2015. The tectonic evolution of a critical segment of the Dinarides–Alps connection: kinematic and geochronological inferences from the Medvednica Mountains, NE Croatia. *Tectonics*, **34**, 1952–1978, https://doi.org/10.1002/2015TC003937

van Hinsbergen, D.J.J., Torsvik, T.H. *et al.* 2020. Orogenic architecture of the Mediterranean region and kinematic reconstruction of its tectonic evolution since the Triassic. *Gondwana Research*, **81**, 79–229, https://doi.org/10.1016/j.gr.2019.07.009

Vishnevskaya, V.S., Djerić, N. and Zakariadze, G.S. 2009. New data on Mesozoic radiolaria of Serbia and Bosnia, and implications for the age and evolution of oceanic volcanic rocks in the Central and Northern Balkans. *Lithos*, **108**, 72–105, https://doi.org/10.1016/j.lithos.2008.10.015

Vukovski, M., Kukoč, D., Grgasović, T., Fuček, L. and Slovenec, D. 2023. Evolution of eastern passive margin of Adria recorded in shallow- to deep-water successions of the transition zone between the Alps and the Dinarides. *Facies*, **69**, 18, https://doi.org/10.1007/s10347-023-00674-7

Wakabayashi, J. 2015. Anatomy of a subduction complex: architecture of the Franciscan Complex, California, at multiple length and time scales. *International Geology Review*, **57**, 669–746, https://doi.org/10.1080/00206814.2014.998728

Whitney, D.L. and Evans, B.W. 2010. Abbreviations for names of rock-forming minerals. *American Mineralogist*, **95**, 185–187, https://doi.org/10.2138/am.2010.3371

Winchester, J.A. and Floyd, P.A. 1977. Geochemical discrimination of different magma series and their differentiation products using immobile elements. *Chemical Geology*, **20**, 325–343, https://doi.org/10.1016/0009-2541(77)90057-2

Wood, D.A. 1980. The application of a Th–Hf–Ta diagram to problems of tectonomagmatic classification and establishing the nature of crustal contamination of basaltic lavas of the British Tertiary volcanic province. *Earth and Planetary Science Letters*, **50**, 11–30, https://doi.org/10.1016/0012-821X(80)90116-8

# 5. UNRAVELLING THE TECTONIC EVOLUTION OF THE DINARIDES—ALPS—PANNONIAN BASIN TRANSITION ZONE: INSIGHTS FROM STRUCTURAL ANALYSIS AND LOW-TEMPERATURE THERMOCHRONOLOGY FROM IVANŠČICA MT., NW CROATIA

By

**Matija Vukovski**, Marko Špelić, Duje Kukoč, Tamara Troskot-Čorbić, Tonći Grgasović, Damir Slovenec & Bruno Tomljenović

*Accepted for publication in Swiss Journal of Geosciences*

*DOI: https://doi.org/10.1186/s00015-024-00464-5*

Matija Vukovski et al. *Swiss Journal of Geosciences* (2024) 117:16
https://doi.org/10.1186/s00015-024-00464-5

Swiss Journal of Geosciences

RESEARCH

Open Access

# Unravelling the tectonic evolution of the Dinarides—Alps—Pannonian Basin transition zone: insights from structural analysis and low-temperature thermochronology from Ivanščica Mt., NW Croatia

Matija Vukovski[1*], Marko Špelić[1], Duje Kukoč[1], Tamara Troskot-Čorbić[2], Tonći Grgasović[1], Damir Slovenec[1] and Bruno Tomljenović[3]

**Abstract**

A comprehensive study, including geological mapping, structural and thermochronological analysis, has been carried out on Ivanščica Mountain (NW Croatia), with the aim to reconstruct the tectonic history of the Dinarides, Southern/Eastern Alps and Pannonian Basin transitional zone. Implementation of structural and thermochronological methods enabled a subdivision of Ivanščica Mt. into two structural domains (from bottom to top): Ivanščica Parautochthon and Ivanščica Imbricate Fan and Cenozoic sedimentary cover. In addition, a sequence of deformational events in tectonic history of this transitional zone is proposed, comprising three extensional and four contractional events starting from Middle Triassic until present times. The two oldest deformational events indicate Middle Triassic (D1) and Early Jurassic (D2) extensional pulses and only occur in volcano-sedimentary successions of the Ivanščica Mt. The oldest contractional event (D3) is related to the obduction of a Neotethyan ophiolitic mélange over an Upper Triassic to Lower Cretaceous succession of the eastern margin of the Adriatic microplate, which resulted in thermal overprint of the Ivanščica Imbricate Fan structural domain in Berriasian—Valanginian times (~ 140 Ma). This event was soon followed by a second contractional event (D4), which resulted in thrusting and imbrication of the Adriatic passive margin successions together with previously emplaced ophiolitic mélange, thermal overprint of the footwall successions, fast exhumation and erosion. Apatite fission track data together with syn-tectonic deposits indicate an Hauterivian to Albian age of this D4 event (~ 133–100 Ma). These Mesozoic structures were dextrally rotated in post-Oligocene times and brought from the initially typically Dinaridic SE striking and SW verging structures to the recent SW striking and NW verging structures. The following extensional event (D5) is associated with the formation of SE striking and mostly NE dipping normal listric faults, and ENE striking dextral faults accommodating top-NE extension in the Pannonian Basin. Deformations were coupled with hanging wall sedimentation of Ottnangian to middle Badenian (middle Burdigalian to upper Langhian; ~ 18–14 Ma) syn-rift deposit as observed from the reflection seismic and well data. A short-lasting contraction (D6) was registered in the late Sarmatian (late Serravallian; ~ 12 Ma). The youngest documented deformational event (D7) resulted in reactivation of ENE striking dextral faults, formation of SE

Handling editor: Stefan Schmid

*Correspondence:
Matija Vukovski
mvukovski@hgi-cgs.hr
Full list of author information is available at the end of the article

striking dextral faults as well as the formation of E to ENE trending folds and reverse faults. This event corresponds to late Pannonian (late Messinian; ~ 6 Ma) to Present NNW-SSE contraction driven by the indentation and counterclockwise rotation of Adriatic microplate. Recognized tectonic events and their timings indicate that Ivanščica was mainly affected by deformational phases related to the Mesozoic evolution of the Neotethys Ocean as well as Cenozoic opening and inversion of the Pannonian Basin. Therefore, the Mesozoic tectono-sedimentary evolution of Ivanščica Mountain proves the paleogeographic affiliation of its non-ophiolitic Mesozoic structural-stratigraphic entities to the Pre-Karst unit of the Dinarides.

**Keywords** Northern Neotethys, Adriatic passive margin, Ophiolite obduction, Nappe stacking, Imbricate fan, Structural inheritance, Tectonic inversion, Pre-Karst unit

## 1 Introduction

Synchronous mountain building of neighbouring orogens often results in complex structural architectures and overprinting relationships. Such complex relationships can only be resolved by comprehensive studies that integrate lithostratigraphic, structural and thermochronological data obtained at local to regional scales of observations. In particular, such an approach is required in cases when both orogens are affected by post-orogenic extensional and/or strike-slip tectonics, a geodynamic scenario known from the past and at present in almost all peri-Mediterranean orogens (e.g., Meulenkamp et al., 1988; Jolivet & Faccenna, 2000; Faccenna et al., 2004, 2013; Kissling et al., 2006). This scenario, which commonly includes post-orogenic local- to regional-scale translations and rotations of differently sized tectonic blocks dismembered from previously formed collisional nappe stacks, is also known from the Dinarides—Alps—Pannonian Basin transitional zone (Fig. 1; e.g., Placer, 1999a; Haas et al., 2000; Tomljenović et al., 2008; van Gelder et al., 2015). This area records complex tectonic histories in the orogenic build-up of the Southern and Eastern Alps as well as the Dinarides, followed by several phases of extension and contraction in the tectonic evolution of the SW margin of the Pannonian Basin (e.g., Fodor et al., 1998; Vrabec & Fodor, 2006; Tomljenović & Csontos, 2001; van Gelder et al., 2015; Fodor et al., 2021). Here, Mesozoic formations of both Alps and Dinarides preserve records of geodynamic processes that resulted with opening and closure of the northern branch of the Neotethys Ocean (e.g., Pamić et al., 1998; Pamić, 2002; Schmid et al., 2008; 2020; Ustaszewski et al., 2010; the Balkan Neotethys sensu van Hinsbergen et al., 2020). In addition, the Alps record a separate and younger collisional event related to the closure of the Alpine Tethys Ocean (e.g., Neubauer et al., 1999; Willingshofer et al., 1999a; Schmid et al., 2008; 2020; van Hinsbergen et al., 2020). Both oceanic realms contemporaneously existed during a part of Mesozoic times, separating the Adria microplate from Eurasia (e.g., van Hinsbergen et al., 2020). However, during the time of their closure, which differs for each of these oceanic realms, the Adriatic microplate was in a different tectonic position with respect to the European plate: lower plate in the Dinarides and upper plate in the Alps (e.g., Doglioni et al., 1999; Schmid et al., 2008, 2020).

Due to the complex Mesozoic and Cenozoic geodynamics at the Dinarides-Southern/Eastern Alps-Pannonian Basin transitional zone (Fig. 1a, b), a detailed reconstruction of the tectonic and depositional history, in its part in the northern Croatia, is still lacking. Among several inselbergs in this area (Fig. 1c), Medvednica Mt. is the most comprehensively studied so far, providing a large data set on different topics regarding Mesozoic stratigraphy (e.g., Halamić et al., 1999, 2005; Babić et al., 2002, with references therein), metamorphic and igneous petrology (e.g., Belak & Tibljaš, 1998; Slovenec & Pamić, 2002; Lugović et al., 2007; Judik et al., 2008; Belak et al., 2022; Mišur et al., 2023;), paleomagnetism, structural architecture and tectonics (e.g., Tomljenović et al., 2008; van Gelder et al., 2015). The results of most of these studies, in

(See figure on next page.)

**Fig. 1** **a** Topographic map of the northern Adriatic realm. Note the red polygon representing outlines of Ivanščica Mt. **b** Tectonic map after Schmid et al. (2020) showing constituent tectonic units of the Dinarides and the Alps. Ivanščica Mt. (marked with yellow line) occupies position at the junction of the Western Vardar ophiolitic unit of the Dinarides and South Alpine unit of the Alps in the southwestern part of the Pannonian Basin (white outlines). PFS—Periadriatic Fault System. Location of figure is shown in **a**. **c** Geological map of the Ivanščica Mt. and wider surrounding area in the Dinarides—Alps—Pannonian Basin transitional zone (simplified and modified after Basic Geological Maps of former Yugoslavia on the 1:100,000 scale, sheets Celje (Buser, 1977), Rogatec (Aničić & Juriša, 1984), Varaždin (Šimunić et al., 1982), Novo Mesto (Pleničar et al., 1975), Zagreb (Šikić et al., 1977) and Ivanić (Basch, 1981)). Location of figure is shown in **b**

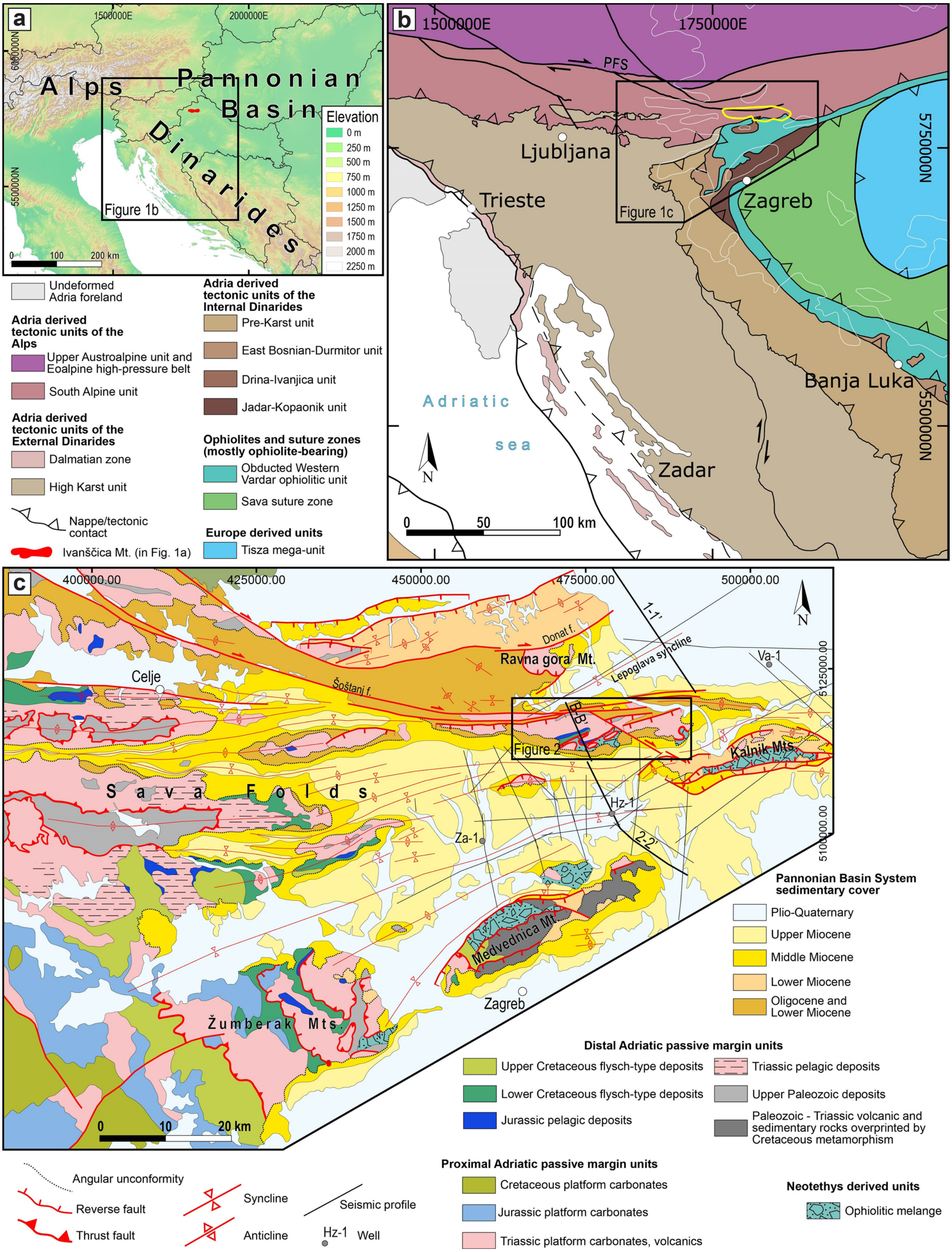


**Fig. 1** (See legend on previous page.)

combination with data from the Basic Geological Map of Yugoslavia, sheet Rogatec (Aničić & Juriša, 1984) and sheet Varaždin (Šimunić et al., 1982), were so far used for the correlation of pre-Neogene tectonic units in this transitional zone, only exposed in inselbergs, with corresponding tectonic units defined within a much wider surrounding area (e.g., Haas et al., 2000; van Gelder et al., 2015) and across the entire Alpine-Carpathian-Dinaridic-Hellenic orogenic system (e.g., Schmid et al., 2008, 2020; van Hinsbergen et al., 2020). Compared with the neighbouring Medvednica Mt., modern data on the geology of the Ivanščica Mt. were relatively scarce (Babić et al., 2002; Goričan et al., 2005; Lužar-Oberiter et al., 2009, 2012), until recently when a series of studies were released by the 'GOST' project (https://projectgost.wordpress.com). These studies provide new data set on stratigraphy (Slovenec et al., 2020; Kukoč et al., 2023, 2024), petrology (Slovenec & Šegvić, 2024; Slovenec et al., 2023; Šegvić et al., 2023) and lithostratigraphy of the Adriatic passive margin successions (Vukovski et al., 2023), tectonically assembled into the structural architecture of Ivanščica Mt.

Being a supplement to published studies of the GOST project, this paper aims to present new and more detailed data on the spatial arrangement, kinematics and age of deformational structures in Mesozoic and Cenozoic rocks of Ivanščica Mt. and neighbouring area. These data were obtained by a multi-scale structural analysis, including geological mapping, interpretation of reflection seismic sections, vitrinite reflectance and apatite fission track measurements. After a short overview on geological and structural setting of Ivanščica Mt. based on previously published data, this paper presents new data on the structural architecture and low-temperature thermochronology of the study area.

These data are then used to propose a sequence of deformational events in the study area. The presented deformational sequence is correlated with deformational events revealed in neighbouring areas of the Dinarides, Southern and Eastern Alps and SW Pannonian Basin. Obtained deformational events are discussed in the context of tectonic evolution of the region, starting from the Middle Triassic until present. Finally, we propose a new correlation between the established tectonic units of Ivanščica Mt. with those known from the Internal Dinarides.

## 2 Geological setting of Ivanščica Mountain

Ivanščica Mt. is built by upper Paleozoic and Mesozoic sedimentary successions belonging to the northern Gondwana margin and later to the Adriatic margin, a Neotethyan ophiolitic mélange and an uppermost Oligocene to Quaternary sedimentary cover (Figs. 2, 3; Šimunić et al., 1982; Aničić & Juriša, 1984).

### 2.1 Lithostratigraphic characteristics of Paleozoic and Mesozoic rock units

The oldest rocks on Ivanščica Mt. are Permian brown–red conglomerates, sandstones and black shales conformably overlain by Lower Triassic clastic deposits, including sporadic1-2 m thick dolomite layer along the contact (Šimunić et al., 1982; Šimunić & Šimunić, 1997). Lower Triassic sediments consist of micaceous sandstone, mica siltstone, shale and marl in the lower part and dark-grey, tabular, thin-bedded limestone in the upper part (Šimunić & Šimunić, 1997). Paleozoic and Lower Triassic deposits have spatially limited exposure on the northern slopes of the mountain. These deposits originated from a shallow-marine environment (Šimunić et al., 1982).

The largest part of the mountain is built up of several hundred meters thick Middle Triassic deposits, predominantly shallow-marine dolomite and limestone (Fig. 2; Šimunić et al., 1982). Pelagic successions consisting of upper Anisian to Ladinian pelagic limestone and radiolarian chert are intercalated with basic to acidic volcanic and volcaniclastic lithologies (Goričan et al., 2005; Slovenec et al., 2020, 2023; Kukoč et al., 2023; Smirčić et al., 2024). These pelagic successions are several tens of meters thick, tectonically deformed and their contacts with the underlying and overlying formations are rarely exposed. Deep-marine basins formed during this period were relatively short-lived and carbonate platform sedimentation was reestablished in the Late Ladinian (Goričan et al., 2005). Upper Triassic sediments of Ivanščica Mt. are exclusively shallow-marine and consist of several hundred meters thick series of dolomite and limestone (Šimunić et al., 1982; Šimunić & Šimunić, 1997). These are the equivalent of the Hauptdolomit and Dachstein Limestone found in the Alps (Vukovski et al., 2023). Lower Jurassic to Lower Cretaceous deposits are exposed in the central part of Ivanščica Mt. The successions composed of these deposits differ in the southern and northern parts of central Ivanščica Mt. (Fig. 2). In the northern part, shallow-marine Lower Jurassic limestone conformably overlies Upper Triassic carbonates and is in turn overlain by Middle Jurassic pelagic limestone (Fig. 3; Vukovski et al., 2023). In contrast, in the southern part, Upper Triassic deposits are overlain by Lower Jurassic thick pelagic series consisting of pelagic limestone, carbonate breccia, marl and calcarenite (Fig. 3; Babić, 1974; Vukovski et al., 2023). Middle to Upper Jurassic radiolarian cherts are recorded in both areas, however, their contact with underling deposits and complete thickness is not known. In both areas, radiolarian cherts conformably pass up-section into Tithonian to Valanginian

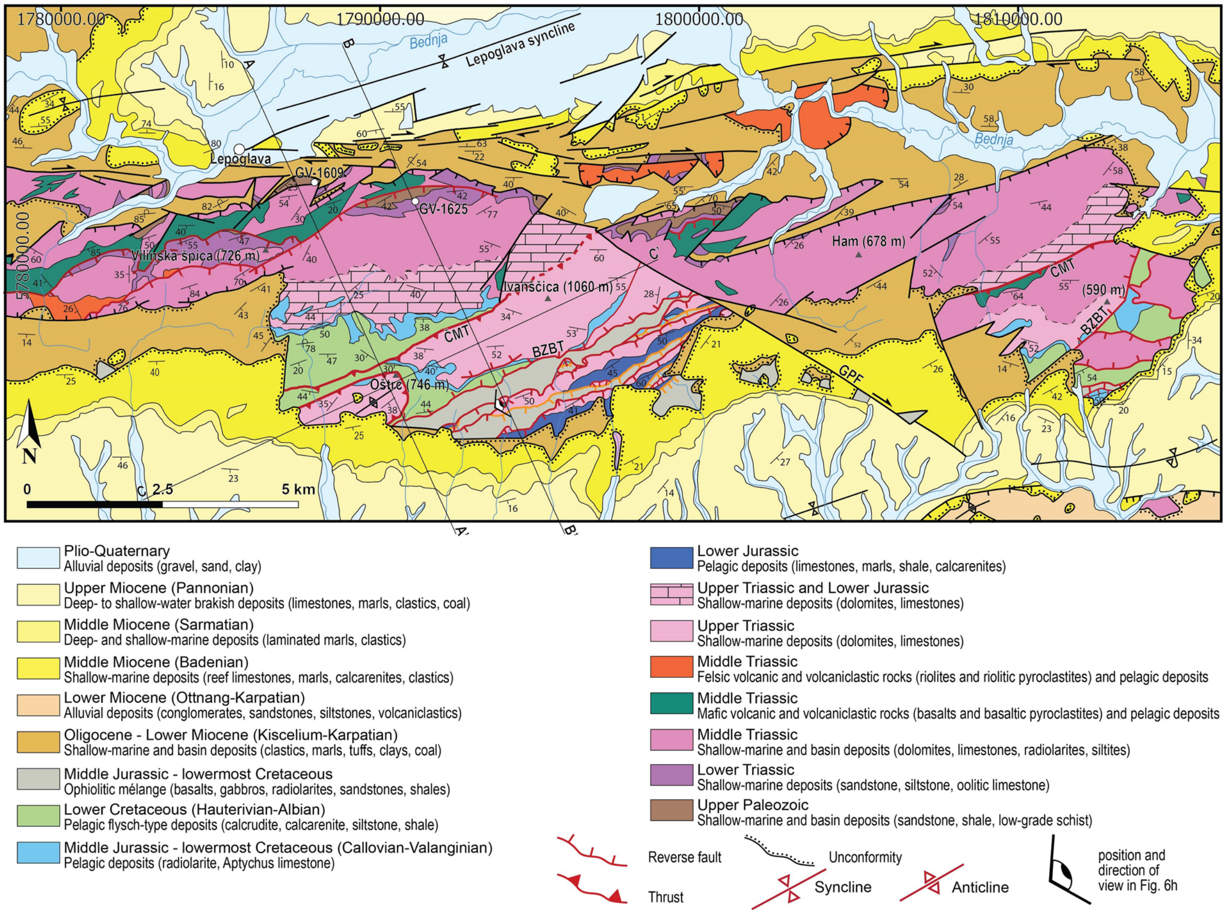


**Fig. 2** Geological map of Ivanščica Mt. compiled from Šimunić et al. (1982) and the results of this study. The map shows the locations of cross-sections **A**-**A**′; **B**-**B**′ and **C**–**C**′ (shown in Fig. 5) and sample locations used for apatite fission track dating. The location of the figure is shown in Fig. 1c. For colour coding of the tectonic features, please refer to Fig. 3. *ČMT* Črne Mlake thrust, *BZBT* Babin Zub back-thrust, *GPF* Gotalovec-Prigorec fault

pelagic Aptychus limestone with several beds of calcarenites sporadically occurring at the contact as recorded in the southern part of central Ivanščica (Fig. 3; Babić & Zupanič, 1973; Vukovski et al., 2023). The youngest Mesozoic deposits are mixed carbonate-siliciclastic turbidites of the Hauterivian to Albian Oštrc Formation (Zupanič et al., 1981; Lužar-Oberiter et al., 2009, 2012), which overly the Aptychus limestone. On the southern slopes of Ivanščica Mt., in its central and eastern parts, an ophiolitic mélange is widely exposed, named as the Repno complex (Fig. 2; Babić & Zupanič, 1978; Babić et al., 2002). This ophiolitic mélange is composed of centimeter to hundred meters sized blocks of sandstone, chert, basalt and gabbro chaotically embedded within a shaly-silty matrix (Babić et al., 2002; Slovenec et al., 2011; Kukoč et al., 2024). The age of the blocks varies from late Anisian to late Oxfordian (Slovenec et al., 2011; Kukoč et al., 2024) while the ages derived from palynomorphs found in the matrix ranges from Hettangian to Bajocian (Babić et al., 2002).

Permian to Middle Triassic deposits were mostly deposited in the shallow-marine depositional environments along the northern Gondwana margin. Middle Triassic successions reflect a period of intense tectonic activity related to the continental rifting and breakup of Gondwana, which resulted in the opening of the Neotethys Ocean and formation of the Adriatic passive margin with horst-and-graben depositional environments (Goričan et al., 2005; Kukoč et al., 2023). Upper Triassic to Lower Cretaceous sedimentary successions of Ivanščica Mt. are interpreted as deposited on the eastern passive margin of the Adria microplate (Lužar-Oberiter et al., 2012; Vukovski et al., 2023), which was facing the evolving Neotethys Ocean from the Middle Triassic until the ophiolite obduction in latest Jurassic-earliest Cretaceous (Schmid et al., 2008, 2020). Sedimentation on the margin reflected regional tectonic activity. Resedimented shallow-marine material was likely supplied from the adjacent Adriatic Carbonate Platform (Vukovski et al., 2023). Hauterivian to Albian turbidites of the Oštrc Fm. have been interpreted as deposited in a clastic wedge in front of the advancing nappes carrying the Neotethys ophiolites (Lužar-Oberiter et al., 2009, 2012). The ophiolitic mélange is interpreted to have formed during the Middle Jurassic intra-oceanic subduction in the northern branch of the Neotethys Ocean (Western Vardar ophiolitic unit sensu Schmid et al., 2020) and subsequent Late Jurassic to earliest Cretaceous obduction of ophiolites of this oceanic realm on the eastern Adriatic margin (Babić et al., 2002; Kukoč et al., 2024).

### 2.2 Lithostratigraphic characteristics of Cenozoic rock units

The oldest Cenozoic deposits on Ivanščica Mt. comprise upper Egerian (lower Aquitanian) clastic deposits with coal seams (Fig. 3; Šimunić et al., 1982). On the southern slopes of the mountain, these deposits lay unconformably over different Mesozoic formations, locally also in tectonic contact with underlying Mesozoic formations (Fig. 2). On the northern slopes, upper Egerian (lower Aquitanian) clastic deposits are found in tectonic contact and steeply dip underneath the Mesozoic formations (Figs. 2, 5; Šimunić et al., 1982). In the neighboring area, only a few kilometers to the NW, complete Oligocene to Lower Miocene succession of dominantly marine clastic deposits have been described (Aničić & Juriša, 1984; Avanić et al., 2021). This around two kilometers thick Oligocene to Lower Miocene succession is interpreted as deposited within the so-called Hrvatsko Zagorje Basin (Fig. 3), a marginal basin of the Central Paratethys Sea (Avanić et al., 2021). The southern margin of the Hrvatsko Zagorje Basin is interpreted to be located along the present-day southern foothills of Ivanščica Mt. (Pavelić & Kovačić, 2018). Further to the south, the deposition of Cenozoic rocks commenced significantly later, in the Ottnangian (middle to late Burdigalian) or locally even Badenian (Langhian and early Serravallian; Pavelić & Kovačić, 2018). The deposition of Ottnangian to middle Badenian (middle to upper Burdigalian to upper Langhian) alluvial to marine succession with volcaniclastics marks the syn-rift period in the evolution of the newly formed so-called North Croatian Basin (Fig. 3; Pavelić, 2001; Pavelić & Kovačić, 2018). Further continuation of extension and accompanying transgression resulted in the unification of the Hrvatsko Zagorje and North Croatian basins during the early to middle Badenian (Langhian). Since then, both areas represent a single basin with a uniform lithostratigraphy (Fig. 3), occupying the south-western position in the Pannonian Basin (Pavelić & Kovačić, 2018). Middle Badenian (late Langhian) sediments are predominantly characterised by widespread sedimentation of marls and limestones (Pavelić & Kovačić, 2018). Regional late Badenian (early Serravallian) transgression and cessation of volcanic activity mark the end of the rifting stage and the onset of post-rift thermal subsidence (Pavelić & Kovačić, 2018). Sarmatian (late Serravallian) and early Pannonian (early Tortonian) sediments are characterized by marine to brackish marl and limestone. During the Late Miocene and Pliocene, the brackish lake was continuously in-filled by a turbiditic, deltaic, and finally alluvial clastic sequence (Pavelić & Kovačić, 2018), reflecting the diachronous regressive trend observed across the entire Pannonian Basin (Magyar et al., 2013). These were overlain by Quaternary clastic deposits (Šimunić et al., 1982).

### 2.3 Structural characteristics

Structurally, Ivanščica Mt., together with other mountains in northern Croatia, is considered as the eastern part of an area locally known as the “Sava folds” (Fig. 1c; Šimunić et al., 1979, 1982; Šimunić 1992), a name characterizing a wedge-shaped tectonic domain in the Dinarides—Alps transition zone in eastern Slovenia and northern Croatia, with kilometer-sized E to ENE trending relatively open folds that deformed earlier formed tectonic units during Latest Cenozoic times (Winkler, 1923; Placer, 1999b). During their work on the Basic Geological Map of Yugoslavia, sheet Varaždin, Šimunić et al., (1979, 1982) considered all mapped faults on Ivanščica to be of Cenozoic age, the main contractional deformations occurring during the Miocene. These authors interpreted Ivanščica as a N verging nappe, which brought Paleozoic and Mesozoic formations over upper Oligocene and lowermost Miocene sediments during the Early Miocene (in Eggenburgian; late Aquitanian to early Burdigalian). The occurrences of Triassic-Jurassic carbonates in the

(See figure on next page.)

**Fig. 3** Tectonostratigraphic columns showing detail lithostratigraphy of Middle Triassic to Lower Cretaceous successions of two structural domains and Cenozoic sedimentary cover. Note the difference in the Lower Jurassic deposits of ČMT footwall succession (IP structural domain) and ČMT hanging wall succession (IIF structural domain). Mesozoic lithostratigraphic columns are cut by faults of different ages and ČMT hanging wall succession is doubled in order to schematically show structural setting, ages and relations between different deformational structures as a result of different deformational events. Note the differences and similarities in Cenozoic deposits N of Šoštanj fault and those of Ivanščica Mountain

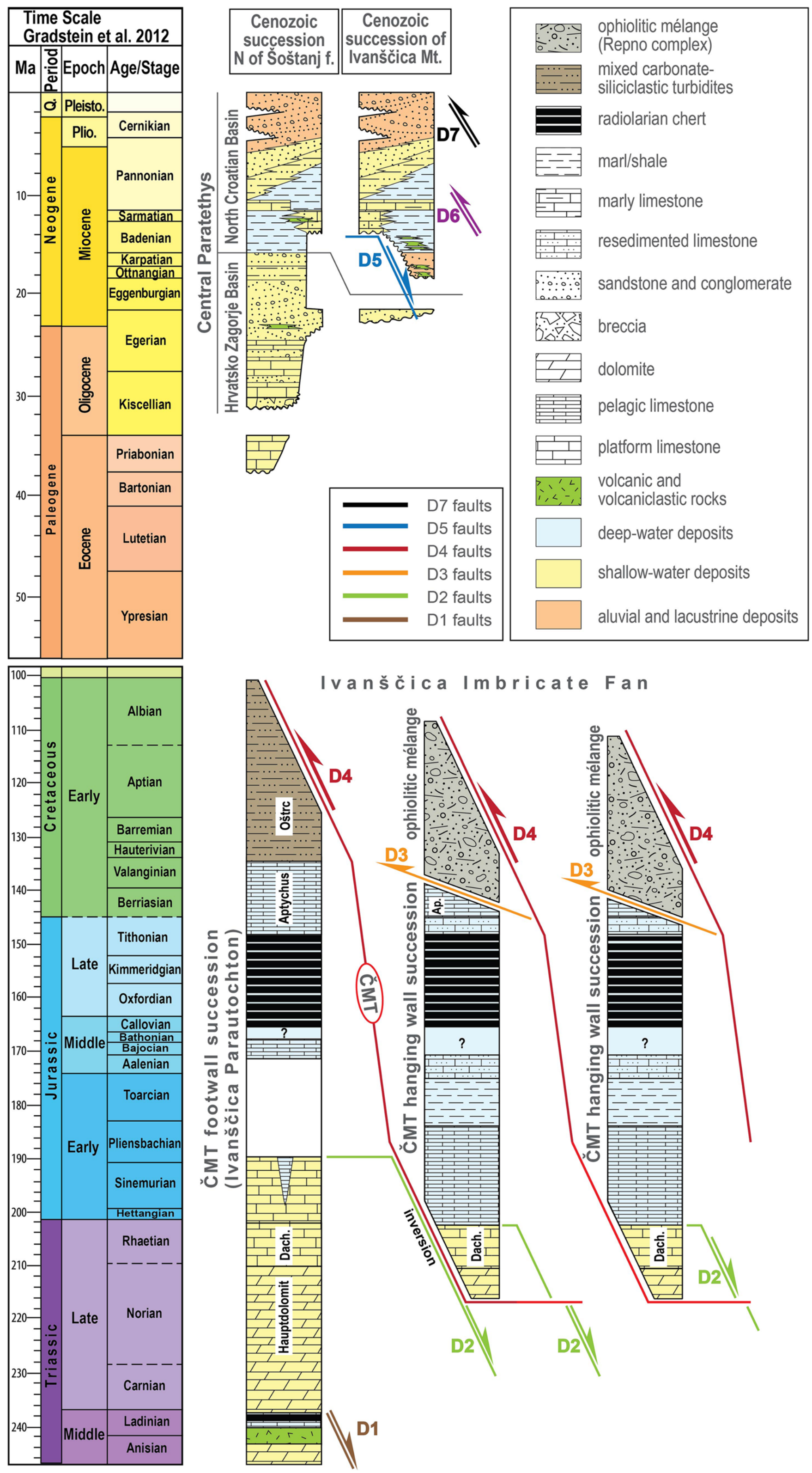


**Fig. 3** (See legend on previous page.)

southern part of central Ivanščica were interpreted as erosional remains of a structurally higher nappe (Šimunić et al., 1979, 1982) or as olistoliths embedded in the Repno complex (Babić & Zupanič, 1978). As we will show below, we newly interpret those occurrences as a stack of imbricates built up of Adriatic passive margin successions and the Repno complex that essentially formed during an Early Cretaceous contractional event.

More recent studies consider the northern Croatian mountains, including Ivanščica Mt., to be a part of the Southern Alps unit (Placer, 1999a). According to van Gelder et al. (2015) and Schmid et al., (2008, 2020) the continental units of Ivanščica Mt. are presently a part of the S verging South Alpine nappe emplaced over earlier formed Internal Dinaridic units during Miocene times. Prior to this south directed emplacement, the tectonic block carrying the northern Croatian mountains rotated 130° clockwise in Oligocene–earliest Miocene, as interpreted by Tomljenović et al. (2008). This interpretation is based on paleomagnetic data measured in Upper Cretaceous deposits on Medvednica Mt. The rotation resulted from earliest Miocene eastward lateral extrusion of the Alps and Dinaridic fragments, accompanied by strong dextral displacements along the Periadriatic fault system and Mid-Hungarian fault zone representing its eastern continuation (Fodor et al., 1998; Schmid et al., 2008). A prominent dextral strike-slip Šoštanj fault which tangent northern foothills of Ivanščica Mt. (Fig. 1c) represents the southernmost branch of the Periadriatic fault system (Fig. 1b; Vrabec & Foor, 2006; Atanackov et al., 2021). Subsequent normal faulting related to Early Miocene rifting and opening of this part of the Pannonian Basin overprinted older structures (Tomljenović & Csontos, 2001; van Gelder et al., 2015). Basin inversion, which was initiated in Late Miocene-Pliocene, caused folding and reverse faulting resulting in the final uplift of the north Croatian mountains (Tomljenović & Csontos, 2001). This inversion was synchronous with approximately 35° counterclockwise (CCW) rotation, active in Late Miocene to recent times, presumably driven by the CCW rotation and indentation of the Adriatic microplate (Tomljenović & Csontos, 2001; Márton et al., 2002).

## 3 Methods and results

### 3.1 Description of deformational structures

Ivanščica is a densely forested mountain with rather scarce high-quality geological outcrops. For this reason, extensive fieldwork was carried out. At locations considered as essential for better understanding of the deformational history of study area, detailed geological mapping at scales of 1:25,000 and 1:5000 was conducted. Special attention was given to the collection of structural and kinematic data, like orientation of bedding, meso-scale

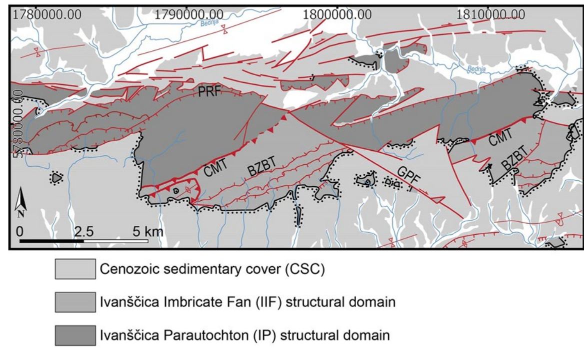


**Fig. 4** Simplified tectonic map of the Ivanščica Mt. showing spatial distribution of structural domains and Cenozoic sedimentary cover. *ČMT* Črne Mlake thrust, *BZBT* Babin Zub back-thrust, *GPF* Gotalovec-Prigorec fault, *PRF* Prigorec reverse fault

folds, axial planar cleavage, S-C fabrics, intersection lineations, fault planes and their kinematic indicators, many of these recorded for the first time in the area. Based on measured structural data, observed differences in deformation styles and mapped tectonic and depositional contacts shown in maps (Figs. 2, 4) and cross-sections (Fig. 5), the study area is subdivided into two structural domains that are from bottom to top: (1) Ivanščica Parautochthon (IP) and (2) Ivanščica Imbricate Fan (IIF). These are overlain by Cenozoic sedimentary cover (CSC) representing the post-tectonic sedimentary cover regarding the Mesozoic deformational events.

#### *3.1.1 Ivanščica Parautochthon (IP) structural domain*

The Ivanščica Parautochthon (IP) structural domain comprises Permo-Mesozoic formations exposed along its northern slopes (Figs. 2, 5). As shown below, our new data do not suggest that IP structural domain would be of allochthonous nature nor do represent a part of a nappe. Therefore, we conclude that parautochthon is an appropriate term for this structurally lower domain. This domain is cut and broken apart into two structural blocks to the west and east of a prominent SE striking Gotalovec—Prigorec dextral strike-slip fault (GPF; see Fig. 2). In both structural blocks, IP structural domain is overthrust by the Ivanščica Imbricate Fan (IIF) structural domain along the SE dipping Črne Mlake roof thrust (ČMT; Figs. 2, 4 and 5). On its SW margin, the IP structural domain is unconformably overlain by upper Egerian (lower Aquitanian) and Miocene sediments. However, in part of the mountain SW of the Vilinska špica peak (726 m), Middle Triassic formations of the IP structural domain are brought over upper Egerian (lower Aquitanian) deposits by two NNW dipping reverse faults, with only locally preserved original depositional contact (Fig. 2). In contrast, no original depositional contacts between Cenozoic sedimentary

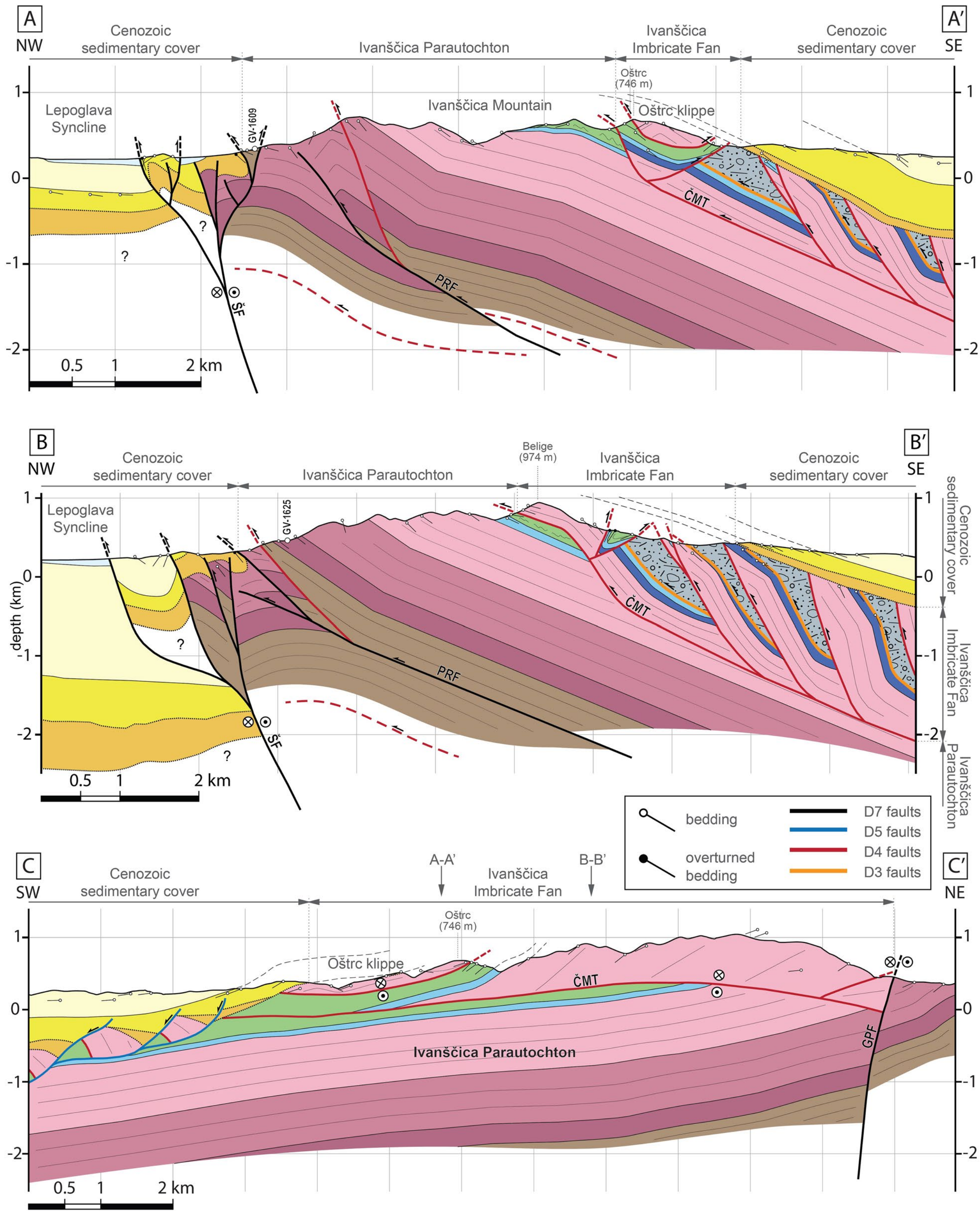


**Fig. 5** Cross-sections across Ivanščica Mt. Cross-sections **A**-**A**′ and **B**-**B**′ are perpendicular to the strike of structures in IIF and IP structural domains. Cross-section **C**–**C**′ is longitudinal to the same structures. Positions of cross sections are shown in Fig. 2. For colour coding of the lithostratigraphic units, please refer to Fig. 2. *ČMT* Črne Mlake thrust, *GPF* Gotalovec-Prigorec fault, *PRF* Prigorec reverse fault, *ŠF* Šoštanj fault

cover and Permo-Mesozoic formations of the IP structural domain are preserved in the northern slopes of Ivanščica Mt. Here, Permo-Mesozoic formations of the IP structural domain are thrusted northward over upper Egerian (lower Aquitanian) sediments (Figs. 2, 5). In the central part of the mountain, the well preserved Permo-Mesozoic succession dips towards S to SE below the IIF structural domain and the upper Egerian (lower Aquitanian) to Miocene cover (Fig. 5). This homoclinal structure of the IP structural domain is thrusted towards NW over the rest of Permo-Mesozoic units belonging to the IP structural domain (Figs. 2, 5). These footwall units are arranged in several SE dipping imbricates and thrusted NW-ward over upper Egerian (lower Aquitanian) sediments at the northern margin of the mountain (Figs. 2, 5). The youngest strata found in this homocline are Hauterivian to Albian turbidites of the Oštrc Fm. They represent the highest footwall strata overthrust by Upper Triassic to Lower Cretaceous shallow- to deep-marine sedimentary succession in a hanging wall of the SE dipping ČMT (Figs. 4, 5). The Oštrc Fm. turbidites are characterized by meter- to meso-scale tight asymmetric folds with NE trending and dominantly SW dipping fold axes (Fig. 6a, b). In the same formation, this folding is associated with an axial planar cleavage (Fig. 6a, b). Moreover, in the underlying Aptychus limestone, similar but predominantly open asymmetric folds are documented showing the same NE trending orientation of fold axes as in the overlying turbidites. Overall consistency of fold asymmetries and SE dipping axial planes and axial planar cleavage (Fig. 6a, b) with respect to the stratification, indicate NW-ward direction of tectonic transport in present-day coordinates. This is in accordance with the tectonic transport direction observed for the structurally higher IIF structural domain (see below) and the overall kinematics of the ČMT.

#### *3.1.2 Ivanščica imbricate fan (IIF) structural domain*

This structural domain occupies southern parts of central and eastern Ivanščica Mt. To the northwest, the domain thrusts over the IP structural domain along the SE dipping ČMT floor thrust (Figs. 2, 4 and 5). In the south, it is unconformably overlain by the upper Egerian (lower Aquitanian) and Miocene cover (Figs. 2, 4 and 5). The main structural characteristics of this domain are a series of SE dipping reverse faults splaying off the ČMT floor thrust (decollement), thus forming a stack of NW verging imbricates in their present-day orientation (Figs. 2, 5). These imbricates are made up of Upper Triassic platform carbonates, overlain by Lower Jurassic to Lower Cretaceous pelagic succession, dipping underneath the ophiolitic mélange of the Repno Complex. The latter was previously tectonically emplaced over the pelagic Jurassic to Lower Cretaceous succession (Figs. 2, 5). Thus, the formation of these imbricates postdates the emplacement of the ophiolitic mélange related to the obduction of the West Vardar ophiolites (Schmid et al., 2020). The lithostratigraphic composition of the imbricates changes towards NW in that the Repno complex thrusts over progressively younger formations starting with Lower Jurassic in the SE up to lowermost Cretaceous pelagic deposits in the NW (Figs. 2, 5). The Oštrc Fm. is present only in the NW-most imbricate, locally sandwiched between the ČMT and the antithetic reverse fault named the Babin Zub back-thrust (BZBT; Figs. 2, 4, 5). The formation of the BZBT was probably favoured by a steep ramp in the SE dipping ČMT (Fig. 5). The top SE transport along the BZBT is supported by the geometry of the overturned syncline with its parasitic folds and axial planar cleavage well developed in the pelagic Aptychus limestone and the Oštrc Fm. (Figs. 5, 6d-f). Thus, the BZBT and the first imbricate to the SE form a NE striking triangle structure (Figs. 2, 5 and 6h). Within the IIF, with the exception of the Repno complex, bedding planes and axial planar cleavage prevailingly dip towards SE (Figs. 5, 6c, g). In the overturned and tight syncline formed in the hanging wall of the BZBT bedding planes and axial planar cleavage dip to the NW (Figs. 5, 6c-e).

The outcrops of the Repno complex are characterized by pervasive scaly cleavage. The planar fabric is mainly represented by clay minerals. Shaly matrix incorporates variously sized blocks of basalt, gabbro, chert, and sandstone (Fig. 7b). Basalt and gabbro blocks are usually tens and up to hundred meters in diameter, while chert and sandstone blocks are centimetre up to tens of meters in diameter. Well-developed kinematic indicators (S-C fabrics, asymmetric and symmetric boudins) record inconsistent sense of shear (Fig. 7a–c). However, close to imbricate-bounding reverse faults, kinematic indicators in the Repno complex show a sense of shear consistent with the larger scale kinematics of these faults (i.e. top NW; Fig. 7c). In the southwestern part of the IIF, the structurally highest pre-Oligo-Neogene tectonic unit, the so-called Oštrc klippe thrusts over the Oštrc Fm. of the leading imbricate (Figs. 2, 5). This klippe comprises Upper Triassic platform carbonates and subordinately Jurassic pelagic deposits, both folded in a form of NE trending anticline (Figs. 2, 5).

#### *3.1.3 Cenozoic sedimentary cover (CSC)*

The Cenozoic sedimentary cover unconformably overlays the Permo-Mesozoic units and seals all the older structures of the structural domains described above. Thus, the Cenozoic sediments represent the post-tectonic cover of the previously described two structural domains. This can be observed on the southern slopes of Ivanščica Mt. where none of the NW verging reverse faults in the IIF structural domain extend into the upper Egerian (lower

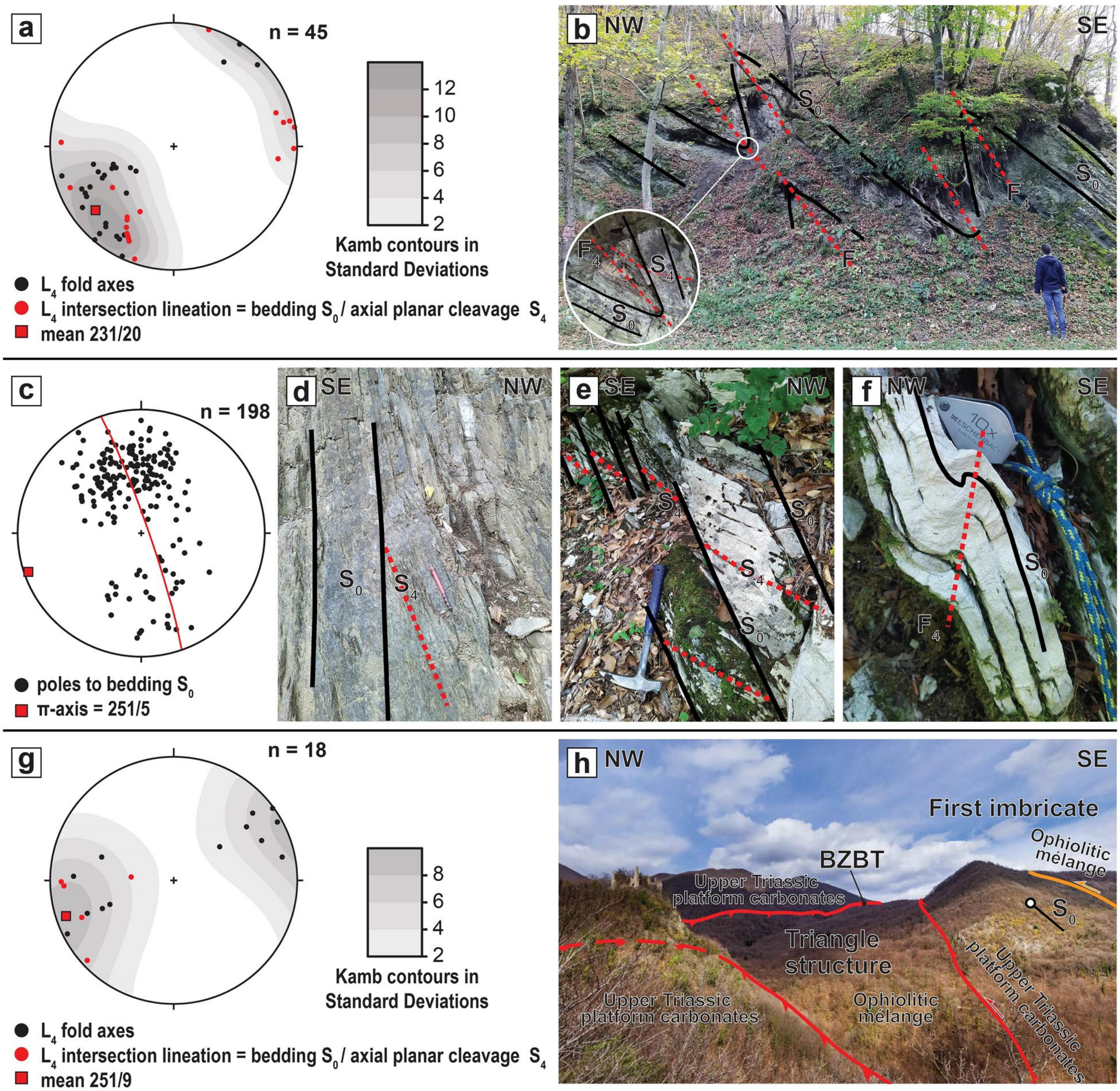


**Fig. 6** Examples of kinematic data. **a** Stereoplot of the fold axes ($L_4$) and intersection lineation ($L_4$) of bedding ($S_0$) – axial planar cleavage ($S_4$), projected on top of the Kamb contour plot. Mean orientation of the fold axes is 231/20. The measurements are taken from pelagic Aptychus limestone and Oštrc Fm. exposed within the IP structural domain. **b** Tight asymmetric folding of siltstones and calcarenites of the Lower Cretaceous Oštrc Fm. exposed within the IP structural domain (46.172552, 16.058040). **c** Stereoplot of the poles to the bedding ($S_0$), best fit Π-circle (shown with red line) and Π-axis. The measurements are taken from the Upper Triassic to lowermost Cretaceous deposits exposed within the IIF structural domain. **d** Slightly overturned NE dipping bedding ($S_0$) and pervasive axial planar cleavage ($S_4$) within siltstones and calcarenites of the Oštrc Fm. exposed within the IIF structural domain. Outcrop is located on the NW overturned limb of the syncline in the hanging wall of the BZBT (46.166424, 16.111421; see the cross-section B-B′ in Fig. 5) **e** NW dipping overturned bedding ($S_0$) and pervasive axial planar cleavage ($S_4$) within pelagic Aptychus limestone exposed in the IIF structural domain. Outcrop is located on the NW overturned limb of the syncline in the hanging wall of the BZBT (46.166978, 16.110589; see the cross-section B-B′ in Fig. 5). **f** Second-order S-type parasitic folding of Aptychus limestone exposed within the IIF structural domain (46.164857, 16.095013). **g** Stereoplot of the fold axes ($L_4$) and intersection lineation ($L_4$) of bedding ($S_0$) – axial planar cleavage ($S_4$), projected on top of the Kamb contour plot. Mean orientation of the fold axes is 251/9. The measurements are taken from the Jurassic to lowermost Cretaceous deposits exposed within the IIF structural domain. **h** Field photo of the SE dipping imbricate, NW dipping BZBT and Triangle structure in between. See Fig. 2 for the photo location

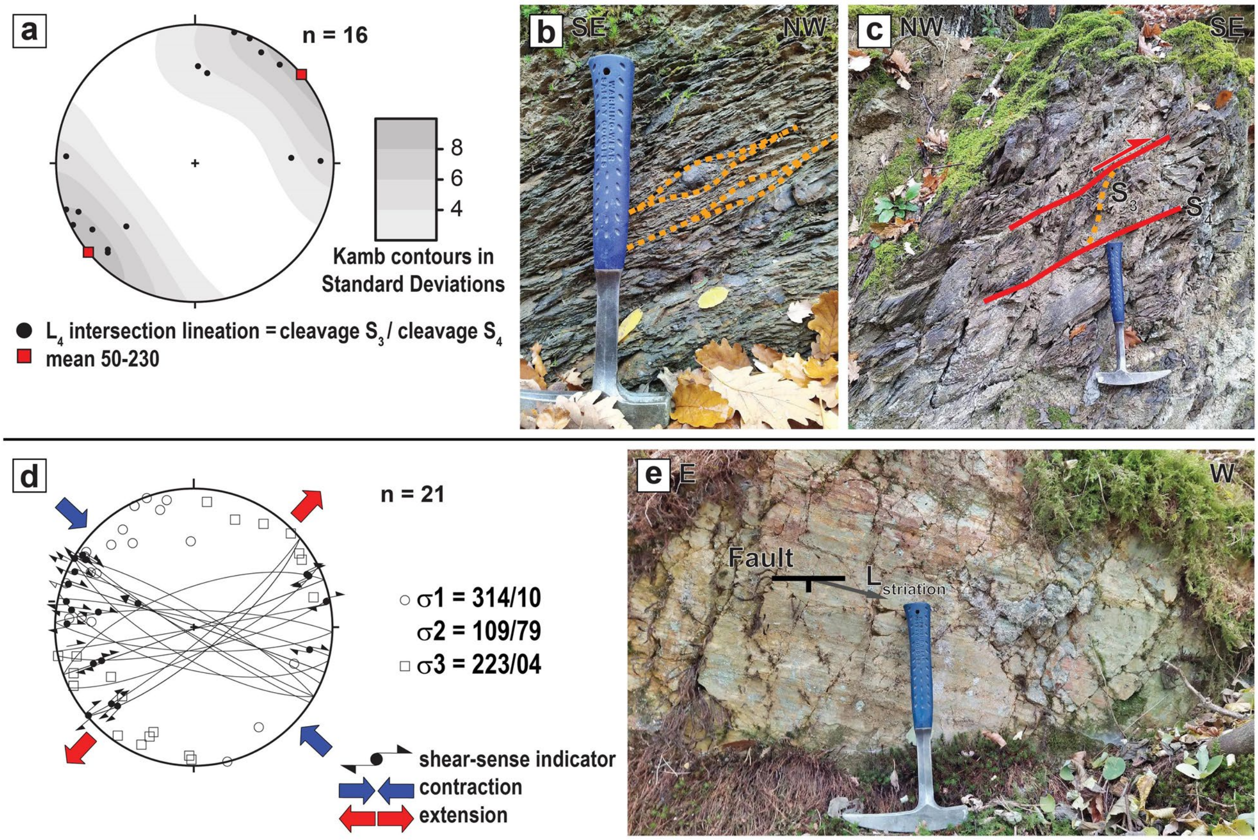


**Fig. 7** Examples of kinematic data. **a** Stereoplot of the cleavage ($S_3$) – cleavage ($S_4$) intersection lineation ($L_4$), projected on top of the Kamb contour plot. Mean orientation of the fold axes is 50–230. The measurements are taken from the ophiolitic mélange unit exposed within the IIF structural domain. Black poles represent intersection lineation derived from NW verging structures and red poles from SE verging structures. **b** Ophiolitic mélange exposed within the IIF structural domain (46.156851, 16.110643) embedding deformed symmetric blocks of sandstones in a shaly matrix. **c** S-C structures in the ophiolitic mélange exposed in the footwall just below the BZBT within the IIF structural domain (46.159118, 16.096405). **d** Stereoplot and associated paleostress tensor of strike-slip faults from the CSC. Measurements were taken along a generally ENE striking strike-slip faults to the north of Ivanščica Mt. **e** Strike-slip fault from the ENE striking dextral fault zone to the north of Ivanščica Mt. (46.219420, 16.192191), fault plane 140/82, striations 228/20, dextral displacement

Aquitanian) sedimentary cover (Figs. 2, 5). Instead, the upper Egerian (lower Aquitanian) sediments gently dip towards S-SE and except for this gentle tilt do not show other deformational structures. In contrast, severe tectonic deformations affecting the Cenozoic deposits are observed along the northern margin of Ivanščica Mt. where upper Egerian (lower Aquitanian) sediments are overthrust by Permo-Mesozoic units of the IP structural domain along Prigorec reverse fault (PRF; Fig, 5). In addition to this, formations of the IP structural domain and the Cenozoic sedimentary cover are severely affected by transpressional faulting along a set of generally ENE striking dextral faults (Figs. 2, 5, and 7d, e). This fault set separates the Lepoglava syncline from the northwestern part of Ivanščica Mt. (see area of the left upper corner of Fig. 2) and is considered as an eastward prolongation of the dextral Šoštanj strike-slip fault (see Fig. 1c; Vrabec & Fodor, 2006; Atanackov et al., 2021). The youngest sediments clearly affected by this dextral fault set are of late Pannonian (late Messinian) age, but younger activity cannot be excluded. Another prominent structure is the SE striking Gotalovec – Prigorec dextral strike-slip fault (GPF in Figs. 2, 4) affecting uppermost Pannonian (Fig. 2) or possibly even younger deposits. South of Ivanščica Mt., similar dextral faults are not present or only have insignificant impact on the structural setting. Here folds and minor reverse faults of E-W to NE-SW orientation are most prominent structures (Figs. 2, 7).

#### *3.1.4 Oligocene-Quaternary structures in the wider study area revealed by reflection seismic data*

2D reflection seismic sections and well data are used to interpret and map structures in the subsurface in order to better understand the tectonic history of the study area. Traces of used seismic sections and positions of wells are shown in Fig. 1c. Pervasive polyphase deformation is registered across the whole study area, encompassing the entire Oligocene-Quaternary sedimentary sequence in which five characteristic types of structures were identified: extensional listric faults, inverted extensional listric faults, folds associated with reverse faults, positive flower structures, and reverse faults (Fig. 8).

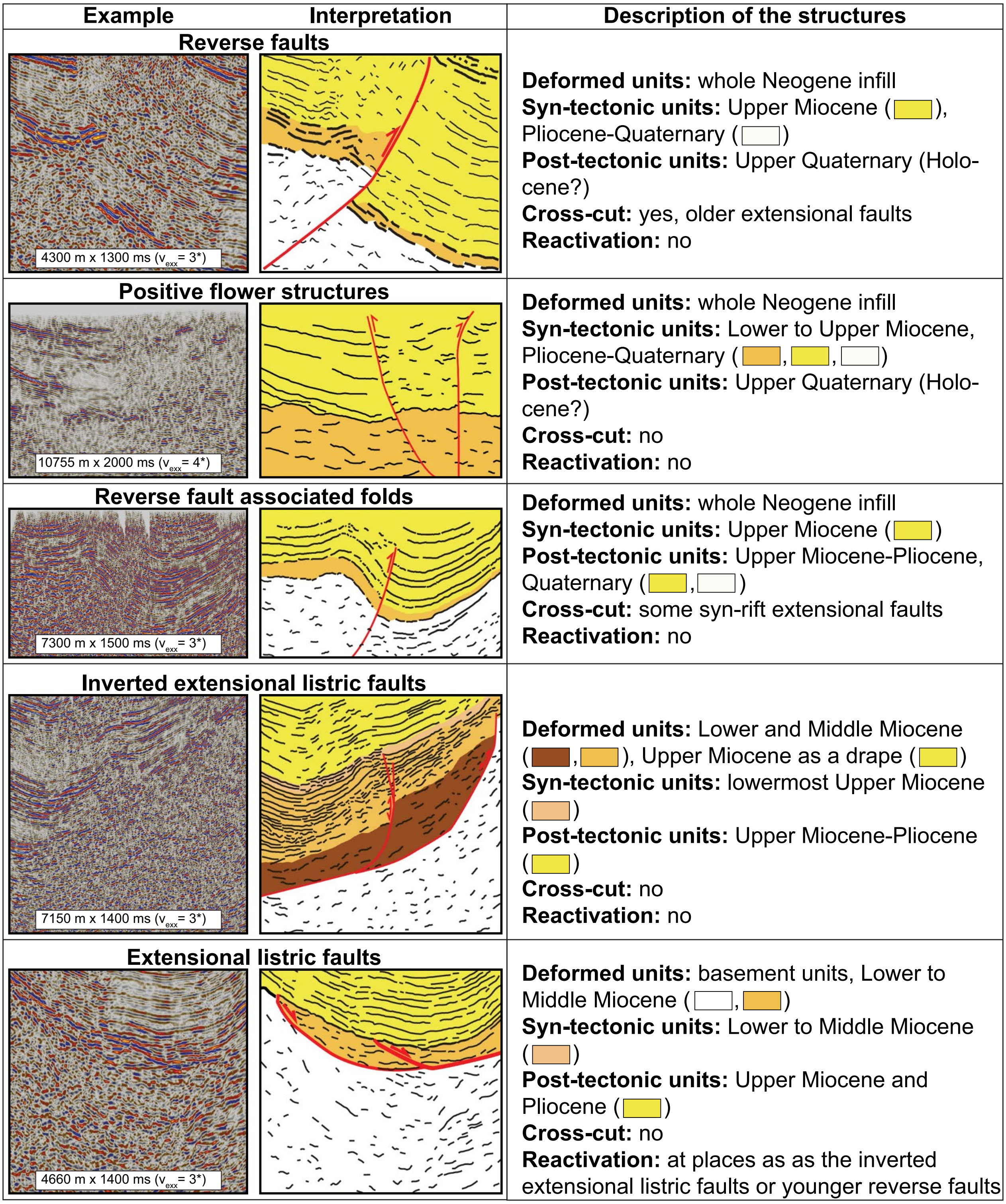


**Fig. 8** Characteristic deformational structures interpreted on the seismic profiles

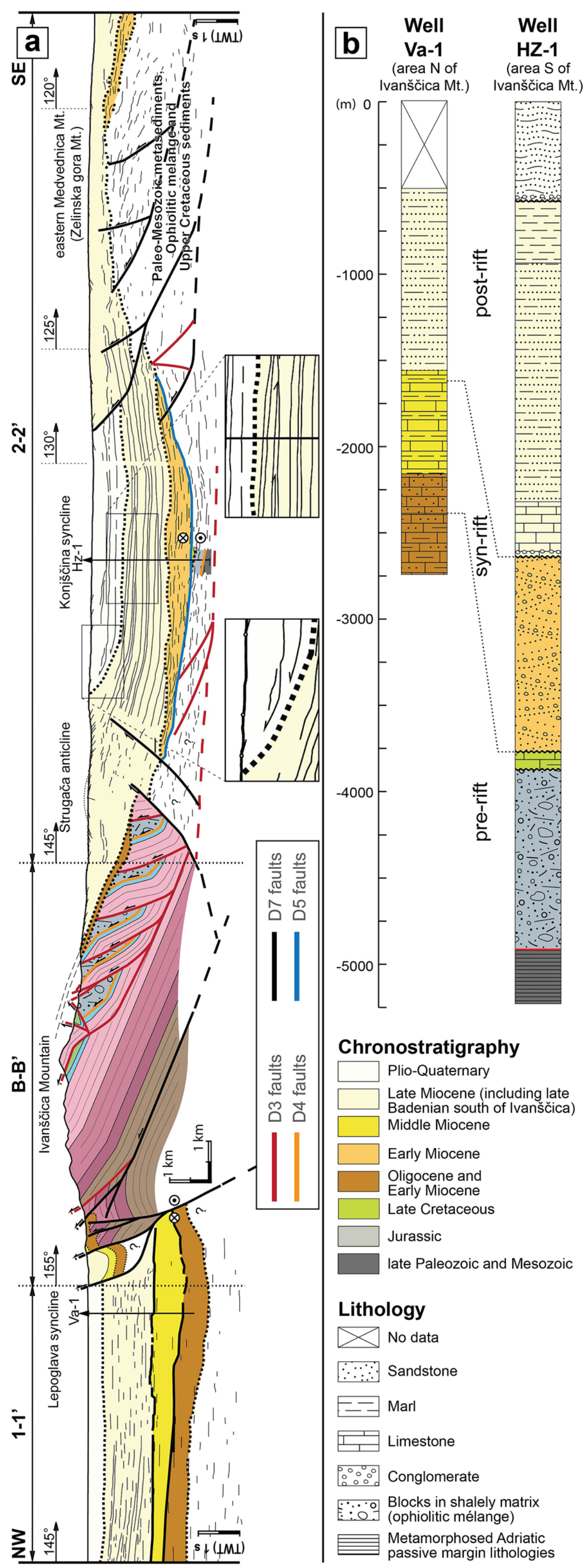


◀ **Fig. 9** **a** Regional composite cross-section composed of three segments. Segment 1–1′ is located to the north of Ivanščica Mt. Note the offset between section segment 1–1′ and B-B′. Segment B-B′ represents the homonymous cross-section from the Fig. 5. The legend for this section is shown in Fig. 2. Segment 2–2′ is located to the south of Ivanščica Mt. and ends at the easternmost slopes of Medvednica Mt. For exact location of the composite cross-section and its segments see Fig. 1c. **b** Lithostratigraphic columns of penetrated deposits from the wells Va-1 and HZ-1. For the locations of the wells see Fig. 1c. Note that the well Va-1 is not originally positioned but projected on the section segment 1–1′

The Oligocene to Middle Miocene sedimentary sequences in the research area indicate the existence of two simultaneous and contrasting paleo-environments. Specifically, during this time interval, the area north of Ivanščica Mt. was characterised by the deposition of around two kilometres thick Oligocene to Lower Miocene dominantly marine deposits (Figs. 3, 9). These deposits are cut by the Šoštanj fault and except for the upper Egerian (lower Aquitanian) deposits, do not appear south of that dextral strike-slip fault. Upper Egerian (lower Aquitanian) deposits pinch-out to the south of Ivanščica Mt., where the oldest Cenozoic deposits are of Ottnangian (middle Burdigalian) or even late Badenian (early Serravallian) age.

The syn-rift structures are the oldest Neogene structures observed in the research area. According to reflector geometry and seismic facies characteristics, it is possible to differentiate Lower to Middle Miocene syn-rift units from older basement units (Fig. 9). Inside the basement, slightly inclined to horizontal echelon zones of sub-parallel, discontinuous, high amplitude reflectors are present (Figs. 8, 9), interpreted as listric normal faults that merge in depth into a detachment dipping towards the NE. Different generations of half-grabens developed in their hanging walls are observed on seismic sections. Based on well data, half-graben formation is constrained by thick syn-rift Lower to Middle Miocene deposits (Figs. 8, 9) penetrated by the Hz-1 well (Fig. 9, see also Tomljenović & Csontos, 2001). The post-rift deposits are of late Middle Miocene and/or early Late Miocene age (Figs. 8, 9). Notably, the absence of cross-cut features indicates a coherent deformation history during Early and Middle Miocene, however, in some cases with reactivation of earlier formed normal faults, and inversion of extensional listric faults into reverse faults (Fig. 8). This tectonic inversion is coeval with Sarmatian (late Serravallian) to earliest Pannonian (early Tortonian) deposition.

Three groups of structures are observed in the deformed post-rift Upper Miocene and Pliocene deposits. The first are reverse faults with SE and NW vergence, predominantly in the area between Ivanščica and Medvednica Mt. (Figs. 8, 9). Displacement on these faults is commonly up to hundreds of meters. As a result, the basement units are brought above Upper Miocene deposits in their footwalls. Between the Ivanščica Mt. and the Hz-1 well (Figs. 2, 9), a general vergence of these faults is towards SE, while in between this well and Medvednica Mt. reverse faults mostly dip towards SE and have NW vergence (Fig. 9). These reverse faults are usually formed as conjugate faults, and commonly bound the E-W to NE-SW striking, open and symmetric anticlines or pop-ups in their hanging walls. The most prominent structure between Ivanščica and Medvednica mountains is the Konjščina syncline (Fig. 9). In the core of this syncline 2000 m of Upper Miocene, Pliocene, and Quaternary deposits were penetrated by the Hz-1 well (Fig. 9). Onlap and downlap reflection terminations are common, but mainly connected to the syn-depositional clinoform architecture related to the basin-scale morphological shelf progradation (Fig. 9). However, the onlap features observed above the Upper Miocene clinoform unit around Hz-1 well, are folded together with the prominent reflector on which they onlap (Fig. 9). Considering the data from the Hz-1 well, this unit is represented by an alternation of sandstone and marls, which are unconformably overlain by Plio-Quaternary gravels at depth of 580 m (Fig. 9). This unconformity surface is folded and pinches out towards Strugača anticline to the N and eastern Medvednica Mt. to the S. As observed on seismic and surface structural data, the overlying Plio-Quaternary deposits are also folded and faulted (Fig. 9). The next prominent syncline is the SE trending Lepoglava syncline located to the N of Ivanščica Mt. between two regional dextral faults, the Šoštanj fault to the S and Donat fault to the N (Figs. 1, 2).

### 3.2 Apatite fission track

Apatite fission track (AFT) analyses were carried out by the Institute of Geology at Czech Academy of Sciences. Samples for AFT analysis were collected from both Permo-Mesozoic structural domains to compare their thermal histories and reconstruct the uplift path of the Alpine—Dinaridic transitional zone. Since the study area consists mostly of carbonate sedimentary rocks and thus lacking apatite-rich lithologies, we selected the only three potentially suitable lithostratigraphic units for apatite extraction. Among overall eight samples collected from Permian to Lower Triassic sandstones, Middle Triassic volcanic rocks and Lower Cretaceous turbidites, only three samples from Permian to Lower Triassic sandstones gave enough apatites for analysis and only two of them (GV-1609 and GV-1625; Fig. 2) were successfully analysed Table 1. The apatite extraction from the rock samples (8 kg per sample) was done following standard mineral separation (REF) and their preparation for counting and subsequent measurement of uranium content by using LA-ICP-MS (Laser Ablation Inductively Coupled Plasma Mass Spectrometry) following the procedure and age calculation described by Hasebe et al. (2004). IsoplotR software (Vermeesch, 2018) and Durango apatite standard were used for zeta factor calculation and final calculation of ages.

The results of two AFT analyses are presented in Table 1. Two analysed detrital samples from the IP structural domain yield a central age of 56.36 ± 2.50 Ma for GV-1609 and 67.27 ± 5.38 Ma for GV-1625 (Fig. 10). Measured mean track length is 11.12 ± 2.54 µm for the sample GV-1609 and 11.76 ± 1.76 µm for the sample GV-1625. The AFT age and length measurements were combined with paleo temperature and stratigraphic constraints in order to derive the cooling trajectories for both samples by using HeFTy software based on fission track annealing algorithms (Ketcham, 2005; Ketcham et al., 2007). The obtained time–temperature model of both samples (Fig. 10) indicates fast, tectonically induced cooling that took place immediately after peak temperature conditions reached in the Early Cretaceous (ca. 140 Ma). The model suggests a drop of a temperature from a minimum 300 to 100 °C between 140 and 125 Ma

**Table 1** Apatite fission track analytical data

| Sample | Lithology | Coordinates | | Central age (Ma ± 1σ) | $N_{Gr}$ | $\rho_s$ ($N_S$) ($10^5$ cm$^{-2}$) | $^{238}U$ (ppm) | 2σ | MSWD | P(χ2) | Disp. (%) | Pooled age (Ma ± 1σ) | MTL (µm ± $SD_L$) | $N_L$ | $D_{par}$ (µm) |
|---|---|---|---|---|---|---|---|---|---|---|---|---|---|---|---|
| | | Latitude | Longitude | | | | | | | | | | | | |
| GV-1609 | Upper Permian sandstone | 46.20068 | 16.08756 | 56.36 ± 2.5 | 63 | 0.09 (3396) | 21.50 | 1.03 | 5.5 | 0 | 28.43 ± 3.54 | | 11.12 ± 2.54 | 40 | 1.90 |
| GV-1625 | Lower Triassic sandstone | 46.20293 | 16.06070 | 67.27 ± 5.38 | 39 | 0.24 (1788) | 26.90 | 0.99 | 7 | 0 | 42.29 ± 6.19 | 56.2 ± 8.5 | 11,76 ± 1.76 | 37 | 1.74 |

The data presented in table are discussed in the text, see also Fig. 10. $N_{Gr}$ number of dated apatite crystals, $\rho_s$ spontaneous track densities, $N_S$ sum of spontaneous fission-tracks, $^{238}U$ mean $^{238}$U content value, *MSWD* mean square of weighted deviates, $P(\chi^2)$ probability of obtaining chi-square ($\chi^2$) for n degrees of freedom (n is the number of crystals), *Disp.* dispersion in single-grain ages, *MTL* C axis projected mean track length with ± the standard deviation ($SD_L$), $N_L$ number of measured confined tracks, $D_{par}$ average etch pit diameter

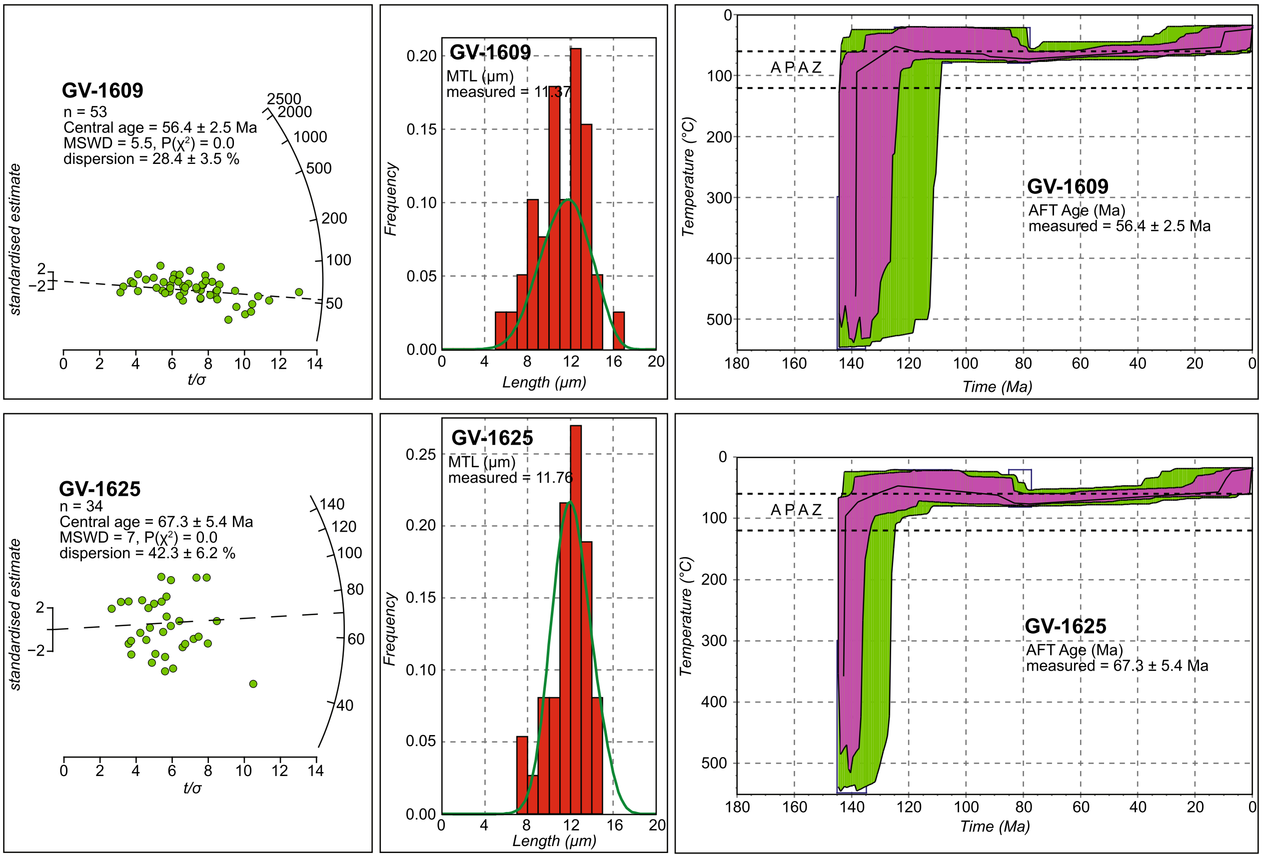


**Fig. 10** Apatite fission track data. Radial plots (plots to the left) showing the distribution of cooling ages according to the relative error and standard deviation for the apatites, accompanied by a graphs showing the distribution of the track lengths in the apatites (graphs in the middle) and a t/T graphs (graphs to the right) showing the results of HeFTy modeling based on track length and age distribution of the apatite fission tracks. *n* number of used data, *MSWD* mean square of weighted deviates, P($\chi^2$) = probability of obtaining chi-square ($\chi^2$) for n degrees of freedom (n is the number of crystals; *APAZ* apatite partial annealing zone

and a minimum cooling rate of 13.33 °C/Ma. This implies denudation rate of 0.53 km/Ma when assuming an average thermal gradient of 25 °C/km. The length of the apatite fission tracks corrected for the angle of measurement indicates a subsequent and relatively slow cooling period through the apatite partial annealing zone (APAZ) followed by a stable period with only minor fluctuations around the lower temperature limit of the APAZ (Fig. 10).

### 3.3 Vitrinite reflectance

Vitrinite reflectance (VR, %$R_o$) was measured on isolated organic matter using Zeiss Axio Imager microscope equipped with MSP 210 microscope spectrometer (oil immersion) following standard procedures (Stach et al., 1982; Taylor et al., 1998). First, total organic carbon (TOC) content was determined on selected samples (siltstones and mudstones of Cretaceous, Jurassic, and Triassic age). The TOC content was measured on Leco C744 carbon analyser. To remove carbonate material, samples were pre-treated with hot 18% HCl. Then, organic matter (kerogen) was isolated. Organic matter concentrate was obtained after standard HCl/HF/$ZnCl_2$ treatment of rock. Standards used for calibration were Spinel (0.426%$R_o$), Sapphire (0.596%$R_o$), Yttrium–Aluminium-Garnet (0.905%$R_o$), Gadolinium-Gallium-Garnet (1.721%$R_o$), Cubic-Zirconia (3.12%$R_o$), Strontium-Titanate (5.38%$R_o$). VR was converted to peak paleotemperatures using formulas defined by Barker & Pawlewicz (1994) for burial heating ($T_{peak} = (\ln Rr + 1.68)/0.0124$). Organic matter was examined on Olympus BX-51 microscope.

The organic matter content in the analysed siltstones and mudstones ranges from 0.16 to 1.16 wt% TOC (Table 2). Generally, organic matter content is low (TOC < 0.3%) except in Jurassic (GV-476) and Triassic (GT-240) siltstones (0.91 and 1.16% TOC, respectively). Organic matter is mainly fine detrital and of terrigenous origin, represented either with vitrinite macerals

**Table 2** Vitrinite reflectance analytical data

| Sample (structural domain) | Lithology | Coordinates | | $TOC_{Leco}$ (%) | VR %$R_o$ | No. | SD | %$R_{min}$ | %$R_{max}$ | TAI | Conversion TAI-%$R_o$ | $T_{peak}$ (°C) | Range $T_{peaK}$ (°C) |
|---|---|---|---|---|---|---|---|---|---|---|---|---|---|
| | | Latitude | Longitude | | | | | | | | | | |
| GV-224 (IP) | Lower Cretaceous Siltstone | 46.174581 | 16.066425 | 0.31 | 2.10 | 35 | 0.27 | 1.63 | 2.57 | $4^-$ | 2–3 | 200 | 180–220 |
| GV-1416 (IIF) | Lower Cretaceous Siltstone | 46.163606 | 16.093678 | 0.16 | – | | | | | 4 | > 3 | > 230 | > 230 |
| GV-1633 (IIF) | Lower Cretaceous Siltstone | 46.162534 | 16.061793 | 0.22 | 2.19 | 24 | 0.21 | 1.80 | 2.54 | $4^-$ | 2–3 | 200 | 190–220 |
| DJI-8,30 (IP) | Lower Cretaceous Siltstone | 46.175544 | 16.073502 | 0.20 | – | | | | | $4^-$ | 2–3 | > 200 | 190–220 |
| GV-476 (IIF) | Jurassic Siltstone | 46.159107 | 16.096391 | 0.,91 | 1.81 | 140 | 0.18 | 1.44 | 2.27 | $3^+–4^-$ | 1.,8–2.2 | 185 | 170–200 |
| GV-1257A (IIF) | Jurassic Siltstone | 46.156935 | 16.121706 | 0.27 | – | | | | | $4^-$ | 2–3 | > 200 | > 200 |
| GV-1257B (IIF) | Jurassic Siltstone | 46.156935 | 16.121706 | 0.21 | – | | | | | $4^-$ | 2–3 | > 200 | > 200 |
| GV-1477 (IIF) | Lower Jurassic Mudstone | 46.172566 | 16.159687 | 0.19 | 2.93 | 7 | 0.30 | 2.45 | 3.26 | $4^-$ | 2–3 | 225 | 210–230 |
| GV-1585 (IIF) | Lower Jurassic Mudstone | 46.174929 | 16.161486 | 0.24 | 1.86 | 5 | 0.07 | 1.76 | 1.95 | $3^+–4^-$ | 1.8–2.2 | 190 | 180–190 |
| MR-24,50 (IIF) | Lower Jurassic Mudstone | 46.164998 | 16.135985 | 0.26 | 1.95 | 45 | 0.53 | 0.92 | 2.80 | $3^+–4^-$ | 1.8–2.2 | 190 | 135–220 |
| GV-113 (IP) | Middle Triassic Siltstone | 46.192836 | 15.98391 | 0.40 | – | | | | | 4 | > 3 | > 230 | > 230 |
| GT-240 (IP) | Middle Triassic Siltstone | 46.181091 | 16.196046 | 1.16 | 3.84 | 31 | 0.42 | 3.05 | 4.71 | 4 | > 3 | 245 | 220–260 |

The data are discussed in the text. *TOC* total organic carbon, *VR* vitrinite reflectance, *No*. number of measurements, *SD* standard deviation; $R_{min}$ minimum vitrinite reflectance, $R_{max}$ maximum vitrinite reflectance, *TAI* thermal alteration index, *IIF* Ivanščica Imbricate Fan, *IP* Ivanščica Parautochton, *o.m.* ophiolitic mélange or with dark, non-fluorescent, highly thermally altered amorphous organic matter. Inertinite, mainly fusinite particles are evidenced as well.

Middle Triassic organic matter is highly thermally altered. VR (3.84%$R_o$) corresponds to paleo-temperatures of ≥ 245 °C (Bostick, 1979; Barker & Pawlewicz, 1994; Rainer et al., 2016). Organic matter in Lower Jurassic mudstones is mainly amorphous while in Jurassic siltstones vitrinite macerals prevailed. VR and TAI (thermal alteration index) in all Jurassic samples indicate transition from catagenesis into metagenesis except in GV-1477 sample. VR in GV-1477 is higher (2.93%Ro) than in two others measured (1.86 and 1.95 respectively) pointing to higher paleotemperatures (> 225 °C) in that sample in relation to other ones (≈ 190 °C). According to VR and TAI Lower Cretaceous siltstones have reached onset of metagenesis. VR is slightly higher than 2%$R_o$ indicating paleotemperatures ≥ 200 °C.

## 4 Discussion

### 4.1 Tectonic evolution of the study area and correlation with the Dinarides and the Alps

Integration of structural, AFT and VR data, together with the existing sedimentological and biostratigraphic data, enabled a reconstruction of the five deformational events that affected Permo-Mesozoic and/or Cenozoic formations of Ivanščica Mt. In addition, based on lithostratigraphic characteristics of volcano-sedimentary successions and their superposition, two older Mesozoic extensional events are also supposed. These events are discussed below in the context of the tectonic evolution of Ivanščica Mt. and in the context of the tectonic evolution of the Dinarides, Southern and Eastern Alps. The chronology of deformational events was partly derived from overprinting relations between documented deformational structures and partly based on new biostratigraphic ages of Mesozoic successions (Vukovski et al., 2023) considered as pre-, syn- and post-tectonic deposits with respect to particular deformational events. Additional time constraints were established based on AFT data.

#### *4.1.1 Pre-Cretaceous tectonic evolution*

The oldest deformational event (D1 extension) on Ivanščica Mt., although not directly confirmed by deformational structures, is indicated by the presence of syn-rift volcano-sedimentary successions of Middle Triassic age. Anisian to Ladinian pelagic successions documented in the IP structural domain (Figs. 2, 3), are interpreted as having been deposited in relatively deep depocenters arranged in the form of half-grabens controlled by steep normal faults (Goričan et al., 2005; Slovenec et al., 2020, 2023; Kukoč et al., 2023). On Ivanščica Mt., the oldest pelagic deposits are Illyrian (late Anisian) radiolarian cherts (Goričan et al., 2005; Slovenec et al., 2020; Kukoč et al., 2023), while on nearby Kuna gora Mt. ammonites from pelagic limestones indicate a Pelsonian (middle Anisian) age (Kukoč et al., 2023). Thus, according to our interpretation, this oldest deformation (D1) represents an extensional event that is related with the opening of the Neotethys Ocean during Middle Triassic times. These half-graben depocenters were short-lived, and a shallow-marine carbonate sedimentation was re-established again in the Late Ladinian (Šimunić & Šimunić, 1997; Goričan et al., 2005). Such an Anisian-Ladinian extensional event is well-documented throughout the Alps and the Dinarides, characterized by deposition of coeval and lithologically similar volcano-sedimentary successions (for correlation, see Kukoč et al., 2023).

During the Early Jurassic, after a period of Late Triassic shallow-marine sedimentation proved by Upper Triassic carbonates found in both pre-Miocene structural domains of Ivanščica Mt. (i.e., in IP and IIF structural domains), a dramatic change in depositional environments took place. In the IP structural domain, deposition of shallow-marine carbonates continued from Late Triassic into Early Jurassic until the Pliensbachian. In contrast, in the IIF structural domain the Upper Triassic shallow-marine carbonates are covered by Lower Jurassic pelagic deposits. This sharp deepening of depositional environments is assumed as related to yet another extensional event of Early Jurassic age (D2). As IP and IIF structural domains are separated by the ČMT (Figs. 2, 4 and 5), this NW verging thrust (recent orientation) is likely an inverted Early Jurassic normal fault. However, since Pliensbachian, pelagic conditions prevailed in both structural domains (Vukovski et al., 2023). This Early Jurassic extensional event correlates well with Jurassic rifting recorded in the Dinarides (Blanchet et al., 1970; Babić, 1976; Dragičević & Velić, 2002) and in the Southern and Eastern Alps, where similar lithostratigraphic successions are documented (e.g. Bertotti et al., 1993; Bohm, 2003; Goričan et. al 2012; Rožič et al., 2017). In the Alps, this Early Jurassic extension led to formation of the Alpine Tethys passive continental margin (e.g., Froitzheim & Eberli, 1990; Froitzheim & Manatschal, 1996).

#### *4.1.2 Early Cretaceous tectonic evolution*

The tectonic emplacement of the Repno Complex over the stratigraphic succession of the Adriatic continental passive margin recorded in the IIF structural domain (Figs. 2, 5, 11) marks the oldest contractional event recorded on Ivanščica Mt. (D3). Age constraints for this event on Ivanščica Mt. are provided by the youngest formations that are directly overthrust by the Repno Complex, which is uppermost Tithonian to Valanginian Aptychus limestone (Fig. 5). This indicates that the D3 event occurred during the Valanginian or slightly earlier.

The peak temperature conditions of approximately 200 °C recorded in the passive margin successions within the IIF structural domain (Table 2) were likely reached during this event. The obtained temperatures, calculated using the vitrinite reflection method, are only slightly higher than those estimated from the colour of pollen and dinoflagellate cysts obtained from the Repno Complex (Babić et al., 2002). This is in line with the structurally higher position of the Repno Complex with respect to the underlying passive margin successions.

Late Jurassic to earliest Cretaceous obduction of the Neotethyan ophiolites on the eastern continental margin of Adria is well documented throughout the Dinarides and the Hellenides (e.g., Bortolotti et al., 2013; Tremblay et al., 2015; Nirta et al., 2018; Schmid et al., 2020 with references). It is proposed that this obduction is responsible for a low-grade metamorphic overprint recorded in Paleo-Mesozoic units of the distal Adriatic margin underlying the ophiolites (see Fig. 11; e.g., Tomljenović et al., 2008; Porkoláb et al., 2019; Mišur et al., 2023). On Medvednica Mt., monazite dating indicates a Berriasian metamorphic event (~ 143 Ma; Mišur et al., 2023), while in the central Dinarides, K/Ar ages indicate Tithonian to Valanginian age of this metamorphic overprint (150–135 Ma; Porkoláb et al., 2019). Therefore, Valanginian age assumed for the D3 deformational event on Ivanščica Mt. is only slightly younger than these metamorphic ages. However, as Permian to Lower Cretaceous formations of Ivanščica Mt. are not affected by this metamorphic overprint but only a minor thermal overprint, at the time of the obduction they were in a more external (i.e., continent-ward) paleogeographic position on the Adriatic margin than units affected by this metamorphism (Fig. 11). In the central Dinarides, the youngest deposits directly overthrust by the Neotethyan ophiolites and ophiolitic mélange have so far been described from

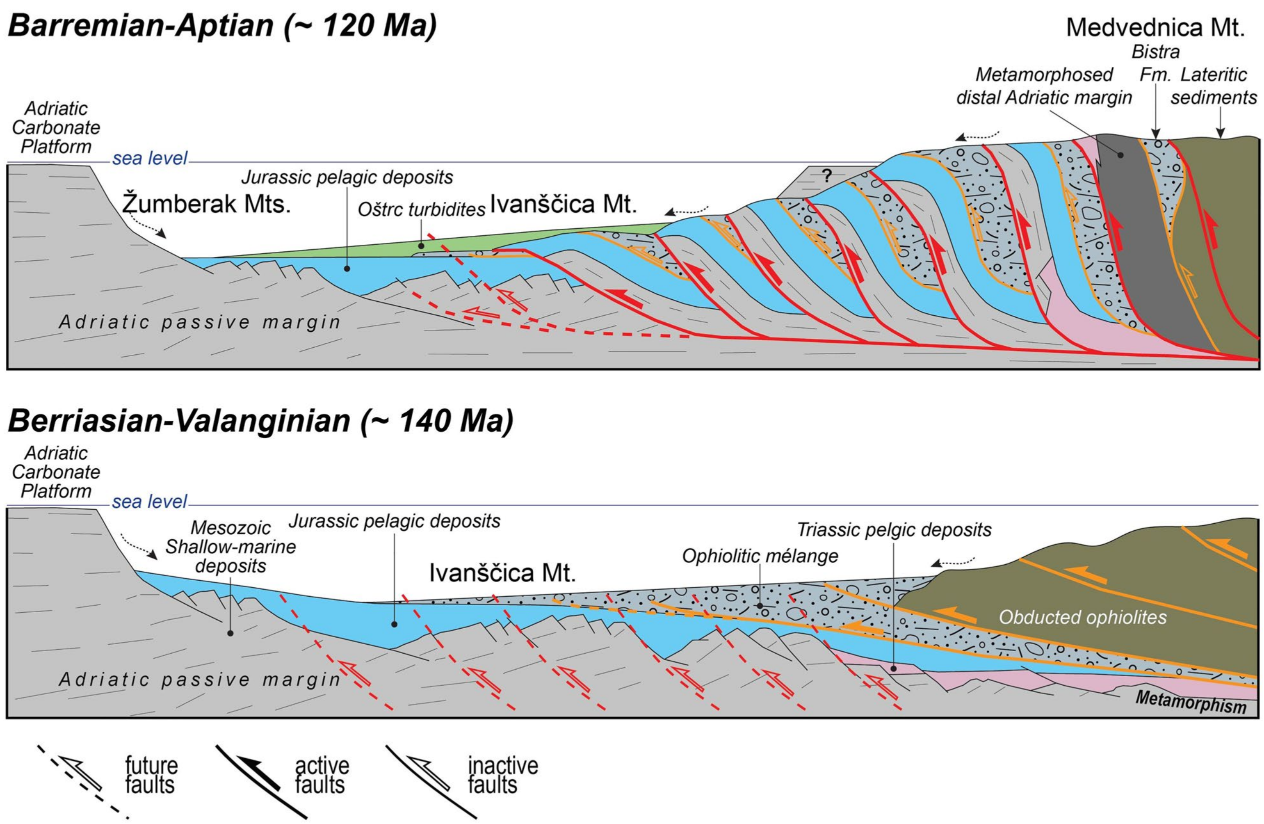


**Fig. 11** Schematic geodynamic reconstruction of the wider study area (northwesternmost Internal Dinarides) during Early Cretaceous. Different symbology is used for the faults to represent different stages in their activity as explained in the legend. Orange coloured faults were formed during D3 event related to the obduction of ophiolites and ophiolitic mélange. D3 obduction caused metamorphism in the distal domains of the Adriatic passive margin (e.g. Medvednica Mt.), while proximal domains experienced thermal overprint. Red coloured faults were formed in subsequent D4 event and are responsible for the exhumation of Adriatic passive margin successions together with overlaying ophiolitic mélange, which enable their erosion and resedimentation within turbidites of the Oštrc Fm

the East Bosnian-Durmitor thrust sheet where the ophiolitic mélange is found in a tectonic position above Tithonian to Berriasian pelagic limestone (Vishnevskaya et al., 2009). This limestone is correlative to the Aptychus Limestone from Ivanščica, although its age is constrained within a shorter stratigraphic range. Middle Triassic to Lower Cretaceous succession exposed on Ivanščica Mt. and attributed to the Adriatic continental margin correlate well with contemporaneous successions described from the Pre-Karst unit of the central Dinarides (Vukovski et al., 2023 with references).

Population of detrital zircons from the Oštrc Fm. with an Early Cretaceous cooling ages (ca. 145 – 134 Ma; Lužar-Oberiter et al., 2012) was sourced from these more internal units (e.g. Medvednica Mt.), where zircons were reset due to obduction (D3) and exhumed during subsequent D4 event.

The second contractional event recorded by deformational structures documented in the IIF and IP structural domains of Ivanščica Mt. is the D4 event. It resulted in the formation of contractional structures observed at different scales. These include NW verging imbricates of the IIF structural domain, which comprise the Repno complex and its tectonic footwall consisting of the Upper Triassic and Jurassic Adriatic passive margin succession (Figs. 5, 11). NW-ward directed thrusting of the IIF structural domain over the IP structural domain along the ČMT (Fig. 5), the formation of the BZBT (Figs. 5, 6h), NW-ward reverse faulting in the IP structural domain (Fig. 2) and intense pervasive folding of non-competent Jurassic to Lower Cretaceous pelagic deposits within both structural domains are also attributed to this deformational event (Fig. 6a–f). Sedimentological evidence supports a late Early Cretaceous age of this contractional event. The youngest deposits affected by this event are turbidites of the Hauterivian to Albian Oštrc Fm., thus indicating that this event should be at least partly post Albian in age. However, as the Oštrc Fm. contains lithoclasts of the underlying uppermost Tithonian to Valanginian Aptychus limestone (Zupanič et al., 1981), we consider this formation as syn-tectonic with respect to D4 deformational event. In addition to lithoclasts of the Aptychus limestone, the Oštrc Fm. contains other shallow-marine to pelagic lithoclasts of Triassic-Jurassic age, as well as mafic volcanic lithoclasts and abundant Cr-spinel grains (Zupanič et al., 1981). The source of all these lithoclasts and Cr-spinels is seen in the imbricates of the IIF (Figs. 5, 11). This indicates a strong, tectonically induced, fast syn-sedimentary Hauterivian to Albian exhumation and erosion of the uppermost Triassic to lowermost Cretaceous Adria passive margin succession together with the tectonically overlaying Repno complex (Fig. 11). This is in agreement with our AFT time–temperature models (Fig. 10) suggesting fast tectonically induced Early Cretaceous cooling and exhumation. The upper age limit of D4 event cannot be precisely constrained on Ivanščica Mt. due to the lack of post-tectonic cover deposits older than upper Egerian (lower Aquitanian). However, on the neighbouring Medvednica Mt. a correlative deformational event, D1 of van Gelder et al. (2015) or D2 of Tomljenović et al. (2008), predates the Late Cretaceous transgression and deposition of the Gosau-type sediments (Glog Fm.; Lužar-Oberiter et al., 2012 with references). Considering an Oligocene-earliest Miocene ca. 130° clockwise rotation of the block carrying Medvednica and neighbouring northern Croatian mountains (including Ivanščica) proposed by Tomljenović et al. (2008), the original trend of the D4 deformational structures documented on Ivanščica would be NW–SE and with top SW direction of tectonic transport. In that case, the initial pre-Miocene orientation and vergence of the D4 structures on Ivanščica Mt. would correspond well with contemporaneous and commonly observed SW verging structures in the Internal Dinarides (Dimitrijević, 1997; Tari, 2002; Schmid et al., 2008; Schefer, 2010; Porkoláb et al., 2019, Nirta et al., 2020).

The thermal overprint recorded in Mesozoic sediments of the IP structural domain likely reflect the D4 deformational event, since unlike the IIF structural domain, the IP was not overthrust by an ophiolitic mélange unit. Instead, continuous sedimentation of the Oštrc Fm. on top of the Aptychus limestone is recorded in the IP structural domain (Figs. 2, 5). Therefore, we propose that peak temperature conditions in the IP structural domain were reached during D4 thrusting of the IIF structural domain over the IP, soon followed by the exhumation and cooling due to propagation of this thrusting towards the Adriatic foreland. In-sequence D4 thrusting is supported by the presence of the syn-tectonic Oštrc Fm. exclusively found in the leading sector of the IIF (Figs. 2, 5 and 11). Conodont fragments from Middle Triassic limestone exhibit CAI (conodont alteration index) value of 5–6 (Kukoč et al., 2023) corresponding to a minimum temperature of 300 °C which is slightly higher but still comparable with our VR results.

In the central Internal Dinarides, contractional deformational event correlative with the D4 documented on Ivanščica postdates the ophiolite obduction and predates the deposition of Upper Cretaceous 'overstepping' sequences (see in Nirta et al., 2020). Here, this event is manifested in SW-ward nappe stacking, exhumation, erosion and re-deposition of passive margin units of the distal Adriatic margin together with overlaying ophiolitic units (Schmid et al., 2008; Schefer 2010; Tremblay et al., 2015; Porkolab et al., 2019; Nirta et al., 2020), also affecting the syn-orogenic turbiditic Vranduk Fm. and its proximal equivalent the Pogari Fm. (Mikes et al., 2008; Nirta et al., 2020). These formations are correlative with syn-orogenic Hauterivian to Albian Oštrc Fm. and Aptian–Albian shallow-water Bistra Fm. (Gušić, 1975; Crnjaković, 1989; Lužar-Oberiter et al., 2012) unconformably overlying the Repno Complex in Medvednica Mt. Still, Oštrc and Bistra formations are younger than the Vranduk and Pogari formations (Mikes et al., 2008; Nirta et al., 2020 with references therein; Hrvatović, 2022), thus suggesting younger age of D4 deformations and more forelandward position of Ivanščica Mt. during this event.

In the Eastern Alps, Early Cretaceous contractional deformational event correlative with the D4 event of Ivanščica is well-known as the Eo-Alpine event characterized by WNW-ward stacking of the Austroalpine nappe units (Fig. 12; Neubauer et al., 1999; Schmid et al., 2008, 2020 and references therein) and a deposition of the syn-orogenic Rossfeld Formation of late Valanginian to Aptian age (~ 135 – 110 Ma; Faupl & Wagreich, 2000). Moreover, a regional Early Cretaceous event is documented along the whole East Alpine-Dinaridic-Hellenic belt (Neubauer et al., 1999; Schefer, 2010; Bortolotti et al., 2013), including the Western Carpathians (Plašienka et al., 1997a, b). In general, it is interpreted as related to the closure of the northern branch of the Neotethys Ocean (Fig. 12; Schmid et al., 2008; 2020; Nirta et al., 2018, 2020).

The D4 event resulted in a regional emersion recorded on Ivanščica Mt. as well as throughout the Dinarides and the Eastern Alps. The oldest sediments covering Mesozoic formations on Ivanščica Mt. are upper Egerian (lower Aquitanian) clastic deposits (Fig. 2). Locally across the Dinarides, this emersion was considerably shorter and lasted until the Late Cretaceous when 'overstepping sediments' were deposited on top of Mesozoic formations (Nirta et al., 2020; Hrvatović, 2022). Similarly, in the Medvednica Mt. these sediments are known as Gosau-type deposits and are of Santonian to Paleocene age (Crnjaković, 1979). Additionally, lateritic sediments on top of serpentinites are found at the base of a Campanian rudist limestone (Palinkaš et al., 2006; Moro et al., 2010). Another evidence of emersion can be found in bauxite deposits on the neighbouring Ravna gora Mt. formed on top of Triassic dolomites, likely exhumed during the D4 event. Bauxites are sealed by upper Eocene Foraminiferal limestone (Šimunić et al., 1981; Šimunić, 1992; Ćosović & Drobne, 2000). Post Early Cretaceous emersion in the study area suggests that Late Cretaceous to Eocene sedimentary burial cannot be the explanation for the thermal overprint, as it is interpreted for the area of "Sava folds" and further westward in Slovenian Basin where continuous latest Cretaceous to middle Eocene sedimentation resulted in deposition of at least 5 km of flysch type sediments (Rainer et al., 2016). Records of this emersion, which lasted from latest Jurassic to earliest Cretaceous until the Late Turonian transgression and the deposition of the Lower Gosau Group are found in the Austroalpine unit and the Western Carpathians (Wagreich & Faupl, 1994; Wagreich & Marschalko, 1995; Stern & Wagreich; 2013; Steiner et al., 2021).

The cooling trajectories of the AFT samples obtained in this study indicate a tectonically stable period with only minor fluctuations after the fast cooling related to the D4 event (Fig. 10). The central ages of 56.4 ± 2.5 Ma for sample GV-1609 and 67.3 ± 5.4 Ma for sample GV-1625 are the result of a long-lasting period during which these samples remained around the lower limit of the APAZ (Fig. 10). For this reason, we suppose that the IP and the IIF structural domains were not affected by any major deformation postdating D4 Early Cretaceous contraction and predating D5 Early Miocene extension.

#### *4.1.3 Neogene-recent tectonic evolution*

NE dipping low angle listric normal growth faults documented on reflection seismic sections (Fig. 8), associated with ENE striking dextral strike-slip faults around the prominent Early Miocene syn-rift depocenters N of Ivanščica Mt. (Figs. 1c, 2) are attributed to the D5

(See figure on next page.)

**Fig. 12** An overview and correlation of the most important tectonic events documented on Ivanščica Mt. (Kukoč et al., 2023, Slovenec et al., 2023; Vukovski et al., 2023 and the results of this study), in the eastern Southern Alps (Doglioni & Bosellini, 1987; Castellarin et al., 1992; Doglioni, 1992; Sarti et al., 1992; Bertotti et al., 1993; Channell, 1996; Schönborn, 1999; Mandl, 2000), the Eastern Alps (Kozur, 1991; Ratschbacher et al., 1991; Schmid et al., 1996; Dunkl & Demény, 1997; Froitzheim et al., 1997; Neubauer et al., 1999; Willingshofer et al., 1999a, b; Faupl and Wagreich, 2000; Mandl, 2000; Böhm, 2003; Thöni, 2006; Gawlick et al., 2009; Missoni & Gawlick, 2011a, b; Favaro et al., 2015; Rosenberg et al., 2015; Gawlick & Missoni, 2019; Fodor et al., 2021), Dinarides (Gušić & Babić, 1970; Lanphere et al., 1975; Dragičević & Velić, 2002; Lugović et al., 2006; Schmid et al., 2008; Ustaszewski et al., 2009; Smirčić et al., 2018, 2020; Porkolab et al., 2019; van Unen et al., 2019a, b; Nirta et al., 2020; Šegvić et al., 2020; Balling et al., 2023; Slovenec & Šegvić, 2024), Pannonian Basin (Tomljenović, 2002; Tomljenović & Csontos, 2001; Horváth et al., 2006; Balázs et al., 2016) and nearby Medvednica Mt. (Tomljenović et al., 2008; van Gelder et al., 2015; Mišur et al., 2023). Note how the tectonic events are linked with the geodynamic processes within the Neotethys Ocean (Channell & Kozur, 1997; Stampfli & Borel, 2002; 2004, Schmid et al., 2004). Time scale after Cohen et al., (2013; updated). *DLS* Dinaride Lake System, *SSZ* supra subduction zone

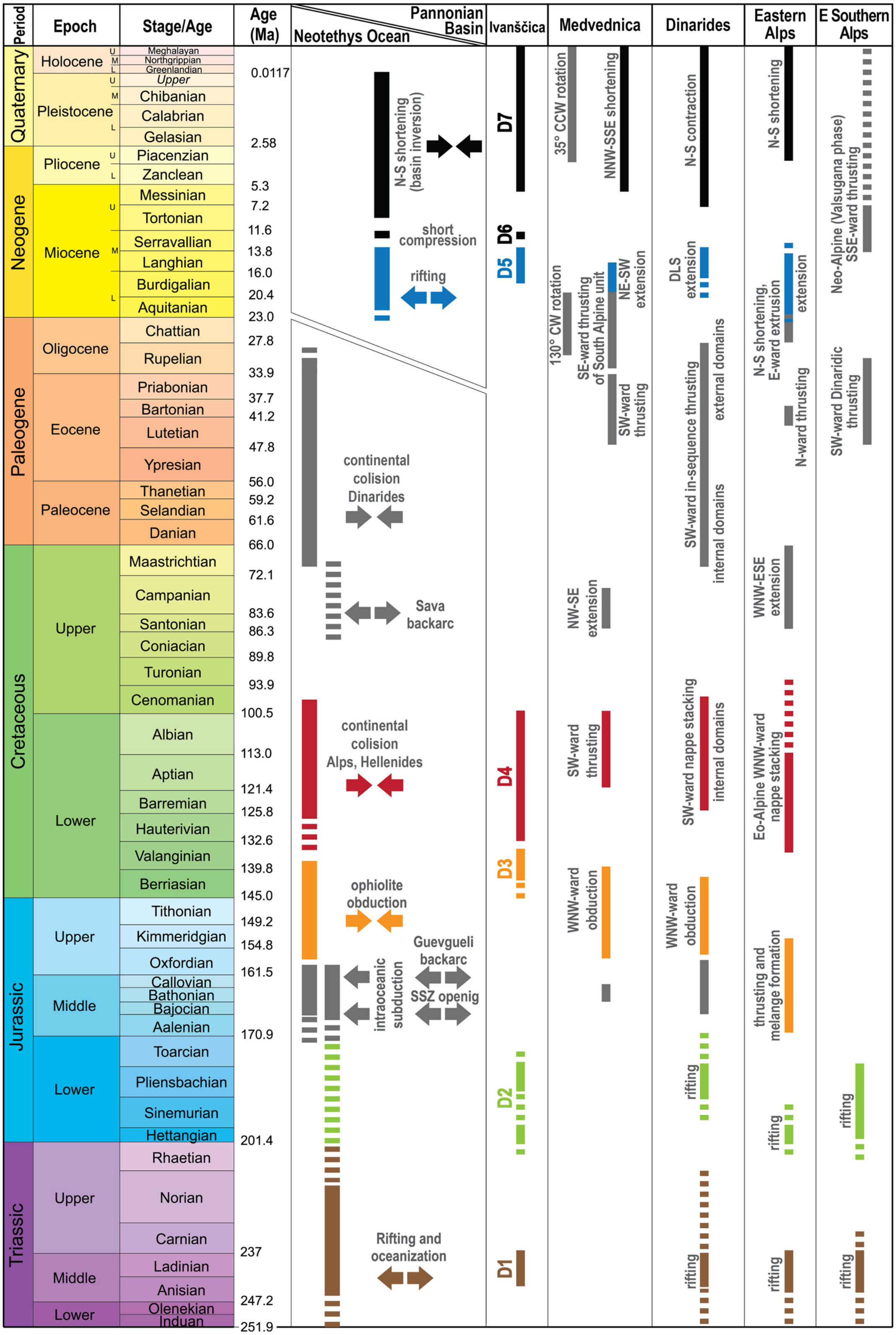


**Fig. 12** (See legend on previous page.)

deformational event that resulted in Early Miocene NE-SW directed extension. The D5 normal faults crosscut older structures (Fig. 5) with only sporadic evidence for their later inversion or reactivation. The termination of D5 extension is marked by the late Badenian (early Serravallian) transgression and deposition of clastic to carbonate sediments, which seal Early Miocene rift structures (Figs. 8, 9). The termination of this event corresponds with a gradual decrease in volcanic activity during late Middle Miocene in the Pannonian Basin (Balázs et al., 2016; Pavelić & Kovačić, 2018). Onlapping of Pannonian (Tortonian to lower Zanclean) over Sarmatian (upper Serravallian) sediments indicates a late Sarmatian (latest Serravallian) short-lived contraction (D6), also documented in reflection seismic sections near Medvednica Mt. by Tomljenović & Csontos (2001). It resulted in partial reactivation of the D5 normal listric faults into reverse faults (Fig. 8). The subsequent stage of thermal subsidence well documented across the entire Pannonian Basin area was characterised by filling of accommodation space and gradual filling of the basin during Late Miocene and Pliocene times (Kovačić et al., 2004; Sebe et al., 2020).

The youngest deformation event (D7) is of Late Miocene to recent age, and characterized by NNW-SSE contraction. To the north of Ivanščica Mt., this contraction is accommodated by the reactivation of ENE striking dextral faults (e.g. Šoštanj fault; Fig. 7d, e) and by formation of E to ENE trending km large folds and SE striking dextral faults (Fig. 2). Here, reverse faulting is mostly accommodated along local transpressional ramps of major strike-slip faults. The influence of strike-slip faulting decreases sharply to the south at the N to NW verging Prigorec reverse fault (Figs. 2, 5), which possibly represents Early Cretaceous D4 fault reactivated during D7 Late Miocene-Present contraction. This fault is responsible for NW-ward high angle thrusting of the Permo–Mesozoic units of the IP and passively transported IIF over upper Oligocene and Miocene deposits, inclination of homoclinal S to SE dipping Miocene strata in the southern slopes of the mountain (Fig. 5), and final uplift of Ivanščica. The SE striking Gotalovec – Prigorec dextral fault is attributed to the D7 event according to the late Pannonian (late Messinian) age of deformed strata. To the south and towards the Medvednica Mt., the same NNW-SSE contraction resulted in the formation of series of E to ENE trending, tens of kilometres long anticlines and synclines, with small offset reverse faults developed in the limbs of anticlines (Figs. 8, 9). Onlapping and thinning of syn-tectonic strata along the flanks of anticlines indicate that the main stage of folding started in the late Pannonian (late Messinian; Figs. 8, 9). This deformation and timing correlates well with previous field kinematic studies and interpretations of seismic data from wider study area (Placer, 1999b; Tomljenović & Csontos, 2001; van Gelder et al., 2015; Balázs et al., 2016).

### 4.2 Tectonic position of Ivanščica Mt.

Earlier studies considered Ivanščica, for the most part, as a S verging Neogene nappe of the South Alpine unit, thrusted over the ophiolitic mélange of the Western Vardar ophiolitic unit of the Dinarides (Repno complex; Fig. 1c; Placer, 1999a; Schmid et al., 2008, 2020; van Gelder et al., 2015). Our investigation did not reveal any S to SE verging thrust of Miocene age. The only SE verging fault is the BZBT, the location and kinematics of which partially coincides with the frontal thrust of the South Alpine unit according to Placer, (1999a), van Gelder et al. (2015) and Schmid et al. (2020). However, the BZBT is sealed by upper Egerian (lower Aquitanian) deposits and thus predates Oligocene–earliest Miocene rotation. Furthermore, we interpret the BZBT to be Early Cretaceous in age (see Sect. 4.1.2.). Therefore, the initial top-NE vergence of the BZBT and its Early Cretaceous age oppose the interpretation about SE-ward Miocene thrust. In addition, the main shortening phase in the South Alpine unit (the Valsugana phase, ca. 14–8 Ma, Castellarin et al., 1992; Doglioni, 1992; Castellarin & Canteli, 2000; Zattin et al., 2003, 2006), was coeval with the regional transgression and the deposition of shallow-water to pelagic sediments in the study area (Fig. 12), including whole Pannonian Basin (Balázs et al., 2016; Pavelić & Kovačić, 2018 and references therein). However, the same driving process which caused thrusting within the South Alpine unit, the indentation and CCW rotation of Adria, is responsible for the late Pannonian (late Messinian; ~ 6 Ma) to recent contraction (D7). In the area of the Dinarides and the Pannonian Basin, this contraction resulted in folding, reverse and strike-slip faulting (Tomljenović & Csontos, 2001; Balázs et al., 2016; van Unen et al., 2019a, b). In contrast, at the same time the South Alpine unit was characterised by thrusting (Castellarin et al., 1992; Picotti et al., 2022). Hence, in contrast to the previous studies, our data suggest that the study area was not affected by the Miocene S-ward retro wedge thrusting characteristic for the South Alpine unit. Instead of S-ward thrusting, in the study area indentation of Adria was manifested by folding, reverse and strike-slip faulting. Considering the Mesozoic tectono-sedimentary evolution of Ivanščica Mt. (Figs. 3, 12) as described earlier in the discussion, we interpret paleogeographic affiliation of its non-ophiolitic Mesozoic structural-stratigraphic entities to the Pre-Karst unit of the Dinarides. The Repno complex belongs to the Western Vardar ophiolitic unit representing its northwesternmost outcrops. Up to now, this is the only known location where ophiolitic mélange of the Western Vardar ophiolitic unit is in the primary obduction thrust contact with underlying successions of the Pre-Karst unit (Figs. 5, 11).

## 5 Conclusion

Ivanščica Mt., an inselberg in the Alpine—Dinaridic transitional zone of northern Croatia, is divided into two structural domains: Ivanščica Parautochthon and Ivanščica Imbricate Fan overlain by Cenozoic sedimentary cover.

By implementation of a multi-scale structural analysis, AFT, and VR data, four contractional and one extensional event have been recorded on Ivanščica Mt. In addition, two older extensional events were recognized based on the Mesozoic tectono-sedimentary record. Middle Triassic (D1) and Early Jurassic (D2) extensional events related to the opening of the Neotethys Ocean and Alpine Tethys respectively are recorded in volcano-sedimentary successions of the IP and the IIF structural domains.

Late Berriasian to Valanginian (~ 140 Ma) contraction (D3) is manifested with tectonic emplacement of the ophiolitic mélange of the Repno Complex over the stratigraphic successions of the Adriatic passive margin in the IIF structural domain and their thermal overprint.

The following contractional event (D4) was a NW-ward imbrication, thrusting of the IIF structural domain over the IP structural domain along the ČMT and thermal overprint of sedimentary succession of the IP. Syn-deformational Hauterivian to Albian Oštrc Fm. and our AFT modelling results provide age constraints for this deformational event (~ 133–100 Ma). When considering the post Oligo-Miocene rotations, initial NW trending and SW verging structures attributed to D4 deformational event coincide with the typical Dinaridic structural trend. This deformational event is a result of continued contraction related to the closure of the northern branch of the Neotethys Ocean and finally resulted in long lasting emersion in the Ivanščica Mt.

The youngest extensional event (D5) is characterized by formation of NE dipping predominantly listric normal faults and ENE striking dextral faults, as a consequence of ongoing extension in the Pannonian Basin. Timing of deformation is constrained by the Ottnangian (middle Burdigalian) to middle Badenian (late Langhian) age (~ 18–14 Ma) of syn-rift deposits observed on the reflection seismic and well data. In the early post-rift stage, short lasting late Sarmatian (late Serravallian; ~ 12 Ma) contraction is registered (D6), preceding the main stage of the basin inversion.

The youngest recorded deformational event (D7) characterised by late Pannonian (late Messinian; ~ 6 Ma) to recent NNW-SSE contraction, resulted in reactivation of ENE striking dextral faults, formation of new SE striking dextral faults as well as the formation of E to ENE trending folds and reverse faults. This event is a result of the N-ward indentation and CCW rotation of the Adriatic microplate. Overall Miocene and post-Miocene deformation history of the study area is in agreement with well-known Pannonian back-arc tectonics starting in the Early Miocene.

Our results infer that the study area was affected by tectonic processes related to the different stages of the evolution of the Neotethys Ocean, opening of the Alpine Tethys Ocean, as well as the opening and inversion of the Pannonian Basin. Mesozoic tectono-sedimentary evolution of Ivanščica Mt. proves the paleogeographic affiliation of its non-ophiolitic Mesozoic structural-stratigraphic entities to the Pre-Karst unit of the Dinarides.

**Abbreviations**

| | |
|---|---|
| AFT | Apatite fission track |
| APAZ | Apatite partial annealing zone |
| BZBT | Babin Zub back-thrust |
| CCW | Counter clockwise |
| CSC | Cenozoic sedimentary cover |
| ČMT | Črne Mlake thrust |
| Dn | Deformational event (n is the number indicating the relative age of the event where the number 1 is the oldest event) |
| DLS | Dinaride Lake System |
| GPF | Gotalovec-Prigorec fault |
| IIF | Ivanščica Imbricate Fan |
| IP | Ivanščica Parautochthon |
| MSWD | Mean square of weighted deviates |
| n | Number of used data |
| PRF | Prigorec reverse fault |
| P(χ2) | Probability of obtaining chi-square ($\chi^2$) for n degrees of freedom (n is the number of crystals |
| SSZ | Supra subduction zone |
| ŠF | Šoštanj fault |
| TAI | Thermal alteration index |
| VR | Vitrinite reflectance |

**Acknowledgements**

László Csontos (MOL Group) and Michele Marroni (Università di Pisa) are gratefully acknowledged for their reviews and suggestions that have significantly improved the first version of the manuscript. The authors would like to thank to Matija Šimunić for providing the photo in Fig. 6h. The authors are especially grateful to the editors Daniel Marty (Naturhistorisches Museum Basel) and Stefan M. Schmid (Universität Basel) for coordinating the publishing process and additional and very helpful comments and suggestions by Stefan M. Schmid. This research was supported by the Croatian Science Foundation under the project "Revealing the Middle Triassic Paleotethyan Geodynamics Recorded in the Volcano-Sedimentary Successions of NW Croatia (GOST)" (IP-2019–04-3824).

**Author contributions**

Matija Vukovski: conceptualization, methodology, field work (lead), analysis (structural), investigation, writing—original draft, review and editing (lead); Marko Špelić: analysis (seismic sections), writing—original draft, review and editing (equal); Duje Kukoč: field work (supporting), writing—original draft, review and editing (equal); Tamara Troskot-Čorbić: analysis (vitrinite reflectance), writing—original draft, review and editing (equal); Tonći Grgasović: field work (supporting), writing—review and editing (supporting); Damir Slovenec: writing—review and editing (supporting); Bruno Tomljenović: conceptualization, methodology, field work (supporting), writing—original draft, review and editing (supporting).

**Funding**
This research was funded by the Croatian Science Foundation under the project "Revealing the Middle Triassic Paleotethyan Geodynamics Recorded in the Volcano-Sedimentary Successions of NW Croatia (GOST)" (IP-2019-04-3824).

**Data availability**
All data generated or analysed during this study are included in this article.

## Declarations

**Competing interests**
The authors have no competing interests to declare that are relevant to the content of this article.

**Author details**
[1]Croatian Geological Survey, Sachsova 2, 10000 Zagreb, Croatia. [2]INA -Oil Company, Plc., Exploration & Production, E&P Laboratory, Lovinčićeva 4, 10000 Zagreb, Croatia. [3]Faculty of Mining, Geology and Petroleum Engineering, University of Zagreb, Pierottijeva 6, 10000 Zagreb, Croatia.

Received: 26 February 2024 Accepted: 13 June 2024
Published online: 02 September 2024

**References**

Aničić, B. & Juriša, M. (1984). Osnovna geološka karta SFRJ 1:100,000, list Rogatec L33–68 (Basic Geological Map of SFRY 1:100,000, Rogatec sheet). Geološki zavod Ljubljana and Geološki zavod Zagreb, Savezni geološki zavod.

Atanackov, J., Jamšek Rupnik, P., Jež, J., Celarc, B., Novak, M., Milanič, B., Markelj, A., Bavec, M. & Kastelic, V. (2021). Database of active faults in Slovenia: Compiling a new active fault database at the junction between the Alps, the Dinarides and the Pannonian Basin Tectonic Domains. *Frontiers in Earth Science*, *9*, 604388. https://doi.org/10.3389/feart.2021.604388.

Avanić, R., Pavelić, D., Pécskay, Z., Miknić, M., Tibljaš, D., & Wacha, L. (2021). Tidal deposits in the Early Miocene Central Paratethys: The Vučji Jarek and Čemernica members of the Macelj formation (NW Croatia). *Geologia Croatica, 74*, 41–56.

Babić, Lj. (1974). Jurassic-Cretaceous sequence of Mt Ivanščica (Northern Croatia). *Bulletin Scientifique Conseil Des Académies Des Sciences Yougoslavie, 19*(7–8), 181–182.

Babić, Lj. (1976). Pomak granice između unutrašnje i vanjske Dinarske regije, primjer šireg područja Žumberka (Migration of the boundary between "inner" and "outer" Dinaric zones). *The 8th Yugoslavian Geological Congress, 2*, 45–51.

Babić, Lj., Hochuli, P. A., & Zupanič, J. (2002). The Jurassic ophiolitic mélange in the NE Dinarides: Dating, internal structure and geotectonic implications. *Eclogae Geologicae Helvetiae, 95*, 263–275.

Babić, Lj., & Zupanič, J. (1973). Uppermost Jurassic and Early Cretaceous deposits on Mt. Ivanščica—northern Croatia. *Geološki Vjesnik, 26*, 267–272.

Babić, Lj., & Zupanič, J. (1978). Mlađi mezozoik Ivanščice. In Lj. Babić & V. Jelaska (Eds.), *Vodič ekskurzije 3. Skupa sedimentologa Jugoslavije* (pp. 11–23). Zagreb: Croatian Geological Society.

Balázs, A., Matenco, L., Magyar, I., Horváth, F., & Cloetingh, S. (2016). The link between tectonics and sedimentation in back-arc basins: New genetic constraints from the analysis of the Pannonian Basin. *Tectonics, 35*(6), 1526–1559.

Balling, P., Tomljenović, B., Herak, M., & Ustaszewski, K. (2023). Impact of mechanical stratigraphy on deformation style and distribution of seismicity in the central External Dinarides: A 2D forward kinematic modelling study. *Swiss Journal of Geosciences, 116*, 7.

Barker, C. E., & Pawlewicz, M. J., et al. (1994). Calculation of vitrinite reflectance from thermal histories and peak temperatures a comparison of methods. In P. Mukhopadhyay (Ed.), *Vitrinite reflectance as a maturity parameter. ACS Symposium Series* (pp. 216–229). American Chemical Society.

Basch, O. (1981). Osnovna geološka karta SFRJ 1:100,000, list Ivanić-Grad L33–81 (Basic Geological Map of SFRY 1:100,000, Ivanić-Grad sheet). Geološki zavod Zagreb, Savezni geološki zavod.

Belak, M., Slovenec, D., Kolar Jurkovšek, T., Garašić, V., Pécskay, Z., Tibljaš, D., & Mišur, I. (2022). Low-grade metamorphic rocks of the Tethys subduction–collision zone in the Medvednica Mt. (NW Croatia). *Geologica Carpathica, 73*(3), 207–229.

Belak, M., & Tibljaš, D. (1998). Discovery of blueschists in the Medvednica Mountain (Northern Croatia) and their significance for the interpretation of the geotectonic evolution of the area. *Geologia Croatica, 51*(1), 27–32.

Bertotti, G., Picotti, V., Bernoulli, D., & Castellarin, A. (1993). From rifting to drifting: Tectonic evolution of the South-Alpine upper crust from the Triassic to the Early Cretaceous. *Sedimentary Geology, 86*, 53–76.

Blanchet, R., Cadet, J.-P., & Charvet, J. (1970). Sur l'existence d'unites intermediaires entre la zone du Haut-Karst et l'unite du flysch bosniaque, en Yougoslavie; la sous-zone prekarstique. *Bulletin De La Société Géologique De France, S7-XII*(2), 227–236.

Böhm, F. (2003). Lithostratigraphy of the Adnet Group (Lower to Middle Jurassic, Salzburg, Austria). In W. E. Piller (Ed.), *Stratigraphia Austriaca—Österr Akad Wiss Schriftenr Erdwiss Komm* (Vol. 16, pp. 231–268). VÖAW.

Bortolotti, V., Chiari, M., Marroni, M., Pandolfi, L., Principi, G., & Saccani, E. (2013). Geodynamic evolution of ophiolites from Albania and Greece (Dinaric–Hellenic belt): One, two, or more oceanic basins? *International Journal of Earth Sciences, 102*, 783–811.

Bostick, N. H. (1979). Microscopic measurements of the level of catagenesis of solid organic matter in sedimentary rocks to aid exploration for petroleum and to determine former burial temperatures—A review. *SEPM, Special Publication, 26*, 17–43.

Buser, S. (1977). Osnovna geološka karta SFRJ 1:100,000, list Celje L33–67 (Basic Geological Map of SFRY 1:100,000, Celje sheet). Geološki zavod Ljubljana, Savezni geološki zavod.

Castellarin, A., & Canteli, L. (2000). Neo-Alpine evolution of the Southern Eastern Alps. *Journal of Geodynamics, 30*, 251–274.

Castellarin, A., Cantelli, L., Fesce, A. M., Mercier, J. L., Picotti, V., Pini, G. A., Prosser, G., & Selli, L. (1992). Alpine compressional tectonics in the Southern Alps. Relationships with the N-Apennines. *Annales Tectonicae, 6*(1), 62–94.

Channell, J. E. T. (1996). Palaeomagnetism and palaeogeography of Adria. *Geological Society, London, Special Publications, 105*(1), 119–132.

Channell, J. E. T., & Kozur, H. W. (1997). How many oceans? Meliata, Vardar, and Pindos oceans in Mesozoic Alpine palaeogeography. *Geology, 25*, 183–186.

Cohen, K. M., Finney, S. C., Gibbard, P. L., & Fan, J.-X. (2013). The ICS International Chronostratigraphic Chart. *Episodes, 36*, 199–204.

Ćosović, V., & Drobne, K. (2000). Some remarks on Nummulites specimens from localities in south-eastern Slovenia and north-western Croatia. In D. Bassi (Ed.), *Shallow water benthic communities at the Middle-Upper Eocene boundary (Southern and north-eastern Italy, Slovenia, Croatia, Hungary)* (pp. 14–15). Annali dell'Università di Ferrara.

Crnjaković, M. (1979). Sedimentation of transgressive Senonian in Southern Mt. Medvednica [In Croatian with English summary]. *Geološki Vjesnik, 32*, 81–95.

Crnjaković, M. (1989). Lower Cretaceous shallow marine deposits in Mt. Medvednica [In Croatian with English summary]. *Acta Geologica Zagreb, 19*, 61–93.

Dimitrijević, M. D. (1997). *Geology of Yugoslavia* (2nd ed.). Geoinstitute.

Doglioni, C. (1992). Relationships between Mesozoic extensional tectonics, stratigraphy and Alpine inversion in the Southern Alps. *Eclogae Geologicae Helvetiae, 85*, 105–126.

Doglioni, C., & Bosellini, A. (1987). Eoalpine and mesoalpine tectonics in the Southern Alps. *Geologische Rundschau, 76*, 735–754.

Doglioni, C., Harabaglia, P., Merlini, S., Mongelli, F., Peccerillo, A., & Piromallo, C. (1999). Orogens and slabs vs their direction of subduction. *Earth Science Reviews, 45*(3–4), 167–208.

Dragičević, I., & Velić, I. (2002). The northeastern margin of the Adriatic Carbonate Platform. *Geologia Croatica, 55*(2), 185–232.

Dunkl, I., & Demény, A. (1997). Exhumation of the Rechnitz Window at the border of the Eastern Alps and Pannonian Basin during Neogene extension. *Tectonophysics, 272*(2–4), 197–211.

Faccenna, C., Becker, T. W., Conrad, C. P., & Husson, L. (2013). Mountain building and mantle dynamics. *Tectonics, 32*, 1–15.

Faccenna, C., Piromallo, C., Crespo-Blanc, A., Jolivet, L., & Rosetti, F. (2004). Lateral slab deformation and the origin of the western Mediterranean arcs. *Tectonics*. https://doi.org/10.1029/2002TC001488

Faupl, P., & Wagreich, M. (2000). Late Jurassic to Eocene palaeogeography and geodynamic evolution of the Eastern Alps. *Mitteilungen der Österreichischen Geologischen Gesellschaft, 92*, 79–94.

Favaro, S., Schuster, R., Handy, A., Scharf, A., & Pestal, G. (2015). Transition from orogen-perpendicular to orogen-parallel exhumation and cooling during crustal indentation—Key constraints from 147Sm/ 144Nd and 87Rb/ 87Sr geochronology (Tauern Window, Alps). *Tectonophysics, 665*, 1–16.

Fodor, L., Balázs, A., Csillag, G., Dunkl, I., Héja, G., Jelen, B., Kelemen, P., Kövér, S., Németh, A., Nyíri, D., Selmeczi, I., Trajanova, M., Vrabec, Ma., & Vrabec, Mi. (2021). Crustal exhumation and depocenter migration from the Alpine orogenic margin towards the Pannonian extensional back-arc basin controlled by inheritance. *Global and Planetary Change*. https://doi.org/10.1016/j.gloplacha.2021.103475

Fodor, L., Jelen, B., Márton, E., Skaberne, D., Car, J., & Vrabec, M. (1998). Miocene-Pliocene tectonic evolution of the Slovenian Periadriatic fault: Implications for Alpine-Carpathian extrusion models. *Tectonics, 17*(5), 690–709.

Froitzheim, N., Conti, P., & van Daalen, M. (1997). Late Cretaceous, synorogenic, low-angle normal faulting along the Schlinig fault (Switzerland, Italy, Austria) and its significance for the tectonics of the Eastern Alps. *Tectonophysics, 280*(3–4), 267–293.

Froitzheim, N., & Eberli, G. P. (1990). Extensional detachment faulting in the evolution of a Tethys passive continental margin, Eastern Alps, Switzerland. *Geological Society of America Bulletin, 102*(9), 1297–1308.

Froitzheim, N., & Manatschal, G. (1996). Kinematics of Jurassic rifting, mantle exhumation, and passive-margin formation in the Austroalpine and Penninic nappes (eastern Switzerland). *Bulletin of the Geological Society of America, 108*, 1120–1133.

Gawlick, H. J., & Missoni, S. (2019). Middle-Late Jurassic sedimentary mélange formation related to ophiolite obduction in the Alpine-Carpathian-Dinaridic Mountain Range. *Gondwana Research, 74*, 144–172.

Gawlick, H. J., Missoni, S., Schlagintweit, F., Suzuki, H., Frisch, W., Krystyn, L., Blau, J., & Lein, R. (2009). Jurassic Tectonostratigraphy of the Austroalpine domain. *Journal of Alpine Geology, 50*(1), 1–152.

Goričan, Š, Halamić, J., Grgasović, T., & Kolar-Jurkovšek, T. (2005). Stratigraphic evolution of Triassic arc-backarc system in northwestern Croatia. *Bulletin De La Société Géologique De France, 176*(1), 3–22.

Goričan, Š, Košir, A., Rožič, B., Šmuc, A., Gale, L., Kukoč, D., Celarc, B., Črne, A. E., Kolar-Jurkovšek, T., Placer, L., & Skaberne, D. (2012). Mesozoic deep-water basins of the eastern Southern Alps (NW Slovenia). *Journal of Alpine Geology, 54*, 101–143.

Gušić, I. (1975). Lower Cretaceous imperforate Foraminiferida of Mt. Medvednica, Northern Croatia (Families: Litoulidae, Ataxophragmidiidae, Orbitolinidae). *Paleontologica Jugoslavica, 14*, 7–48.

Gušić, I., & Babić, Lj. (1970). Neke biostratigrafske i litogenetske osobine jure Žumberka. *Geološki Vjesnik, 23*, 39–49.

Haas, J., Mioč, P., Pamić, J., Tomljenović, B., Arkai, P., Berczi-Makk, A., Koroknai, B., Kovács, S., & Felgenhauer, E. R. (2000). Complex structural pattern of the Alpine-Dinaridic-Pannonian triple junction. *International Journal of Earth Sciences, 89*, 377–389.

Halamić, J., Goričan, Š, Slovenec, D., & Kolar-Jurkovšek, T. (1999). A Middle Jurassic Radiolarite-Clastic Succession from the Medvednica Mt. (NW Croatia). *Geologia Croatica, 52*(1), 29–57.

Halamić, J., Marchig, V., & Goričan, Š. (2005). Jurassic radiolarian cherts in northwestern Croatia: Geochemistry, material provenance and depositional environment. *Geologica Carpathica, 56*(2), 123–136.

Hasebe, N., Barbarand, J., Jarvis, K., Carter, A., & Hurford, A. J. (2004). Apatite fission track chronometry using laser ablation ICP-MS. *Chemical Geology, 207*, 135–145.

Horváth, F., Bada, G., Szafián, P., Tari, G., Ádám, A., & Cloetingh, S. (2006). Formation and deformation of the Pannonian Basin: Constraints from observational data. *Geological Society London Memoirs, 32*(1), 191–206.

Hrvatović, H. (2022). *Geološki vodič kroz Bosnu i Hercegovinu*. Akademija nauka i umjetnosti Bosne i Hercegovine.

Jolivet, L., & Faccenna, C. (2000). Mediterranean extension and the Africa-Eurasia collision. *Tectonics, 19*(6), 1095–1106.

Judik, K., Rantitsch, G., Rainer, T. M., Árkai, P., & Tomljenović, B. (2008). Alpine metamorphism of organic matter in metasedimentary rocks from Mt. Medvednica (Croatia). *Swiss Journal of Geosciences, 101*, 605–616.

Ketcham, R. A. (2005). Forward and inverse modeling of low-temperature thermochronometry data. *Reviews in Mineralogy and Geochemistry, 58*(1), 275–314.

Ketcham, R. A., Carter, A., Donelick, R. A., Barbarand, J., & Hurford, A. J. (2007). Improved modeling of fission-track annealing in apatite. *American Mineralogist, 92*(5–6), 799–810.

Kissling, E., Schmid, S. M., Lippitsch, R., Ansorge, J., & Fügenschuh, B. (2006). Lithosphere structure and tectonic evolution of the Alpine arc: New evidence from high-resolution teleseismic tomography. *Geological Society, London, Memoirs, 32*(1), 129–145.

Kovačić, M., Zupanič, J., Babić, Lj., Vrsaljko, D., Miknić, M., Bakrač, K., Hećimović, I., Avanić, R., & Brkić, M. (2004). Lacustrine basin to delta evolution in the Zagorje Basin, a Pannonian sub-basin (Late Miocene: Pontian, NW Croatia). *Facies, 50*, 19–33.

Kozur, H. (1991). The evolution of the Meliata-Hallstatt ocean and its significance for the early evolution of the Eastern Alps and western Carpathians. *Palaeogeography Palaeoclimatology Palaeoecology, 87*, 109–135.

Kukoč, D., Slovenec, D., Šegvić, B., Vukovski, M., Belak, M., Grgasović, T., Horvat, M., & Smirčić, D. (2024). The early history of the Neotethys archived in the ophiolitic mélange of northwestern Croatia. *Journal of the Geological Society*. https://doi.org/10.1144/jgs2023-143

Kukoč, D., Smirčić, D., Grgasović, T., Horvat, M., Belak, M., Japundžić, D., Kolar-Jurkovšek, T., Šegvić, B., Badurina, L., Vukovski, M., & Slovenec, D. (2023). Biostratigraphy and facies description of Middle triassic rift-related volcano-sedimentary successions at the junction of the Southern Alps and the Dinarides (NW Croatia). *International Journal of Earth Sciences, 112*, 1175–1291.

Lanphere, M., Coleman, R. G., Karamata, S., & Pamić, J. (1975). Age of amphibolites associated with Alpine peridotites in the Dinaride ophiolite zone, Yugoslavia. *Earth and Planetary Science Letters, 26*, 271–276.

Lugović, B., Šegvić, B., Babajić, E., & Trubelja, F. (2006). Evidence for short-living intraoceanic subduction in the Central Dinarides, Konjuh Ophiolite Complex (Bosnia–Hercegovina). International Symposium on the Mesozoic Ophiolite Belts of the Northern Part of the Balkan Peninsula. Serbian Academy of Sciences and Arts, Commitee of Geodynamics, Belgrade, pp. 72–75. May 31st–June 6th, 2006.

Lugović, B., Slovenec, D., Halamić, J., & Altherr, R. (2007). Petrology, geochemistry and geotectonic affinity of the Mesozoic ultramafic rocks from the southwesternmost Mid-Transdanubian Zone in Croatia. *Geologica Carpathica, 58*(6), 511–530.

Lužar-Oberiter, B., Mikes, T., Dunkl, I., Babić, Lj., & von Eynatten, H. (2012). Provenance of cretaceous synorogenic sediments from the NW Dinarides (Croatia). *Swiss Journal of Geosciences, 105*, 377–399.

Lužar-Oberiter, B., Mikes, T., von Eynatten, H., & Babić, Lj. (2009). Ophiolitic detritus in Cretaceous clastic formations of the Dinarides (NW Croatia): Evidence from Cr-spinel chemistry. *International Journal of Earth Sciences, 98*, 1097–1108.

Magyar, I., Radivojević, D., Sztanó, O., Synak, R., Ujszászi, K., & Pócsik, M. (2013). Progradation of the paleo-Danube shelf margin across the Pannonian Basin during the Late Miocene and Early Pliocene. *Global and Planetary Change, 103*, 168–173.

Mandl, G. W. (2000). The Alpine sector of the Tethyan shelf—Examples of Triassic to Jurassic sedimentation and deformation from the Northern Calcareous Alps. *Mitteilungen Österreichische Geologische Gesellschaft, 92*, 61–77.

Márton, E., Pavelić, D., Tomljenovicć, B., Avanić, R., Pamić, J., & Márton, P. (2002). In the wake of a counterclockwise rotating Adriatic microplate: Neogene paleomagnetic results from Northern Croatia. *International Journal of Earth Sciences, 91*, 514–523.

Meulenkamp, J. E., Wortel, M. J. R., Van Wamel, W. A., Spakman, W., & Hoogerduyn Strating, E. (1988). On the Hellenic subduction zone and thegeodynamical evolution of Crete since the late middle Miocene. *Tectonophysics, 146*, 203–215.

Mikes, T., Christ, D., Petri, R., Dunkl, I., Frei, D., Báldi-Beke, M., et al. (2008). Provenance of the Bosnian Flysch. *Swiss Journal of Geosciences, 101*, 31–54.

Missoni, S., & Gawlick, H. J. (2011a). Evidence for Jurassic subduction from the Northern Calcareous Alps (Berchtesgaden; Austroalpine, Germany). *International Journal of Earth Sciences, 100*, 1605–1631.

Missoni, S., & Gawlick, H. J. (2011b). Jurassic mountain building and Mesozoic-Cenozoic geodynamic evolution of the Northern Calcareous Alps as proven in the Berchtesgaden Alps (Germany). *Facies, 57*, 137–186.

Mišur, I., Balen, D., Klötzli, U., Belak, M., Massonne, H. J., Brlek, M., & Brčić, V. (2023). Petrochronological study of chloritoid schist from Medvednica Mountain (Zagorje Mid-Transdanubian zone, Croatia). *Geologia Croatica, 76*(1), 13–36.
Moro, A., Ćosović, V., Benić, J., & Dokmanović, J. (2010). Taxonomy of Rudists from the Campanian Transgressive Sediments of Brašljevica, Donje Orešje and Sv. Martin, Northern Croatia. *Turkish Journal of Earth Sciences, 19*, 613–633.
Neubauer, F., Genser, J., & Handler, R. (1999). The Eastern Alps: Result of a two-stage collision process. *Mitteilungen Gesellschaft Geologische, 92*, 117–134.
Nirta, G., Aberhan, M., Bortolotti, V., Carras, N., Menna, F., & Fazzuoli, M. (2020). Deciphering the geodynamic evolution of the Dinaric orogen through the study of the 'overstepping' Cretaceous successions. *Geological Magazine, 157*(8), 1238–1264.
Nirta, G., Moratti, G., Piccardi, L., Montanari, D., Carras, N., Catanzariti, R., Chiari, M., & Marcucci, M. (2018). From obduction to continental collision: New data from Central Greece. *Geological Magazine, 155*(2), 377–421.
Palinkaš, L., Bermanec, V., Moro, A., Dogančić, D. & Strmić-Palinkaš, S. (2006). The northernmost Ni-lateritic weathering crust in the Tethyan domain, Gornje Orešje, Medvednica Mt., Mesozoic ophiolite belts of northern part of the Balkan. *Balkan Peninsula Proceedings*, 97–101.
Pamić, J. (2002). The Sava-Vardar Zone of the Dinarides and Hellenides versus the Vardar Ocean. *Eclogae Geologicae Helvetiae, 95*, 99–113.
Pamić, J., Gušić, I., & Jelaska, V. (1998). Geodynamic evolution of the Central Dinarides. *Tectonophysics, 297*, 251–268.
Pavelić, D. (2001). Tectonostratigraphic model for the North Croatian and North Bosnian sector of the Miocene Pannonian Basin System. *Basin Research, 13*(3), 359–376.
Pavelić, D., & Kovačić, M. (2018). Sedimentology and stratigraphy of the Neogene rift-type North Croatian Basin (Pannonian Basin System, Croatia): A review. *Marine and Petroleum Geology, 91*, 455–469.
Picotti, V., Romano, M. A., Ponza, A., Guido, F. L., & Peruzza, L. (2022). The Montello thrust and the active mountain front of the eastern Southern Alps (northeast Italy). *Tectonics, 41*, e2022TC007522.
Placer, L. (1999a). Contribution to the macrotectonic subdivision of the border region between Southern Alps and External Dinarides. *Geologija, 41*, 223–255.
Placer, L. (1999b). Structural meaning of the Sava folds. *Geologija, 41*, 191–221.
Plašienka, D., Grecula, P, Putiš, M., Hovorka, D. & Kovać, M. (1997a). Evolution and structure of the Western Carpathians: an overview. In: Grecula, P. Hovorka, D. & Putiš M. (Eds) Geological evolution of the Western Carpathians, Mineralia Slovaca Monograph, Bratislava, pp. 1–24.
Plašienka, D., Putiš, M., Kovać, M., Šefara, J. & Hrušecký, I. (1997b). Zones of Alpidic subduction and crustal underthrusting in the Western Carpathians. In: Grecula, P., Hovorka, D. & Putiš M. (Eds.) Geological evolution of the Western Carpathians, Mineralia Slovaca Monograph, Bratislava, pp. 35–42.
Pleničar, M., Premru, U. & Herak, M. (1975). Osnovna geološka karta SFRJ 1:100,000, list Novo Mesto L33–79 (Basic Geological Map of SFRY 1:100,000, Novo Mesto sheet). Geološki zavod Ljubljana, Savezni geološki zavod.
Porkolab, K., Köver, S., Benko, Z., Heja, G. H., Fialowski, M., Soos, B., Gerzina Spajić, N., Đerić, N., & Fodor, L. (2019). Structural and geochronological constraints from the Drina-Ivanjica thrust sheet (Western Serbia): Implications for the Cretaceous-Paleogene tectonics of the Internal Dinarides. *Swiss Journal of Geosciences, 112*, 217–234.
Rainer, T., Sachsenhofer, R. F., Greenb, P. F., Rantitscha, G., Herlec, U., & Vrabec, M. (2016). Thermal maturity of Carboniferous to Eocene Sediments of the Alpine-Dinaric Transition Zone (Slovenia). *International Journal of Coal Geology, 157*, 19–38.
Ratschbacher, L., Frisch, W., Linzer, H. G., & Merle, O. (1991). Lateral extrusion in the Eastern Alps, part 2: Structural analysis. *Tectonics, 10*(2), 257–271.
Rosenberg, C. L., Berger, A., Bellahsen, N., & Bousquet, R. (2015). Relating orogen width to shortening, erosion, and exhumation during Alpine collision. *Tectonics, 34*(6), 1306–1328.
Rožič, B., Jurkovšek, T. K., Rožič, P. Ž, & Gale, L. (2017). Sedimentary record of subsidence pulse at the Triassic/Jurassic boundary interval in the Slovenian Basin (eastern Southern Alps). *Geologica Carpathica, 68*(6), 543.
Sarti, M., Bosellini, A., & Winterer, E. L. (1992). Basin geometry and architecture of a Tethyan Passive Margin, Southern Alps, Italy: Implications for rifting mechanisms: Chapter 13: African and Mediterranean Margins. In J. S. Watkins, F. Zhiqiang, & K. J. McMillen (Eds.), *Geology and geophysics of continental margins*. The American Association of Petroleum Geologists.
Schefer, S. (2010). Tectono-metamorphic and magmatic evolution of the Internal Dinarides (Kopaonik area, southern Serbia) and its significance for the geodynamic evolution of the Balkan Peninsula. PhD thesis University of Basel, 230pp.
Schmid, S. M., Bernoulli, D., Fügenschuh, B., Maţenco, L., Schefer, S., Schuster, R., Tischler, M., & Ustaszewski, K. (2008). The Alpine-Carpathian-Dinaridic orogenic system: Correlation and evolution of tectonic units. *Swiss Journal of Geosciences, 101*, 139–183.
Schmid, S. M., Fügenschuh, B., Kissling, E., & Schuster, R. (2004). Tectonic map and overall architecture of the Alpine orogen. *Eclogae Geologicae Helvetiae, 97*, 93–117.
Schmid, S. M., Fügenschuh, B., Kounov, A., Matenco, L., Nievergelt, P., Oberhänsli, R., Pleuger, J., Schefer, S., Schuster, R., Tomljenović, B., Ustaszewski, K., & Van Hinsbergen, D. J. J. (2020). Tectonic units of the Alpine collision zone between Eastern Alps and Western Turkey. *Gondwana Research, 78*, 308–374.
Schmid, S. M., Pfiffner, O. A., Froitzheim, N., Schönborn, G., & Kissling, E. (1996). Geophysical-geological transect and tectonic evolution of the Swiss-Italian Alps. *Tectonics, 15*, 1036–1064.
Schönborn, G. (1999). Balancing cross sections with kinematic constraints: The Dolomites (northern Italy). *Tectonics, 18*, 527–545.
Sebe, K., Kovačić, M., Magyar, I., Krizmanić, K., Špelić, M., Sütő-Szentai, M., Kovács, A., Korecz-Szuromi, A., Bakrač, K., Hajek-Tadesse, V., Troskot-Čorbić, T., & Sztanó, O. (2020). Correlation of upper Miocene-Pliocene Lake Pannon deposits across the Drava Basin, Croatia and Hungary. *Geologia Croatica, 73*(3), 177–195.
Šegvić, B., Slovenec, D., & Badurina, L. (2023). Major and rare earth element mineral chemistry of low-grade assemblages inform dynamics of hydrothermal ocean-floor metamorphism in the Dinaridic Neotethys. *Geological Magazine, 160*(3), 444–470.
Šegvić, B., Slovenec, D., Schuster, R., Babajić, E., Badurina, L., & Lugović, B. (2020). Sm-Nd geochronology and petrologic investigation of sub-ophiolite metamorphic sole from the Dinarides (Krivaja-Konjuh, Ophiolite Complex, Bosnia and Herzegovina). *Geologia Croatica, 73*(2), 119–130.
Šikić, K., Basch, O. & Šimunić, An. (1977). Osnovna geološka karta SFRJ 1:100,000, list Zagreb L33–80 (Basic Geological Map of SFRY 1:100,000, Zagreb sheet). Institut za geološka istraživanja Zagreb, Savezni geološki zavod.
Šimunić, An. (1992). Geološki odnosi središnjeg dijela Hrvatskog Zagorja. PhD thesis, Zagreb, 208pp.
Šimunić, An., Pikija, M. & Hećimović, I. (1982). Osnovna geološka karta SFRJ 1:100,000, list Varaždin L33–69 (Basic Geological Map of SFRY 1:100,000, Varaždin sheet). Geološki zavod Zagreb, Savezni geološki zavod.
Šimunić, An., Pikija, M., Hećimović, I. & Šimunić, Al. (1981). Osnovna geološka karta SFRJ 1:100,000, Tumač za list Varaždin L 33–69 (Basic Geological Map of SFRY 1:100,000 Explanatory notes for Varaždin sheet). Institut za geološka istraživanja Zagreb, Savezni geološki zavod.
Šimunić, An., & Šimunić, Al. (1997). Triassic deposits of Hrvatsko Zagorje. *Geologia Croatica, 50*(2), 243–250.
Šimunić, An., Šimunić, Al., & Milanović, M. (1979). Geološka građa Ivanščice i Ravne gore. *Geološki Vjesnik, 31*, 157–174.
Slovenec, D., Horvat, M., Smirčić, D., Belak, M., Badurina, L., Kukoč, D., Grgasović, T., Byerly, K., Vukovski, M., & Šegvić, B. (2023). On the evolution of Middle Triassic passive margins of the Greater Adria Plate: Inferences from the study of calc-alkaline and shoshonitic tuffs from NW Croatia. *Ofioliti, 48*(1), 31–46.
Slovenec, D., Lugović, B., Meyer, H., & Garapić Šiftar, G. (2011). A tectonomagmatic correlation of basaltic rocks from ophiolite mélanges at the North-Eastern tip of the Sava-Vardar suture Zone, Northern Croatia, constrained by geochemistry and petrology. *Ofioliti, 36*(1), 77–100.
Slovenec, D., & Pamić, J. (2002). Geology of the Vardar Zone ophiolites of the Medvednica Mountain area located along the Zagreb-Zemplin line (NW Croatia). *Geologica Carpathica, 53*(1), 53–59.

Slovenec, D., & Šegvić, B. (2024). The evolution of the Mesozoic lithosphere of northwestern Neotethys: A petrogenetic and geodynamic perspective. *Journal of the Geological Society*. https://doi.org/10.1144/jgs2023-132

Slovenec, D., Šegvić, B., Halamić, J., Goričan, Š., & Zanoni, G. (2020). An ensialic volcanic arc along the northwestern edge of paleotethys—Insights from the Mid-Triassic volcano-sedimentary succession of Ivanščica Mt. (northwestern Croatia). *Geological Journal, 55*, 4324–4351.

Smirčić, D., Aljinović, D., Barudđija, U., & Kolar-Jurkovšek, T. (2020). Middle Triassic syntectonic sedimentation and volcanic influence in the central part of the External Dinarides, Croatia (Velebit Mts.). *Geological Quarterly, 64*(1), 220–239.

Smirčić, D., Kolar-Jurkovšek, T., Aljinović, D., Barudžija, U., Jurkovšek, B., & Hrvatović, H. (2018). Stratigraphic definition and correlation of Middle Triassic Volcaniclastic Facies in the External Dinarides: Croatia and Bosnia and Herzegovina. *Journal of Earth Science, 29*, 864–878.

Smirčić, D., Vukovski, M., Slovenec, D., Kukoč, D., Šegvić, B., Horvat, M., Belak, M., Grgasović, T., & Badurina, L. (2024). Facies architecture, geochemistry and petrogenesis of Middle Triassic volcaniclastic deposits of Mt Ivanščica (NW Croatia)—Evidence of bimodal volcanism in the Alpine-Dinaridic transitional zone. *Swiss Journal of Geosciences*. https://doi.org/10.1186/s00015-024-00453-8

Stach, E., Mackowsky, M. T. H., Teichmüller, M., Taylor, G. H., Chandra, D., & Teichmüller, R. (1982). *Coal petrology* (p. 535). Berlin-Stuttgart.

Stampfli, G. M., & Borel, G. D. (2002). A plate tectonic model for the Paleozoic and Mesozoic constrained by dynamic plate boundaries and restored synthetic oceanic isochrons. *Earth and Planetary Science Letters, 196*, 17–33.

Stampfli, G. M., & Borel, G. (2004). The TRANSMED transects in space and time: Constraints on the paleotectonic evolution of the Mediterranean domain. In W. Cavazza, F. M. Roure, W. Spakman, G. M. Stampfli, & P. A. Ziegler (Eds.), *The TRANSMED Atlas: The Mediterranean Region from Crust to Mantle* (pp. 53–80). Springer.

Steiner, T. M. C., Gawlick, H. J., Melcher, F., & Schlagintweit, F. (2021). Ophiolite derived material as parent rocks for Late Jurassic bauxite: Evidence for Tithonian unroofing in the Northern Calcareous Alps (Eastern Alps, Austria). *International Journal of Earth Sciences, 110*, 1847–1862.

Stern, G., & Wagreich, M. (2013). Provenance of Upper Cretaceous to Eocene Gosau Group around and beneaththe Viena Basin (Austria and Slovakia). *Swiss Journal of Geosciences, 106*, 505–527.

Tari, V. (2002). Evolution of the northern and western Dinarides: A tectonostratigraphic approach. In G. Bertotti, K. Schumann, & S. Cloetingh (Eds.), *Neotectonics and surface processes: The Pannonian Basin and Alpine/Carpathian System, Stephan Mueller Special Publication Series* (pp. 105–120). Copernicus.

Taylor, G. H., Teichmüller, M., Davis, A., Diessel, C. F. K., Littke, R., & Robert, P. (1998). *Organic petrology* (p. 704). Berlin-Stuttgart.

Thöni, M. (2006). Dating eclogite-facies metamorphism in the Eastern Alps—Approaches, results, interpretations: A review. *Mineralogy and Petrology, 88*, 123–148.

Tomljenović, B. (2002). Strukturne značajke Medvednice i Samoborskog gorja. PhD thesis, Zagreb, 208pp.

Tomljenović, B., & Csontos, L. (2001). Neogene-Quaternary structures in the border zone between Alps, Dinarides and Pannonian Basin (Hrvatsko zagorje and Karlovac basins, Croatia). *International Journal of Earth Sciences, 90*, 560–578.

Tomljenović, B., Csontos, L., Márton, E., & Márton, P. (2008). Tectonic evolution of the northwestern Internal Dinarides as constrained by structures and rotation of Medvednica Mountains, North Croatia. *Geological Society, London, Special Publications, 298*, 145–167.

Tremblay, A., Meshi, A., Deschamps, T., Goulet, F., & Goulet, N. (2015). The Vardar zone as a suture for the Mirdita ophiolites, Albania: Constraints from the structural analysis of the Korabi-Pelagonia zone. *Tectonics, 34*(2), 352–375.

Ustaszewski, K., Kounov, A., Schmid, S. M., Schaltegger, U., Krenn, E., Frank, W., & Fügenschuh, B. (2010). Evolution of the Adria-Europe plate boundary in the northern Dinarides: From continent-continent collision to back-arc extension. *Tectonics, 29*(TC6017), 1–34.

Ustaszewski, K., Schmid, S. M., Lugović, B., Schuster, R., Schaltegger, U., Bernoulli, D., Hottinger, L., Kounov, A., Fügenschuh, B., & Schefer, S. (2009). Late Cretaceous intra-oceanic magmatism in the internal Dinarides (northern Bosnia and Herzegovina): Implications for the collision of the Adriatic and European plates. *Lithos, 108*, 106–125.

van Gelder, I. E., Maţenco, L., Willingshofer, E., Tomljenović, B., Andriessen, P. A. M., Ducea, M. N., Beniest, A., & Gruić, A. (2015). The tectonic evolution of a critical segment of the Dinarides-Alps connection: Kinematic and geochronological inferences from the Medvednica Mountains, NE Croatia. *Tectonics, 34*(9), 1952–1978.

van Hinsbergen, D. J. J., Torsvik, T. H., Schmid, S. M., Maţenco, L. C., Maffione, M., Vissers, R. L. M., Gürer, D., & Spakman, W. (2020). Orogenic architecture of the Mediterranean region and kinematic reconstruction of its tectonic evolution since the Triassic. *Gondwana Research, 81*, 79–229.

van Unen, M., Matenco, L., Demir, V., Nader, F. H., Darnault, R., & Mandic, O. (2019a). Transfer of deformation during indentation: Inferences from the post-middle Miocene evolution of the Dinarides. *Global and Planetary Change, 182*, 103027.

van Unen, M., Matenco, L., Nader, F. H., Darnault, R., Mandić, O., & Demir, V. (2019b). Kinematics of foreland-vergent crustal accretion: Inferences from the Dinarides evolution. *Tectonics, 38*(1), 49–76.

Vermeesch, P. (2018). IsoplotR: A free and open toolbox for geochronology. *Geoscience Frontiers, 9*, 1479–1493.

Vishnevskaya, V. S., Djeric, N., & Zakariadze, G. S. (2009). New data on Mesozoic Radiolaria of Serbia and Bosnia, and implications for the age and evolution of oceanic volcanic rocks in the Central and Northern Balkans. *Lithos, 108*(1–4), 72–105.

Vrabec, M., & Fodor, L. (2006). Late Cenozoic tectonics of Slovenia: structural styles at the Northeastern corner of the Adriatic microplate. In N. Pinter, N. Grenerczy, J. Weber, S. Stein, & D. Medak (Eds.), *The Adria microplate: GNSS geodesy, tectonics and hazards (NATO science series IV, Earth and environmental Sciences 61)* (pp. 151–168). Springer.

Vukovski, M., Kukoč, D., Grgasović, D., Fuček, L., & Slovenec, D. (2023). Evolution of eastern passive margin of Adria recorded in shallow- to deepwater successions of the transition zone between the Alps and the Dinarides. *Facies*. https://doi.org/10.1007/s10347-023-00674-7

Wagreich, M., & Faupl, P. (1994). Paleogeography and geodynamic evolution of the Gosau Group of the Northern Calcareous Alps (Late Cretaceous, Eastern Alps, Austria). *Palaeogeography, Palaeoclimatology, Palaeoecology, 110*, 235–254.

Wagreich, M., & Marschalko, R. (1995). Late Cretaceous to Early Tertiary palaeogeography of the Western Carpathians (Slovakia) and the Eastern Alps (Austria): Implications from heavy mineral data. *Geologische Rundschau, 84*, 187–199.

Willingshofer, E., Neubauer, F., & Cloetingh, S. (1999a). The significance of Gosau-type basins for the late cretaceous tectonic history of the Alpine-Carpathian belt. *Physics and Chemistry of the Earth, Part A, 24*(8), 687–695.

Willingshofer, E., van Wees, J. D., Cloetingh, S., & Neubauer, F. (1999b). Thermomechanical consequences of Cretaceous continent-continent collision in the eastern Alps (Austria)—Insights from two-dimensional modeling. *Tectonics, 18*(5), 809–826.

Winkler, A. (1923). Ueber den Bau der östlichen S üdalpen. Mitt. Geol. Ges., XVI, 1–272, Wien.

Zattin, M., Cuman, A., Fantoni, R., Martin, S., Scotti, P., & Stefani, C. (2006). From Middle Jurassic heating to Neogene cooling: The thermochronological evolution of the southern Alps. *Tectonophysics, 414*, 191–202.

Zattin, M., Stefani, C., & Martin, S. (2003). Detrital fission-track analysis and petrography as keys of Alpine exhumation: The example of the Veneto foreland (Southern Alps, Italy). *Journal of Sedimentary Research, 73*, 1051–1061.

Zupanič, J., Babić, Lj., & Crnjaković, M. (1981). Lower Cretaceous basinal clastics (Oštrc Formation) in the Mt. Ivanščica (Northwestern Croatia). *Acta Geologica, 11*(1), 1–44.


## Publisher's Note

# 6. DISCUSSION

The main goal of this research was to unravel the Mesozoic and Cenozoic tectono-stratigraphic evolution of Ivanščica Mt. and its tectonic position at the junction of the Alps, Dinarides and Pannonian Basin. However, to be able to clearly distinguish tectonic relations between distinct lithostratigraphic rock units, it was of crucial importance to reconstruct the complete tectonically undisturbed Mesozoic and Cenozoic sedimentary successions and to characterize the primary sedimentological relations between spatially and temporally adjacent lithostratigraphic units. Considering the knowledge of the results of all the studies carried out so far on the Ivanščica Mt., the aim of this study was summed up in four main objectives: (1) to improve the existing knowledge on the age, lithostratigraphic features and paleogeographic provenance of the Mesozoic deposits of Ivanščica Mt.; (2) to determine the present-day spatial arrangement and geodynamic features of the main tectonostratigraphic units and kinematic characterization of their bounding faults; (3) to reconstruct tectono-thermal evolution, kinematics and paleostress regimes during the main Mesozoic and Cenozoic deformation events in the geodynamic development of the researched area; (4) to propose regional correlation of tectonostratigraphic units and deformational events with the corresponding units and events in the surrounding area of the Alps, Dinarides and Pannonian Basin.

To achieve the research objectives, seven hypotheses were tested using an interdisciplinary approach including various geological mapping, sedimentological, biostratigraphic, structural and thermochronological methods. In response to the set hypotheses, a synthesis of the results obtained within this research is presented and discussed below.

## 6.1. Response to the set hypotheses

*Hypothesis #1: Sedimentological and biostratigraphic analyses of Middle Triassic and Jurassic sedimentary successions can provide information on their precise age and paleogeographic provenance as well as the age of syn-sedimentary tectonic events.*

Middle Triassic volcano-sedimentary successions are well known throughout the Dinarides (**Aubouin et al., 1970; Pamić, 1984; Gawlick et al., 2012; Smirčić et al., 2016, 2018**), Southern and Eastern Alps (**Celarc et al., 2013; De Min et al., 2020; Gawlick et al., 2021**). These successions were deposited on the newly formed Adriatic passive margin (***sensu*** **Schmid et al.,**

**2008**). In the area of N Croatia, Middle Triassic syn-rift deposits are found on Ivanščica, Strahinjčica, Kuna gora and Desinić gora Mts. Lithological descriptions, interpretation of depositional mechanisms and detail biostratigraphy of these deposits were studied in less details.

In the mountains of Hrvatsko zagorje region, nine Middle Triassic lithostratigraphic sections were recorded (**Kukoč et al., 2023**). These deposits consist of volcanic and volcaniclastic deposits, pelagic limestone, radiolarian chert, siltstone and sandstone. The primary contact of the volcano-sedimentary succession with the underlying deposits is recorded exclusively in the Brezovica I section. These basement deposits consist of Anisian xenotopic anhedral crystalline dolostone (**Kukoč et al., 2023**). The shallow-marine dolostone is overlain by hemipelagic limestone, whose Middle to late Anisian age has been determined based on ammonites. The hemipelagic limestone is overlain by upper Anisian to lower Ladinian radiolarian chert, which alternates with felsic *Pietra Verde* volcaniclastic deposits. Basalts or basic volcaniclastic deposits are locally found underlying the *Pietra Verde*-radiolarian chert unit. Their late Anisian age is determined indirectly by conodonts from pelagic limestones intercalated within the basalts (**Kukoč et al., 2023**). Felsic volcaniclastic and radiolarian chert deposits are continuously overlain by the alternation of siltstones and sandstones representing secondary or redeposited volcaniclastic deposits in form of medium- to fine-grained turbidites. Although radiolarians extracted from the turbidites point to the late Anisian age, they are likely resedimented. Thus, late Ladinian age of the turbidites is suggested considering the local and regional correlation. Coeval existance of diverse depositional environments, variable thicknesses and poor spatial and temporal correlation of deposits indicate that the area was characterized by highly irregular topography, which was pre-determined by escarpments of steep normal faults. Direct contact of late Ladinian turbidites with the overlying deposits was not observed in the sections, although field observations suggest a sharp transition of turbidites into the shallow-marine crystalline dolostones. These dolostones continuously pass to the Upper Triassic dolostones (**Šimunić et al., 1981, 1982).** Time constraints for Middle Triassic syn-rift deposits indicate middle Anisian to late Ladinian age of this rifting event (**Kukoč et al., 2023**). Late Triassic shallow-marine carbonates are presented by a several hundred meters thick Main Dolomite ("*Hauptdolomit*" or "*Dolomia Principale*") and overlying up to 200 m thick Dachstein limestone (**Šimunić & Šimunić, 1979, 1997; Vukovski et al., 2023**). Such a relationship was recorded in the Gradinovec lithostratigraphic section (**Vukovski et al., 2023**).

In the Hrvatsko zagorje region, Jurassic deposits are best exposed on Ivanščica Mt. Besides these occurrences, very rare outcrops occur in the Burnjak creek NE of Gornja Stubica settlement. This primarily refers to upper Tithonian to Valanginian Aptychus limestone. Apart from a small occurrence of Lower Jurassic limestone near the Mrzljak peak on the S slopes of Ivanščica Mt., the presence of Jurassic deposits older than the Aptychus limestone has not been documented (**Šimunić et al., 1981, 1982**). As a result, various interpretations have emerged regarding the depositional environments that existed during the Jurassic times. One interpretation suggested the deposition of Aptychus limestone directly above Upper Triassic shallow-marine carbonates after an emersion phase that lasted from the end of the Lower Jurassic (**Šimunić et al., 1981**). In contrast, another interpretation assumed continuous deep-marine pelagic sedimentation starting in the early Jurassic and persisting continuously into the Lower Cretaceous (**Babić, 1974**).

In the central part of Ivanščica Mt., detailed field investigations have been conducted, proving the existence of sedimentary rocks that, based on their relative field relationships, must have represented deposits of the Jurassic age. Two contrasting successions could have been distinguished, differing from each other in the type of deposits which underlay radiolarian chert and Aptychus limestone. These two successions are spatially distributed in a systematic manner: one exclusively NW of the Črne Mlake fault and the other exclusively SE of the same fault. In the NW part, due to poor exposure, suitable locations for recording sedimentological columns could not be found. However, field observations indicate continuous sedimentation of shallow-marine limestone on top of Upper Triassic Dachstein limestone (**Vukovski et al., 2023**). Their Hettangian to Pliensbachian age was determined based on dasycladal algae and benthic foraminifera (**Vukovski et al., 2023**). Lower Jurassic shallow-marine limestone is directly overlain by pelagic filament rich limestone. Abundant protoglobigerinids and local to regional scale correlation with matching microfacies indicate Bajocian to Bathonian age of this limestone (**Vukovski et al., 2023**). In the underlying Lower Jurassic shallow-marine limestone centimeter-sized neptunian dykes, composed of the overlaying Middle Jurassic pelagic limestone components, were recorded. Red to brownish radiolarian chert is found on top of Middle Jurassic pelagic limestone (**Vukovski et al., 2023**). The age of chert could not be determined due to dissolved radiolarian tests. Radiolarian chert is conformably overlain by uppermost Tithonian to Valanginian Aptychus limestone (**Vukovski et al., 2023**).

In the area SE of the Črne Mlake fault, four lithostratigraphic sections were recorded within the Upper Triassic to Lower Cretaceous deposits. In contrast to the area NW of the Črne Mlake fault, here Upper Triassic Dachstein limestone is conformably overlain by Hettangian to Pliensbachian pelagic limestone and Toarcian shale and marl as evident in the Mrzljak and Mala Ivanščica sections (**Vukovski et al., 2023**). The age of this pelagic limestone is determined by benthic foraminifera. Shale and marl were barren of fossil content, so their age is assumed to be Toarcian based on local and regional correlations. Shale and marl are followed by calcarenites whose early Middle Jurassic age is supposed based on the superposition (**Vukovski et al., 2023**). Such development is recorded in the Mrzljak section. Field observations indicate that calcarenites are overlain by Callovian to Tithonian radiolarian chert. Radiolarian chert represents the oldest Jurassic pelagic formation that was deposited throughout the entire pelagic domain and thus is present in both areas, NW and SE of the Črne Mlake fault (**Vukovski et al., 2023**). Equally, uppermost Tithonian to Valanginian Aptychus limestone continuously overlay radiolarian chert in both areas regarding the Črne Mlake fault (**Vukovski et al., 2023**).

Investigations of Upper Triassic and Jurassic deposits of Ivanščica Mt. revealed yet another extensional deformational event recorded in the Lower Jurassic sedimentary succession (**Vukovski et al., 2023**). Ultimately, this event resulted in a diachronous, but complete, drowning of till then shallow-marine depositional environments. This event was related to the opening of the Alpine Tethys (**Vukovski et al., 2023**). The deposition of pelagic Aptychus limestone is interrupted in the Hauterivian when mixed carbonate–siliciclastic turbidites of the Oštrc Formation were deposited (**Babić et al., 1979; Babić & Zupanič, 1973, 1978; Šimunić et al., 1982**). These flysch-type deposits are interpreted as the foreland basin sediments, located in front of the obducting nappes containing ophiolites and distal Adriatic passive margin units (**Zupanič et al., 1981; Lužar-Oberiter et al., 2009, 2012**) and present regional syn-orogenic deposits (**Faupl & Wagreich, 2000; Mikes et al., 2008; Goričan et al., 2018**).

*Hypothesis #2: The unit of the volcanogenic-sedimentary complex can be separated in two formations, turbidites of the Oštrc Fm. and an ophiolitic mélange of the Repno Complex, with the determination of their spatial distribution and the character of their geological boundary.*

The first papers that differentiate two various units within the so-called volcanogenic-sedimentary complex were published already in the late 1970s (**Babić & Gušić, 1978; Babić &**

**Zupanič 1978; Babić et al., 1979**). Considering lithological and paleontological characteristics, these authors distinguished Hauterivian to Albian well-bedded, fossiliferous, mixed carbonate-siliciclastic deposits named Oštrc Formation, and overlying Cenomanian to Turonian chaotic, non-fossiliferous, siliciclastic deposits containing ophiolites, named Repno Complex. The latter was recognized as an ophiolitic mélange of Late Jurassic age (**Babić et al., 2002**). However, despite the earlier recognition of these two formations, authors of the Basic geological map of the SFRY, sheet Varaždin and associated explanatory notes considered Oštrc turbidites and Repno ophiolitic mélange as a single formation called volcanogenic-sedimentary complex of Hauterivian to Turonian age (**Šimunić et al., 1981, 1982**). Consequently, information on the exact spatial distribution, relationship and character of the contact between these two formations remained unclear.

To approach this issue, detailed geological mapping has been carried out in the area where the volcanogenic-sedimentary complex crops out. Once such locations were found, special attention was given to the contact between Oštrc turbidites and Repno ophiolitic mélange with the emphasis on the collection of structural data. Analogous to the relationships described in the Dinarides (**Schmid et al., 2008; Nirta et al., 2020**), within this research it was assumed that turbidites of Oštrc Fm. occupy lower structural position regarding the overthrust Repno ophiolitic mélange.

Collected field data clearly shows that, in fact, Repno ophiolitic mélange occupies lower structural position regarding the Oštrc turbidites (**Vukovski et al., 2024**). Oštrc turbidites and underlying Adriatic passive margin successions were thrusted SE-ward along Babin Zub back-thrust over the Repno ophiolitic mélange during late Early Cretaceous times (**Vukovski et al., 2024**). Primary contact between Repno ophiolitic mélange and Oštrc turbidite was not found in the field. However, as the deposition of the Oštrc turbidites postdates the tectonic emplacement of the ophiolitic mélange on the continental passive margin, it is assumed that the distalmost (oceanward) portion of Oštrc turbidites overlay Repno ophiolitic mélange (**Vukovski et al., 2023**). Similarly, Bistra Fm. representing a shallow-marine time equivalent of the basinal Oštrc turbidite, unconformably overlies the Repno ophiolitic mélange in the Medvednica Mt. (**Halamić, 1998; Lužar-Oberiter at al., 2012**).

Results obtained from investigations of the volcanogenic-sedimentary complex, enabled the first spatial delineation of Hauterivian to Albian Oštrc turbidites from the uppermost Jurassic to lowermost Cretaceous Repno ophiolitic mélange, as well as the characterization of their boundary.

*Hypothesis #3: Isolated bodies of Upper Triassic carbonates represent either tectonic klippes, olistoliths within ophiolitic mélange or erosional remnants of the ophiolitic mélange basement preserved in the cores of the anticlines.*

In the S slopes of Ivanščica Mt., Basic geological map of the SFRY, sheet Varaždin shows a number of tectonic klippes made of Upper Triassic and subordinately Lower Jurassic shallow-marine carbonates, overlying the volcanogenic-sedimentary complex (**Šimunić et al., 1981, 1982**). However, alternative interpretation proposes that these carbonate bodies do not represent tectonic klippes, but rather olistoliths embedded in the ophiolitic mélange (**Babić & Zupanič, 1978**). In this thesis a third hypothesis is proposed, assuming that Upper Triassic carbonate bodies represent erosional remnants of the ophiolitic mélange basement preserved in the cores of the anticlines. This hypothesis is supported by the fact that the carbonate bodies are elongated and spatially aligned in a linear arrangement.

In order to test each of the three hypotheses, detailed geological mapping was conducted around the carbonate bodies. Special attention was given to the collection of structural data, particularly the orientation of bedding planes within the carbonate bodies and the surrounding volcanogenic-sedimentary complex. Another important question to be addressed was whether the carbonate bodies are surrounded by the Repno ophiolitic mélange and/or the Oštrc turbidites.

The newly collected field data increased the number of bedding orientations measured within carbonate bodies for several tens of times (**Vukovski et al., 2024**) and strongly improved the knowledge on their structural position. This bedding data firmly refuted each of the proposed hypotheses. Orientation of all bedding planes measured within carbonate bodies homoclinally dips exclusively to the S to SE, which strongly opposes the hypothesis of anticlines emerging from the basement of the ophiolitic mélange. This also contradicts the hypothesis that favors the olistolith interpretation since it is extremely unlikely that all twenty isolated olistoliths would have identical bedding orientation. Instead, the uniform orientations of bedding planes in all carbonate bodies could indicate that these bodies once belonged to a single, unified nappe, now eroded and preserved only in the form of isolated klippes, as proposed by **Šimunić et al. (1981)** and **Šimunić (1992)**. However, geological mapping has revealed that these carbonate bodies do not represent isolated entities but are connected along the strike of the bedding planes. The results of this research refuted the initial working hypotheses about the carbonate bodies, but also suggested a new one. This new hypothesis indicated a structural setting in the form of the SE dipping and NW verging imbricate fan whose geometry, kinematics and origin are extensively described in **Vukovski et al. (2024)**. This hypothesis was extensively tested in the field and ultimately confirmed (**Vukovski et al., 2024**).

*Hypothesis #4: Apart from the faults which, according to the OGK 1:100,000 sheet Varaždin at the Ivanščica Mt. are exclusively of Cenozoic age, it is possible to cartographically separate faults whose age is pre-Cenozoic.*

Considering the Basic geological map of the SFRY, sheet Varaždin (**Šimunić et al., 1981, 1982**), some of the faults shown on the Ivanščica Mt. are certainly at least pre-Miocene and potentially Mesozoic in age, as they are sealed by lowermost Miocene deposits. However, implementation of structural, sedimentological and thermochronological methods indicates a sequence of deformational events, comprising three extensional and four contractional events starting from Middle Triassic until present times (**Vukovski et al., 2024**). Some of the faults that were formed in Mesozoic deformational events are still recognizable in the field.

Although characteristics of Middle Triassic syn-rift deposits indicate highly irregular topography of depositional environment, which was predetermined by the steep normal faults (**Kukoč et al., 2023**), in the field it was not possible to distinguish Middle Triassic faults from younger faults.

As detailed described in the response to the Hypothesis #1, NE striking and SE dipping Črne Mlake fault separates shallow-marine Lower Jurassic deposits in its footwall from deep-marine Lower Jurassic deposits in its hanging wall (**Vukovski et al., 2023**). This indicates that the Črne Mlake fault was initially formed in the Early Jurassic extensional event (D2) as a normal fault, which allowed the fast deepening of the depositional environments in its hanging wall (**Vukovski et al., 2024**), while shallow-marine sedimentation was still retained in its footwall until the Pliensbachian (**Vukovski et al., 2023**).

Geological mapping revealed that Repno Complex occupies a structurally higher position with respect to the pelagic Jurassic to Lower Cretaceous deposits and was tectonically emplaced over the Adriatic passive margin successions. Age constraints for this event on Ivanščica Mt. are provided by the youngest formation that is directly overthrust by the Repno Complex, which is uppermost Tithonian to Valanginian Aptychus limestone (**Vukovski et al., 2024**). This indicates that tectonic emplacement of Repno Complex (D3) and formation of its basal thrust occurred during the earliest Cretaceous times.

Main characteristics of the Ivanščica Imbricate Fan structural domain is a stack of NW verging imbricates (**Vukovski et al., 2024**). These imbricates are made of Upper Triassic platform carbonates, overlain by Lower Jurassic to Lower Cretaceous pelagic succession, dipping underneath the ophiolitic mélange of the Repno Complex (**Vukovski et al., 2024**). Hauterivian to Albian age of the imbrication (D4), the formation of related reverse faults, the Babin Zub back-thrust and inversion of the Črne Mlake fault is indicated by the age of the syn-orogenic Oštrc turbidites and the apatite fission track time-temperature modeling (**Vukovski et al., 2024**).

Majority of the faults shown on the Basic geological map of the SFRY sheet Varaždin deform the earliest Miocene or younger deposits (**Šimunić et al., 1981, 1982**). The youngest strata deformed by the ENE striking dextral faults observed in the N of Ivanščica are of late Pannonian age (**Šimunić et al., 1981, 1982).** Nevertheless, their Early Miocene activity (D5) is proposed based on correlation with similar transfer faults reported from the E Slovenia (**Fodor et al., 2021**) and the distribution of earliest Miocene sediments that are spatially closely related to ENE striking dextral faults (**Vukovski et al., 2024**). Additionally, low angle normal faults of Early to Middle Miocene age are found in the subsurface by reflection seismic sections (**Tomljenović & Csontos, 2001; Vukovski et al., 2024**). The scarce occurrences of Early to Middle Miocene syn-rift faults on the surface is explained by the absence of outcrops of the syn-rift deposits on the surface and later sealing of syn-rift structures with thick Late Miocene post-rift succession.

Reverse faults related to the short lasting late Sarmatian contraction (D6) were not found on the surface. Their presence in the subsurface is recorded in the reflection seismic sections (**Tomljenović & Csontos, 2001; Vukovski et al., 2024**)

The youngest faults that correspond to the late Pannonian contractional event (D7) are the most abundant in the field. These are primary E to ENE trending reverse faults such as the

Prigorec fault, SE striking dextral strike-slip faults such as Gotalovec-Prigorec fault and reactivated ENE striking Early to Middle Miocene dextral strike-slip faults (**Vukovski et al., 2024**).

Although Cenozoic faults (D5, D6 and D7) are the most abundant faults in the study area, these new results confirm the existence of faults of Hauterivian to Albian (D4), Berriasian to Valanginian (D3), Lower Jurassic (D2) and possibly Middle Triassic (D1) age.

*Hypothesis #5: Some of the faults that were created in the former active regime of tectonic stress, were subsequently reactivated or inverted under the influence of younger tectonic stress.*

Present day geometry and kinematics of the Črne Mlake thrust clearly evidence its contractional character (**Vukovski et al., 2024**). Still, there are few points that indicate its polyphase evolution and an initial extensional origin. The first argument has already been explained above under the Hypotheses #1 and #4, and it concerns the fact that this fault separates two completely different depositional environments from the Early Jurassic times. The second argument is evident in the fact that Črne Mlake thrust locally thrusts younger deposits over older ones (**Fig. 2 in Vukovski et al., 2024**). Such a structural relationship is not possible when thrusting a normal stratigraphic sequence. However, during inversion of normal faults, the stratigraphic sequence was already disrupted before the thrusting, allowing the possibility that parts of the fault do not show a reverse relationship due to progressive inversion.

As already described above under the Hypothesis #4, ENE striking dextral faults located north of Ivanščica Mt. are supposed to have initially formed in the Early to Middle Miocene extensional event as transfer faults, and reactivated later in the late Pannonian to recent inversion of the Pannonian Basin (**Vukovski et al., 2024**).

Some of the late Pannonian reverse faults observed in the reflection seismic sections exhibit typical growth strata of Lower to Middle Miocene age in their hanging walls. Such geometry indicates that their initial formation was associated with the Early to Middle Miocene syn-rift stage. Inversion of these normal faults took place in late Pannonian to recent times under the contractional regime of tectonic stress causing the inversion of the Pannonian Basin.

Results of this thesis indicate multiple stages of fault inversion, dominantly from extensional normal faults to compressional reverse faults or thrusts.

*Hypothesis #6: During Mesozoic and Cenozoic, study area was affected by Dinarides, Alps and Pannonian Basin related tectonic deformational events whose effects and deformational structures is possible to determine in the field.*

As Ivanščica Mt. is positioned at the junction of the Alps and the Dinarides in the SW part of the Pannonian Basin, it is assumed that evidence of the deformation events related to the formation of the Alps, Dinarides and the Pannonian Basin should be preserved in the outcrops. Results of this research carried out in the area of Ivanščica Mt. reveal a sequence of seven different deformational events (**Vukovski et al., 2024**).

The oldest deformational event representing the Middle Triassic extension (D1) is attributed to the opening of the Neotethys Ocean (**Kukoč et al., 2023, 2024**). Subsequent Early Jurassic extension (D2) is interpreted as a result from the opening of the Alpine Tethys (**Vukovski et al., 2023**).

Late Berriasian to Valanginian tectonic emplacement of the ophiolitic mélange of the Repno Complex (D3) is related to regional process of the obduction of the Neotethyan ophiolites (Western Vardar ophiolitic unit) on the eastern passive continental margin of Adria (**Vukovski et al., 2024**). The following Hauterivian to Albian contraction (D4) resulted in exhumation of Adriatic margin units and previously obducted ophiolitic mélange (**Lužar-Oberiter et al., 2012; Vukovski et al., 2024**). Both closely followed Early Cretaceous contractional events are related to the closure of the Neotethys Ocean. Deformational structures and ophiolites that testify for the closure of the Neotethys Ocean are best exposed in the Dinarides and Hellenides, but are also found in the Eastern Alps and Western Carpathians whose main mountain building phase commenced later and is related to the closure of the Alpine Tethys Ocean (**Schmid et al., 2008, 2020 and references therein**). Therefore, it is not appropriate to attribute deformation events to individual orogens, but rather to the oceans whose opening and closure caused deformational processes.

Early to Middle Miocene extension (D5) and following Late Sarmatian (D6) and Late Pannonian to recent (D7) contractions are attributed to the well-known Pannonian Basin back-arc extension and the following basin inversion as a result of N-ward indentation and CCW rotation of the Adriatic microplate.

Structural data, in combination with lithostratigraphic and thermochronological data, reveal three extensional deformational events linked with the rifting related to the opening of the Neotethys Ocean, Alpine Tethys Ocean and back-arc Pannonian Basin, and four contractional deformational events, two of them related to the closure of the Neotethys Ocean, and two related to the inversion of the Pannonian Basin.

*Hypothesis #7: Kinematic characteristics of the first order thrust between the nappe of the South Alpine unit and the Dinarides can be determined and the thrust contact can be mapped and traced on the field.*

Earlier studies (**Placer, 1999a; Schmid et al., 2008, 2020; van Gelder et al., 2015**) considered a major part of Ivanščica Mt. as a Neogene nappe of the South Alpine unit, thrusted S-ward over the ophiolitic mélange of the Western Vardar unit of the Internal Dinarides. Within this research, existence of S verging thrust of Miocene age has not been confirmed as explained in detail in **Vukovski et al. (2024)**. Detailed geological mapping reveal that the hypothetical trace of that first order thrust on the Ivanščica Mt. partly represents the continuous Jurassic succession of the Adriatic passive margin, partly the NW verging Early Cretaceous Črne Mlake thrust and partly the SE verging Early Cretaceous Babin Zub back-thrust (**Fig. 2 in Vukovski et al., 2024**). Consequently, the entire hypothesis is refuted.

## 6.2. Mesozoic and Cenozoic tectono-stratigraphic evolution of the Alps and the Dinarides transition zone in the SW Pannonian Basin

The oldest rocks on Ivanščica Mt. are Permian brown-red conglomerates, sandstones and black shales, conformably overlain by Lower Triassic clastic and later carbonate deposits (equivalents of the Seis and Campil members from the Southern Alps; **Šimunić et al., 1981, 1982**). Shallow-marine carbonate sedimentation continued into the Middle Triassic. The entire Permian to lowermost Middle Triassic unit of Ivanščica Mt. is corelative with coeval clastic and carbonate deposits from the rest of the Dinarides and Southern and Eastern Alps, which are interpreted as deposits of the epeiric platform located along the northern Gondwana margin (**Pamić & Jurković, 2001; Sremac, 2005; Vlahović et al., 2005; Aljinović et al., 2018; Palatinuš et al., 2024**).

In the Middle Triassic times, continental rifting led to the break-up of Adria from Gondwana, opening of the Neotethys Ocean and formation of Adriatic passive margin (**Stampfli & Borel, 2004; Schmid et al., 2008).** This extensional event is the oldest registered deformational event in the study area (D1) and is registered in the sedimentary record of Ivanščica Mt. and other mountains of N Croatia. The result of such an event is seen as an abrupt deepening of the depositional environment in the Late Anisian (**Goričan et al., 2005; Kukoč et al., 2023**). The Middle Triassic deeper marine deposits were formed within the so-called Northwestern Croatian Triassic Rift Basin (***sensu*** **Kukoč et al., 2023**), situated on the newly formed eastern Adriatic passive margin. In this deep-marine setting, pelagic and hemipelagic limestones and radiolarian cherts were deposited, alternating with sub-alkaline, middle to high-K calc-alkaline, and shoshonitic volcanic and volcaniclastic rocks corelative to the Buchenstein Formation in the Southern Alps and Transdanubian Range (**Fig. 5; Kukoč et al., 2023, Slovenec et al., 2023; Smirčić et al., 2024**).

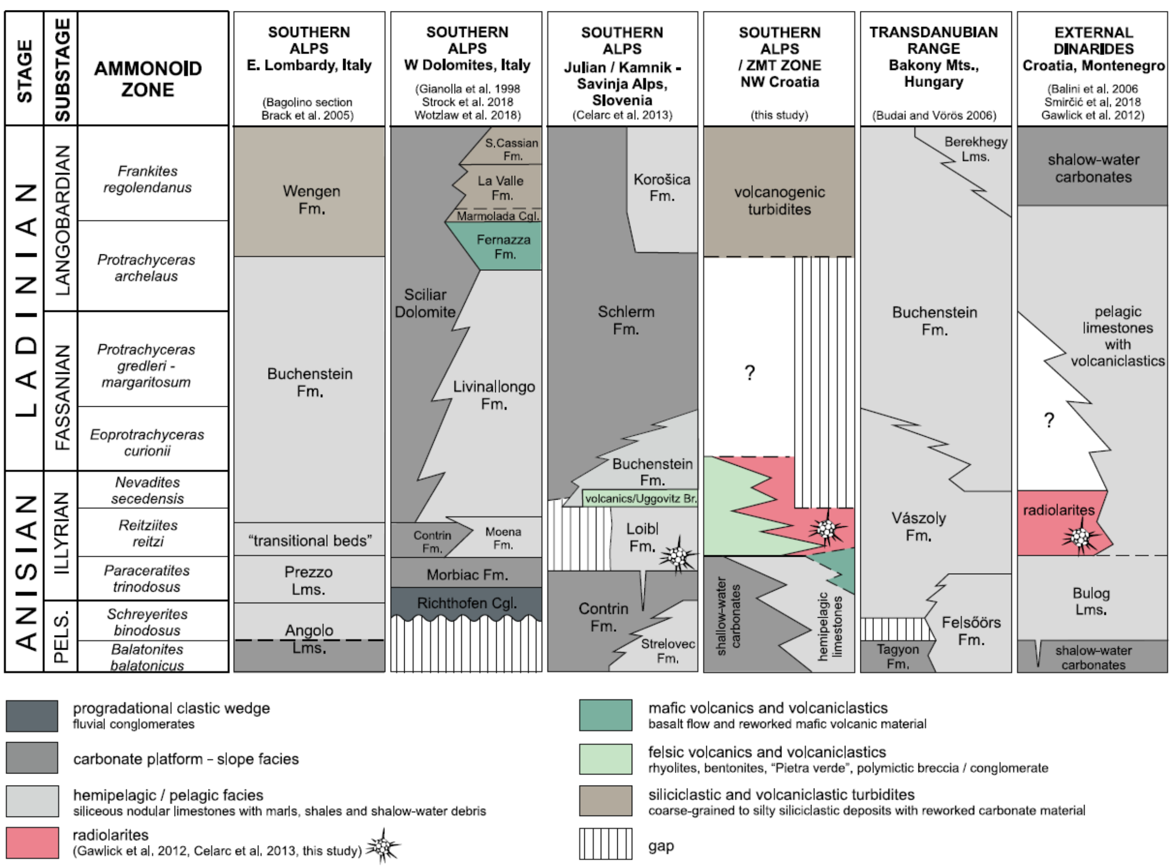


***Figure 5.*** *Correlation of successions of the Northwestern Croatian Triassic Rift Basin with the Middle Triassic deposits of the Southern Alps, Transdanubian Range and External Dinarides. Adopted from* ***Kukoč et al. (2023)***

Locally, basic to acidic calc-alkaline rift related volcanic rocks also appear (**Goričan et al., 2005; Kukoč et al., 2023; Slovenec et al., 2023**). Sedimentation processes in the Northwestern Croatian Triassic Rift Basin during late Anisian to early Ladinian were controlled by the complex horst-and-graben topography (**Fig. 6; Kukoč et al., 2023**). Middle Triassic syn-rift succession ends with the deposition of Late Ladinian black siltstones and sandstones representing the equivalent to the Wengen Formation in the Southern Alps (**Fig. 5; Kukoč et al., 2023**). These deposits were generated by the rapid reworking of unconsolidated or poorly consolidated volcaniclastic detritus and its redeposition into the deep-marine environment in the form of turbidites (**Fig. 6**), promoting the gradual filling of the Northwestern Croatian Triassic Rift Basin (**Kukoč et al., 2023**). Shallow-marine carbonate sedimentation reestablished already in the Late Ladinian (**Goričan et al., 2005**) and continued in the Late Triassic.

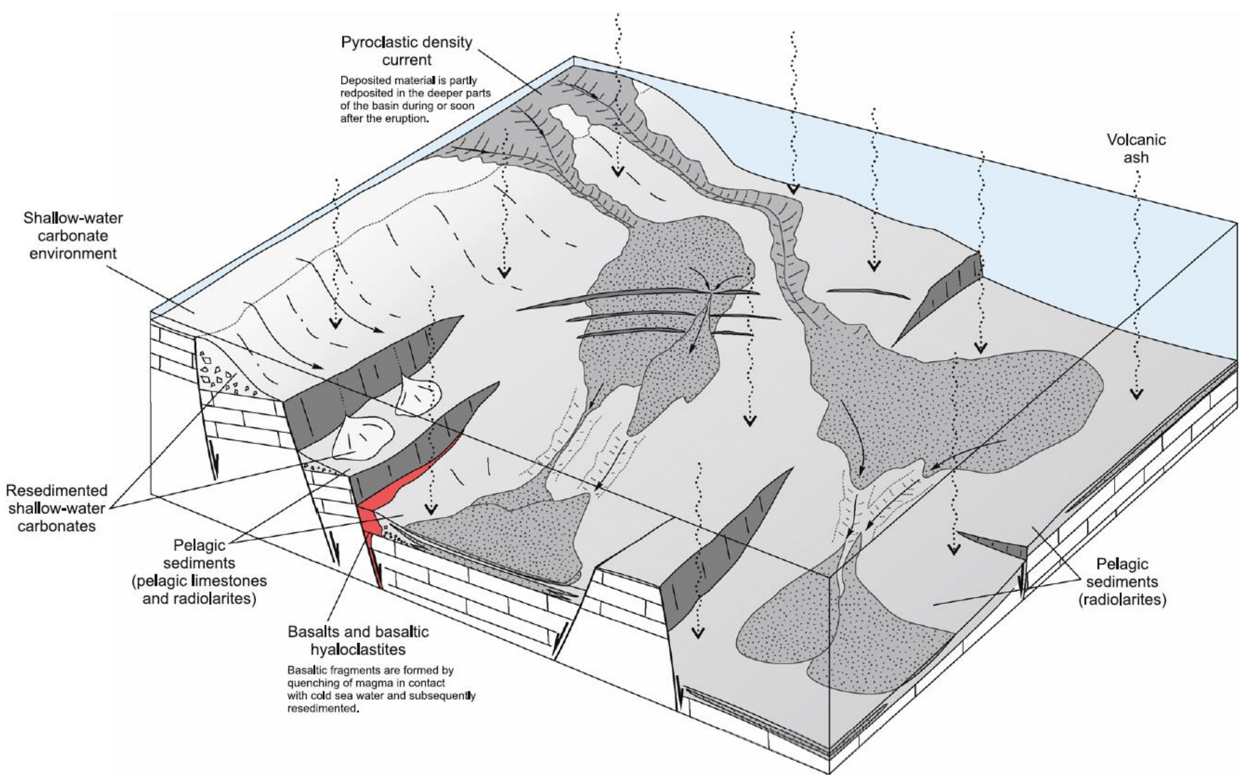


***Figure 6.*** *Schematic reconstruction of depositional environments in the Northwestern Croatian Triassic Rift Basin during the Middle Triassic. Adopted from* ***Kukoč et al. (2023)***

Coeval formation of Neotethyan oceanic crust in the newly formed oceanic domain (**Fig. 7**) is evidenced by the Middle Triassic enriched mid-ocean ridge basalts (E-MORB) and overlying radiolarian cherts, nowadays preserved as blocks in the ophiolitic mélange of the Ivanščica Mt. (**Kukoč et al., 2024**).

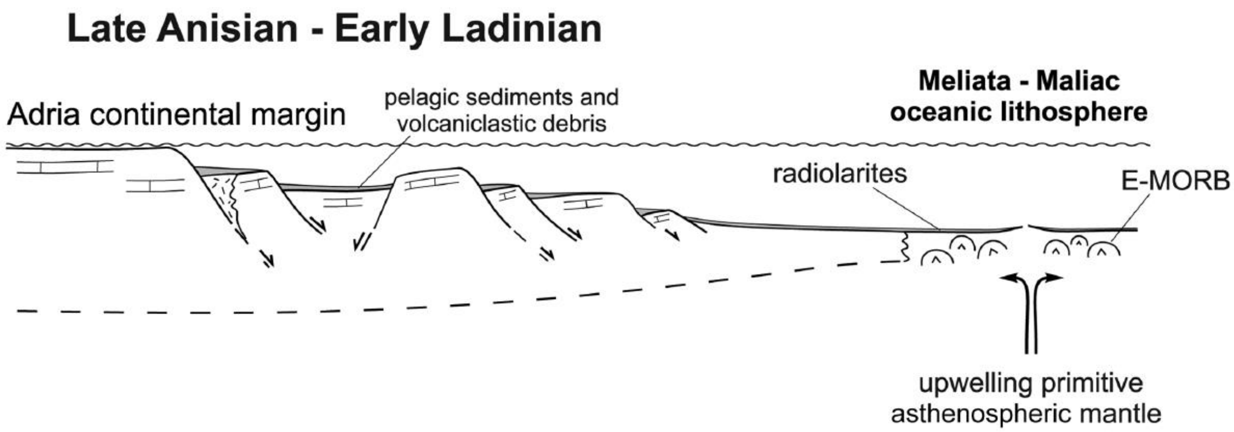


***Figure 7.*** *Schematic cross-section across the eastern Adriatic passive continental margin and newly formed oceanic crust. Adopted from* ***Kukoč et al. (2024)***

The existence of Carnian deposits belonging to the Adriatic passive margin succession preserved on Ivanščica Mt., has never been biostratigraphically proven. However, local and regional correlation suggests that Upper Triassic carbonate siliciclastic deposits found in the W Ivanščica Mt. could correspond to the Carnian age. Sedimentation during Norian and Rhaetian was characterized by the deposition of shallow-marine carbonates. Most of these deposits consist of the Main Dolomite which is continuously overlain by Rhaetian Dachstein limestone (**Vukovski et al., 2023**).

At the beginning of the Early Jurassic, a new phase of rifting (D2) associated with the opening of the Alpine Tethys caused a fast drowning of a part of the Adriatic passive margin preserved in the investigated area (**Vukovski et al., 2023**). In this Early Jurassic pelagic domain, that occupies the area SE of the Črne Mlake thrust, Upper Triassic shallow-marine Dachstein limestone is continuously overlain by Lower Jurassic pelagic limestone, shale, marl and calcareous resediments (**Fig. 8; Vukovski et al., 2023**). In the same time, more landward domain occupying the area NW of the Črne Mlake thrust, retained shallow-marine carbonate sedimentation until the Pliensbachian (**Fig. 8; Vukovski et al., 2023**). Here, NW of the Črne Mleke fault, Lower Jurassic shallow-marine limestone is overlain by lower Middle Jurassic pelagic limestone rich in Bositra-shell filaments and protoglobigerinids (**Vukovski et al., 2023**). Middle to Upper Jurassic radiolarian cherts were found overlaying Lower and Middle Jurassic calcareous pelagic deposits in both domains (**Fig. 8**) that now represent the unified pelagic depositional environment (**Vukovski et al., 2023**). Radiolarian cherts represent regional Middle to Late Jurassic pelagic facies typical of the deep-marine passive margin basins in the western Neotethys Ocean and probably present the first post-rift deposits after the Early Jurassic rifting event (D2). Middle Jurassic shift from carbonate to siliceous sedimentation (**Fig. 8**) was associated with the changes in the ocean surface fertility attributed to the paleoclimatic changes (**Bartolini et al., 1999; Baumgartner, 2013**).

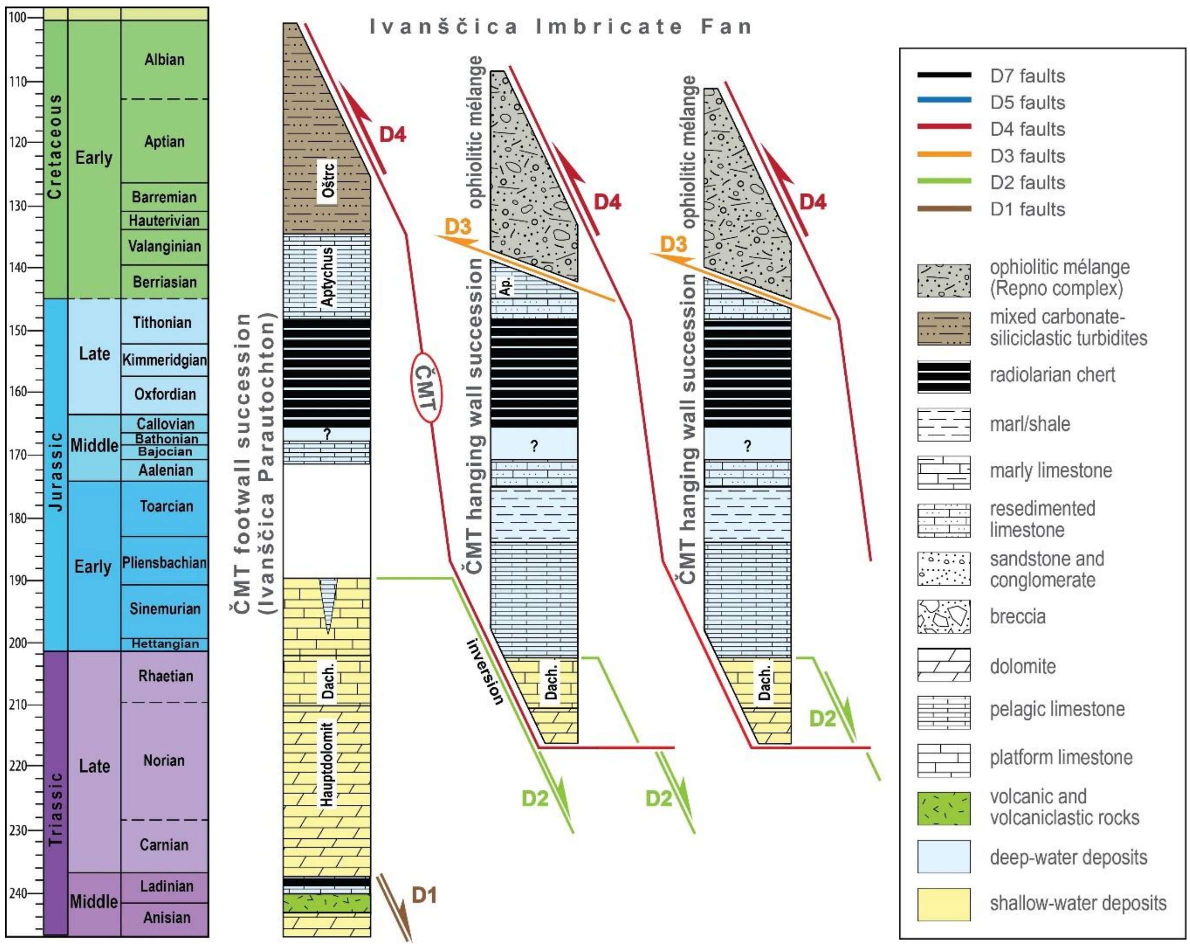


***Figure 8.*** *Tectonostratigraphic columns showing detail lithostratigraphy of Middle Triassic to Lower Cretaceous successions of two structural domains: Ivanščica Imbricate Fan and Ivanščica Parautochthon. Note the difference in the lithostratigraphy of the Jurassic successions preserved in the footwall and hanging wall of the Črne Mlake thrust, and the tectonic position of the ophiolitic mélange which is found only in the Ivanščica Imbricate Fan structural domain. Modified after* ***Vukovski et al. (2024)***

Latest Tithonian evolutionary rise of calcareous nanoplankton resulted in the shift from siliceous back to carbonate sedimentation (**Bronemann et al., 2003**) and the onset of the

Aptychus limestone (equivalent of *Biancone*, *Maiolica* and *Oberalm* facies in the Alps; **Fig. 8**). A few meters thick calcarenite unit is occasionally found at the contact between radiolarian chert and Aptychus limestone (**Babić & Zupanič, 1973; Vukovski et al., 2023**). All Jurassic age calcarenites represent redeposited material from the adjacent Adriatic Carbonate Platform (**Vukovski et al., 2023**). Jurassic to Lower Cretaceous successions preserved on Ivanščica Mt. were deposited on the eastern Adriatic passive margin and thus correlate well with coeval successions preserved in the Dinarides, Southern Alps, and Eastern Alps (**Vukovski et al., 2023).** In the more distal (oceanward) part of the passive margin preserved on Ivanščica Mt., the deposition of Aptychus limestone was interrupted by the late Berriasian to Valanginian obduction (D3) of the ophiolitic mélange referred as the Repno Complex (**Fig. 9; Kukoč et al., 2024; Vukovski et al., 2024**).

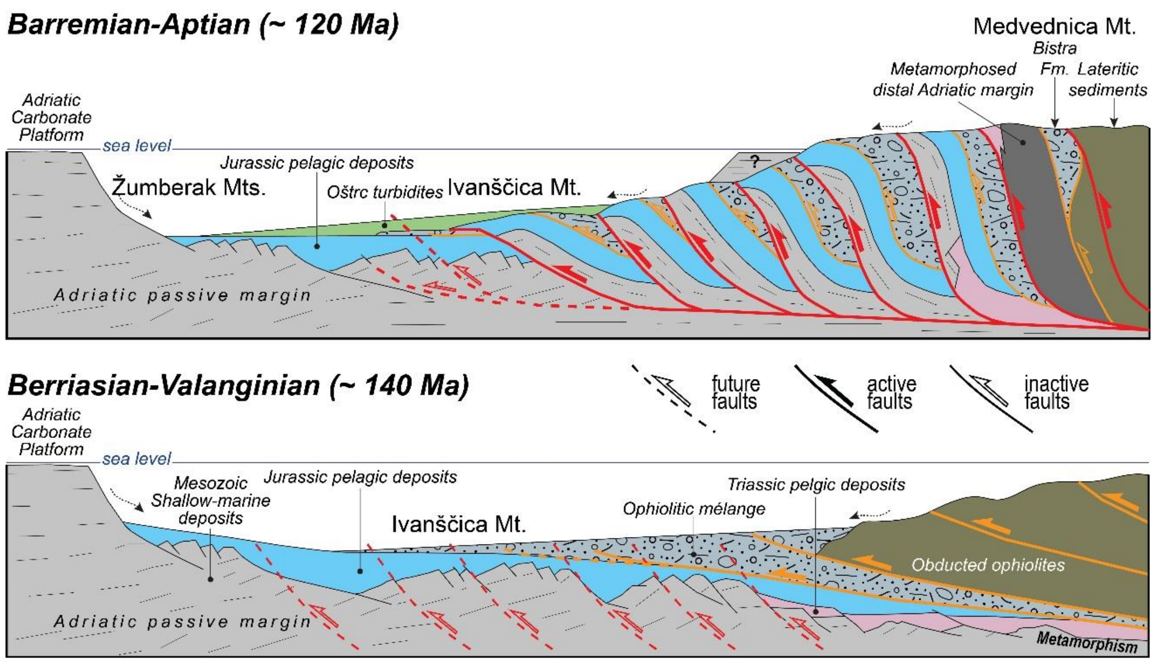


***Figure 9.*** *Schematic geodynamic reconstruction of the wider study area (northwesternmost Internal Dinarides) during Early Cretaceous D3 and D4 deformational events. Adopted from* ***Vukovski et al. (2024)***

Within this ophiolitic mélange, blocks of various ophiolitic rocks including enriched mid-ocean ridge basalts (E-MORB), back-arc ridge basalts (BARB) and island-arc tholeiites (IAT) indicate continuous development of the Neotethyan oceanic lithosphere from the Middle Triassic to the Late Jurassic times (**Lugović et al., 2015; Šegvić et al., 2023; Kukoč et al., 2024; Slovenec et al., 2011, 2024**). More proximal (landward) part of the passive margin preserved on the Ivanščica

Mt. was not affected by the obduction of the ophiolitic mélange and thus retained pelagic carbonate sedimentation until the first influx of mixed carbonate–siliciclastic deposits in the Hauterivian (**Zupanič et al., 1981; Vukovski et al., 2024**). Hauterivian to Albian carbonate-siliciclastic turbidites of the Oštrc Formation (equivalent of the *Vranduk*, *Studor* and *Rossfeld* formations in the Dinarides and the Alps) were deposited in the foreland basin developed in front of advancing nappes containing ophiolites and units of the distal Adriatic margin (**Fig. 9; Zupanič et al., 1981; Lužar-Oberiter et al., 2009, 2012**). This late Early Cretaceous compressional event (D4) resulted in thrusting and imbrication of the Adriatic passive margin successions together with previously emplaced ophiolitic mélange, fast exhumation and erosion (**Fig. 9; Vukovski et al., 2024**). The same contraction finally resulted in a regional emersion (**Fig. 9**) that lasted until the late Egerian in the Ivanščica Mt. (**Vukovski et al., 2024**).

A long-lasting emersion was interrupted in the late Egerian by the sedimentation of brackish to marine siliciclastic deposits (**Fig. 3; Avanić, 2012; Avanić et al., 2021**) above the tectonically disrupted and lithologically diverse Mesozoic basement (**Figs. 8 and 9; Vukovski et al., 2024**). These strata were deposited on the SW margin of the Central Paratethys, close to its connection with the Mediterranean. The deposition lasted for a short time as the new emersion commenced in the Egenburgian and lasted until the late Badenian (**Šimunić et al., 1981, 1982**). Ottnangian to middle Badenian syn-rift deposits are missing on the surface since the local depocenters, created by the Early to Middle Miocene back-arc extension (D5), were at that time located further S of Ivanščica Mt. The area N of Ivanščica was characterized by the higher rate and different style of extension (**Fodor et al., 2021**) resulting in a formation of a dextral transfer fault zone including Šoštanj fault, passing only a few kilometers N of Ivanščica Mt. This dextral fault is responsible for the right lateral displacement of Kiscellian to Karpatian shallow-marine siliciclastic succession of the Central Paratethys and pre-Kiscellian basement including the Middle Triassic acidic volcanic rocks for several decades of kilometers from the W-NW. Regional late Badenian transgression resulted in flooding over late Egerian, only locally over Mesozoic deposits (**Fig. 3; Šimunić et al., 1981**) and mark the beginning of the post-rift stage in the SW part of the Pannonian Basin (**Pavelić & Kovačić, 2018**). Deposition of late Badenian clastic and carbonate deposits continued in Sarmatian by the deposition of laminated marls (**Fig. 3; Šimunić et al., 1981**). In the late Sarmatian a short-lasting contraction (D6) resulted in uplift, local emersions and deposition of clastic deposits (**Tomljenović & Csontos, 2001; Vukovski et al., 2024**).

During the Pannonian and Cernikian, deep-water brackish lake was continuously in-filled by a turbiditic, deltaic, and finally alluvial clastic sequence (**Šimunić et al., 1981; Pavelić & Kovačić, 2018**), reflecting the diachronous regressive trend observed across the entire Pannonian Basin. The closure of the lake system was additionally favored by the onset of late Pannonian to recent contraction (D7). This contraction resulted in reverse faulting, reactivation of older and formation of new dextral faults and extensive folding of the entire study area and wider region (**Tomljenović & Csontos, 2001; van Gelder et al., 2015; Vukovski et al., 2024**).

### 6.3. Tectonic position of the pre-Neogene units of Ivanščica Mt. with respect to tectonic subdivision of the Alps and the Dinarides

The South Alpine tectonic unit occupies the area of northern Italy and Slovenia, south of the Periadriatic fault system (**Schmid et al., 2004, 2008**). It is characterized by the Neogene top-S thrusting of Adriatic passive margin units and its underlying Variscan basement (**Schönborn, 1992, 1999**). Prior to Neogene contraction, area of the eastern Southern Alps was additionally affected by the late Paleogene "Dinaridic" SW verging thrusting (**Doglioni, 1987; Doglioni & Bosellini, 1987; Caputo, 1996**). Therefore, in the eastern Southern Alps the Dinaridic SW verging structures are cut and/or refolded by the younger S verging structures of the Southern Alps. Similarly, earlier studies considered the largest part of Ivanščica Mt. as a S verging Neogene nappe of the South Alpine unit, which thrust Adriatic passive margin succession over the ophiolitic mélange of the Western Vardar ophiolitic unit of the Dinarides (Repno complex; **Fig. 1b; Placer, 1999a; Schmid et al., 2008, 2020; van Gelder et al., 2015**).

Research conducted within the framework of this thesis did not reveal any S verging thrust, nor any other S verging structures (**Vukovski et al, 2024**). As shown in the new geological map (**Fig. 10**), huge part of the terrain previously thought to exhibit the ophiolitic mélange in fact represent Hauterivian to Albian turbidites of the Oštrc Fm. (compare **Fig. 4** with **Fig. 10**). Consequently, almost half of this hypothetical contact between the typically Dinaridic ophiolitic mélange and tectonically overlying Triassic to lowermost Cretaceous Adriatic passive margin succession previously interpreted to represent the thrust contact between South Alpine unit and the Dinarides (**Placer, 1999a; Schmid et al., 2008, 2020; van Gelder et al., 2015**) in fact appears as the continuous conformable contact of the latest Tithonian to Valanginian Aptychus limestone and Hauterivian to Albian turbidites of the Oštrc Fm. (**Vukovski et al., 2023, 2024**). The rest of that first order thrust contact undoubtedly represent a thrust contact. However, obtained results prove that frontal thrust of the nappe ascribed to the South Alpine unit according to **Placer (1999a)**, **van Gelder et al. (2015)** and **Schmid et al. (2020)** is sealed by the upper Egerian deposits and thus predates the main shortening phase in the South Alpine unit and Oligocene to Neogene rotations of the wider study area. Moreover, this thrust, known as Črne Mlake thrust, as well as its Babin Zub back-thrust, were formed earlier, in the Early Cretaceous during D4 deformational event with initial top-SW vergence of the thrust and top-NE vergence of the back-thrust (**Vukovski et al., 2024**). Their present-day orientation and vergence is a consequence of the Oligocene to early Miocene 130° clockwise rotation and Miocene to recent 30° of counterclockwise rotation (**Tomljenović & Csontos, 2001; Márton et al., 2002; Tomljenović et al., 2008; Vukovski et al., 2024**).

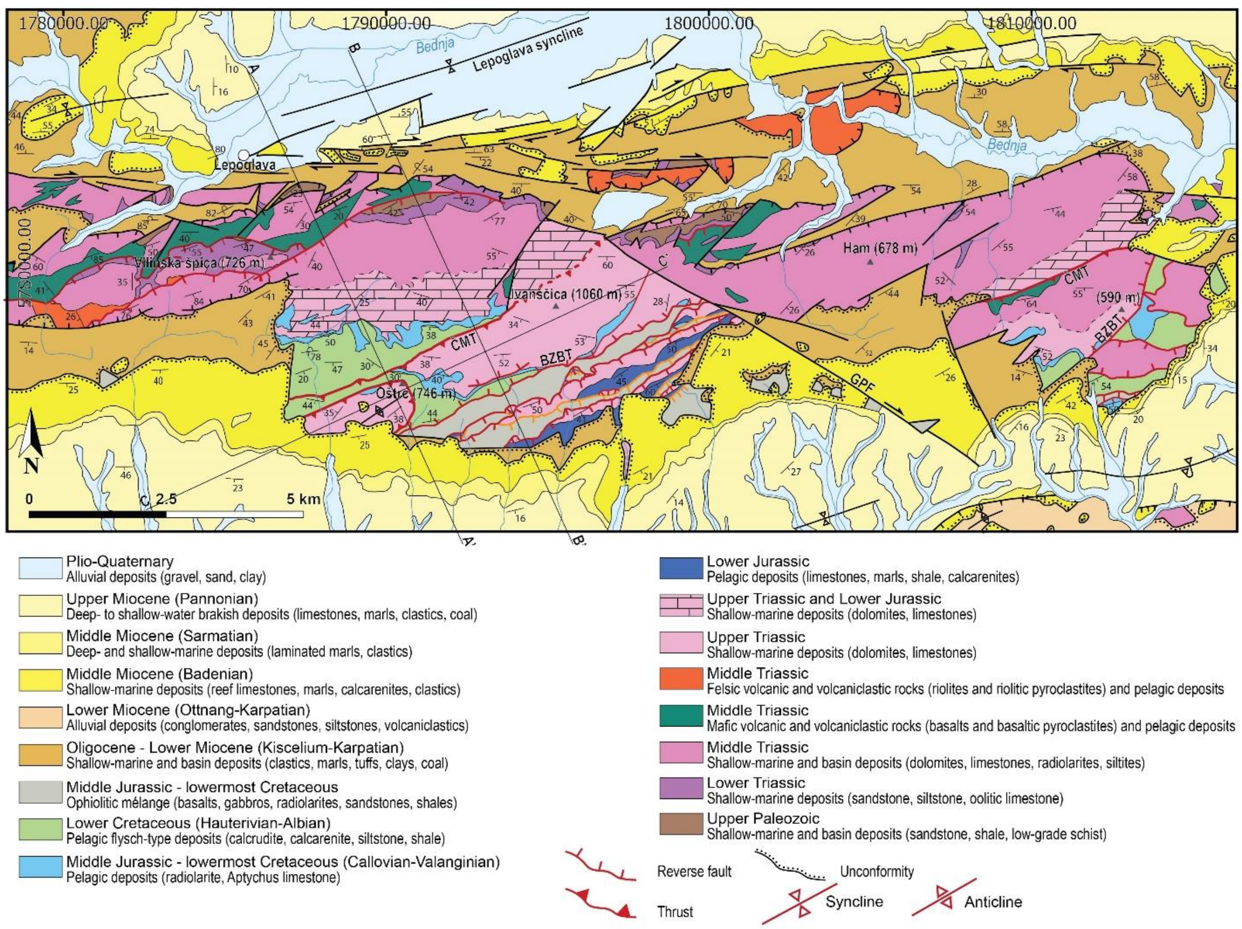


***Figure 10.*** *Geological map of Ivanščica Mt. compiled from* ***Šimunić et al. (1982)*** *and* ***Vukovski et al. (2024)****. The map shows the locations of cross-sections A-A'; B-B' and C–C' (shown in* ***Fig. 5*** *of chapter 5 (****Vukovski et al., 2024****)). The location of the figure is shown in* ***Fig. 1b****. For*

*color coding of the tectonic features, please refer to **Fig. 8.** Modified after **Vukovski et al. (2024)***

Hence, in contrast to previous studies, the results of this thesis indicate that the study area was not affected by the Miocene S-ward thrusting characteristic for the South Alpine unit. Therefore, the Mesozoic and Cenozoic tectono-stratigraphic evolution of Ivanščica Mt. indicates the tectonic and paleogeographic affiliation of its non-ophiolitic Mesozoic structural-stratigraphic entities belonging to the Pre-Karst unit of the Internal Dinarides (**Vukovski et al., 2024**). The Repno complex represents the northwesternmost occurrence of the Western Vardar ophiolitic unit. Up to now, this is the only location where ophiolitic mélange of the Western Vardar ophiolitic unit is in primary obduction thrust contact with underlying successions of the Pre-Karst unit (**Vukovski et al., 2024**). This new cognition represents a significant contribution to the knowledge of the structure and dynamics of the Dinaridic orogen.

# 7. CONCLUSION

This thesis has explored the complex tectono-stratigraphic evolution and the present-day tectonic position of Ivanščica Mt. This is accomplished using the interdisciplinary approach by implementation of structural, sedimentological, biostratigraphic, petrological, geochemical, thermochronological methods and methods of geological mapping.

Sedimentological and biostratigraphic investigations indicate the existence of two extensional events. The older, Middle Triassic extensional event (D1) resulted in the drowning of the earlier shallow-marine depositional environment and formation of the short-lasting Northwestern Croatian Triassic Rift Basin. Ultimately, this event led to the formation of the Adriatic passive margin and opening of the Neotethys Ocean in the more distal domains. Lower Jurassic extensional event (D2) resulted in diachronous drowning of Late Triassic carbonate platform and the final establishment of pelagic depositional environments that lasted until the end of the Early Cretaceous.

Implementation of geological mapping, multi-scale structural analysis and thermochronology enabled recognition of four contractional and one extensional event. Late Berriasian to Valanginian (~ 140 Ma) contraction (D3) is manifested with obduction-related tectonic emplacement of the ophiolitic mélange, referred as the Repno Complex, over the stratigraphic succession of the Adriatic passive margin. The following Hauterivian to Albian contractional event (D4) was responsible for NW-ward (in present day coordinates) imbrication and thrusting of the Adriatic passive margin succession and previously tectonically emplaced ophiolitic mélange, and for the deposition of syn-orogenic Oštrc turbidites. Ultimately, this contraction resulted in regional emersion.

Analysis of reflection seismic sections revealed three deformational events of Miocene age. The following rifting event (D5) is associated by extension that was accompanied by the NE dipping listric normal faults and ENE striking dextral transfer faults, and the deposition of Ottnangian to middle Badenian syn-rift deposits. A short-lasting contraction (D6) responsible for reactivation of Early Miocene normal faults and creation of new reverse faults was registered in the late Sarmatian. The youngest documented deformational event (D7) resulted in the late Pannonian to Present reactivation of ENE striking dextral faults, formation of SE striking dextral faults as well as the formation of E to ENE trending folds and reverse faults. This contraction is driven by the indentation and counterclockwise rotation of the Adriatic microplate.

Documented stratigraphic evolution of the Ivanščica Mt. is in good accordance with the passive margin successions originating from the Adria plate, preserved today in the South Alpine unit and Austroalpine units of the Alps and the Pre-Karst unit of the Dinarides. Recognized deformational events and their ages indicate that Ivanščica was mainly affected by deformational phases related to the Mesozoic evolution of the Neotethys Ocean as well as Miocene opening and inversion of the Pannonian Basin. No deformational events related to the closure of the Alpine Tethys were recognized in the study area. These new findings on the Mesozoic and Cenozoic tectono-stratigraphic evolution of Ivanščica Mt. proves the tectonic and paleogeographic affiliation of its non-ophiolitic Mesozoic structural-stratigraphic entities to the northernmost part of the Pre-Karst unit of the Dinarides, located in the SW part of the Pannonian Basin. The ophiolitic mélange, known as the Repno complex, marks the northwesternmost occurrence of the Western Vardar ophiolitic unit. To date, this is the only location where ophiolitic mélange of the Western Vardar ophiolitic unit is in primary obduction thrust contact with the underlying successions of the Pre-Karst unit.

# 8. REFERENCES

Aljinović, D., Horacek, M., Krystyn, L., Richoz, S., Kolar-Jurkovšek, T., Smirčić, D. & Jurkovšek, B. (2018). Western Tethyan Epeiric Ramp Setting in the Early Triassic: An Example from the Central Dinarides (Croatia). *Journal of Earth Science*, *29*(4), 806–832.

Aničić, B. & Juriša, M. (1984). Osnovna geološka karta SFRJ 1:100,000, list Rogatec L33–68 (Basic Geological Map of SFRY 1:100,000, Rogatec sheet). Geološki zavod Ljubljana and Geološki zavod Zagreb, Savezni geološki zavod.

Aničić, B. & Juriša, M. (1985). Osnovna geološka karta SFRJ 1:100,000, Tumač za list Rogatec L 33-68 (Basic Geological Map of SFRY 1:100,000 Explanatory notes for Rogatec sheet). Geološki zavod Ljubljana i Institut za geološka istraživanja Zagreb, Savezni geološki zavod.

Aubouin, J., Blanchet, R., Cadet, J.-P., Celet, P., Charvet, J., Chorowitz, J., Cousin, M. & Rampnoux, J.-P. (1970). Essai sur la géologie des Dinarides. *Bull Soc Géol Fr 12*(6), 1060–1095.

Avanić, R. (2012). Litostratigrafske jedinice donjeg miocena sjeverozapadne Hrvatske [Lower Miocene lithostratigraphic units from north-western Croatia – in Croatian]. Unpubl. PhD Thesis, Faculty of Science, University of Zagreb, 162 p.

Avanić, R., Pavelić, D., Pécskay, Z., Miknić, M., Tibljaš, D. & Wacha, L. (2021). Tidal deposits in the Early Miocene Central Paratethys: The Vučji Jarek and Čemernica members of the Macelj formation (NW Croatia). *Geologia Croatica 74*, 41–56.

Babić, Lj. & Gušić, I. (1978). Pregled fosila iz "klastičnog kompleksa" Ivanščice I njihovo stratigrafsko značenje. *Geološki vjesnik, 30*(1), 1-19.

Babić, Lj. & Zupanič, J. (1973). Uppermost Jurassic and Early Cretaceous deposits on Mt. Ivanščica – northern Croatia. *Geološki Vjesnik, 26*, 267–272.

Babić, Lj. & Zupanič, J. (1978). Mlađi mezozoik Ivanščice. In: Babić Lj, Jelaska V (ed) Vodič ekskurzije 3. Skupa sedimentologa Jugoslavije. Croatian Geological Society, Zagreb, pp 11–23.

Babić, Lj. (1974). Jurassic-Cretaceous sequence of Mt. Ivanščica (Northern Croatia). *Bull. Sci. Cons. Acad. Yugosl., 19*(7–8),181–182.

Babić, Lj. (1976). Stratigrafski slijed I paleogeografska evolucija Ivanščice od gornjeg trijasa do sredine krede. 8. Jugosl. Geol. Kongres, Bled 1974. 2, 53-62, Ljubljana.

Babić, Lj., Hochuli, P.A. & Zupanič, J. (2002). The Jurassic ophiolitic mélange in the NE Dinarides: dating, internal structure and geotectonic implications. *Eclogae Geologicae Helvetiae 95*, 263–275.

Babić, Lj., Zupanič, J. & Crnjaković, M. (1979). Recognition of two units in the "Clastic Formation with ophiolites " of Mt. Ivanščica and the role of a magmatic belt and an active continental margin (In Croat., Engl. Summ.). Proc. 4lh Meeting of the Section for geol., geophys. and geochem., Scientific Council for oil. 115-123. Zagreb.

Bartolini, A., Baumgartner, P.O. & Guex, J. (1999). Middle and Late Jurassic radiolarian palaeoecology versus carbon-isotope stratigraphy. *Palaeogeography Palaeoclimatology Palaeoecology 145*, 43–60.

Baumgartner, P.O. (2013). Mesozoic radiolarites – accumulation as a function of sea surface fertility on Tethyan margins and in ocean basins. *Sedimentology 60*, 292–318.

Brlek, M., Richard Tapster, S., Schindlbeck-Belo, J., Gaynor, S.P., Kutterolf, S., Hauff, F., Georgiev, S.V., Trinajstić, N., Šuica, S., Brčić, V., Wang, K.-L., Lee, H.-Y., Beier, C., Abersteiner, A.B., Mišur, I., Peytcheva, I., Kukoč, D., Németh, B., Trajanova, M., Balen, D., Guillong, M., Szymanowski, D. & Lukács, R. (2023). Tracing widespread Early Miocene ignimbrite eruptions and petrogenesis at the onset of the Carpathian-Pannonian Region silicic volcanism. *Gondwana Research 116*, 40–60.

Bronemann, A., Aschwer, U. & Mutterlose, J. (2003). The impact of calcareous nannofossils on the pelagic carbonate accumulation across the Jurassic-Cretaceous boundary. *Palaeogeography Palaeoclimatology Palaeoecology 199*, 187–228.

Caputo, R. (1996). The polyphase tectonics of the Eastern Dolomites, Italy. *Mem. Sci. Geol., 48*, 93–106.

Celarc, B., Goričan, Š. & Kolar-Jurkovšek, T. (2013). Middle Triassic carbonate- platform break-up and formation of small-scale half-grabens (Julian and Kamnik-Savinja Alps, Slovenia). *Facies 59*, 583–610.

Ćosović, V. & Drobne, K. (2000). Some remarks on Nummulites specimens from localities in south-eastern Slovenia and north-western Croatia. Annali del Museo Civico di Storia Naturale di Ferrara. str. 14-15-x.

De Min, A., Velicogna, M., Ziberna, L., Chiaradia, M., Alberti, A., & Marzoli A. (2020). Triassic magmatism in the European Southern Alps as an early phase of Pangea break-up. *Geological Magazine.*

Doglioni, C. (1987). Tectonics of the Dolomites. *Journal of Structural Geology 9*, 181–193.

Doglioni, C. & Bosselini, A. (1987). Eoalpine and Mesoalpine tectonics in the Southern Alps. *Geol Rundsch 76*(3), 735–754.

Faupl, P. & Wagreich, M. (2000). Late Jurassic to Eocene palaeogeography and geodynamic evolution of the Eastern Alps. *Mitteilungen der Österreichischen Geologischen Gesellschaft 92*, 79–94.

Fodor, L., Balázs, A., Csillag, G., Dunkl, I., Héja, G., Jelen, B., Kelemen, P., Kövér, S., Németh, A., Nyíri, D., Selmeczi, I., Trajanova, M., Vrabec, Ma. & Vrabec, Mi. (2021). Crustal exhumation and depocenter migration from the Alpine orogenic margin towards the Pannonian extensional back-arc basin controlled by inheritance. *Global and Planetary Change 201*.

Fodor, L., Jelen, B., Márton, E., Skaberne, D., Car, J. & Vrabec, M. (1998). Miocene-Pliocene tectonic evolution of the Slovenian Periadriatic fault: Implications for Alpine-Carpathian extrusion models. *Tectonics 17*(5), 690–709.

Gawlick, H.-J., Goričan, Š., Missoni, S. & Lein, R. (2012). Late Anisian platform drowning and radiolarite deposition as a consequence of the opening of the Neotethys ocean (High Karst nappe, Montenegro). *Bull Soc Géol France 183*(4):349–358.

Gawlick, H.-J., Lein, R. & Bucur, I.I. (2021). Precursor extension to the final Neo-Tethys break-up: flooding events and their significance for the correlation of shallow-water and deep marine organisms (Anisian, Eastern Alps, Austria). *Int J Earth Sci 110*, 419–446.

Goričan, Š., Halamić, J., Grgasović, T. & Kolar-Jurkovšek, T. (2005). Stratigraphic evolution of Triassic arc-backarc system in northwestern Croatia. *Bulletin de la Société Géologique de France 176*(1), 3–22.

Goričan, Š., Žibret, L., Košir, A., Kukoč, D. & Horvat, A. (2018). Stratigraphic correlation and structural position of Lower Cretaceous flysch-type deposits in the eastern Southern Alps (NW Slovenia). *Int J Earth Sci 107*, 2933–2953.

Gorjanović-Kramberger, D. (1904). Geologijska prijegledna karta Kraljevine Hrvatske i Slavonije. Krapina i Zlatar 1:75.000. Izd. zemalj. vlade, Odjela za unutarnje poslove, Zagreb.

Gorjanović-Kramberger, D. (1907). Die geotektonischen Verhaltnisse des Agramer Gebirges und die mit denselben im Zusammenhage stedenden Erscheinungen. Verh. Geol. Reichansts., 13, 313-314, Wien.

Halamić, J. (1998). The lithostratigraphic characterisation of Jurassic andCretaceous sediments with ophiolite of Mts. Medvednica, Kalnik andIvanščica. PhD Thesis, Zagreb University, 1-184 (in Croatian, with English abstract).

Hauer, F. (1868). Geologische Ubersichkarte der Osterrieischen Monarchie, Batt 6, tlstliche Alpenlander, Jahrb. Geol. Reichsanst., 18, 1-44, Wien.

Jurković, I. & Pamić, J. (2001). Geodynamics and metallogeny of Variscan complexes of the Dinarides and South Tisia as related to plate tectonics. *Nafta 52(9)*, 267–284.

Kukoč, D., Slovenec, D., Šegvić, B., Vukovski, M., Belak, M., Grgasović, T., Horvat, M. & Smirčić, D. (2024). The early history of the Neotethys archived in the ophiolitic mélange of northwestern Croatia. *Journal of the Geological Society*. doi: 10.1144/jgs2023-143.

Kukoč, D., Smirčić, D., Grgasović, T., Horvat, M., Belak, M., Japundžić, D., Kolar-Jurkovšek, T., Šegvić, B., Badurina, L., Vukovski, M. & Slovenec, D. (2023). Biostratigraphy and facies description of Middle triassic rift-related volcano-sedimentary successions at the junction of the Southern Alps and the Dinarides (NW Croatia). *International Journal of Earth Sciences 112*, 1175–1291.

Lugović, B., Slovenec, D., Schuster, R., Schwarz, W.H. and Horvat, M. (2015). Petrology, geochemistry and tectono-magmatic affinity of gabbroic olistoliths from the ophiolite mélange in the NW Dinaric–Vardar ophiolite zone (Mts. Kalnik and Ivanščica, North Croatia). *Geologia Croatica 68*, 25–49.

Lužar-Oberiter, B., Mikes, T., von Eynatten, H. & Babić, Lj. (2009). Ophiolitic detritus in Cretaceous clastic formations of the Dinarides (NW Croatia): evidence from Cr-spinel chemistry. *International Journal of Earth Sciences 98*, 1097–1108.

Lužar-Oberiter, B., Mikes, T., Dunkl, I., Babić, Lj. & von Eynatten, H. (2012). Provenance of cretaceous synorogenic sediments from the NW Dinarides (Croatia). *Swiss Journal of Geosciences 105*, 377–399.

Mikes, T., Christ, D., Petri, R., Dunkl, I., Frei, D., Báldi-Beke, M., et al. (2008). Provenance of the Bosnian Flysch. *Swiss Journal of Geosciences 101*, 31–54.

Márton, E., Pavelić, D., Tomljenović, B., Avanić, R., Pamić , J. & Márton, P. (2002). In the wake of a counterclockwise rotating Adriatic microplate: Neogene paleomagnetic results from Northern Croatia. *International Journal of Earth Sciences 91*, 514–523.

Nirta, G., Aberhan, M., Bortolotti, V., Carras, N., Menna, F., & Fazzuoli, M. (2020). Deciphering the geodynamic evolution of the Dinaric orogen through the study of the ‘overstepping’ Cretaceous successions. *Geological Magazine 157*(8), 1238–1264.

Palatinuš, I., Gobo, K., Fio-Firi, K., Marković, F. & Srecam, J. (2024). Lower Permian Košna conglomerates of the Velebit Mt. (Croatia): modal composition, provenance and depositional environment. *Geologia Croatica 77*(1), 1–14.

Pavelić, D. & Kovačić, M. (2018). Sedimentology and stratigraphy of the Neogene rift-type North Croatian Basin (Pannonian Basin System, Croatia): A review. *Marine and Petroleum Geology 91*, 455–469.

Pavelić, D., Avanić, R., Bakrač, K. & Vrsaljko, D. (2001). Early Miocene braided river and lacustrine sedimentation in the Kalnik Mountain area (Pannonian Basin System, NW Croatia). *Geol Carpathica 52*, 375–386.

Petković, K. (1961). Tektonska karta FNR Jugoslavije. Glas SAZU, 249, Jubil sv, 129-144.

Placer, L. (1999a). Contribution to the macrotectonic subdivision of the border region between Southern Alps and External Dinarides. *Geologija 41*, 223–255.

Placer, L. (1999b). Structural meaning of the Sava folds. *Geologija 41*, 191–221.

Schmid, S. M., Fügenschuh, B. Kissling, E. & Schuster, R. (2004). Tectonic map and overall architecture of the Alpine orogen. *Eclogae Geologicae Helvetiae 97*, 93–117.

Schmid, S. M., Bernoulli, D., Fügenschuh, B., Maţenco, L., Schefer, S., Schuster, R., Tischler, M. & Ustaszewski, K. (2008). The Alpine-Carpathian-Dinaridic orogenic system: correlation and evolution of tectonic units. *Swiss Journal of Geosciences 101*, 139–183.

Schmid, S. M., Fügenschuh, B., Kounov, A., Matenco, L., Nievergelt, P., Oberhänsli, R., Pleuger, J., Schefer, S., Schuster, R., Tomljenović, B., Ustaszewski, K. & Van Hinsbergen, D. J. J. (2020). Tectonic units of the Alpine collision zone between Eastern Alps and Western Turkey. *Gondwana Research, 78*, 308–374.

Schönborn, G., (1992). Alpine tectonics and kinematic models of the central Southern Alps. *Memorie Scienze Geologiche Padova 44*, 229–393.

Schönborn, G., (1999). Balancing cross sections with kinematic constraints: the Dolomites (northern Italy). *Tectonics 18*, 527–545.

Slovenec, D., Lugović, B., Meyer, H.-P. & Garapić-Šiftar, G. (2011). A tectonomagmatic correlation of basaltic rocks from ophiolite mélanges at the northeastern tip of the Sava-Vardar suture Zone, northern Croatia, constrained by geochemistry and petrology. *Ofioliti, 36*, 77–100.

Slovenec, D. & Šegvić, B. (2024). The evolution of the Mesozoic lithosphere of northwestern Neotethys: a petrogenetic and geodynamic perspective. *Journal of the Geological Society.* doi: 10.1144/jgs2023-132.

Sremac, J. (2005). Equatorial Shelf of the Palaeozoic Supercontinent – Cradle of the Adriatic Carbonate Platform. *Geologia Croatica 58*(1), 1–19.

Stampfli, G.M. & Borel, G.D. (2004). The TRANSMED transects in space and time: Constraints on the paleotectonic evolution of the Mediterranean domain. In: W. Cavazza, F. Roure, W. Spakman, G.M. Stampfli and P.A. Ziegler (Eds.), The TRANSMED Atlas: the Mediterranean Region from crust to mantle. Springer-Verlag, Berlin, p. 53-80.

Šegvić, B., Slovenec, D. & Badurina, L. (2023). Major and rare earth elements mineral chemistry of the low-grade assemblages inform dynamics of hydrothermal ocean-floor metamorphism in the Dinaridic Neotethys. *Geological Magazine 160*, 444−470.

Šimunić, A. (1992). Geološki odnosi središnjeg dijela Hrvatskog Zagorja. PhD thesis, Zagreb, 208pp.

Šimunić, A., Pikija, M. & Hećimović, I. (1982). Osnovna geološka karta SFRJ 1:100,000, list Varaždin L33–69 (Basic Geological Map of SFRY 1:100,000, Varaždin sheet). Geološki zavod Zagreb, Savezni geološki zavod.

Šimunić, An. & Hećimović, I. (1980). Tektonski odnosi sjeverozapadne Hrvatske (centralni dio Hrvatskog zagorja I dio Kalničkoh prigorja). Fond struč. dok. Inst. za geol. istraž. Zagreb.

Šimunić, An. & Šimunić, Al. (1987). Rekonstrukcija neotektonskih zbivanja u sjeverozapadnoj Hrvatskoj na temelju analize pontskih sedimenata. Rad Jugosl. akad. znan. umjet., 431, Razred za prir. znanosti, 22, 155- 177, Zagreb.

Šimunić, An. & Šimunić, Al. (1997). Triassic deposits of Hrvatsko Zagorje. *Geologia Croatica 50*(2), 243–250.

Šimunić, An., Pikija, M., Hećimović, I. & Šimunić, Al. (1981). Osnovna geološka karta SFRJ 1:100,000, Tumač za list Varaždin L 33-69 (Basic Geological Map of SFRY 1:100,000 Explanatory notes for Varaždin sheet). Institut za geološka istraživanja Zagreb, Savezni geološki zavod.

Šimunić, An., Pikija, M., Šimunić, Al., Šikić, L. & Milanović, M. (1976). Stratigrafsko-tektonski odnosi centralnog I istočnog dijela Ivanščice. 8. Jugoslav. Geol. Congress, 2, 303-314.

Šimunić, An., Šimunić, Al. & Milanović, M. (1979). Geološka građa Ivanščice i Ravne gore. *Geološki Vjesnik 31*, 157–174.

Slovenec, D., Horvat, M., Smirčić, D., Belak, M., Badurina, L., Kukoč, D., Grgasović, T., Byerly, K., Vukovski, M. & Šegvić, B. (2023). On the evolution of Middle Triassic passive margins of the Greater Adria Plate: inferences from the study of calc-alkaline and shoshonitic tuffs from NW Croatia. *Ofioliti 48*(1), 31–46.

Slovenec, D., Šegvić, B., Halamić, J., Goričan, Š. & Zanoni, G. (2020). An ensialic volcanic arc along the northwestern edge of paleotethys— insights from the Mid-Triassic volcano-sedimentary succession of Ivanščica Mt. (northwestern Croatia). *Geological Journal 55*, 4324–4351.

Smirčić, D., Kolar-Jurkovšek, T., Aljinović, D., Barudžija, U., Jurkovše,k B. & Hrvatović, H. (2018). Stratigraphic definition and correlation of the Middle Triassic volcaniclastic facies in the External Dinarides: Croatia and Bosnia and Herzegovina. *J Earth Sci 29*, 864–878.

Smirčić, D., Lugović, B., Aljinović, D., Hrvatović, H., Kolar-Jurkovšek, T., Jurkovšek, B. & Gajšak F (2016). Middle Triassic autoclastic deposits in the vicinity of Bosansko Grahovo (SW Bosnia and Herzegovina). *Rud Geol Naft Zb 31*(2),1–12.

Smirčić, D., Vukovski, M., Slovenec, D., Kukoč, D., Šegvić, B., Horvat, M., Belak, M., Grgasović, T. & Badurina, L. (2024). Facies architecture, geochemistry and petrogenesis of Middle Triassic volcaniclastic deposits of Mt. Ivanščica (NW Croatia) – evidence of bimodal volcanism in the Alpine-Dinaridic transitional zone. *Swiss Journal of Geosciences 117*, 5.

Tomljenović, B. & Csontos, L. (2001). Neogene-Quaternary structures in the border zone between Alps, Dinarides and Pannonian Basin (Hrvatsko zagorje and Karlovac basins, Croatia). *International Journal of Earth Sciences 90*, 560–578.

Tomljenović, B., Csontos, L., Márton, E. & Márton, P. (2008). Tectonic evolution of the northwestern Internal Dinarides as constrained by structures and rotation of Medvednica

Mountains, North Croatia. In: Tectonic Aspects of the Alpine- Dinaride-Carpathian System (Siegesmund, S. et al. Eds.). *Geological Society, London, Special Publications, 298,* 145–167.

van Gelder, I. E., Mațenco, L., Willingshofer, E., Tomljenović, B., Andriessen, P. A. M., Ducea, M. N., Beniest, A. & Gruić, A. (2015). The tectonic evolution of a critical segment of the Dinarides-Alps connection: kinematic and geochronological inferences from the Medvednica Mountains. NE Croatia. *Tectonics, 34*(9), 1952–1978.

Vlahović, I., Tišljar, J., Velić, I. & Matičec, D. (2005) Evolution of the Adriatic carbonate platform: palaeogeography, main events and depositional dynamics. *Palaeogeogr Palaeoclimatol Palaeoecol 220*, 333–360.

Vukovski, M., Kukoč, D., Grgasović, T., Fuček, L. & Slovenec, D. (2023). Evolution of eastern passive margin of Adria recorded in shallow- to deepwater successions of the transition zone between the Alps and the Dinarides. *Facies 69,* 18.

Vukovski, M., Špelić, M., Kukoč, D., Troskot-Čorbić, T., Grgasović, T., Slovenec, D. & Tomljenović, B. (2024). Unravelling the tectonic evolution of the Dinarides—Alps—Pannonian Basin transition zone: insights from structural analysis and low-temperature thermochronology from Ivanščica Mt., NW Croatia. *Swiss Journal of Geosciences*.

Winkler, A. (1923). Uber den Bau der östlichen Südalpen. Mitt. Geol. Ges., XVI, 1-272, Wien.

Winkler-Hermaden, A. (1957). Geologisches kraftespiel und landformen. Grundsatzliche erkenntnisse zur frage junger gebirgsbildung und landformung. Springer Ver., XX, 822, Wien.

Zupanič, J., Babić, Lj. & Crnjaković, M. (1981). Lower Cretaceous basinal clastics (Oštrc Formation) in the Mt. Ivanščica (Northwestern Croatia). *Acta Geologica, 11*(1), 1–44.

## 9. BIOGRAPHY OF THE AUTHOR

Matija Vukovski was born on October 17, 1994, in Zagreb. After completing elementary school, he enrolled in Vladimir Prelog Science School, specializing in Geological Technician, and graduated in 2013. In the same year, he began his undergraduate studies in Geological Engineering at the Faculty of Mining, Geology, and Petroleum Engineering, University of Zagreb. In 2016, he earned the academic degree of University Bachelor of Geological Engineering by defending his bachelor thesis titled "Petrogenetic Characteristics of Lasinja Spilites, Pokuplje." That same year, he enrolled in the Master study program in Geology, specializing in Mineral Resources Geology and Geophysical Exploration. He graduated in 2019 by defending his master thesis "Structural Analysis of Mesozoic and Cenozoic Deformation Structures in the Area of Western Papuk," earning the academic degree of Master of Geology. During the 2016/2017 academic year, he took a study break to participate in an international scientific project, "Miocene Evolution and Inferences for Petroleum Potential in the External Dinarides (Croatia): 2D Basin Modelling of Complex Geological Domains," and completed a six-month professional internship at the French Institute of Petroleum (IFP Energies nouvelles). In the academic year 2018/2019, he received the Excellence Scholarship by the City of Zagreb. In 2020, he got employed as an assistant at the Croatian Geological Survey, Department of Geology, within the project "Volcano-Sedimentary Successions of Northwestern Croatia and Their Role in Understanding the Geodynamics of the Paleotethys During the Middle Triassic (GOST)." The topic and research of his doctoral work are part of the GOST project. He is a member of the Croatian Geological Society (HGD) and the Swiss Geological Society (SGG/SGS).

**List of published scientific papers (28/10/2024):**

Pollak, D., Gulam, V., Novosel, T., Avanić, R., Tomljenović, B., Hećej, N., Terzić, J., Stipčević, J., Bačić, M., Kurečić, T., **Vukovski, M.** et al. (2021) The preliminary inventory of coseismic ground failures related to December 2020 – January 2021 Petrinja earthquake series. *Geologia Croatica 74*(2), 189-208.

Baize, S., Amoroso, S., Belić, N., Benedetti, L., Boncio, P., Budić, M., Cinti, F., Henriquet, M., Jamšek Rupnik, P., Kordić, B., **Vukovski, M.** et al. (2022) Environmental effects and seismogenic source characterization of the December 2020 earthquake sequence near Petrinja, Croatia. *Geophysical journal international 230*(2), 1394-1418.

Henriquet, M., Kordić, B., Métois Marianne, Lasserre Cecile, BAIZE, S., Benedetti, L., Špelić, M. & **Vukovski, M.** (2022) Rapid Remeasure of Dense Civilian Networks as a Game-Changer Tool for Surface Deformation Monitoring: The Case Study of the Mw 6.4 2020 Petrinja Earthquake, Croatia. *Geophysical research letters 49*(24), 1-11.

Slovenec, D., Horvat, M., Smirčić, D., Belak, M., Badurina, L., Kukoč, D., Grgasović, T., Byerly, K., **Vukovski, M.** & Šegvić, B. (2023) On the evolution of Middle Triassic passive margins of the Greater Adria Plate: inferences from the study of calc-alkaline and shoshonitic tuffs from NW Croatia. *Ofioliti, 48*(1), 31-46.

Kukoč, D., Smirčić, D., Grgasović, T., Horvat, M., Belak, M., Japundžić, D., Kolar-Jurkovšek, T., Šegvić, B., Badurina, L., **Vukovski, M.** & Slovenec, D. (2023) Biostratigraphy and facies description of Middle Triassic rift-related volcano-sedimentary successions at the junction of the Southern Alps and the Dinarides (NW Croatia). *International journal of earth sciences, 112*(4), 1175-1201.

**Vukovski, M.,** Kukoč, D., Grgasović, T., Fuček, L. & Slovenec, D. (2023) Evolution of eastern passive margin of Adria recorded in shallow- to deep-water successions of the transition zone between the Alps and the Dinarides (Ivanščica Mt., NW Croatia). *Facies 69,* 18.

Kukoč, D., Slovenec, D., Šegvić, B., **Vukovski, M.**, Belak, M., Grgasović, T., Horvat, M. & Smirčić, D. (2024) The early history of the Neotethys archived in the ophiolitic mélange of northwestern Croatia. *Journal of the geological society 181,* 1.

Smirčić, D., **Vukovski, M.**, Slovenec, D., Kukoč, D., Šegvić, B., Horvat, M., Belak, M., Grgasović, T. & Badurina, L. (2024) Facies architecture, geochemistry and petrogenesis of Middle Triassic volcaniclastic deposits of Mt. Ivanščica (NW Croatia): evidence of bimodal volcanism in the Alpine-Dinaridic transitional zone. *Swiss journal of geosciences 117,* 5.

Brlek, M., Trinajstić, N., Schindlbeck-Belo, J.C., Kutterlof, S., **Vukovski, M.** et al. (2024) A distal record of the Middle Miocene silicic eruption of the Carpathian-Pannonian Region stored within the Dinaride Lake System: implications for tephrostratigraphy and emplacement of volcaniclastic deposits. *International journal of earth sciences*.

**Vukovski, M.**, Špelić, M., Kukoč, D., Troskot-Čorbić, T., Grgasović, T., Slovenec, D. & Tomljenović, B. (2024) Unravelling the tectonic evolution of the Dinarides—Alps—Pannonian Basin transition zone: insights from structural analysis and low-temperature thermochronology from Ivanščica Mt., NW Croatia. *Swiss journal of geosciences, 117*, 16.